UNIVERSIDAD D SEVILLA

Caracterización de las royas del trigo en Andalucía y uso de sensores remotos para su detección temprana

Tesis doctoral de: Jaime Nolasco Rodríguez Vázquez

Tutor: Manuel Pérez Ruiz

Director 1: Fernando Martínez Moreno

Director 2: Orly Enrique Apolo Apolo

Sevilla, diciembre 2023

Caracterización de las royas del trigo en Andalucía y uso de sensores remotos para su detección temprana

D. Manuel Pérez Ruiz, Dr. Ingeniero Agrónomo y catedrático de la Universidad de Sevilla. Tutor

D. Fernando Martínez Moreno, Dr. Ingeniero Agrónomo y profesor titular de la Universidad de Sevilla. Director 1

D. Orly Enrique Apolo Apolo, Dr. Ingeniero Agrónomo, investigador postdoctoral en la Universidad de Hasselt y profesor sustituto interino en la Universidad de Sevilla. Director 2

Certifican:

Que el trabajo: Caracterización de las royas del trigo en Andalucía y uso de sensores remotos para su detección temprana; realizado por D. Jaime Nolasco Rodríguez Vázquez bajo su dirección, se considera ya finalizado y puede ser presentado para su exposición y defensa como Tesis Doctoral en el Dpto. Ingeniería Aeroespacial y Mecánica de Fluidos ´Área Agroforestal´

Fdo: Manuel Pérez Ruiz

Fdo: Fernando Martínez Moreno

Fdo: Orly Enrique Apolo Apolo

Agradecimientos

Una vez finalizada esta tesis doctoral, me gustaría expresar mi más sincero agradecimiento a todas las personas, que han contribuido a la realización de este trabajo con su ayuda y colaboración, y que, sin ellas, no estaría defendiendo esta tesis.

En primer lugar, agradecerles a mis padres, a mi hermano y a Mercedes el apoyo incondicional desde el primer al último día, siempre han conseguido sacarme una sonrisa en los momentos más oscuros. Y a mis abuelos, Cecilio y Encarna, quienes además de generar en mí la ilusión por esta profesión, me llevan inculcando valores 28 años.

Me gustaría reconocer la gran tarea de mis directores de tesis: Fernando Martínez y Enrique Apolo, disponibles a todas horas y días del año, para ayudar en lo que fuera preciso, y poner a mi disposición sus conocimientos para realizar el trabajo. También a mi tutor: Manuel Pérez, aconsejándome y guiándome cada vez que ha sido necesario.

Al Global Rust Reference Center (GRRC), por la rápida y eficaz caracterización de las muestras de royas.

Al CIMMYT, por el material vegetal suministrado, y especialmente al Dr. Karim Ammar, colaborador en varios de los capítulos de esta tesis, aportando su dilatada experiencia y conocimiento sobre las tres royas del trigo, dándole un enfoque más global al trabajo, y ayudándonos a comprender cómo "encajaban" nuestros datos con el actual desarrollo de estas enfermedades a nivel mundial.

Agradecer la colaboración de las personas que me ayudaron, en el fitotrón o en campo, a tomar datos de enfermedad, altura de las plantas, montar sensores, analizar imágenes, etc., principalmente: Jose Antonio Muñoz, Francisco Ruiz, Pedro Castro y José Luis Lagares.

Me gustaría hacer una mención especial a todo el equipo de AGROVEGETAL. Buenas personas, trabajadores, humildes, con un amor incondicional por su trabajo y por su empresa, y siempre con disposición de ayudar. Me acogieron como uno más del equipo desde el primer día, hace ya casi ocho años, y desde entonces siento "La Aceñuela" como mi segunda casa. Ellos son: Ignacio Solís, Luis Tomás, José Antonio Muñoz, Francisco Ruiz, Inmaculada Izquierdo, Clara Márquez, Antonio García, José Luis Tomás y Alberto Pascual.

Para terminar, darle las gracias a Ignacio Solís, quien fuera mi profesor de Mejora Vegetal, hace ya nueve años, y desde entonces sigo aprendiendo de él diariamente. Gracias por darme la oportunidad de formar parte de Agrovegetal, gracias por compartir tus conocimientos conmigo, y gracias por instarme a hacer esta tesis, en la que he aprendido mucho más de lo que podía imaginarme en un principio.

ÍNDICE GENERAL

Índice de tablas

Índice de figuras

Abstract

Rusts are a significant disease in wheat cultivation, causing yield loss and economic losses in the cereal sector. We can distinguish three rust species causing three different diseases: leaf (or brown), yellow (or stripe) and stem (or black) rust. Until the 2019-2020 season, leaf rust was controlled since the most planted cultivars in southern Spain had resistance genes against it, and susceptible cultivars were protected with fungicides. A problem arose in the spring of 2020 when all durum wheat cultivars began to become infected with a kind of leaf rust. The leaves had large pustules, different from those of typical rust caused by *P. triticina*, and the teliospores sprouted rapidly after a few days of infections. The symptoms fitted *P. tritici-duri*, another wheat leaf rust species already reported in the western Mediterranean basin. This study, evaluated the severity of leaf rust in durum wheat field trials during the 2019-20, 2020-21 and 2021-22 seasons in Huelva, Seville, Cádiz and Córdoba provinces. Additionally, during the spring of 2020 and 2021, isolates from individual leaf rust pustules were collected from different durum wheat cultivars. Inoculation of the isolate into a differential set of lines showed that five different races were present, of which two were of the *P. tritici-duri* subspecies. This subspecies is not new in southern Spain. Still, in the last 25 years, it has not been observed with such severity in almost all durum wheat cultivars (susceptible and resistant to *P. triticina*). Cultivar Calero constantly resisted all races of *P. tritici-duri* used in this study. Furthermore, effective mitigation of the current threat of yellow rust and the potential threat of stem rust to wheat production in southern Spain requires the characterization of the breeds currently present in the region. The results of this study indicated that the primary races of yellow rust now present in southern Spain are PstS10, PstS13 and PstS14, to which several widely planted commercial cultivars (possessing, among others, *Yr27* gene) are resistant. Stem rust does not pose a severe threat yet during the regular wheat growing season but can be a potential biotic stress soon. The primary races were Clade IV-B and Clade IV-F, as in most Europe and North Africa. For this rust species, the available resistances are always incomplete. The evaluation of differential series and unique breeding lines with known genes in local conditions (such as *Sr27* and *Sr35*) has indicated the availability of several genetic options that could be used in breeding/selection programs to provide adequate levels of resistance to stem rust. However, for any of the three rusts affecting wheat, in undertaking these efforts, it is essential to consider not only the races currently present in the region but also to consider effective resistance options against races that are being developed elsewhere and that they could very probably reach the south of Spain soon.

The other way to control rust in wheat is through chemical control; for this, early detection of the disease is essential. Therefore, this work studied the detection of yellow and leaf rust using hyperspectral data. An experiment was carried out in a greenhouse, with inoculated and non-inoculated wheat plants, with this disease. Each wheat plant was planted in separate pots, and their spectral reflectance was measured. Data pre-processing included standardization and the synthetic minority oversampling technique (SMOTE)

for data balance. Four machine learning models (ANN, SVM, RF, GNB) were tested with different SMOTE applications, focusing on accuracy and F1 score. The SVM and RF models showed the highest accuracies, especially with SMOTE (enhanced datasets). However, concerns were raised about real-world applications due to the use of synthetic data. The study highlighted the mixed impact of SMOTE on the data and identified RF and SVM as the best models for yellow and leaf rust detection, respectively. The findings emphasize the potential of spectral data and machine learning in crop disease detection and the need for data processing in future research. Another part of the study focuses on an alternative method to detect rust in wheat plants early, taking advantage of 3D LiDAR technology to discern the impact of this disease on wheat cultivars from the moment of its infection. Despite rust inoculation, variations in plant height and biomass were negligible. However, notable drops in grain yield were recorded, especially in cultivars susceptible to rust. LiDAR-derived data demonstrated a substantial correlation with disease severity, underscoring its promise for reliable biomass assessment and early detection of rust. The study affirms the vital role of LiDAR in precision agriculture, offering a proactive approach to disease management and safeguarding the stability of wheat production yields. Using new technologies for the early detection of rust in wheat plants, the precision, and results of the F1 score have been analyzed in different models and data sets. The data sets used can be considered comparatively small compared to other studies; this challenge is related to the current insufficiency of the size and diversity of the data sets in the application of plant disease classification models In addition, it is essential to consider all possible capture conditions, symptom variations and sensors. For these reasons, it is inevitable to have incomplete data sets and therefore the models in their application are limited in scope. There are several alternatives to address the effects of using incomplete data sets. One of the most common is data augmentation through various techniques that can be combined. However, each data augmentation technique can affect model accuracy differntly. Finding a design pattern to select the most optimal method presents a challenge. In this study, the SMOTE algorithm is applied to varying degrees to a small data set for a single disease with three categories. This demonstrates how, in general, precision increases with the application of data augmentation techniques. Regarding the data set, where the SMOTE algorithm was applied only to the training set, the accuracy for yellow rust detection decreased, and the accuracy for leaf rust detection increased. The classification models that achieved the highest accuracy values in this study were SVM and RF. In the study with LiDAR sensors, the estimation of disease severity using LiDAR reflectance intensities presents a novel method that aligns with the growing interest in precision agriculture, and the need for timely disease management. The findings of this study reveal that disease severity can be quantitatively assessed through LiDAR. In conclusion, while applying LiDAR technology for severity estimation is promising, it is imperative to consider the variability between different wheat cultivars and stages of disease progression. Future studies should focus on refining estimation models and exploring integrating LiDAR data with other remote sensing modalities to improve the accuracy and reliability of disease severity assessments.

Resumen

Las royas son una enfermedad importante en el cultivo del trigo, generando pérdidas de producción y, por tanto, económicas, en el sector cerealista. Podemos distinguir principalmente tres especies que causan tres enfermedades diferentes: roya de la hoja (o parda), amarilla (o lineal) y del tallo (o negra). Hasta la temporada 2019-2020, la roya de la hoja estaba controlada, ya que los cultivares más sembrados en el sur de España tenían genes de resistencia contra ella, y los cultivares susceptibles estaban protegidos con fungicidas. Pero un problema surgió en la primavera de 2020, cuando todos los cultivares de trigo duro comenzaron a infectarse con una roya parecida a la de la hoja. Las hojas presentaban pústulas grandes, diferentes a las de la roya de la hoja causada por *P. triticina*, y las teliosporas aparecían rápidamente después de unos días. Los síntomas claramente encajaban con *P. tritici-duri*, otra especie de roya de la hoja del trigo ya reportada en la cuenca occidental del Mediterráneo. Se evaluó la severidad de la roya de la hoja en ensayos de campo de trigo duro durante las temporadas 2019-20, 2020-21 y 2021-22 en las provincias de Huelva, Sevilla, Cádiz y Córdoba. Además, durante la primavera de 2020 y 2021, se recolectaron aislados de pústulas individuales de roya de la hoja de diferentes cultivares de trigo duro. La inoculación del aislado en un conjunto de líneas diferenciales, mostró que estaban presentes cinco razas diferentes, de las cuales dos eran de la subespecie *P. tritici-duri*. Esta subespecie no es nueva en el sur de España, pero en los últimos 25 años nunca se había observado con tanta severidad en casi todos los cultivares de trigo duro (susceptibles y resistentes a *P. triticina*). La mayor parte de los cultivares presentaron una respuesta mesotética frente a esta especie de roya, que crecía a un ritmo lento pero constante en casi todos los cultivares. Solo el cultivar Calero mostró una resistencia constante a las dos razas de *P. tritici-duri* empleadas en este estudio. Por otra parte, la mitigación efectiva de la amenaza actual de la roya amarilla, y la amenaza potencial de la roya del tallo, a la producción de trigo en el sur de España, requiere la caracterización de las razas actualmente presentes en la región. Los resultados de este estudio indicaron que las principales razas de roya amarilla actualmente presentes en el sur de España son: PstS10, PstS13 y PstS14, a los que son resistentes varios cultivares comerciales de trigo harinero (que seguramente tengan *Yr27*), especie más susceptible a esta roya. La roya del tallo apenas está presente durante la temporada de cultivo regular, pero puede ser una enfermedad importante en el futuro. Se identificaron las principales razas como Clade IV-B y Clade IV-F, al igual que en la mayor parte de Europa y partes del norte de África. Para esta roya, las resistencias siempre son incompletas. La evaluación de series diferenciales y líneas de mejora especiales, con genes conocidos en condiciones locales (como *Sr27* y *Sr35*) ha indicado la disponibilidad de varias opciones genéticas que podrían usarse en programas de mejoramiento/selección, con el fin de proporcionar niveles efectivos de resistencia a la roya del tallo. Sin embargo, para cualquiera de las tres royas que afectan al trigo, al emprender estos esfuerzos, es importante considerar no sólo las razas actualmente presentes en la región, sino, también considerar, opciones de resistencia efectivas contra razas que se están desarrollando en

otros lugares y que muy probablemente podrían llegar al sur de España en un futuro próximo.

La otra forma de controlar las royas en el trigo es mediante el control químico; y para ello, es imprescindible la detección precoz de la enfermedad. Por ello, en este trabajo se estudió la detección de roya amarilla y de la hoja en el trigo, utilizando datos hiperespectrales. Se realizó un experimento en invernadero, con plantas de trigo inoculadas y no inoculadas, con esta enfermedad. Cada planta de trigo se sembró en macetas separadas, y se midió la reflectancia espectral en cada una de ellas. El pre-procesamiento de datos incluyó la estandarización y la técnica de sobre muestreo de minorías sintéticas (SMOTE), para el equilibrio de datos. Cuatro modelos de aprendizaje automático (ANN, SVM, RF, GNB) se probaron con diferentes aplicaciones SMOTE, centrándose en la precisión y la puntuación F1. Los modelos SVM y RF mostraron las mayores precisiones, especialmente con SMOTE (conjuntos de datos mejorados). Sin embargo, surgieron preocupaciones sobre la aplicación en el mundo real, debido al uso de datos sintéticos. El estudio destacó el impacto mixto de SMOTE en los datos, e identificó RF y SVM como los mejores modelos para la detección de la roya amarilla y de la hoja, respectivamente. Los hallazgos enfatizan el potencial de los datos espectrales y aprendizaje automático en la detección de enfermedades de cultivos y la necesidad de procesamiento de datos en futuras investigaciones. Otra parte del estudio se centró en un método alternativo para detectar de forma precoz las royas en las plantas de trigo, y es, aprovechando la tecnología LiDAR 3D para discernir el impacto de esta enfermedad en los cultivares de trigo, desde el momento de su infección. A pesar de la inoculación de roya, las variaciones en la altura de las plantas y la biomasa fueron insignificantes; sin embargo, se registraron caídas notables en el rendimiento de granos, especialmente en cultivares susceptibles a la roya. Los datos derivados de LiDAR demostraron una correlación sustancial con la gravedad de la enfermedad, lo que subraya su promesa de una evaluación confiable de la biomasa y una detección temprana de la roya. El estudio afirma el papel vital de LiDAR en la agricultura de precisión, ofreciendo un enfoque proactivo para el manejo de enfermedades y salvaguardando la estabilidad de los rendimientos de las producciones de trigo. Utilizando nuevas tecnologías para la detección precoz de la roya en plantas de trigo, en el presente estudio, se han analizado la precisión y los resultados de la puntuación F1, en diferentes modelos y conjuntos de datos. Los conjuntos de datos utilizados pueden considerarse comparativamente pequeños a otros estudios, este desafío, se relaciona con la insuficiencia actual del tamaño y la diversidad de los conjuntos de datos, en la aplicación de modelos de clasificación de enfermedades en plantas, además, es fundamental considerar todas las posibles condiciones de captura, variaciones de síntomas y sensores. Por estas razones, es inevitable tener conjuntos de datos incompletos y, por tanto, los modelos en su aplicación tienen un alcance limitado. Existen varias alternativas para abordar los efectos del uso de conjuntos de datos incompletos. Uno de los más comunes, es el aumento de datos a través de diversas técnicas que se pueden combinar entre sí. Sin embargo, cada técnica de aumento de datos puede afectar la precisión del modelo de una manera diferente. Encontrar un patrón de diseño para seleccionar el método óptimo presenta un desafío. En

este estudio, el algoritmo SMOTE se aplica en diversos grados a un pequeño conjunto de datos, para una sola enfermedad con tres categorías. Esto demuestra, cómo en general, la precisión aumenta con la aplicación de técnicas de aumento de datos. Con respecto al conjunto de datos, donde el algoritmo SMOTE se aplicó solo al conjunto de entrenamiento, disminuyó la precisión para la detección de roya amarilla, y aumentó la precisión para la detección de roya de la hoja. Los modelos de clasificación que alcanzaron los valores de precisión más altos en este estudio fueron SVM y RF. En el estudio con sensores LiDAR, la estimación de la gravedad de la enfermedad utilizando intensidades de reflectancia LiDAR, presenta un método novedoso que se alinea con el creciente interés en la agricultura de precisión, y la necesidad de un manejo oportuno de las enfermedades. Los hallazgos de este estudio revelan que la gravedad de la enfermedad se puede evaluar cuantitativamente a través de LiDAR. En conclusión, si bien la aplicación de la tecnología LiDAR para la estimación de la gravedad es prometedora, es imperativo considerar la variabilidad entre los diferentes cultivares de trigo y las etapas de progresión de la enfermedad. Los estudios futuros deberían centrarse en perfeccionar los modelos de estimación, y explorar la integración de datos LiDAR con otras modalidades de detección remota, para mejorar la precisión y confiabilidad de las evaluaciones de la gravedad de las enfermedades.

Capítulo 1. Introducción

1.1 Los cereales

Los cereales constituyen un grupo de cultivos fundamental para la agricultura. La mayor parte de las civilizaciones han consumido un tipo de cereal específico, creando una cultura gastronómica en torno a ellos. Son plantas herbáceas monocotiledóneas de ciclo vegetativo anual que comprenden varias especies, como el trigo, cebada, avena, centeno, triticale, maíz, etc. (López Bellido, 1991). Actualmente, la producción de cereal a nivel mundial es de 2.815 Mt (millones de toneladas) al año (FAO, 2023). La semilla (o grano) tiene un alto contenido en carbohidratos, y se puede conservar durante mucho tiempo. También contienen una cantidad apreciable de un complejo de proteínas (en torno al 14%), que en el trigo y centeno forman el gluten (cuando se mezcla la harina con agua), responsables de la esponjosidad y la textura del pan, que históricamente ha sido el producto más común obtenido del grano (Zohary et al., 2000; Abdullaeva et al., 2021). El grano de los cereales se puede usar para la fabricación de otros productos para alimentación humana y animal, y a la fabricación de bioetanol (Guerrero, 1999). El grano o semilla está formado por:

- **Germen o embrión:** órgano de la semilla, a partir del cual se desarrolla una nueva planta. Está formado por ácidos grasos, enzimas, proteínas, vitaminas y minerales (Gili, 2018).
- **Endospermo:** estructura harinosa que envuelve al embrión y que le proporciona los nutrientes necesarios para la germinación de la semilla. Se encuentra formado por almidón y por proteínas, algunas de las cuales forman el gluten que hace posible la panificación (Shewry, 2009).
- **Testa:** capa exterior laminar que recubre al grano y proporciona nutrientes y vitaminas (Marikkar et al., 2020).
- **Cubiertas:** son las capas más exteriores (pericarpo, testa y capa de aleurona) y tiene cierta dureza ya que protege a la semilla. Está formada por fibras vegetales y en la molienda constituyen el salvado (López Bellido, 1991).

1.2 El trigo

El trigo se considera en muchos países (Europa, norte de África, oeste de Asia y parte de América), un alimento básico, debido a sus múltiples nutrientes, a sus propiedades y a la extraordinaria calidad de su harina. Desde la antigüedad, representaba alrededor del 20% de las calorías totales consumidas por el ser humano (Liu et al., 2019). Actualmente (campaña 2022/23), la producción mundial es de 781 Mt al año y la superficie cultivada es de 220 Mha (millones de hectáreas), lo que lo convierte en el tercer cereal más producido del mundo (detrás del maíz y el arroz), y el primero en cuanto a superficie cultivada (FAO, 2023). Esta gran superficie cultivada se debe, entre otros

factores, a que el trigo se adapta a condiciones climáticas muy diversas, encontrándose cultivado en prácticamente todas las regiones del planeta, a excepción de las zonas entre trópicos y los casquetes polares, aunque, como se puede ver en la figura 1.1, en Europa y Asia es donde más se cultiva (Hyles et al., 2020). Las condiciones ideales para su cultivo son:

- **Clima:** temperatura mínima de 3 °C y máxima de 30 a 33 °C, siendo la temperatura óptima entre 10 y 25 °C. Los requerimientos de temperatura varían algo con el estadio de crecimiento de la planta, y también depende de los requisitos de vernalización del cultivar (Gouis et al., 2020).
- **Humedad:** requiere una humedad relativa de entre el 40 y el 70 %; desde el espigado hasta la maduración del grano es la época que tiene mayores requerimientos en este aspecto, ya que exige una humedad relativa entre el 50 y el 60 % y un clima seco para su maduración (Bahri et al., 2019).
- **Agua:** tiene unos requerimientos moderados de agua, ya que se puede cultivar en zonas donde caen precipitaciones entre 250 y 2.800 mm anuales de agua, aunque un 75% del trigo sembrado en el mundo crece entre los 400 y 1000 mm (Ahmed et al., 2022).
- **Suelo:** los mejores suelos para su crecimiento deben ser sueltos, profundos, fértiles y libres de inundaciones, y deben tener un pH entre 6,0 y 7,5. En terrenos ácidos es difícil lograr un adecuado crecimiento y producción (Khan et al., 2019).

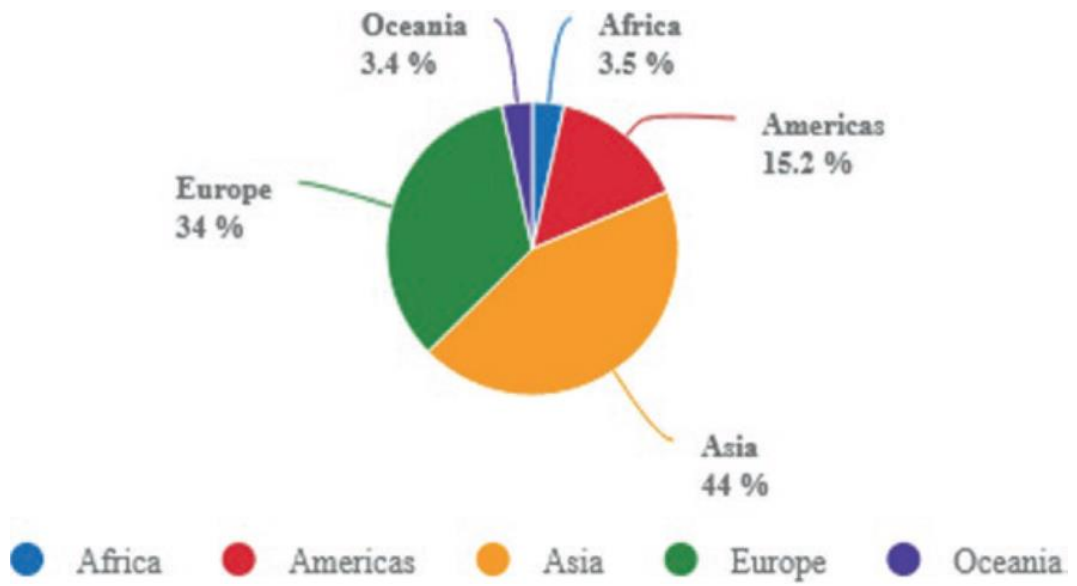

Figura 1.1 Producción mundial de trigo por continentes (Reynolds y Braun, 2022).

1.2.1 El trigo harinero

El trigo harinero, *Triticum aestivum* L. ssp. *aestivum*, es una planta alohexaploide, debido a su conformación de 42 cromosomas repartidos en seis juegos o subgenomas

(AABBDD), que proceden de tres genomas de tres especies de trigos silvestres diferentes. El trigo harinero se produjo en campos de agricultores del suroeste de la Cuenca del Mar Caspio (actual norte de Irán) hace unos 9.000 años, cuando una especie de trigo tetraploide cultivado se cruzó con una gramínea silvestre local, *Aegilops tauschii* (2n=2x=14; DD). El posterior cruce de gametos naturalmente no reducidos (óvulo y polen) en meiosis dio lugar a los primeros genotipos de trigos harineros. Esta poliploidía le confiere a la especie una gran adaptabilidad a los diferentes ambientes, sobre todo en climas fríos o secos, mayor que sus parientes tetraploides o diploides. Esta mejor adaptación del trigo harinero alohexaploide es debida, entre otras razones, a la plasticidad alélica de poseer seis alelos para el mismo locus (dos por cada genoma), lo que da lugar a numerosas combinaciones de alelos (Levy y Feldman, 2022). Constituye la mayoría del trigo cultivado en el mundo, ya que en esta campaña 2022/23, de los 781 millones de toneladas producidas, 743 fueron de trigo harinero, es decir un 95% del trigo mundial (Song et al., 2023). Su grano se usa para elaborar harina, con la que se elaboran una multitud de productos, siendo el principal el pan, pero también galletas, tartas, dulces, crackers, etc. (Shewry, 2009).

1.2.2 El trigo duro

El trigo duro, *Triticum turgidum* L. subsp. *durum* (Desf.) Husn., es un trigo alotetraploide (AABB), cuyo uso principal es la elaboración de pastas, cuscús y otros productos a través de su grano (Saini et al., 2023). A pesar de que apenas aporta un 5% de la producción de trigo mundial, es de elevada importancia en nuestra región, ya que el 50% de la producción mundial de trigo duro se cultiva en la cuenca mediterránea (Chairi et al., 2020). El trigo duro procede de la evolución de la escanda cultivada (*Triticum turgidum* L. subsp. *dicoccum*) (2n=2x=28), cuya selección de plantas con grano desnudo dio origen a esta especie. La escanda silvestre (*Triticum turgidum* L. subsp. *dicoccoides*) se domesticó hace unos 10.069±160 años (según una estimación hecha en 2023 a partir de datos del genoma) en el sudeste de Turquía-norte de Siria (o norte del Levante mediterráneo), dando lugar a la escanda cultivada, especie de trigo de grano vestido (Zhao et al., 2023). Un factor clave para la obtención de la escanda cultivada fue la selección de plantas con un raquis más fuerte o tenaz, que favorecía el trillado y que es debido a las mutaciones de los genes *TtBtr1-A* y *TtBtr1-B*. Los primeros trigos tetraploides de grano desnudo y de fácil trilla (no exactamente como el trigo duro actual, pero parecidos) surgieron hace 9.269±98 años en el sudeste de Turquía (Zhao et al., 2023). Otra mutación dominante producida en locus *q*, en el cromosoma 5A, produjo plantas de cuyos granos se soltaban fácilmente de las glumas, dando lugar a plantas de grano desnudo (Faris, 2014).

Andalucía es la región de España con mayor producción de trigo duro, aportando el 70% de la producción del país, y un 9% de la Unión Europea. De las 320.000 hectáreas sembradas de trigo en Andalucía, 200.000 hectáreas son trigo duro, frente a 120.000

hectáreas de trigo harinero, de ahí la importancia de este cultivo en la región, a pesar del poco peso a nivel mundial (Martínez-Moreno et al., 2022).

1.3 El CIMMYT

El CIMMYT (Centro Internacional de Mejoramiento de Maíz y Trigo) surgió de un programa piloto de investigación científica patrocinado por el Gobierno de México y la Fundación Rockefeller en las décadas de 1940 y 1950 destinado a elevar la productividad agrícola en México (Borlaug, 2007). Norman Borlaug (1914-2009), un mejorador estadounidense, junto con investigadores y agricultores mexicanos, desarrollaron cultivares de trigo de tallo corto (enanas, resistentes al encamado), y que producían más grano que las variedades locales o criollas (figura 1.2). Después de que fueron mejoradas y seleccionadas en diversos sitios de Méjico, se obtuvieron cultivares que se adaptaron a diversas condiciones climáticas (Borlaug, 2007). Esos cultivares ayudaron a Méjico a lograr su autosuficiencia en trigo a partir de la década de 1960, y sus semillas fueron exportadas a India y a Pakistán en dicha década (como Sonora 64), que ayudaron a salvar a la población de una inminente hambruna y en poco tiempo a elevar de manera impresionante la producción de trigo en ambos países. Estos hechos produjeron la adopción generalizada de cultivares de trigo mejorados junto con prácticas agronómicas más intensivas (mejora de la siembra, fertilización, riego, protección de cultivos, etc.) (Borlaug, 2007). La adopción de estas técnicas dio lugar a la llamada Revolución Verde. El CIMMYT se estableció oficialmente en 1966 como organización internacional. El Dr. Borlaug recibió el Premio Nobel de la Paz en 1970 por su enorme contribución a la Revolución Verde y a la lucha contra el hambre. Fue mejorador, científico y líder de investigación sobre trigo en el CIMMYT hasta 1979, cuando se jubiló, y posteriormente consultor del Centro hasta su fallecimiento en 2009. El CIMMYT se encarga de mejorar el rendimiento del trigo a nivel mundial para países en vías de desarrollo, donde la falta de alimentos básicos ricos en hidratos de carbono es uno de los problemas principales de la sociedad (Borlaug, 2007).

Figura 1.2 El Dr. Norman Borlaug con algunos de los cultivares de porte corto creadas en el CIMMYT.

Hay cuatro factores que explican el éxito de los cultivares de la Revolución Verde:

1. Enanismo. El encamado o caída del trigo era un accidente frecuente debido a la altura de la planta, que se doblaba al final de su ciclo debido al viento, a la lluvia y al propio peso de la planta. Debido al aumento de la fertilización química y a la llegada de nuevos modelos de segadoras y cosechadoras a principios del siglo XX, el encamado pasó a ser uno de los principales problemas del trigo. Borlaug recibió semillas del cultivar de talla baja japonés Norin 10 (con los genes *Rht1* o *RhtB1b*, y *Rht2* o *RhtD1b*) y semillas del cruce Brevor×Norin 10 del mejorador estadounidense O. Vogel (Universidad del Estado de Washington). A partir de ellas se obtuvieron plantas con menor altura que, además, tenían mayor índice de cosecha, que pasó de 0,3 a 0,5. Posteriormente, se observó que los cultivares semienanos (dos genes de enanismo), tenían un mayor rendimiento que los enanos (solo uno). El desarrollo de cultivares semienanos sigue siendo la línea actual del CIMMYT. Se buscan genes de enanismo que además tengan un coleóptilo largo, como el gen *Rht18*, que permite una siembra más profunda y un mejor establecimiento del cultivo, lo cual es ventajoso en regiones cálidas y secas (Borlaug, 2007; Yang et al., 2015).

2. Alto potencial de rendimiento. Desde inicios del siglo XX se introdujeron diferentes tipos de fertilizantes (como la urea) que aumentaron el rendimiento en grano del trigo. Brevor y Gaines eran cultivares obtenidos por O. Vogel, con buena respuesta al abonado nitrogenado. En 1953, Borlaug comienza a cruzar las líneas semienanas de Brevor×Norin 10 con variedades locales mejicanas para conseguir un nuevo tipo de trigo harinero enano de primavera (Brevor y Norin 10 eran cultivares de invierno). También eran de mayor rendimiento debido a un mayor número de flores por espiguilla y del ahijado. Dos de los mejores cultivares que surgieron de este programa fueron Sonora 64 y Lerma Rojo 64, que tuvieron tanto éxito en México, como después en India y Pakistán. Después llegaron todavía mejores cultivares, como Siete Cerros 66, que llegó a sembrarse en unos 7 Mha.

Pavón 76, Anza, Seri 82, Attila o Borlaug100 han sido cultivares que han superado el rendimiento de las anteriores. Se calcula que el rendimiento de los nuevos cultivares en el periodo 1960-2020 se incrementó un 0.91% anual (63 kg/ha/año) en el Valle del Yaqui (Fisher, 2022).

3. Resistencia a las royas. La roya del tallo era una enfermedad que estaba generando problemas en América del Norte a mediados del siglo XX (epifitias de 1935 y 1954, raza 15b). Para ello, Borlaug recurrió a cultivares resistentes de Estados Unidos como Hope (*Sr2, Sr17*) y Thatcher (*Sr9g, Sr12, Sr16*). Los nuevos ensayos de trigo en el Valle de Toluca (México), con un ambiente húmedo, a unos 2.600 metros sobre el nivel del mar, fueron ideales para que Borlaug evaluara resistencias a royas. Cuando la roya del tallo empezó a disminuir, apareció la roya de la hoja. Para luchar contra esta otra especie de roya, empleó el cultivar resistente brasileño Frontana (*Lr34*) y el australiano Marroqui 588 (*Lr46* y *Lr67*). Fruto de estos cruces fueron los cultivares Yaqui 50 o Bonza 55, claramente previas a los cultivares de la Revolución Verde, pero que contribuyeron a la resistencia a las royas de las mismas (Borlaug, 2007).

4. Insensibilidad al fotoperiodo. Borlaug disponía de dos lugares para realizar sus ensayos de trigos de primavera: el Valle del Yaqui, en el desierto de Sonora, y el Valle de Toluca, en el Altiplano. Las dos zonas distaban 1.200 km y tenían un clima muy diferente. El Valle del Yaqui tiene un clima cálido y seco (siembra en diciembre), mientras que el Valle de Toluca es húmedo (siembra en junio). Borlaug sembró dos generaciones de trigo al año en estos dos sitios para acelerar el proceso de selección de genotipos superiores. Esta idea iba en contra de los tratados de mejora vegetal de la época, donde se decía que la selección de cultivares debía efectuarse en un único ambiente: el mismo donde el agricultor fuera a sembrarlas. De hecho, tuvo enfrentamientos con G. Harrar por esto, pero afortunadamente los ensayos de campo siguieron adelante. Como en el Valle del Yaqui el trigo espiga a día creciente (en primavera) y en Toluca a día decreciente (final de verano), se seleccionaron unos pocos genotipos que podían crecer fácilmente en estos dos ambientes, como se puede ver en la (figura 1.3). Estos individuos eran insensibles al fotoperiodo y se podían cultivar en multitud de ambientes. La insensibilidad al fotoperiodo es la capacidad de algunos cultivares de trigo de espigar en condiciones variables de fotoperiodo, es decir, el espigado ocurre de forma independiente a la duración del día y la noche. Esa adaptación es debida a mutaciones naturales en los genes de fotoperiodo (*PPD1*) que, en su forma natural, promueven el espigado en fotoperiodo creciente (primavera). La insensibilidad al fotoperiodo, favorece una mejor adaptación de los cultivares, cuando se siembran en ambientes y/o fechas diferentes. Desde entonces, el CIMMYT y otras empresas aplican este método de selección en condiciones diferentes (*shuttle breeding*) (Borlaug, 2007).

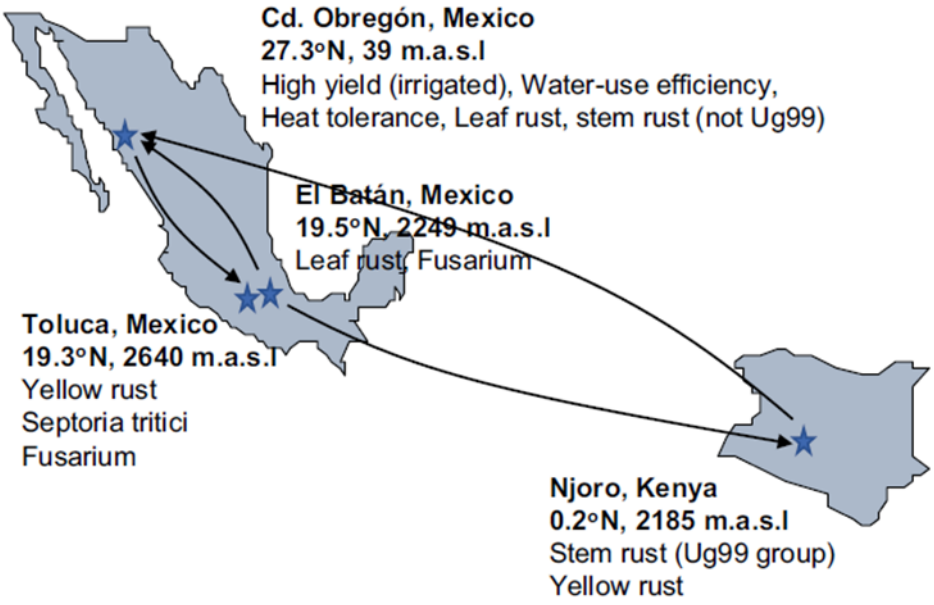

Figura 1.3 Mejora en estación (Cd. Obregón, Sonora) y contraestación (Toluca) (shuttle breeding) en Méjico, realizada por el CIMMYT

1.4 Mecanismos de defensa de las plantas frente a estreses bióticos

Las plantas disponen de una amplia gama de mecanismos de defensa frente a sus enemigos que pueden ser preexistentes al ataque o inducidos por la presencia del patógeno (Song et al., 2020). Los podemos clasificar en cuatro grupos:

- **Escape:** Consiste en la falta de coincidencia entre ambos (en el tiempo o en el espacio), en la ausencia de contacto. No suele ser un mecanismo hereditario, aunque a veces sí, como en el caso de cultivares precoces que maduren antes de que llegue el patógeno, como ha sucedido con los cultivares de trigos de primavera del CIMMYT frente a la roya del tallo (Soleiman et al., 2014).

- **Evitación:** Está basada en mecanismos hereditarios que reducen la probabilidad de contacto. En ella se incluyen tanto la arquitectura de la parte aérea que reduce la superficie de contacto con los patógenos como los mecanismos de antixenosis (no preferencia) de algunas plantas frente a insectos y vertebrados. Frente a enfermedades hay menos casos. Un ejemplo ocurre en la gramínea silvestre *Hordeum chilense* frente a la roya de la hoja de la cebada (*Puccinia hordei*). Las esporas de roya germinan normalmente sobre la superficie foliar y desarrollan el tubo germinativo que crece buscando un estoma. Normalmente los estomas están situados a mayor altura respecto al plano de la superficie foliar. Este elemento es clave para que la roya reconozca la presencia del estoma. Pero debido a la presencia de ceras que cubren el estoma en *H. chilense*, el tubo germinativo de la espora no puede localizar al estoma y formar el apresorio para penetrar dentro de la hoja (Soleiman et al., 2014; Niks et al., 2019).

- **Tolerancia:** El patógeno se multiplica en el huésped, pero los daños son reducidos o inexistentes. Un cultivar puede ser muy susceptible a un patógeno, pero sufrir daños económicos muy reducidos. Tolerante es opuesto a sensible. La tolerancia es un mecanismo de defensa frecuente frente a virus, pero menos frente a hongos fitopatógenos. La tolerancia se ha estudiado muy poco. Por un lado, no es tan abundante como la resistencia, por otro lado, su evaluación no es fácil. En muchos casos, implica medir el rendimiento en plantas con y sin enfermedad, que es un carácter complicado y muy influenciable por el ambiente. Por ejemplo, la línea de tomate ABL portadora del gen *Ty-1* tiene tolerancia frente a un virus del rizado amarillo. El virus está presente en esta línea y, de hecho, su concentración se puede medir mediante una prueba ELISA, pero la planta no muestra prácticamente síntomas (Niks et al., 2019; Mashaheet et al., 2020).

- **Resistencia:** Es la capacidad de la planta de restringir el crecimiento o la reproducción del patógeno una vez que ha penetrado dentro de esta. Puede haber síntomas de la enfermedad, aunque reducidos respecto a una variedad de planta susceptible. La inmunidad es la máxima expresión de la resistencia con ausencia de síntomas. Resistente es opuesto a susceptible (Pazda et al., 2019).

La mayor parte de los esfuerzos de la mejora, se han dirigido a introducir resistencias en los cultivos de mayor importancia económica. Por un lado, son abundantes, suelen ser bastante completas y se pueden encontrar mecanismos de resistencia diferentes, que se pueden combinar en un solo cultivar mediante cruzamientos (Pazda et al., 2019).

1.5 Tipos de resistencia

1.5.1 Resistencia

Puede estar controlada por uno, varios o muchos genes. Entre la planta hospedante y el patógeno puede existir una reacción de compatibilidad o incompatibilidad (Hafeez et al., 2021). Podemos destacar dos tipos de resistencia: horizontal y vertical (Li et al., 2019).

1.5.1.1 Resistencia vertical

La resistencia es vertical (también llamada diferencial o raza-específica), si una variedad del huésped responde de distinta manera a diversas razas fisiológicas del patógeno (Vanderplank, 2012). La resistencia vertical es debida a genes mayores, por tanto, es monogénica, y sigue la relación gen a gen (Vanderplank, 2012). En dicha relación, la resistencia es producto de la interacción del alelo de resistencia de la planta,

con el alelo complementario de avirulencia del patógeno. El resto de combinaciones resulta en susceptibilidad (Flor, 1971).

La resistencia vertical, suele ser una resistencia completa, y es fácil de manejar e introducir por cruzamiento, debido a que la resistencia es debida a un solo gen (Miah et al., 2013). Son resistencias cualitativas; si el individuo tiene el alelo de resistencia, será resistente, y si tiene el alelo de susceptibilidad, será susceptible. El ambiente influye muy poco (alta heredabilidad) (Lamberti et al., 2015).

1.5.1.2 Resistencia horizontal

Desde hace mucho tiempo, se observaba que algunas variedades tenían resistencias intermedias, que se llamaban 'resistencias de campo'. Este tipo de resistencias se corresponden con la resistencia horizontal (uniforme o raza no específica), si una variedad se muestra siempre resistente ante diversas razas del patógeno (Karkman et al., 2019). Las resistencias horizontales suelen tener un control poligénico, en la que cada uno de los genes menores disminuye en una pequeña proporción el desarrollo de la enfermedad por mecanismos diferentes (Vanderplank, 2012). Son resistencias incompletas (o débiles), por eso es también muy común el término resistencia parcial (Johnson et al., 2016). En las variedades con resistencia parcial, el patógeno es capaz de reproducirse dentro de la planta, pero lo hace de forma más lenta, por eso son muy típicas las expresiones slow rusting (desarrollo lento de roya) o slow mildewing (desarrollo lento de mildiu o de oídio). Es también un carácter cuantitativo, en el que el nivel de resistencia depende del número de genes menores del individuo, y del ambiente, el cual tiene una gran influencia (Miedaner y Korzun, 2012). Al tratarse de poligenes su manejo en mejora es más complejo, aunque el desarrollo de marcadores de ADN permite seleccionar los genotipos con los genes menores que produzcan un mayor efecto en la resistencia parcial, como ocurre con el gen *Lr34*, de resistencia a la roya de la hoja del trigo (Niks et al., 2019). El gen *Lr34*, localizado en el cromosoma 7DS y procedente de la variedad de trigo harinero italiana Mentana, causa un incremento notable en el periodo de latencia (periodo de aparición de los síntomas o pústulas). Su efecto es más pronunciado en planta adulta que en plántula. Se ha descrito que este gen en combinación con otros genes mejora la resistencia y la durabilidad. El gen *Lr34* goza de enorme éxito en los programas de mejora, siendo frecuentemente usado en mejora de trigo harinero. Otra ventaja del gen *Lr34* es que es pleiotrópico, es decir que también tiene otros efectos, con los genes *Yr18*, *Sr57* y *Pm38* (resistencia a oídio) (Ellis et al., 2014). El gen *Lr67* se identificó en la línea pakistaní PI250413. Está en el cromosoma 4DL y su expresión fenotípica se parece mucho a la del gen *Lr34*, y también tiene efecto pleiotrópico frente a la roya amarilla y del tallo (Herrera-Foessel et al., 2014; Rodríguez Vázquez et al.,2023). Otro gen similar es el gen *Sr2*, que está en el cromosoma 3B, procede de la variedad escanda rusa Yaroslav y fue transferida al cultivar de trigo harinero de invierno Hope en 1930 (Ellis et al., 2014).

1.5.2 Relación gen a gen

La teoría gen por gen, propone que, por cada gen de resistencia en el hospedante, existe un gen de virulencia complementario en el patógeno (Flor, 1956). La mayor parte de las resistencias a hongos fitopatógenos y a insectos en plantas son debidas a un alelo dominante, mientras que la susceptibilidad suele ser debida a un alelo recesivo (Legarralde et al, 2019). En el patógeno existe un gen complementario que puede ser de virulencia o avirulencia, donde la avirulencia es debida a un alelo dominante, y la virulencia debida a un alelo recesivo (Mendoza, 2020). La resistencia se produce cuando interaccionan los productos de los alelos de avirulencia del patógeno y el de resistencia de la planta, activando una reacción que conduce a la resistencia (reacción incompatible). En el resto de combinaciones de genes no se produce esa reacción, con lo que el patógeno seguirá con el proceso de infección (Rodríguez Gil., 2023). Por lo tanto, una variedad que no lleve ningún gen dominante (en general, de resistencia) será susceptible a todas las razas del patógeno que lleven al menos un gen de virulencia; la que lleve uno será resistente a todas las razas que lleven el complementario del patógeno en la forma requerida para la avirulencia (en general, en alelo dominante) (Flor, 1971). Actualmente, se afirma que el alelo de avirulencia del patógeno produce un efector, es decir, una molécula que manipulan el metabolismo de la planta huésped a favor del patógeno (fundamental para entender la patogénesis). Así, un efector puede desviar el flujo de azúcares desde la célula vegetal hacia el haustorio, o cortar reacciones de defensa de la planta. Un efector del mildiu de la patata, aislado recientemente, es un inhibidor de proteasas. Las proteasas son enzimas que degradan proteínas y son responsables de la resistencia de ciertas variedades de patata frente al mildiu. La planta resistente ha aprendido a detectar este efector, mediante un receptor específico (producto del alelo de resistencia) y activar el sistema de defensa cuando los detecta. Si el receptor (de la planta) reconoce al efector (del patógeno) entonces se desencadena la resistencia. Si no hay reconocimiento, el efector penetra en la célula vegetal y efectúa su labor patogénica. En patógenos que forman haustorios, la relación planta-patógeno (acción del efector y reconocimiento o no por parte del receptor) tiene lugar en el espacio comprendido entre la membrana de la célula vegetal y la membrana del haustorio (del patógeno) (Niks et al., 2019).

1.5.3 Resistencia hipersensible

Este mecanismo se desarrolla con la infección de un hongo biotrofo o hemibiotrofo y es un mecanismo de defensa activa que consiste en una necrosis de las células vegetales que se encuentran alrededor del sitio de penetración, mientras que el crecimiento del patógeno es frenado o retenido (Moerschbacher et al., 1990). En el caso de las royas o mildius, dicha necrosis ocurre durante o después de la formación del primer haustorio (Ferreira et al., 2021). La respuesta hipersensible está además asociada a la producción de fitoalexinas y proteínas relacionadas con la patogénesis (Lin et al., 2022). Un ejemplo de fitoalexina es la pisatina en guisante y un ejemplo de proteínas PR son las

quitinasas, enzimas que degradan la quitina, un componente de la pared celular de los hongos. La respuesta hipersensible depende del gen de resistencia, y cada gen de resistencia puede activar esta de forma más rápida o lenta. Cuando hay una respuesta hipersensible rápida, apenas se aprecia la necrosis de manera macroscópica y se dice que la planta es inmune (Niks et al., 2019).

1.5.4 Raza-especificidad

La resistencia no es solo específica entre especie de patógeno y especie de planta, sino también a ciertas razas de patógenos (Sharma y Bhattarai, 2019). Estas razas donde la resistencia es efectiva son llamadas avirulentas, mientras que aquellos genotipos del patógeno en la que no es efectiva se denominan virulentos (Nicolaides y Charmandari, 2021). Este tipo de resistencia suele corresponderse con la resistencia vertical y es debida a genes mayores, monogénica y sigue la relación gen a gen. Es bastante fuerte (muchas veces completa) y fácil de introducir por cruzamiento por su alta heredabilidad (Niks et al., 2019).

1.5.5 Durabilidad de la resistencia

Es un fenómeno muy común que las variedades que anteriormente eran resistentes se vuelvan susceptibles (Orellana-Torrejón et al., 2022). Las resistencias pueden dejar de funcionar debido a que el patógeno desarrolla mecanismos de adaptación que son consecuencia de una coevolución entra planta y patógeno (Wulff y Krattinger, 2022). El investigador británico Roy Johnson definió el concepto de durabilidad de una resistencia de la siguiente forma: “una variedad tiene resistencia durable cuando ha permanecido efectiva por un largo periodo de tiempo durante la cual ha sido empleada ampliamente en un ambiente propicio para el patógeno” (Johnson 1984). El tiempo medio de duración de la resistencia es variable y, a menudo, corto. Oscila entre 2 y 15 años dependiendo de varios factores, como el tipo de resistencia empleada o la diversidad de variedades en el campo de cultivo. Así, las resistencias en algunos trigos harineros frente a las royas duran de 1 a 6 años. Sin embargo, la resistencia en algunos cultivares de manzano frente al pulgón lanígero sigue siendo efectiva después de 130 años (Niks et al., 2019; Mapuranga et al., 2022). La resistencia vertical desparece con frecuencia cuando se siembra en grandes extensiones un único cultivo y una única variedad (monocultivo monovarietal), ya que cuanto mayor sea el contacto entre patógeno y planta (o cultivo) huésped, mayor será la probabilidad de aparición de nuevas razas virulentas, por lo que es aconsejable evitar la homogeneidad genética y el contacto permanente entre ambos (Bhavani et al., 2022). Por otro lado, la resistencia horizontal está presente en plantas seleccionadas por agricultores durante siglos y a causa de la naturaleza poligénica de la resistencia, no existe peligro de pérdida súbita, por lo que es la más duradera (Niks et al., 2019).

Podemos diferenciar entre durabilidad de la resistencia vertical y horizontal (Babu et al., 2020). La durabilidad de la resistencia vertical suele ser corta o efímera. La pérdida de la resistencia vertical es probable en el transcurso de un reducido número de años. Se puede prolongar la durabilidad si se utilizan los genes de resistencia siguiendo un plan

estratégico, eliminando los huéspedes alternativos y diversificando el uso de genes de resistencia en el espacio y en el tiempo (Podgornik et al., 2021). La resistencia horizontal (resistencia de campo) es durable y está presente en variedades seleccionadas por los agricultores durante siglos (Tomar et al., 2014; Otto et al., 2011). Si un patógeno desaparece por la presencia de un buen gen de resistencia vertical, se pueden perder sistemas poligénicos en la selección de líneas de un programa de mejora. Es lo que se conoce como 'efecto Vertifolia', cuyo nombre deriva de un cultivar de patata con resistencia horizontal al mildiu. Sus hojas permanecían verdes (de ahí su nombre) cuando una nueva raza de mildiu atacó a la mayoría de cultivares de patata que tenían genes de resistencia vertical no efectivo frente a esta raza (Martínez & Solís, 2014). Entonces, al aparecer una nueva raza del patógeno pueden producirse graves daños en el huésped (Sabouri et al.,2022).

1.6 Las royas del trigo

Existen alrededor de 7.000 especies de royas, que afectan a muchas especies de plantas, entre ellas cultivos como ciruelo, pino, habas, café, ajos, etc. (Duplessis et al., 2021). Existen tres especies de royas que afectan al trigo: la roya del tallo, la roya amarilla y la roya de la hoja (McIntosh et al., 1995). Estas han causado graves problemas a lo largo de la historia (Mapuranga et al., 2022). Las uredosporas de roya del tallo son las más antiguas que se han hallado y datan del 1.300 a.C. en Israel. En la antigua Roma y Grecia también había descripciones de royas del trigo, sobre todo roya del tallo (Roelfs et al., 1992).

Las royas son parásitos obligados que suelen penetrar por las estomas, siendo de infección localizada, y se manifiestan en forma de pequeñas pústulas pulverulentas o uredios, en todas las partes aéreas de la planta (Hovmoller et al., 2023). De las pústulas salen grandes cantidades de esporas (uredosporas) que aseguran la dispersión de la enfermedad de manera rápida (Figueroa et al., 2020). La primera persona que descubrió que la roya del trigo estaba causada por un hongo fue Felice Fontana en 1767. Sin embargo, no fue hasta el siglo XIX cuando se hizo distinción entre las royas del trigo (Boa, 2021). Las tres especies de royas del trigo son:

1.6.1 Roya amarilla (o lineal)

Organismo causal: *Puccinia striiformis* West f. sp. *tritici*. Los signos de esta enfermedad son pústulas o uredios de color amarillo-naranja, como se puede observar en la figura 1.4, ordenadas en bandas o estrías que le dan el epíteto específico a esta roya, y que pueden presentarse también en la cara interna de las glumas y en las vainas (Chen et al., 2014). Las pústulas teliosóricas constituidas por teliosporas oscuras tienen una tendencia a ocupar el haz de las hojas también en forma de estrías, y permanecen

recubiertas por tejidos epidérmicos durante mucho tiempo (Jin et al., 2010). Respecto a la epidemiología, el patógeno sobrevive como micelio y urediniosporas en más de 18 géneros de gramíneas, incluido, por supuesto, el trigo (Dammer et al., 2022). Las infecciones primarias son producidas por las uredosporas transportadas por el viento (Zadoks y Bouwman, 1985).

Figura 1.4 Plantas de trigo infectadas con roya amarilla. Variedad muy susceptible a la izquierda vs variedad con resistencia intermedia a la derecha.

De los tres patógenos de las royas del trigo, la roya amarilla es la que necesita temperaturas más bajas para desarrollarse (Ahmad et al., 2010). Las temperaturas mínima, óptima y máxima para la infección con este patógeno son respectivamente, 11, 15 y 23°C (Mboup et al., 2012). A menudo puede sobrevivir al invierno en forma activa en el trigo sembrado en el otoño (Ali et al., 2022). La mayoría de los estudios epidemiológicos sobre esta enfermedad se han efectuado en Europa. Son clásicos los estudios efectuados por J.C. Zadoks en la Universidad de Wageningen (Países Bajos) (Zadoks y Bouwman, 1985). Recientemente el Centro de Referencia Global de Royas de Dinamarca (GRRC) coordina diferentes estudios sobre roya amarilla a nivel mundial (GRRC, 2023).

En 2010, se descubrió que el agracejo es hospedante alterno de la roya amarilla del trigo, cuando hasta dicha fecha se creía que no tenía ninguno hospedante (Jin et al., 2010). Es necesario comprobar que el fenotipo de la virulencia es el mismo en ambos hospedantes, y que se traslada de la gramínea al trigo, durante el ciclo de cultivo (Roelfs et al., 1992; Ding et al., 2021).

1.6.2 Roya de la hoja (o parda)

Organismo causal: *Puccinia triticina* Eriks. Los signos de la roya de la hoja son pústulas de color pardo-rojizo subepidérmicas, como se observa en la figura 1.5. Los uredios o pústulas son de aproximadamente 2 mm de diámetro y contienen miles de uredosporas producidas por reproducción asexual o clonal (Omara et al., 2019). Se distribuyen irregularmente en el haz o envés de la hoja, pudiendo alcanzar las espigas y espiguillas, si la infección es suficientemente fuerte. Al final del ciclo del cultivo aparecen teliosoros de color negro, dispuestos al azar en el envés de las hojas y en las vainas (Mabrouk et al., 2019). Las pústulas se diferencian de las de la roya amarilla por su color más intenso y porque en este último caso la distribución es en líneas o en bandas en lugar de al azar (Zhao et al., 2023). Las condiciones propicias para la infección se relacionan con la existencia de un periodo crítico, el cual involucra una combinación de horas de mojado y una temperatura necesaria para que ocurra la infección. Por lo tanto, para que ocurra la misma, se necesitan días luminosos con una temperatura entre 15 y 22 °C y 4 horas de rocío mínimo. La transmisión es por el viento, que arrastra las uredosporas a grandes distancias, a veces cientos, e incluso miles de kilómetros (Rodríguez-Moreno et al., 2020).

En cuanto a su ciclo, a finales de temporada aparecen soros oscuros (telios o teliosoros). Se trata de la forma invernante, esporas bicelulares, rodeadas de una membrana espesa (Prasad et al., 2020). Germinan en primavera, infectan a las plantas huéspedes alternas (*Thalictrum* spp.), y de las pústulas de estas plantas, salen esporas que pueden volver a infectar al cereal, completando así su ciclo evolutivo (Ren et al., 2023). De todas formas, el hospedante alterno tiene poca importancia para esta roya y la propagación clonal (uredosporas producidas en uredinios que proceden a su vez de otras uredosporas) se hace por el viento a distancias considerables, como se han mencionado anteriormente (Kolmer, 2013).

Figura 1.5 Pústulas de roya de la hoja en cultivar susceptible.

Respecto a la epidemiología de la enfermedad, la mayoría de las epifitias graves se presentan cuando las infecciones son tempranas (Chen, 2020). Se suelen producir epifitias y pérdidas graves cuando la hoja bandera se infecta antes de la apertura de la flor (Yuldasheva et al., 2021). En Andalucía, las primeras pústulas de roya de la hoja aparecen, por lo general, a finales de marzo o principios de abril, y termina cuando las hojas más viejas infectadas mueren (a primeros de mayo). Una combinación de temperaturas favorables (en torno a 20ºC), un salto térmico día-noche corto y un periodo de rocío amplio (o presencia de niebla o lluvia suave) son condiciones adecuadas para el desarrollo de la roya de la hoja (Martínez-Moreno y Solís, 2019; Semagn et al., 2022). Cuando llueve durante el día, se producen algunas infecciones, pero con frecuencia, las temperaturas nocturnas limitan el número de infecciones (Leonova et al., 2020). Los uredinios de la roya de la hoja también pueden desarrollarse en primavera, a partir de infecciones producidas en el otoño o el invierno (inóculo endógeno). Suelen encontrarse en la parte baja del follaje, con las infecciones más antiguas en las hojas más bajas (Morgounov et al., 2020). La roya de la hoja que se desarrolla a partir del inóculo transportado por el aire (exógeno), comúnmente se presenta en las hojas de más arriba, que son las primeras en ser infectadas (Kolmer y Fajolu, 2022). Sobre esta base, generalmente se puede distinguir si el inóculo es local, o si ha sido transportado desde grandes distancias, debido a las mutaciones espontáneas que se dan al realizar la mitosis (Roelfs et al., 1992).

1.6.3 Roya del tallo (o negra)

Es una enfermedad causada por el hongo *Puccinia graminis* Pers. f. sp. *tritici* Eriks. & E. Henn. Los síntomas aparecen comúnmente en tallos y, en caso de ataques severos también afecta hojas y espigas (Singh et al., 2008). Las pústulas son más grandes que las de la roya amarilla y de la hoja, y al romper la epidermis, afloran masas pulverulentas de urediniosporas de color castaño rojizo oscuro, tal como se observa en la figura 1.6 (Patpour et al., 2022). En el haz y envés de las hojas se observan las pústulas negras o teliosoros con teliosporas que desarrollan al final del ciclo del cultivo (Radici et al., 2022). A diferencia de las otras royas, estos teliosoros aparecen descubiertos tempranamente, por rotura de la epidermis; laceran los tejidos del tallo, los que pueden tornarse quebradizos, determinando el volcado de las plantas (Singh et al., 2019). El momento de ataque es a partir de espigado (Sánchez-Espinosa et al., 2023). Las condiciones predisponentes son temperaturas altas (entre 20 y 30 °C) y mojado foliar de 6 a 8 horas (Omara et al., 2020). Debido a los modernos cultivares de trigos de primavera de ciclo corto, y a que necesita una elevada temperatura, aunque se han dado ocasiones de elevada infección, aún no está presente en España de forma común, aunque su presencia se había descrito a comienzos y mediados del siglo XX. Es un caso claro de escape (Martínez-Moreno et al., 2019). La transmisión, como en las otras especies de royas del trigo, es principalmente, por las uredosporas transportadas por el viento a grandes distancias, desde zonas con producción de trigo más temprana (Roelfs et al., 1992).

Figura 1.6 Pústulas de roya el tallo en cultivar susceptible.

1.7 Problemas causados por la roya en el trigo, y búsqueda de genes de resistencia

Las royas provocan en las plantas de trigo una perturbación en la asimilación de nutrientes, y modifican el metabolismo general de la planta, acentuando notablemente la respiración, lo que aumenta el metabolismo y el consumo de nutrientes (Wellings, 2011). El crecimiento de la planta resulta afectado, y baja el rendimiento de la misma, dándose casos de pérdida casi total de la producción en casos extremos de infección y condiciones climáticas propicias (Soko et al., 2018). Otro gran problema de las royas es su fácil dispersión, ya que, gracias al fácil transporte de sus esporas por el viento, pueden infectar cultivos sembrados a kilómetros de distancia (Roelfs et al., 1992). En concreto, la producción de trigo a nivel mundial se ve mermada en un 3,25% por la roya de la hoja, unos 25 Mt de pérdidas anuales, un 2,08% por la roya amarilla, unos 16 Mt de pérdidas y un 0,90% por la roya del tallo, unos 7 Mt de pérdida. La roya de la hoja es la enfermedad que más merma la producción de trigo a nivel mundial, la roya amarilla es la cuarta y la roya del tallo, la décima (Savary et al., 2019). De aquí la importancia para buscar genes de resistencia contra las royas, en las variedades comerciales de trigo, pudiendo ser genes que dotan a la variedad una resistencia completa a la roya de la hoja, como se puede observar en la figura 1.7a, o genes que provocan una resistencia incompleta, como se ve en la figura 1.7b), con la característica necrosis rodeando las pústulas, típico de las resistencias hipersensibles (Martínez y Solís, 2019). En la figura 1.7c, el cultivar no muestra ningún síntoma de resistencia, por lo ese cultivar no tiene ningún gen de resistencia o en el caso de que lo tenga es completamente inefectivo para esa raza de roya.

Figura 1.7 Tipos de resistencia de diferentes cultivares de trigo a roya parda: a, Resistencia completa; b, Resistencia incompleta; c, Ningún tipo de resistencia

Tradicionalmente se buscaban genes de resistencia en el centro de origen de la especie cultivada y especies emparentadas, por la coexistencia de huésped y parásito, pero existen muchas excepciones (Gultyaeva et al., 2021). Debemos buscar genes de resistencia en regiones de coexistencia, sean centros de origen o no, y en todo tipo de material, desde cultivares de otros países, variedades locales, parientes silvestres y especies relacionadas (Riaz y Wong, 2017). Jack Harlan explicaba con este ejemplo el potencial de los recursos fitogenéticos en la búsqueda de resistencias: "En el este de Turquía recogí un trigo que se nombró como PI178383. Es un trigo de aspecto miserable, alto, delgado, que se encama, es susceptible a la roya de la hoja, no resiste el frío, y por tanto difícil de vernalizar, y tiene una pésima calidad panadera. Es lógico que nadie le prestara atención durante 15 años. De repente, apareció la roya amarilla en los estados del noroeste (de los Estados Unidos) y PI178383 resultó ser resistente a 4 razas de roya amarilla, a 35 razas de carbón y buena tolerancia a varias podredumbres. Las nuevas variedades con PI178383 en sus programas de mejora están ahorrando millones de dólares de pérdidas cada año". Ese gen de resistencia a la roya amarilla era el *Yr10*, que sigue siendo eficaz frente a la mayoría de razas encontradas en el mundo. El CIMMYT y otros

organismos de investigación están apostando por el uso de genes con efecto pleiotrópico, es decir, que son resistentes a varias especies de royas u otras enfermedades. Son muy escasos, aunque un ejemplo es el gen *Lr37*, que a su vez es *Yr17* y *Sr38* (Gultyaeva et al., 2023). Gracias a la ingeniería genética se pueden introducir genes de resistencia en nuestro cultivo procedentes de cualquier organismo vivo (Shrawat y Armstrong, 2018). Una idea para conseguir variedades resistentes a la roya mediante ingeniería genética sería la construcción de cassettes multigenéticos que se diseñan poniendo juntos los fragmentos de ADN correspondientes a 5-7 genes de resistencia a una, dos o tres de las royas del trigo. Como ejemplo, el CSIRO (Australia) ha creado un ejemplo de multicassette donde están los siguientes genes: *Sr45*, *Lr67*, *Sr50*, *Sr35* y *Sr22*, como se observa en la figura 1.8, que segregarían como un único gen simplificando su selección (Luo et al., 2021).

Actualmente todos los recursos fitogenéticos están almacenados en bancos de germoplasma o en otras colecciones *in situ* (Priyanka et al., 2021). En el caso del trigo, se conservan miles de entradas en varios bancos de germoplasma repartidos por todo el mundo; destacando el que posee el CIMMYT en Méjico, o el Svalvard Global Seed Vault de Noruega (Sansaloni et al., 2020). En España, tenemos el que posee el CRF (Centro Nacional de Recursos Fitogenéticos) en la finca La Canaleja, donde la colección nacional de variedades locales de trigo ha sido caracterizada fenotípica y genotípicamente (Alcalá de Henares, Madrid) (Pascual et al., 2020).

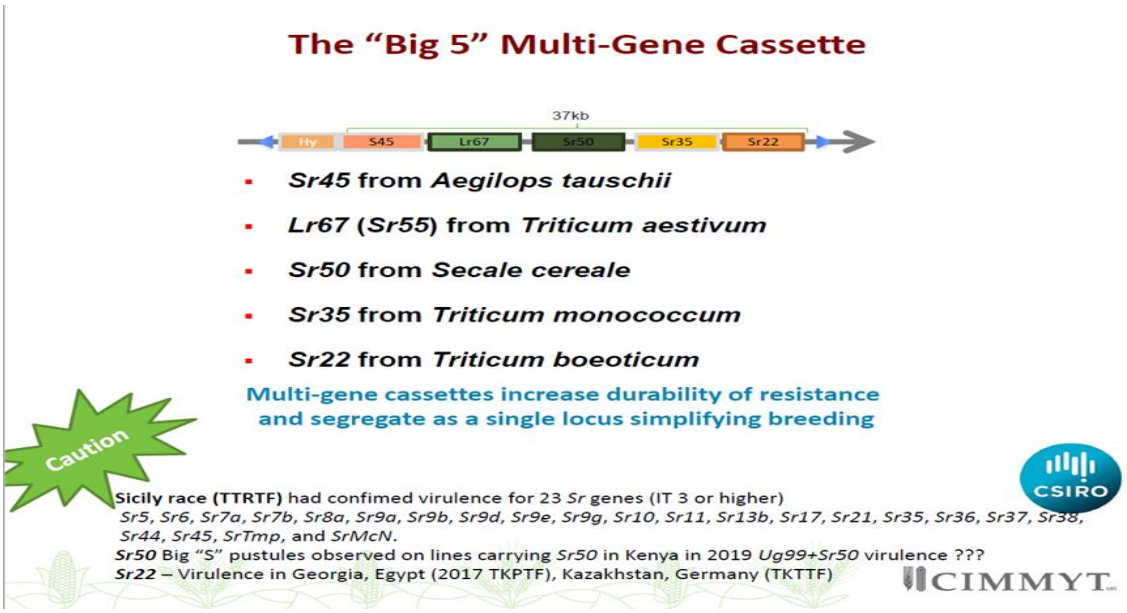

Figura 1.8 Cassette de cinco genes de resistencia a roya del tallo que está investigando el CSIRO (Australia) para introducirlo en sus nuevas líneas avanzadas (Luo et al., 2021).

1.8 Formas de control de las royas en trigo

Una de las formas más efectivas para el control de las tres royas del trigo es la resistencia genética (Niks et al., 2019). Proteger los trigos frente a las royas es uno de los objetivos principales de las empresas de mejora y de organismos internacionales de mejora como el CIMMYT. En sus ensayos, se ha comprobado que, si ataca con virulencia, y en condiciones climáticas favorables, estas pueden llegar a mermar casi el 100% de la producción, y superar el 50% de merma, en bastantes ocasiones (Roelfs et al., 1992; Herrera-Foessel, et al., 2007).

La mayor parte de las resistencias a las royas provenían de un solo gen, es decir resistencia monogénica; pero el desarrollo continuo de razas virulentas como Ug99 en 1999, en roya del tallo, BBG/BN en roya de la hoja de trigo duro en 2001, o la raza Warrior en 2010, en roya amarilla (que provocaban la pérdida de más del 50% del material vegetal de una empresa de mejora por susceptibilidad), ha hecho replantearse el problema (Huerta-Espino et al., 2022). Es entonces cuando se planteó introducir varios genes de resistencia para cada variedad, incluyendo genes de resistencia parcial u horizontal (Singh et al., 2011). Por ejemplo, cuando en 2008, (en Méjico), una raza de roya de la hoja mutó y afectó al cultivar de trigo duro Jupare, que tenía los genes *Lr27+Lr31*, solo se perdió un 20% de las líneas del programa de mejora de trigos duros del CIMMYT por su susceptibilidad a roya de la hoja, porque hubo varias líneas independientes de mejora con genes de resistencia distintos (Huerta-Espino et al., 2009). Durante 2017 hubo otra mutación de la roya de la hoja en Méjico que generó una virulencia que afectó a la variedad Cirno C2008 que tiene el gen *LrCam.* Sin embargo, solo se perdió un 5% de las líneas avanzadas del programa de trigo duro del CIMMYT (Huerta-Espino et al., 2023). Estos hechos, recalcan la importancia de sacar variedades con resistencia poligénica, y con genes de resistencia diferentes entre unas variedades y otras (Singh y Bowden, 2011). Por ello, actualmente se están empleando genes de resistencia horizontal o parcial como los genes *Lr34, Lr46, Lr67* o *Lr68* para roya de la hoja; *Sr2* para roya del tallo e *Yr18* para la roya amarilla. Estos genes siguen siendo efectivos frente a las otras royas (efecto pleiotrópico), por lo que son todavía más deseables (Ellis et al., 2014; Bhavani et al., 2019).

Una forma de facilitar la introducción de diferentes genes de resistencia (o piramidación), en las diferentes variedades, es mediante la ayuda de marcadores moleculares. Todos los genes de resistencia de interés llevan asociado uno o varios marcadores de ADN, que permiten la identificación de los individuos que porten ese gen (Gupta et al., 2006). De esta forma, es relativamente fácil la introducción de dichos genes de resistencia, prolongando el periodo de resistencia a la roya durante varios años (Haider et al., 2023). Un gen muy importante para trigo duro, en roya de la hoja, era *Lr14a*, pero dicho gen fue vencido en España por una nueva raza en 2013 (Soleiman et al., 2016). Los estudios genéticos son muy costosos, pero necesarios a la hora de desarrollar y comprobar los genes de resistencia efectivos para la roya. Se necesita unos 3-4 años entre desarrollo de poblaciones, evaluación, mapa genético, etc., para descubrir y caracterizar los genes de resistencia a las royas del trigo (Yadav et al., 2022).

La roya amarilla, históricamente, afectaba más a trigo harinero que a trigo duro (Martínez-Moreno y Solís, 2019). No obstante, en los últimos años, ha afectado a varios cultivares de trigo duro. En realidad, siempre han sido susceptibles a roya amarilla, pero esta roya solía aparecer en zonas más frías donde se cultivaba principalmente trigo harinero facultativo o de invierno, pero últimamente existen razas de roya amarilla que se adaptan mejor a zonas más cálidas, donde se cultiva trigo duro, de ahí la infección de estos (Chen et al., 2014). Por tanto, debemos de explorar material nuevo, como el que tiene CIMMYT para combatirla con efectividad (Lin et al., 2018). Un dato a tener en cuenta es que, de 2014 a 2016, con la aparición de una nueva raza de roya amarilla, se pasó de un 99% a un 85% de variedades resistentes, en el material avanzado de trigo duro del CIMMYT (Lin et al., 2018). Este hecho, nos alerta del problema potencial que puede suponer la roya amarilla en trigos duros.

Otra roya, que puede suponer un problema en el futuro cercano en España, es la roya del tallo (Patpour et al., 2022). Está en expansión en muchos lugares del mundo, como Turquía o en el este de África, y con razas diferentes muy agresivas como la raza siciliana o la familia de la Ug99 (Salcedo et al., 2017; Patpour et al., 2022). En España, cada vez es más frecuente, sobre todo, en la provincia de Cádiz (Olivera et al., 2022).

Es muy importante, determinar la herencia y la base genética de la resistencia (Niks et al., 2019). Estos estudios ya están en curso en el CIMMYT, y los avances de mejora de resistencia a la roya están avanzando a pasos agigantados, gracias, en parte, al apoyo económico de muchas instituciones (Huerta-Espino et al., 2023). Pero cuando la resistencia genética no es suficiente, bien por una nueva raza muy virulenta de la que no se disponen aún genes de resistencia, o bien porque las condiciones climáticas son excesivamente favorables para la aparición de la roya, por ejemplo, en fincas con riego de apoyo; la alternativa es el control químico, y la importancia de una detección precoz de la enfermedad es fundamental para atajar el problema desde su inicio (Khosrokhani y Nasr, 2022). Es por ello que el uso de nuevas tecnologías como la teledetección o *remote sensing* está jugando un papel muy importante en los últimos años como alternativa a la detección visual por parte del técnico (Khanal et al., 2020).

1.9 Introducción general al uso de sensores remotos para la detección de enfermedades en trigo

La detección remota se basa en el principio de que siempre existe una interacción entre la radiación electromagnética (luz) y un objeto (Taddia et al., 2015). Los objetos absorben, reflejan, dispersan, transmiten o refractan la radiación. Los objetos reflejan la radiación que puede ser captada por diferentes tipos de sensores (Sadeghipoor, 2015). Este tipo de sensores detectan las longitudes de onda reflejadas y los ordenadores las transforman en datos (Weiss et al., 2020). Esto hace posible recopilar información más allá de las imágenes. Principalmente se pueden subdividir en dos tipos de sensores: pasivos y activos (Amiridis et al., 2009).

- **Sensores pasivos**: registra la energía natural que se refleja o emite desde la superficie de la Tierra. La fuente de radiación más común detectada por sensores pasivos es la luz solar reflejada. Un ejemplo de sensor pasivo es una cámara con el flash apagado (Rasti et al., 2021).
- **Sensores activos**: proporcionan su propia fuente de energía, como un láser o radiación electromagnética de microondas, para iluminar los objetos que observan. Un sensor activo puede funcionar día y noche emitiendo radiación en la dirección del objetivo que se va a investigar. Un ejemplo de sensor activo es una cámara con el flash encendido (Zhu et al., 2018).

En parte, la gran utilidad de estos sensores remotos, algunos de ellos observados en la figura 1.9, es debido a que no son estáticos, y se pueden implementar en drones, aviones y otro tipo de plataformas tanto aéreas como terrestres, cubriendo gran superficie en poco tiempo, ahorrando tiempo y esfuerzo a los técnicos (Dabove et al., 2014). Además, pueden ir varios tipos diferentes de sensores remotos montados en una misma máquina, lo que hace que puedan trabajar de forma complementaria (Meivel y Maheswari, 2021).

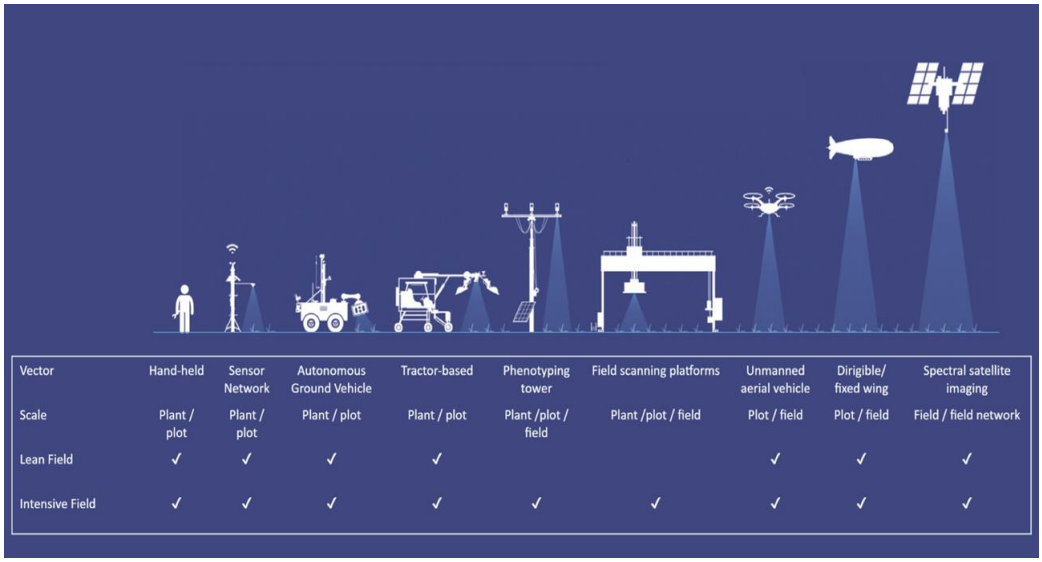

Figura 1.9 Sensores remotos. Descripción general de las plataformas de fenotipado de campo. Los enfoques de fenotipado operan en una variedad de escalas físicas (Shakoor et al., 2017).

1.10 Detección de roya en trigo utilizando sensores remotos

La pérdida de producción de trigo inducida por las royas es enorme cada año a nivel mundial (un 6,2% de la producción mundial) (Savary et al., 2019; Kiani et al., 2021). La detección temprana de la roya del trigo mejoraría el rendimiento del trigo y sus características de calidad (Khosrokhani y Nasr, 2022).

Actualmente, los métodos utilizados para la detección de esta enfermedad son las observaciones visuales de los síntomas en la planta, complementándose con el uso de escalas o claves pictográficas, que relacionan diferentes grados de severidad con el porcentaje del tejido ocupado por las pústulas que provoca la roya en las hojas (Sauceda-Acosta et al., 2015). La evaluación visual de los síntomas es el método más utilizado debido a su sencillez, rapidez y bajo costo (Navarro y Arauz, 1999), pero tiene limitaciones en cuanto a repetitividad, confiabilidad y precisión (Bade y Carmona, 2011). Debido a estas limitaciones, en los últimos años se han ido desarrollando numerosos trabajos basados en el uso de la teledetección, como fuente de obtención de datos, con el objetivo de analizar la información obtenida y elaborar modelos de predicción que permitan conocer, de manera anticipada, la producción esperada o la incidencia de una enfermedad en el cultivo, gracias a que son capaces de obtener información del cultivo a distancia y de manera no destructiva (Araus, 2014; Jing et al., 2022). Un ejemplo, es la plataforma de detección de enfermedades (principalmente royas), con sensor LiDAR incorporado, que se muestra en la figura 1.10. Utilizada en los ensayos de la empresa Agrovegetal, en la localidad de Escacena del Campo (Huelva) (Pérez-Ruiz et al., 2020).

Figura 1.10 Plataforma de detección de enfermedades con sensor LiDAR incorporado.

Estas tecnologías han sido objeto de estudio con el fin de ayudar en la toma de decisiones, evaluar el estado sanitario del cultivo, las etapas de crecimiento o las necesidades nutricionales, así como elaborar modelos de predicción que permitan conocer la producción y el rendimiento esperado o la detección temprana de una enfermedad (Ruan et al., 2022). Para este último caso, estas tecnologías resultan esenciales, ya que tienen potencial para detectar la enfermedad antes de que aparezcan los síntomas visuales en el cultivo (Thirugnana et al., 2022). Esa predicción temprana permite un manejo óptimo de la enfermedad, ya que cuando se visualizan los síntomas, el daño al cultivo ya se ha producido (Balasundram, 2019).

1.11 Sensores LiDAR

1.11.1 Fundamentos de los sensores LiDAR

El LiDAR (Detección y Medición de Distancias por Luz) es una técnica avanzada de teledetección óptica, que emplea luz láser para obtener una muestra densa y detallada de la superficie terrestre, resultando en mediciones exactas en las coordenadas x, y, z (Bates et al., 2021). LiDAR genera conjuntos de datos masivos de nubes de puntos, los cuales pueden ser gestionados, visualizados, analizados y compartidos eficientemente (Heinzler et al., 2019). Este sensor óptico activo emite rayos láser hacia un objetivo, mientras se desplaza a lo largo de rutas topográficas predeterminadas (Lee et al., 2020). Los receptores situados en el sensor captan el reflejo del láser en el objetivo y proceden a su análisis (Bates et al., 2021). Estos receptores registran con precisión el tiempo transcurrido desde la emisión del pulso láser hasta su retorno, lo que permite calcular la distancia exacta entre el sensor y el objetivo (Guo et al., 2019). Al combinar esta información con los datos posicionales proporcionados por el GPS (Sistema de Posicionamiento Global) y el INS (Sistema de Navegación por Inercia), las medidas de distancia se convierten en coordenadas tridimensionales precisas del objeto reflectante en el espacio (Patoliya et al., 2022).

Los componentes de hardware principales de un sistema Lidar incluyen un vehículo de recolección (avión, helicóptero, dron, plataforma de fenotipado, etc.), sistema de escáner láser, GPS e INS (Ramezani et al 2020). Un sistema INS mide la rotación, inclinación y encabezamiento del sistema LiDAR. Los datos, (que son nubes de puntos), se procesan posteriormente después de que la recopilación de los mismos se reconozca dentro de las coordenadas x, y, z, georreferenciadas con alta precisión al analizar el rango de tiempo láser, ángulo de escaneo láser, posición del GPS e información del INS (Patoliya et al., 2019).

1.11.2 Uso de sensor LIDAR en agricultura y detección de enfermedades

En agricultura, los sensores láser, donde se encuentran los sensores LiDAR, son ejemplos de tecnologías intensivas en información, que se utilizan para adquirir rasgos fenotípicos de la estructura de las plantas, siendo una alternativa muy utilizada en agricultura de precisión, como podemos observar en la figura 1.11 (Jiménez-Berni et al., 2018). Los sistemas LiDAR tienen muchas aplicaciones importantes en este contexto, que van desde la reconstrucción 3D de cultivos (Martínez-Guanter et al., 2017), pasando por la navegación asistida de vehículos agrícolas.

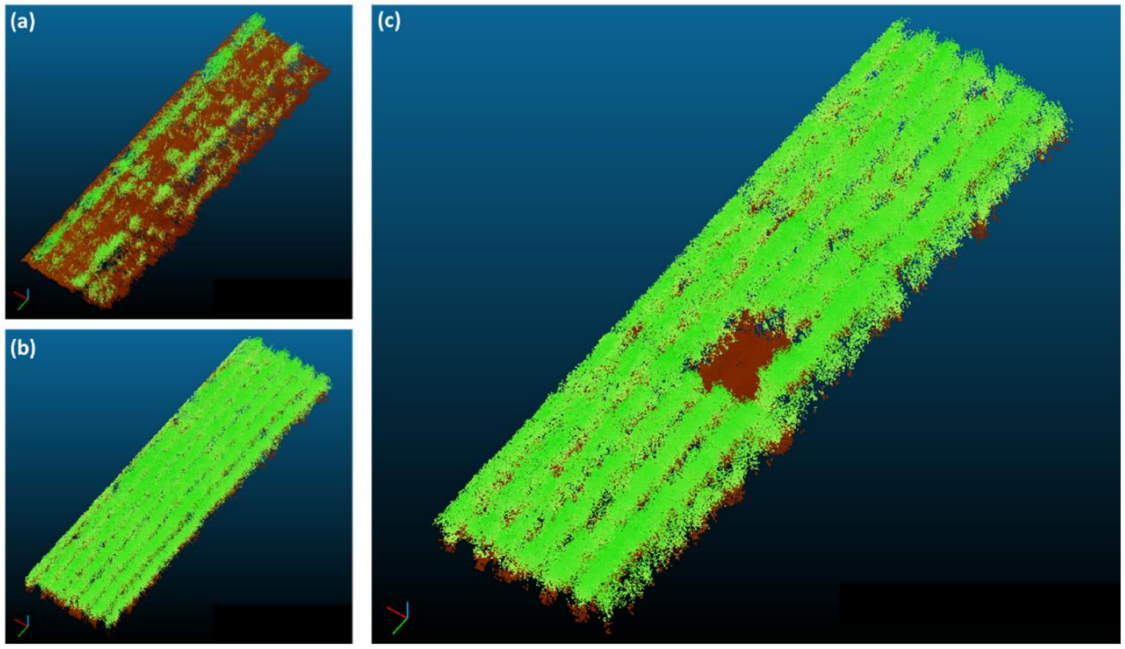

Figura 1.11 Uso de sensores LiDAR, reconstrucción 3D de parcelas de trigo, (a) parcelas como mala nacencia, (b) parcelas con muy buena nacencia, y (c) parcelas con buena nacencia, pero con 'calvas' internas (Jiménez-Berni et al., 2018).

La tecnología LiDAR es vital para la teledetección de enfermedades en los cultivos, ya que ayuda a su detección temprana, la gestión de recursos y las prácticas respetuosas con el medio ambiente (Abdullah et al., 2023). Los avances recientes en la tecnología de teledetección y el procesamiento de datos han convertido a los sensores LiDAR, instalados en vehículos aéreos o terrestres no tripulados, en herramientas valiosas para obtener datos detallados sobre enfermedades de las plantas con alta resolución espacial, temporal y espectral (Kouadio et al., 2023). Ejemplos de ellos son la detección de *Xylella fastidiosa* en olivar (Cubero et al., 2019), o la detección de *Botrytis cinerea* en el cultivo de la fresa (Bélanger et al., 2011).

1.12 Sensores espectrales

1.12.1 Sensores espectrales

Los sensores espectrales representan una herramienta vital en la captura y análisis de información del espectro electromagnético, teniendo aplicaciones en una diversidad de campos que van desde la observación terrestre y la investigación científica hasta la industria y la medicina (Liu et al., 2020), y también, sirven para detectar enfermedades foliares en superficies foliares. Estos dispositivos están diseñados para ser sensibles a longitudes de onda específicas, permitiéndoles registrar detalles precisos sobre un objeto o fenómeno en estudio (Sagan et al., 2020). Su capacidad para detectar energía electromagnética en diferentes partes del espectro, incluyendo las regiones ultravioleta, visible e infrarroja, los hace indispensables en la teledetección (Bian et al., 2022). Aquí,

sensores montados en satélites o aviones capturan la luz reflejada o emitida por la Tierra para estudiar y analizar sus características. Además, su utilidad se extiende a laboratorios para el análisis de materiales, en la medicina, para técnicas de diagnóstico por imagen y en la industria, para el control de calidad (Castro-Valdecantos et al., 2022).

En el contexto de la agricultura y la detección de enfermedades, los índices espectrales emergen como una herramienta clave para la interpretación de los datos capturados por los sensores espectrales (Pérez-Ruiz et al., 2020). En este sentido, numerosos investigadores han estudiado varios índices espectrales de vegetación, los cuales están compuestos por una combinación de bandas espectrales registradas por un sensor, para detectar diferentes enfermedades y estreses en plantas y árboles (Castro-Valdecantos et al., 2022). Cada banda espectral está caracterizada por una longitud de onda, pudiendo estas agruparse en regiones espectrales (Apolo-Apolo et al., 2020). El rango (rango espectral), es el intervalo de longitudes de onda que debe tener la luz para ser procesada por un sensor; cuanto más alto sea el valor, más clara y detallada será la fuente de la imagen (Apolo-Apolo et al., 2020).

Para determinar estos índices espectrales de vegetación, se debe determinar la reflectancia obtenida para cada longitud de onda (Egea et al., 2017). La reflectancia de una superficie se define físicamente como el cociente entre la radiación reflejada y la potencia total recibida por la misma, al ser siempre la radiación reflejada menor que la recibida, la reflectancia tendrá valores comprendidos entre 0 y 1 (Chacon-Iznaga et., al 2019). La representación de la reflectancia para cada longitud de onda da lugar a la firma espectral o curva de reflectancia espectral (Bagnato et al., 2012).

1.12.2 Sensores hiperespectrales

1.12.2.1 Firma espectral

Cada tipo de superficie interactúa con la radiación solar de manera diferente, absorbiendo unas longitudes de onda muy concretas y reflejando otras diferentes en unas proporciones determinadas (Ferreira et al., 2020). Esta característica hace posible que se puedan identificar los distintos objetos: suelo, vegetación, aguas, etc., ya que, mediante experimentos en laboratorio, se ha podido caracterizar el comportamiento de estas distintas superficies al recibir radiación, y cuantificar los porcentajes de reflexión, absorción y transmisión. A este comportamiento concreto de cada tipo de objeto es a lo que se llama firma espectral (Ochsendorf et al., 2011). Cuando hay alteraciones en el sistema, por ejemplo, la irrupción de una enfermedad foliar, como es la roya, la firma espectral varía entre plantas sanas y plantas infectadas, y también entre plantas resistentes y susceptibles, como podemos ver en la figura 1.12 (Apolo-Apolo et al., 2019).

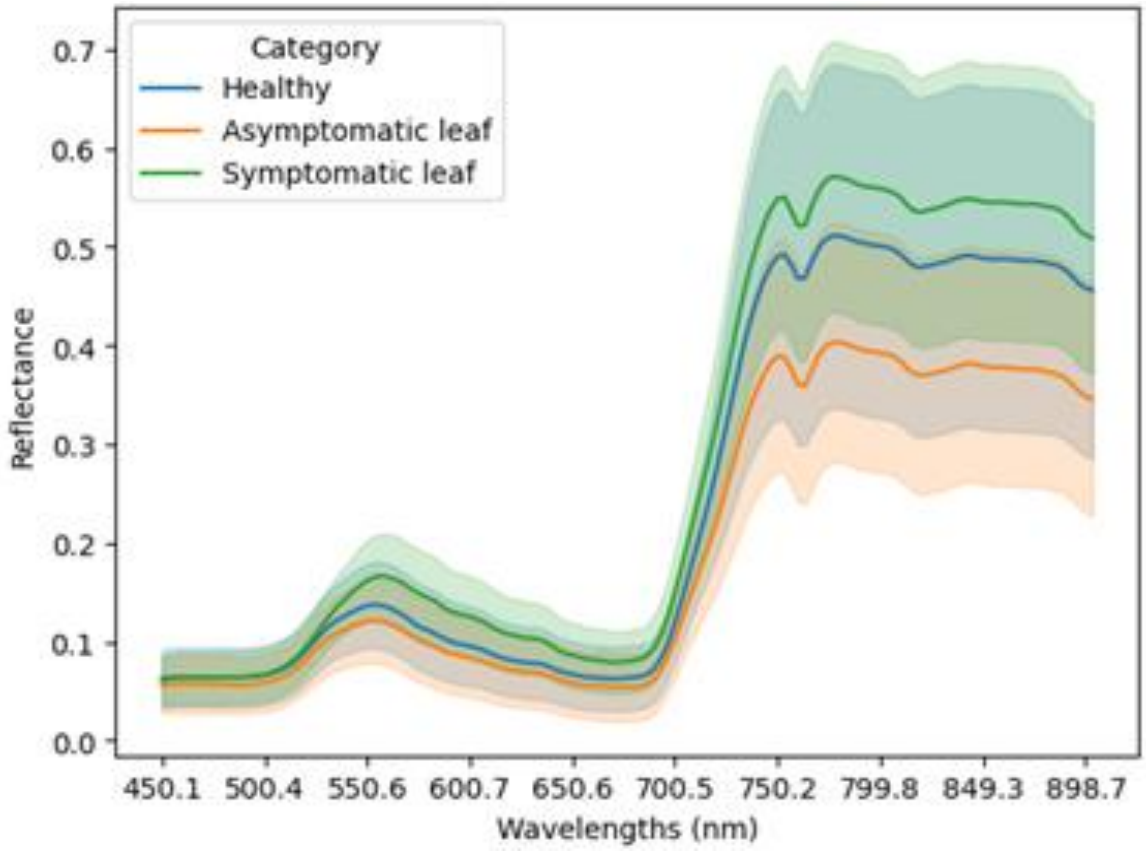

Figura 1.12 Valores medios de reflectancia y desviación estándar en plantas de trigo harinero, inoculadas y no inoculadas con roya amarilla. Azul (no inoculadas), verde (variedades susceptibles) y naranja (variedades resistentes) (Apolo-Apolo et al., 2019).

1.12.2.2 Cámaras hiperespectrales y espectroradiómetros

Las cámaras hiperespectrales son un tipo de cámaras que generan imágenes con mucha más información que otro tipo de dispositivos de captura. Están equipadas con una serie de sensores capaces de percibir centenares de longitudes de onda, dentro y fuera del espectro visible y, como consecuencia, la imagen lograda es mucho más precisa (Camacho Velasco et al., 2016). En su origen, estas cámaras se utilizaban en satélites y aviones para caracterizar la superficie de la tierra, pero hoy en día, su uso se ha extendido y popularizado en otros sectores, como la agricultura (Camacho Velasco et al., 2016). En la figura 1.13, podemos ver de forma esquemática y resumida, cómo funcionan este tipo de cámaras y cómo analizan hojas de trigo infectadas con roya (Yao et al., 2019).

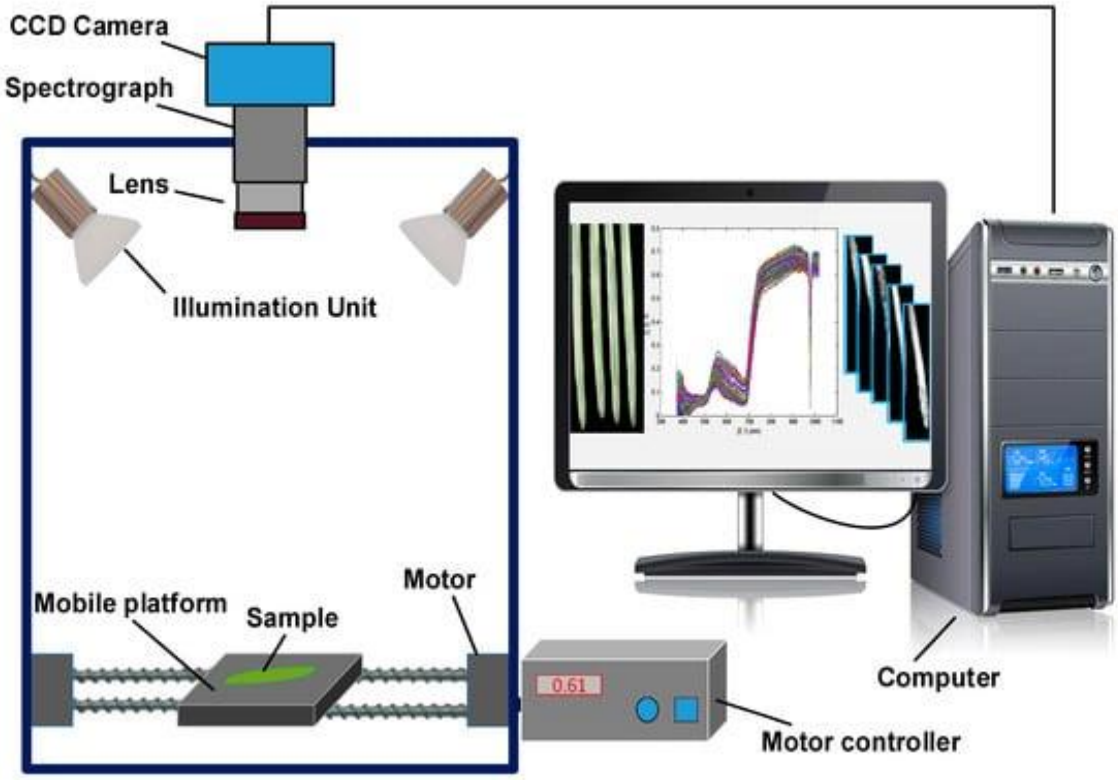

Figura 1.13 Funcionamiento de las cámaras hiperespectrales, analizando hojas de trigo infectadas con roya (Yao et al., 2019).

Por cada píxel de una imagen, una cámara hiperespectral recopila el espectro de radiación electromagnética en cientos de bandas estrechas de longitud de onda (Pérez-Ruiz et al., 2011). Como cada banda puede tener menos de 10 nm de ancho, el espectro parece ser continuo (Appeltans et al., 2021). El rango del espectro se extiende desde el ultravioleta (350nm) hasta el infrarrojo (2500nm), y diferentes técnicas hiperespectrales y/o sensores operan solo en ciertas partes del mismo (Appeltans et al., 2021). Para tener una idea del amplio espectro que tienen las cámaras hiperespectrales, la región del espectro visible está comprendida entre 400 y 700nm, y la región del infrarojo cercano NIR, entre 700 y 1100nm (Xu et al., 2021).

Un espectroradiómetro es un dispositivo para medir la radiación espectral o irradiación a través de varios rangos espectrales (la radiación espectral de un espectro de longitud de onda que se mide en Vatios por metro cuadrado por nanómetro ($W \cdot m^{-2} \cdot nm^{-1}$)) (González-Morales et al., 2020). Los equipos espectroradiómetros poseen un sistema de medición óptica objetiva, capaz de medir luz desde aproximadamente 380 a 780nm (Soylak et al.,2020).

1.13 Detección de roya en trigo utilizando información espectral

Los síntomas de la enfermedad producen una alteración en la composición de los pigmentos y la estructura de la planta. Algunos trabajos como el realizado por Oehler et al. (2008), demuestran que el contenido en pigmentos como la clorofila, siguen una tendencia decreciente a medida que aumenta la severidad de la enfermedad. De igual manera se muestra la modificación que sufre en su respuesta espectral los carotenos al depender de la concentración de clorofila, de manera que el incremento en la respuesta espectral de los carotenos indica una reducción en la concentración de clorofila (Khosrokhani et al., 2022).

Este cambio en la proporción de los pigmentos va acentuándose con el tiempo y se ve reflejado en la firma espectral del tejido, lo que constituye la base para una detección eficaz de la enfermedad. Así mismo, existen determinadas regiones espectrales cuya reflectancia es más sensible a estas variaciones (Devadas et al., 2009).

En los últimos años, se han realizado numerosos análisis para comprobar la efectividad de diferentes índices espectrales de vegetación, en la detección especifica de la roya en el cultivo del trigo, así como la diferenciación entre diferentes tipos de royas, basándose en los cambios producidos en el equilibrio de la composición de los pigmentos. Algunos trabajos, como el realizado por Devadas et al. (2009) o por Zheng et al. (2019), han puesto de manifiesto la capacidad de algunos índices, como el índice de reflectancia de antocianina (ARI), para discriminar entre hojas sanas de enfermas por roya, en una etapa de crecimiento medio-tardío, el índice de absorción de clorofila transformada en reflectancia (TCARI), para detectar roya de la hoja, o el índice de radiación fotosintética (PRI), para etapas de crecimiento tempranas-medias (Furbank et al., 2021). Sin embargo, hasta el momento, ningún índice espectral ha logrado diferenciar entre los diferentes tipos de roya del trigo, ya sea en una etapa temprana o tardía, aunque se ha determinado que los cambios en la combinación de pigmentos con el desarrollo de los síntomas y la degradación de la clorofila podría ser clave (Zheng et al., 2019). Además, al trabajar en condiciones de campo, una fuerte influencia de otros parámetros como el estado nutricional y fisiológico de la planta que, a su vez, puede verse influenciado por la fertilidad y humedad del suelo, la fecha de siembra o la densidad de plantación, pueden afectar a los datos (Furbank et al., 2011). Debido a la fuerte influencia del entorno, surge el requerimiento adicional de desarrollar modelos de predicción específicos para entornos locales que se adapten a sus condiciones (Apolo-Apolo et al., 2020).

A pesar de estas dificultades, trabajos como el realizado por Ashourloo et al. (2014) han logrado formular un índice de severidad de la enfermedad de la roya de la hoja (LRDSI), obteniendo precisiones en la estimación de la gravedad de la enfermedad superiores al 85%. No obstante, dicho índice sigue presentando limitaciones para estimar la enfermedad en los síntomas iniciales por su similitud espectral, entre áreas afectadas y áreas sanas (Mapuranga et al., 2022).

Los índices espectrales constituyen el elemento base para muchas aplicaciones de la teledetección en el manejo de cultivos, esto es debido a que están relacionados con

variables bioquímicas y biofísicas de los cultivos (Martínez-Guanter er al., 2019). El contenido de pigmentos y el cambio en la estructura de la planta provocados por la enfermedad son parámetros útiles para su detección, por lo que gran parte de los índices a calcular serán específicos para un pigmento o estarán relacionados directamente con parámetros fisiológicos (Apolo-Apolo et al., 2019). Así mismo, se han incluido también índices específicos para la detección de roya (LRDSI) (Paz Pellat et al., 2015). Como por ejemplo el indicado por (Yao et al., 2019), que se indica en la figura 1.14, que consiste en la distribución de la clorofila en hojas de trigo durante los días posteriores a la inoculación de las plantas con roya.

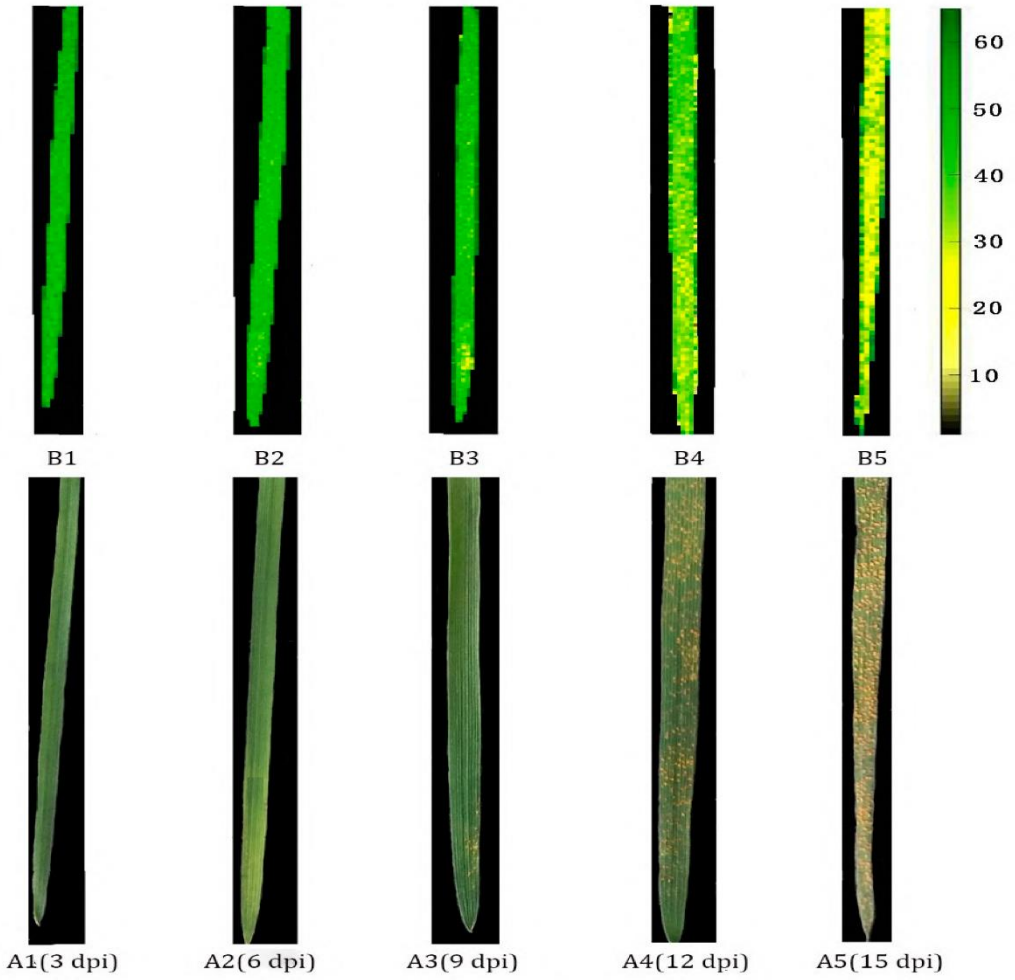

Figura 1.14 Distribución de clorofila en hojas de trigo durante los diferentes días posteriores a la inoculación (Yao et al., 2019).

1.14 Uso práctico para técnicos y agricultores

La roya (de la hoja, amarilla o del tallo), es una enfermedad fúngica que se empieza a desarrollar en rodales de enfermedad, y poco a poco comienza a infectar toda la finca y colindantes (Zhang et al., 2019).

Gracias al desarrollo de estas herramientas, incorporadas en drones, como el que se observa en la figura 1.15a, realizando vuelos periódicos sobre grandes extensiones de cultivo, se puede detectar en campo la enfermedad en su inicio, mucho antes de que el técnico la pueda observar a simple vista (cuando salen las pústulas visibles, la enfermedad ya está desarrollada) (Pérez-Ruiz et al., 2018). Esto permite que los técnicos puedan actuar con rapidez y con precisión, ya que solo sería necesario realizar tratamientos fúngicos en los pequeños rodales donde se esté iniciando la enfermedad, ahorrando así tiempo y dinero (Chavarro et al., 2023). Esta herramienta es una más, dentro del amplio mundo que nos abre la monitorización y digitalización de las parcelas (figura 1.15b) y (figura 1.15c), haciendo los cultivos más rentables y con mayor proyección de futuro (Ozdogan et al., 2017).

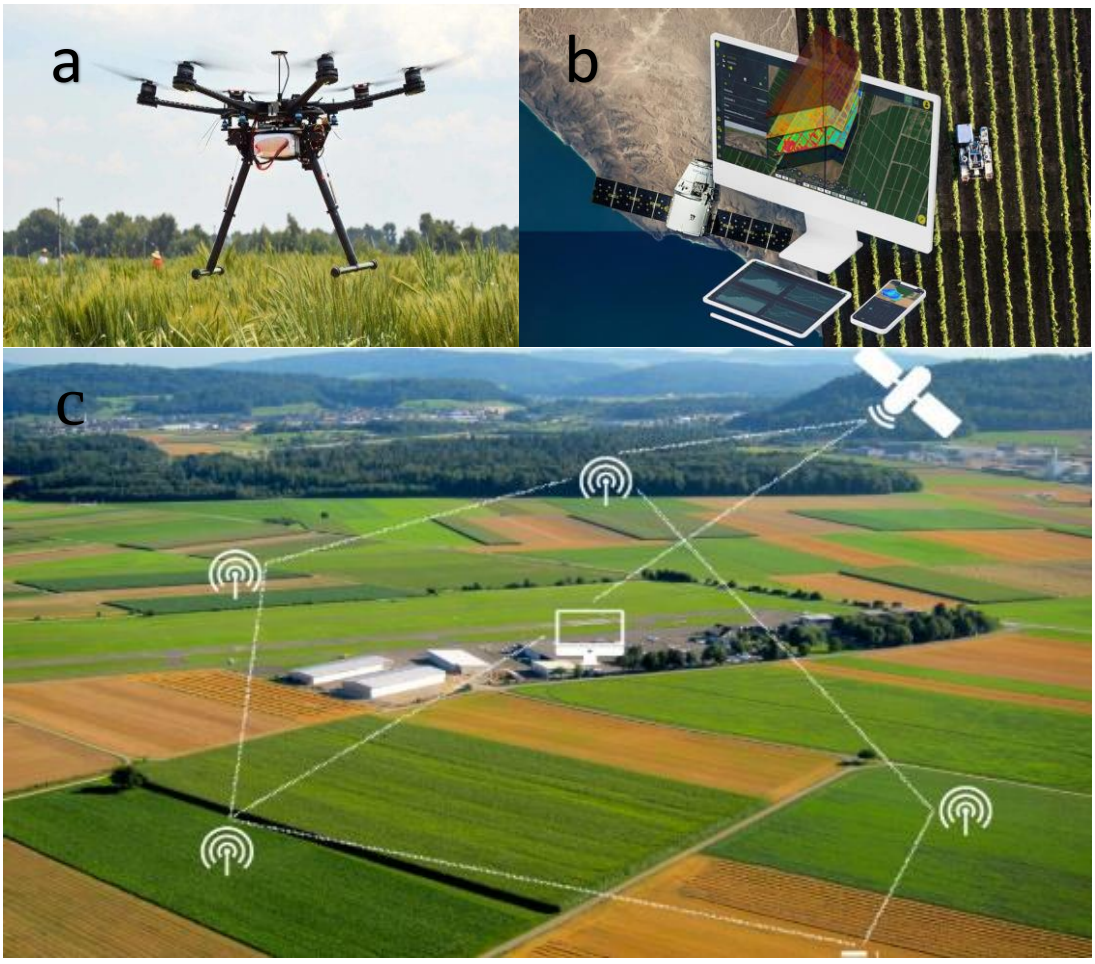

Figura 1.15 Utilidades prácticas para técnicos y agricultores de estas nuevas tecnologías. 1.15a. Drones para la detección precoz de enfermedades (Chen et al., 2022). 1.15b. Monitorización de parcelas agrícolas. 1.15c. Digitalización de parcelas agrícolas (Ozdogan et al., 2017).

Objetivos

El objetivo o propósito general de esta tesis doctoral, es la caracterización de nuevas razas de roya de la hoja, amarilla y del tallo, en el sur de España, con la intención de conocer qué genes de resistencia son vencidos y cuáles son efectivos contra ellas, así como conocer otras razas que, no estando aún en la Península Ibérica, podrían llegar en un futuro cercano. Por otra parte, aprender a utilizar y poner a punto las nuevas tecnologías, como sensores LiDAR o espectroradiometría, para detectar estas royas en los cultivares de forma eficaz y precoz, y así poder realizar control fúngico de forma efectiva. Como objetivos específicos para alcanzar el objetivo general de esta tesis se persiguen los siguientes:

1. Caracterizar la virulencia de aislados de roya de la hoja del trigo (*P. triticina* y *P. tritici-duri*) recolectados en varias localidades del sur de España en 2020, 2021 y 2022, y obtener información que pueda ser utilizada por los mejoradores para abordar el problema de susceptibilidad a *P. tritici-duri.*

2. Caracterizar nuevas razas de roya amarilla y del tallo en el sur de España y su perfil de virulencia de estas razas locales.

3. Caracterizar la resistencia a las tres royas en cultivares de trigo y triticale presentes en Andalucía para, en conjunción con los objetivos anteriores, conocer mejor la reacción cultivar-raza y prever el impacto de las tres royas en el futuro.

4. Evaluar la respuesta de cultivares de trigo duro y harinero con distintos grados de resistencia, afectados por la roya de la hoja y la roya amarilla, respectivamente, utilizando firmas espectrales completas, adquiridas mediante información hiperespectral.

5. Evaluar el impacto del algoritmo SMOTE (Synthetic Minority Over-sampling Technique) en el desarrollo de modelos de aprendizaje automático, para la detección precisa y precoz de ambos tipos de royas en cultivares de trigo.

6. Perfeccionar un sistema de detección precoz de la roya de la hoja, en cultivares de trigo duro, y de la roya amarilla, en cultivares de trigo harinero, aprovechando las capacidades de los sensores LIDAR y la tecnología de nubes de puntos 3D.

Capítulo 2. Virulence of *Puccinia triticina* and *Puccinia tritici-duri* on durum wheat in southern Spain from 2019 to 2022

Publicado: Rodríguez-Vázquez, J. N., Ammar, K., Solís, I., & Martínez-Moreno, F. (2023). Virulence of *Puccinia triticina* and *Puccinia tritici-duri* on durum wheat in southern Spain, from 2019 to 2022. Phytopathologia Mediterranea 62(1): 29-34. doi: 10.36253/phyto-14227

2.1 Abstract

Leaf rust is one of the main wheat diseases in southern Spain, where durum wheat is an important crop. Until the 2019-2020 season leaf rust was controlled, since the most widely planted cultivars in southern Spain had resistance genes against it and the susceptible cultivars were protected with fungicides. A problem arose in the spring of 2020, when every durum wheat cultivar began to be infected with leaf rust. Leaves displayed large pustules, different from those of the normal leaf rust caused by *P. triticina*, and teliospores came out rapidly after a few days. The symptoms clearly fitted with *P. tritici-duri*, another wheat leaf rust species already reported in the western Mediterranean Basin. For this study, leaf rust severity was assessed in durum wheat field trials during the 2019-20, 2020-21 and 2021-22 seasons in the provinces of Huelva, Seville, Cadiz, and Cordoba. In addition, during the spring of 2020 and 2021, single pustule isolates of leaf rust were collected from different cultivars of durum wheat. Inoculation of isolate on a differential set of lines showed that five different races were present, of which two of them were *P. tritici-duri. P. tritici-duri* is not new in southern Spain, but in the last 25 years, it has never been observed with such high severity on almost every durum wheat cultivar (susceptible and resistant to *P. triticina*). Cultivar Calero showed a consistent resistance to all races of *P. tritici-duri* employed in this study.

Keywords: Durum wheat, virulence, leaf rust, *Puccinia triticina*, *Puccinia tritici-duri*, *Puccinia striiformi.*

2.2 Introduction

Wheat is the most cultivated crop worldwide, with an annual acreage of 220 Mha (million ha), and third in grain production (after maize and rice) with 760 Mt (million t, data of 2020/21) (FAOSTAT, 2022). Durum wheat (*T. turgidum* L. subsp. *durum* (Desf.) Husn.) is sown on around 6.2% of the total wheat area (13.14 Mha) but it is much more important regionally such as in the Mediterranean Basin, where it is transformed in different types of food made from its semolina or flour, e.g., pasta, couscous, bulgur, frike and flat breads. Canada, Italy, Turkey, USA, Mexico, and Algeria are the main producing

countries, with Canada, USA, and Mexico being the most important exporters whereas Italy, Turkey, and Algeria are large importers of the durum wheat grain (Martínez-Moreno *et al*., 2022). In Spain, durum wheat is also an important crop, with 0.27 Mha planted in 2019/20, representing 12.5% of the total wheat area (MAPA, 2022). In the southern region of Andalusia, durum wheat has traditionally been the main wheat species (Martínez-Moreno and Solís, 2017), with a current area of 0.18 Mha in 2019/20 (about 60% of all durum area in the country) (MAPA, 2022).

Wheat production is regularly challenged by various fungal diseases such as leaf rust, fusarium head blight, septoria tritici blotch or yellow rust. Leaf rust, caused by the fungus *Puccinia triticina* Eriks., is the main biotic constraint worldwide according to a recent study, causing a global grain loss of 3.25%, about 25.4 Mt (Savary *et al.,* 2019). Genetic and physiologic variation in *P. triticina* is considerable, and many races classified according to their virulence/avirulence on differential wheat genotypes have been recorded since the early 20th century (Chester, 1946). As an example, in the United States *P. triticina* populations are highly variable in terms of their virulence spectra, with over 50 different races identified annually (Kolmer and Hughes, 2018). Mutations regularly occur in wheat fields, due to the tremendous number of spores produced by the pathogen every year (Huerta-Espino *et al*., 2011), and selection of newly virulent races on widely grown cultivars have been described as an important mechanism of *P. triticina* evolution (Park *et al*., 2002). Races collected on bread wheat show a broader and different virulence phenotype compared to those collected from durum wheat (Martinez *et al*., 2005).

The use of resistance genes (or *R*-genes) represents the most effective and environmentally friendly way to control this disease. To date, more than sixty leaf rust resistance genes have been described in wheat (McCallum *et al*., 2012). Most *Lr* genes originated from bread wheat, but others are from durum wheat, rye, and wild relatives (McIntosh *et al*., 1995). Virulence to these genes usually appears some years after the release of a new resistant cultivar, although there is variability in the durability of different *R*-genes. Knowledge of the virulence of the leaf rust races would permit a sensible selection of *R*-genes to be incorporated in breeding programmes. Such studies are annually conducted in many countries worldwide (USA, Australia, Canada) (Kolmer and Hughes, 2018; Park et al., 2020), but were performed only sporadically in Spain (Salazar and Branas, 1972; Martinez *et al.*, 2005).

From 1998 to 2005, leaf rust outbreaks on durum wheat were quite frequent in Andalusia, which forced farmers to apply fungicides, and breeders to ultimately develop resistant cultivars. Resistance was most often based on the very widely used and deployed *Lr14a* gene, including in very extensively grown cultivars such as Colosseo (Maccaferri *et al*., 2010). Since 2013, virulent races to this gene were reported in Spain, including the Andalusian location of Conil de la Frontera (Cádiz) (Soleiman *et al.,* 2016). Durum wheat breeders started to deploy other sources of leaf rust resistance, such as *Lr27+Lr31, LrCamayo, Lr3,* and *Lr61* (Kthiri *et al*., 2018), plus others yet to be characterized. In the spring of 2020, leaf rust uredia (or pustules) were observed in west Andalusia on previously resistant durum wheat cultivars, such as the popular Don Ricardo

(*Lr27+Lr31*). The pustules were scarce but larger than usual, with a tendency to rapidly form telia on the abaxial side of the pustule. The observed and atypical symptoms were consistent with the leaf rust disease produced by the fungus *Puccinia tritici-duri* V. Bourgin that was already reported in Morocco and Portugal and has *Anchusa azurea* Mill. (In the *Boraginaceae*) as alternate host instead of *Thalictrum speciosissimum* (in the *Ranunculaceae*), the alternate host of *P. triticina* (Ezzahiri and Roelfs, 1992; Anikster *et al.*, 1997). The presence of this variant of the leaf rust fungus was associated with atypical field reactions of known resistant durum varieties that were largely inconsistent with previously known reactions to *P. triticina*.

The objective of this study was to characterize the virulence spectra of isolates of *P. triticina* and *P. tritici-duri* collected from several locations of southern Spain in 2020, 2021 and 2022 and obtain information that could be used by breeders to address the issue of susceptibility to *P. tritici-duri*.

2.3 Materials and methods

2.3.1 Field trials

Five durum wheat cultivars popular in southern Spain, namely Don Ricardo, Athoris, Amilcar, Euroduro, and Calero, were sown in field trials with three replications (plots of 8-row of 1,36m × 5m) in the locations of Écija (near Seville), Conil de la Frontera (near Cadiz), Córdoba, Escacena del Campo (near Huelva), and Jerez de la Frontera (near Cadiz). Natural leaf rust infections occurred in during all three seasons the experiment was conducted. Leaf rust severity was assessed using the modified Cobb scale at the time of highest infection (Peterson *et al.,* 1948). The data was analyzed through ANOVA and then Duncan test to statistically separate genotypes according to their rust severity.

2.3.2 Collection and multiplication of isolates

A set of 17 samples were obtained in March-April from infected durum wheat leaves from four locations, namely, Cadiz, Huelva, Seville, and Cordoba, in 2020 (seven isolates) and 2021 (10 isolates). Infected leaves were collected from both breeding plots and commercial fields. With a small lancet, spores from a field leaf infected with leaf rust were inoculated on clean seedlings of the susceptible durum wheat cultivar Atil/Local Red to multiply each single pustule isolate, and Little Club to multiply each single pustule from bread wheat, since bread wheat may be also a host of *P. tritici-duri* (Anikster et al., 1997). Single young pustules from these plants were again inoculated on clean plants to multiply each single pustule isolate. Inoculated plants were placed in a dark dew chamber for 14 hours at 20°C, and 100% relative humidity. Plants infected with each isolate, wrapped in perforated plastic transparent bags with small perforation to prevent cross-

contamination, were returned to the greenhouse at 20-25ºC. Several cycles of reinfection were performed to obtain a sufficient quantity of spores of each single pustule isolate (at least 20 mg). Inoculi from each isolate were dried in a desiccator for seven days and then preserved in an ultra-freezer at -80ºC.

2.3.3 Virulence phenotype

A set of 20 near isogenic lines of the bread wheat cultivar Thatcher was used to determine the virulence spectrum of each isolate. The nomenclature for race designation was as described (Singh *et al*., 2004), but with some modifications. The 20 Thatcher near isogenic lines were grouped in five sets as follows: (1) *Lr1, Lr2a, Lr2c, Lr3; (2) Lr9, Lr16, Lr24, Lr26;* (3) *Lr3ka, Lr11, Lr17, Lr30;* (4) *LrB, Lr10, Lr14a, Lr18;* and (5) *Lr3bg, Lr14b, Lr20, Lr28*. The isolines Thatcher-*Lr19* and Thatcher-*Lr23* were also included. The following durum wheat cultivars, most of them with known resistance genes, were also included: Jupare (*Lr27 + Lr31*), Somateria (*Lr14a+*), (Herrera-Foessel *et al*., 2008), Colosseo (*Lr14a+*), Gallareta (= Altar C84, *Lr72*), Guayacán INIA (*Lr61*) (Herrera-Foessel *et al*., 2008), Storlom (*Lr3+*), Camayo (*LrCam*), Gatcher (*Lr27 + Lr31*), Don Jaime (*Lr14a*), Don Ricardo (*Lr27 + Lr31*), Don Javier, Aconchi-*Lr19*, Aconchi-*Lr47*, Cirno (Lr_{Camayo}) (Herrera-Foessel *et al*., 2007), and Calero. All genotypes were grown in soil (60% peat and 40% sand) trays (60×40×10 cm) in a greenhouse of the University of Seville (Spain). Each tray was sown with 13 genotypes and the cultivar Thatcher was included in all trays as a susceptible check. Six seeds of each line were grown to obtain four plants. All trays of both durum and bread wheat received the same amount of irrigation and nutrients. The plants were inoculated at the first and the fifth fully developed leaf when plants where at DC 12 and DC 16 (Zadoks *et al*., 1974). Leaf at the fifth leaf displays a better correlation with field data than the primary leaf. Each fifth leaf was fixed on the soil surface in a horizontal position by metallic clips to achieve a uniform inoculation. Each tray was inoculated with 6 mg of uredospores mixed with talcum powder (1:50). The mixture was blown over the plants which were then incubated in a dew chamber overnight at 18-20ºC, and 100% relative humidity. The following morning, plants were transferred to their greenhouse compartment at 18-25ºC. Twelve days after inoculation, plants were evaluated. The infection types were scored using a 0-4 scale described by Stakman *et al*. (1962), where 0 = no macroscopic signs of infection, ; = no uredinia with hypersensitive necrotic or chlorotic flecks present, 1 = small uredinia often surrounded by necrosis, 2 = small to medium-size uredinia surrounded by chlorosis or necrosis, X = mesothetic response, few but big uredinia surrounded by some necrosis, accompanied by small necrotic spots, 3 = medium-size uredinia with or without chlorosis, 4 = large uredinia without chlorosis or necrosis. The infection types 0 to 2 (and X) indicated that the isolate was avirulent to the resistance gene of that isoline, whereas the infection type 3 to 4 indicated virulence to the corresponding *R*-gene.

2.4 Results

2.4.1 Field trials

During the 2019-20 season, leaf rust infection was observed in the field on almost all durum wheat cultivars (Table 2.1). The observed reactions were considered atypical as these cultivars had displayed reactions ranging from complete resistance (Don Ricardo) to intermediate resistance (Amilcar), in the farmers' fields the previous seasons. In fact, these five cultivars were in field trials during the two previous seasons (2017-18 and 2018-19 and they did not show leaf rust infections at any locations. The symptoms were also different from those generally observed in the typical leaf rust epidemics. Pustules were larger and exhibited a tendency to very rapidly form teliospores. The cultivar Calero was the only one which hardly showed any symptoms of leaf rust. In 2020-21 and 2021-22, leaf rust severity was lower but nevertheless significant. In 2020-21, records were obtained only in Conil de la Frontera, while in 2021-22 Jerez de la Frontera and Escacena del Campo were the sole locations with leaf rust infections. In any case, the leaf rust severity was maintained in all cultivars but Calero, which maintained its very low infection level.

Table 2.1 Average leaf rust severity (%) on five durum wheat cultivars grown in replicated trials at five locations of southern Spain from 2019-20 to 2021-22.

Cultivar / Location-year [1]	Écija 2020	Jerez 2020	Conil 2020	Cordoba 2020	Conil 2021	Escacena 2022
Don Ricardo	10 b	23 c	25 c	1 c	7 b	3 ab
Athoris	10 b	32 bc	40 b	7 b	10 b	4 ab
Amilcar	18 a	50 a	65 a	5 b	17 a	6 a
Euroduro	18 a	37 b	53 ab	12 a	15 a	11 a
Calero	1 c	1 d	5 d	1 c	1 c	1 b

[1] Duncan test, level of significance 0.05. Within a column, figures that are followed by a common letter are not significantly different.

2.4.2 Virulence phenotype

The data on the infection type of the 20-differential set showed that the 17 isolates corresponded to five different races, as can be seen in Table 2.2. Three races belonged to *Puccinia triticina* (two from durum wheat, one from bread wheat) and two to *P. tritici-duri* (both from durum wheat). The differences between *P. triticina* collected from durum wheat and that collected from bread wheat resides in the latter being virulent to *Lr1, Lr3,*

Lr3bg, and *Lr17*. With regards to *P. tritici-duri*, the mesothetic reaction was frequent when inoculated onto the differential isolines and the set of durum wheat cultivars. The two races of *P. tritici-duri* had also different virulence spectra. *P. tritici-duri 1* was more virulent than *P. tritici-duri 2* on the Thatcher isolines, with the virulence on the durum wheat set of cultivars observed to be similar with the two *P. tritici-duri* races. *P. triticina* from durum wheat differed from *P. tritici-duri* mostly in its virulence spectrum on the durum wheat set of cultivars. The infection type of *P. tritici-duri* was mostly mesothetic, both in cultivars known to be susceptible to known races of *P. triticina* (Gallareta, Somateria) and in those which are resistant to the same (Camayo, Storlom, Jupare, Guayacán, Aconchi-*Lr19*, Aconchi-*Lr47*, etc.).

Table 2.2 Distribution of infection types (IT) at fifth leaf stage on 22 near-isogenic Thatcher, and eight durum cultivars with known *R*-genes inoculated with the five leaf rust races collected in this study.

Resistance gene	**Virulence of races and Infection type**				
	***P. tritici-duri* 1**	***P. tritici-duri* 2**	***P. triticina* new**	***P. triticina* old**	***P. triticina* from bread wheat**
Race nomenclature	PBDSS	BBBBB	DBBTJ	DBRTJ	PBDSJ
Inoculations	Seedling/5th leaf [1]	Seedling/5th leaf	Seedling/5th leaf	Seedling/5th leaf	Seedling/5th leaf
Thatcher	4 / 3	X / 2	4 / 4	3 / 3	3 / 4
Thatcher-*Lr1*	4 / 3	X / 3	1 / ;	2 / 1	3 / 4
Thatcher-*Lr2aLr2c*	1 / 1	1 / 1	2 / 1	2 / 1	2 / 2
Thatcher-*Lr3*	3 / 3	X / 1	3 / 3	3 / 3	3 / 3
Thatcher-*Lr3bg*	3 / 3	X / 2	1 / ;	1 / 1	3 / 3
Thatcher-*Lr3ka*	3 / 3	X / 1	1 / ;	1 / 1	2 / 3
Thatcher-*Lr9*	1 / 2	X / 1	1 / ;	1 / ;	1 / 1
Thatcher-*Lr10*	1 / 2	1 / 1	0 / 0	0 / 0	; / 0
Thatcher-*Lr11*	3 / 4	X / 2	3 / 4	3 / 3	4 / 3
Thatcher-*Lr14a*	X / 3	1 / 1	1 / 1	1 / 1	1 / 2
Thatcher-*Lr14b*	4 / 3	X / 2	3 / 4	3 / 3	4 / 3
Thatcher-*Lr16*	4 / 2	X / 2	3 / 4	3 / 3	3 / 3
Thatcher-*Lr17*	2 / 2	X / 2	1 / 2	1 / 3	2 / 3
Thatcher-*Lr18*	3 / 3	X / 2	; / ;	1 / 1	3 / 3
Thatcher-*Lr20*	X / 2	X / 2	2 / 2	3 / 3	2 / 2
Thatcher-*Lr24*	3 / 3	X / 2	3 / 2	3 / 3	3 / 3
Thatcher-*Lr26*	; / ;	; / ;	; / ;	; / 1	; / ;
Thatcher-*Lr28*	; / ;	; / ;	; / ;	; / 1	; / ;
Thatcher-*Lr30*	; / ;	1 / ;	1 / ;	1 / 1	; / 0
Thatcher-*LrB*	2 / 2	1 / 2	2 / 2	2 / 1	2 / 2
Thatcher-*Lr19*	4 / 3	2 / 2	3 / 3	3 / 3	3 / 3
Thatcher-*Lr23*	1 / 2	; / 1	; / ;	; / 0	0 / 0
Gatcher (*Lr27+Lr31*)	3 / 3	2 / 2	2 / 2	3 / 3	
Atil/Local Red	X / 3	X / 1	4 / 4	4 / 4	
Gallareta (*LrAltar*)	4 / 3	4 / 4	4 / 4	4 / 4	
Somateria (*Lr14a*)	X / X	X / 3	3 / 3	4 / 3	
Camayo (*LrCam*)	X / X	X / X	3 / 4	3 / 3	
Colosseo (*Lr14a+*)	X / X	X / X	1 / ;	1 / ;	
Don Jaime (*Lr14a*)	X / 3	X / X	4 / 4	3 / 3	
	X / X	X / X	4 / 4	3 / 3	

Don Ricardo	X / X	X / X	1 / ;	1 / ;
(*Lr27+Lr31*)	X / 3	X / X	2 / 2	2 / 3
Don Javier	X / X	X / X	; / ;	0 / ;
Storlom (*Lr3*)	X / X	X / X	1 / ;	1 / ;
Jupare (*Lr27+Lr31*)	X / X	X / X	; / ;	; / ;
Guayacán (*Lr61*)	X / X	X / X	0 / 0	0 / 0
Aconchi-*Lr19*	X / X	X / X	; / ;	0 / ;
Aconchi-*Lr47*	X / X	X / X	1 / 1	1 / ;
Cirno	1 / 1	1 / 1	1 / 1	; / ;
Calero				

[1] Infection type assessment according to a 0-4 scale as described by Stakman *et al.* (1962).

The collected samples were classified according to the province from which they were collected and the race to which they belonged. They were also classified by the year in which they were collected (Table 2.3).

Table 2.3. Number of durum wheat isolates collected in different locations during the period 2019-2021.

Races	Huelva	Sevilla	Cordoba	Cadiz	Total	Total	Total	Total
Year					2020	2021	All	All (%)
P. tritici-duri 1	2	0	1	3	3	3	6	35,3
P. tritici-duri 2	0	0	1	2	1	2	3	17,7
P. triticina old	0	0	1	1	1	1	2	11,8
P. triticina new	0	0	0	2	1	1	2	11,8
P. triticina from bread wheat	3	1	0	0	1	3	4	23,5
Total					7	10	17	100

2.5 Discussion

P. tritici-duri has been in the western Mediterranean Basin for a long time. Interestingly, rust-infected *Anchusa azurea* (the alternate host of *P. tritici-duri*) were cited in Spain prior to 1902 (Navarro, 1902) and more specifically in southern Spain little before 1918 (González-Fragoso, 1918). *Anchusa azurea* plants with rust infections could not be found in southern Spain during a survey conducted by our team at different locations. It is likely that *P. tritici-duri* had coexisted with *P. triticina* for a long time, infecting durum wheat fields. From 1992-2005, durum wheat acreage increased in Andalusia and Spain due to subsidies from the European Union (Martínez-Moreno and Solís, 2017). Research on durum wheat leaf rust was reactivated globally when, in 2001, a new race of leaf rust (BBG/BN), virulent on *Lr72* (a gene frequently deployed in durum wheat cultivars globally), appeared in Mexico and later in other parts of the world. Until that time, the resistance mainly relied on two genes globally namely, *Lr72* and *Lr14a* (Singh *et al.,* 2004). However, the development of virulent races against these two genes

made *P. triticina* a major disease in durum wheat globally, including Spain (Martínez-Moreno and Solís, 2019).

Although, in principle, *P. tritici-duri* was detected in the geographical range of *Anchusa azurea*, it may have been able to move from this region to other without any alternate host. This capacity of rust to survive and coexist without the alternate host has been previously reported as indicated by *P. triticina* expansion, outside the area of its alternate host, *Thalictrum spp.*, in southern Europe (Anikster *et al*., 1997).

Rusts have always been a problem in wheat. Their evolving nature and the rapid development of virulence towards cultivars with effective resistance is a feature of these pathogens (Figueroa *et al.*, 2020). Leaf rust is not an exception to this, and the appearance of races virulent to durum wheat cultivars containing *Lr14a* gene in Spain in 2013 is a good example (Soleiman et al., 2016). However, in this study another leaf rust species, *P. tritici-duri*, has emerged in the durum wheat fields of western Andalusia. This rust species is not new, as it has been present in Morocco, Portugal, and even in southern Spain for a long time, but the impact on wheat development was limited to nil (D´Oliveira and Samborski, 1966; Anikster *et al*. 1997). These countries have had a great tradition of planting durum wheat, especially Morocco, but also in the southern Iberian Peninsula (Martínez-Moreno *et al*., 2020). The distance between Morocco and southern Spain is very short (only 14 kilometers at the Strait of Gibraltar), and climatic conditions are similar, so the different races of rust easily get airborne and move from one country to the other (Martínez-Moreno and Solís, 2019). Even though *P. tritici-duri* may have been present in the area for a long time, the recent increase in incidence on durum wheat in Andalusia since 2020 has been very significant and alarming for a region in which 60% of the wheat area is sown to durum wheat.

P. triticina and *P. tritici-duri* showed important differences, primarily in the size of their pustules with those from of *P. tritici-duri* larger than those of *P. triticina*. The other typical difference was the speed with which they develop telia, with the former doing so at 26 days after inoculation, much faster than the latter which developed telia at 45 days under the same conditions. These results were consistent with those reported by Anikster *et al.* (1997). The virulence spectra on the Thatcher differential set were also quite different, with the races of *Puccinia triticina* collected from durum wheat being avirulent on *Lr1, Lr3ka, Lr9, Lr17*, and virulent on *Lr18, Lr20* and the *P. tritici-duri* presenting a constant mesothetic reaction towards almost all Thatcher near isogenic lines, where lesions of infection type 1 where mixed with well formed, but few, pustules of infection type 2-3. Only *Lr24, Lr26* and *Lr28* genes were clearly effective against *P. tritici-duri*. *Lr24* is located in chromosome 3D and cannot be transferred to durum wheat by regular crossing and selection, and its transfer would require cytogenetic transfers before it could be used in regular breeding programs. *Lr26*, located on the translocated chromosome 1B/1R and originating from rye has been very extensively used for decades in bread wheat (McIntosh *et al*., 1995), but to our knowledge has not been deployed commercially in durum wheat. Its potential use as a resistance option against *P. tritici-duri* needs to be critically assessed as the 1B/1R translocation is known to cause

unsuitable sticky dough characteristics in bread wheat and could very well affect the gluten strength and characteristics of durum wheat. Finally, *Lr28*, located on chromosome 4A and originating from *T. speltoides* (McIntosh, 1995), has been used in a more limited fashion in bread wheat but virulence for this gene has been reported as highly frequent in *P. triticina* populations worldwide (McIntosh, 1995). Based on the results from this study, the few well characterized seedling resistance genes used in bread wheat that could be used in durum wheat as resistance options against *P. tritici-duri* come with major drawbacks which may not justify their use in durum wheat breeding programs.

P. tritici-duri is present in western Andalusia and albeit sporadically it can be a serious problem in durum wheat because very few completely resistant genotypes have been identified so far. Most cultivars and genotypes evaluated in this study and in larger sets as part of the screening activities of local breeding programs are characterized by the same severe intermediate reaction. The majority of the cultivars considered resistant to leaf rust, such as Don Ricardo (*Lr27+Lr31*), which has been the most widely planted cultivar in Andalusia for many years (Martínez-Moreno and Solís, 2017), are somewhat susceptible to *P. tritici-duri*. Other genotypes known to exhibit different *Lr* genes, such as Lr_{Camayo} present in the popular Mexican cultivar CIRNO C2008 have also been affected significantly by this rust species. *Lr19* and *Lr47* are globally effective genes originating from wheat wild relatives (Kthiri et al., 2017). They were introduced in bread wheat giving a near immune response, and recently to durum wheat (Ammar, p.c.). *P. tritici-duri* seems to easily overcome the resistance of these two *R*-genes. To date, among the released cultivars grown in Andalusia, only Calero showed an interesting resistance against the two *P. tritici-duri* races employed in this study. The resistance of Calero towards *P. triticina* races is likely to be located on chromosomes 6B, very close to *Lr61* as allelism tests between Calero and Guayacan INIA, the source of *Lr61* (Herrera et al, 2008b) have not yielded any recombinant susceptible plants based on studies conducted at CIMMYT (Ammar, personal communication). Whether or not this is the basis underlying the resistance of Calero to *P. tritici-duri* that cannot be known until proper studies are conducted.

Given the almost generalized and variable levels of susceptibility observed in the relatively small sets of germplasm evaluated in southern Spain against *P. tritici-duri*, and the very limited options available with known *R*-genes to provide complete resistance to *P. triticina*, breeders will need to explore and find new sources of suitable resistance in wider and more diverse sets of germplasm. These resistance discovery activities will have to be conducted under conditions that ensure the exclusive presence of *P. tritici-duri* without the confounding effect of *P. triticina*. However, before such costly initiatives are taken, it is important to accurately assess the probability of *P. tritici-duri* becoming a major and yield-limiting pathogen in southern Spain and estimate the actual economic cost through yield loss when the pathogen is present on cultivars that are otherwise resistant to *P. triticina*.

2.6 Conclusions

In this study, the existence, virulence, symptoms, and severity of *P. tritici-duri* in southern Spain compared to *P. triticina* were described. *P. tritici-duri* was able to infect almost all durum wheat cultivars used in southern Spain, and in the greenhouse showed a mesothetic infection type against most Thatcher near isogenic lines and a collection of durum wheat cultivars and lines known to be resistant to *P. triticina*. Breeders have very little-known options to genetically address resistance to *P. tritici-duri*. If this species is to become much more prevalent in southern Spain and its economic effects can be demonstrated, breeding programs will have to undertake resistance or gene discovery initiatives to identify suitable sources of resistance in much wider and diversified sets of germplasm. The isolates of *P. tritici-duri* obtained in this study will certainly be useful for such future studies.

Capítulo 3. Characterization of wheat yellow rust and stem rust virulence in southern Spain

Publicado: Rodríguez-Vázquez JN, Ammar K, Solís I, Martínez-Moreno F. Characterization of Wheat Yellow Rust and Stem Rust Virulence in Southern Spain. Agriculture. 2023; 13(12):2202. https://doi.org/10.3390/agriculture13122202

3.1 Abstract

Effective mitigation of the current threat from yellow rust and the potential threat from stem rust to the wheat production in the south of Spain requires the characterization of the lineages/races currently present in the region. Results from this study clearly indicated that the main yellow rust lineages currently present in the south of Spain are PstS10, PstS13 and PstS14, to which several widely grown commercial cultivars are resistant. Even tough stem rust is not yet present during the regular cropping season, the main lineages/races as Clade IV-B and Clade IV-F were identified, much like in most of Europe and parts of North Africa. The evaluation of differential series and special breeding lines with known genes under local conditions has indicated the availability of several genetic options that could be used in breeding/selection programs to provide effective levels of resistance to either disease in the future. However, in undertaking these efforts, it is important to consider not only the lineages currently present locally but also consider resistance options effective against lineages/races that rapidly developing elsewhere and could very likely reach the south of Spain in the near future.

Keywords: *Puccinia graminis*, *Puccinia striiformis*, resistance, Warrior race.

3.2 Introduction

Wheat is one of the world's leading cereal grains and represents a staple food for more than one third of its population, contributing more calories and proteins than any other cereal (Curtis et al., 2002). It is the most cultivated crop worldwide with an annual area of 221 Mha (million ha), and third in grain production, after maize and rice, with 771 Mt (million t) in 2021/22 (FAOSTAT, 2023). It provides 21% of the calories and 20% of the protein for more than 4.5 billion people in 94 developing countries (Braun et al., 2010, Arval et al., 2019). According to Choudhary et al. (Choudhary et al., 2018), wheat production needs to be increased annually by 2% in the coming years (Kashyap et al., 2020), representing double the rate of increase currently being achieved (Ray et al., 2013, Bahar et al., 2013). Wheat yields are, on average, around 20% lower than the current crop potential because of biotic and abiotic factors. Among the factors that affect wheat production and prevent the crop from realizing its yield potential are wheat rusts, which

can cause significant yield losses in susceptible cultivars and can be difficult to control chemically in some areas of the world (Vergara-Diaz et al., 2015, Savary et al., 2019). There are three types of rust affecting wheat: leaf rust, yellow rust, and stem rust; and all three can be most effectively controlled through genetic resistance. While fungicides can be excellent means of control, they are not always available in large wheat growing areas worldwide and are not the most environmentally friendly option (Martínez-Moreno y Solís, 2019, Hafeez et al., 2021).

Wheat yellow (or stripe) rust is caused by the fungus *Puccinia striiformis* Westend. f. sp. *tritici* (Pst), a pathogen generally prevalent in temperate regions with cool and wet weather conditions (Figure 3.1) (Chen et al., 2014). In the susceptible plant, chlorotic flecks typically appear after six to eight days from infection, whereas sporulation (characteristic yellow orange uredinia appearing in long, narrow stripes on leaves) starts approximately from 12 to 14 days under favorable conditions (Singh et al., 2008), eventually leading to desiccation of leaves. Urediniospores germinate rapidly in optimum dew conditions and a temperature between 7 and 12°C, with ideal disease development conditions (from infection to sporulation) between 12–15°C (Porras et al., 2022). Global losses inflicted by the disease can reach 20 Mt annually, representing an estimated US$ 1 billion (Beddow et al., 2015, Wellings et al., 2011, Savary et al., 2019). Wheat stripe rust has been reported in more than 60 countries and evidence suggests a significant geographical expansion in the last 50 years (Beddow et al., 2015). According to McIntosh et al. (McIntosh et al., 2013), 67 yellow rust resistance genes (*Yr1* to *Yr67*), and 42 with temporary designations, have been reported. Since the 2000s, aggressive lineages of Pst adapted to higher temperature climates have spread to warmers regions of the world that were previously less affected by this disease (Ali et al., 2014). Although populations of yellow rust appear to be clonal in Europe, Australia and North America, there are significant levels of genetic diversity within some pathogen populations (Chen et al., 2014). Such polymorphic populations are evident in western China and Central Asia, consistent with their reported center of diversity in the Himalayan and nearby regions, where sexual recombination appears to be common (Ali et al., 2014, Hovmoller et al., 2011). Races from that region, such as Warrior or Warrior- reached Europe in recent years, bringing virulence on important resistance genes present in European wheat cultivars (Figueroa et al., 2018, Singh et al., 2015). These linages were reported in Spain starting in 2014 and, more specifically, in the southern region of the country in 2015 (Martínez-Moreno y Solís, 2019).

(a) **(b)**

Figure 3.1 Yellow rust in bread wheat cultivars at Jerez field (2022). (**a**) Susceptible (left, cv. Califa) *vs.* resistant bread cultivar (right, cv. Conil) in field plots; (**b**) Symptoms on bread wheat susceptible plants (leaves).

Wheat stem rust, caused by the basidiomycete *Puccinia graminis* Pers. f. sp. *tritici*, was historically considered the main wheat rust disease due to its devastating impact on grain yield and quality, in some cases even with losses of more than 50% (Figure 3.2) (Singh et al., 2015, Patpour et al., 2022). Stem rust did not appear frequently in European countries in recent decades, thanks to an effective control, starting in the 1950s-1960s (Beard et al., 2004), resulting from the widespread use of host resistance (*Sr2*, *Sr31*), the eradication of the alternate host, common barberry, and the release of early maturing cultivars descending from the Green Revolution (Pretorius et al., 2012). In Eastern African, one of the most stem rust prone areas in the world, the pathogen was well under control thanks to the deployment of *Sr31* gene, very effective against the predominant stem rust races of the time (Bartos et al., 1996). However, the race TTKSK (syn. Ug99), detected in Uganda in 1998 and its subsequent variants, defeated the effectiveness of many designated and undesignated resistance genes, and losses due to Ug99 were reported to be as high as 90% (Pretorius et al., 2000). Many *Sr* genes originated from tetraploid wheats (*Sr7a*, *Sr8b*, several alleles of *Sr9*, *Sr11*, *Sr12*, *Sr13*, *Sr14*, *Sr17*, and *Sr8155-B1*) (McIntsh et al., 1995, Nirmala et al., 2017). Several of these genes are widely used in bread and durum wheat, contributing to the successful control of stem rust worldwide (Dubcovsky et al., 2011). *Sr13b* gene is a major basis of stem rust resistance in durum wheat, worldwide (Klindworth et al., 2007, Luig et al., 1983, Singh et al., 2015). New stem rust from different lineages have emerged in East Africa; Race TKTTF resulted in epidemics in Ethiopia in 2013, with yield losses close to 100% on the most grown cultivar Digalu (Olivera et al., 2015). In 2013, wheat stem rust reappeared at several locations in Germany (Olivera et al., 2017), along with sporadic incidences in southern Denmark, eastern Sweden, and the United Kingdom (Lewis et al., 2018). A more widespread outbreak was reported in Sicily in 2016, where thousands of hectares of both bread and durum wheat were affected (Bhattacharya, 2017). Analyses of infected plant samples from Sicily suggested the presence of a new race in Europe, TTRTF (Bhattacharya, 2017), which carried virulence to *Sr13b* of particular relevance for durum

wheat (Patpour et al., 2020). In southern Spain, this disease was detected regularly since 2018, but with low severity. Stem rust was also detected, with higher severity, in the irrigated off-season wheat trials (August-September) in the south (Conil de la Frontera, Cadiz) and northeast of Spain (Lleida).

Given the increasingly threatening incidences of yellow and stem rust in Spain, there is a need to characterize and understand the virulence spectrum of the local lineages of these pathogens. This objective was addressed through field testing of differential lines and main cultivars in locations where both diseases occurred naturally during the period from 2016 to 2022, by sampling and subsequently analyzing several single pustules isolates of both pathogens collected from several locations during these seven years.

(a) **(b)**

Figure 3.2 Stem rust in durum wheat cultivars at Conil field (2023). (a) Resistant (left, cv. Amilcar) vs. susceptible bread cultivar (right, cv. Athoris), in field plots; (b) Symptoms on susceptible plants (leaves and stems).

3.3 Materials and Methods

3.3.1 Locations, plant material and experimental setup

This research was conducted in experimental sites used by Agrovegetal, a local breeding company, at four locations in southern Spain, namely, Escacena del Campo, near Huelva (37°27'20" N; 6°21'49" W), Jerez de la Frontera near Cadiz (36°42'14" N; 6°10'11" W), Ecija near Sevilla (37°32'23" N; 5° 6' 42" W), and in Conil de la Frontera

near Cadiz (36°18'30" N; 6° 5' 13" W). The first 3 locations were used for evaluations related to yellow rust and were sown during the regular season (December planting) while the fourth was dedicated to evaluations related to stem rust, with a summer, off-season sowing in June, under irrigation. Field trials were under rainfed conditions in winter sowings, and weekly irrigated at the off-season site of Conil. Rainfall during the wheat growing season (November-May) across the years of the present study are shown in Table 1. Experiments were carried out from 2016 to 2022, relying exclusively on natural infections. In all trials, entries were sown in twin rows of 1 meter length using 4 grams of seed per plot. The susceptible checks, Califa for yellow rust, and McNair and Tocayo for stem rust, were planted around their respective nurseries. Tejada and Calero were planted as resistant checks for yellow and stem rust, respectively.

The set of commercial varieties for yellow rust evaluation was planted in a total of 21 location/year combinations, but only the 14 location/year combinations are reported herein, as the other seven were characterized by very low or absent natural disease incidence. The set of yellow rust differential lines was planted in a total of 19 location/year combinations, with only 15 of those reported as they involved high disease incidence. The 52 wheat entries in the yellow rust nurseries were divided into two sets: the old set of 35 genotypes with different *Yr* genes, and a collection of 17 near isogenic lines in the Avocet background. The 100 wheat entries for stem rust evaluations, included (1) 34 advanced durum breeding lines selected by CIMMYT for their different response to the African races of stem rust in Kenya and Ethiopia, (2) 6 advanced breeding lines with known resistance gene(s) introgressed at CIMMYT through marker-assisted selection, (3) 20 cultivars, landraces or other sources of resistance to the African races used in the CIMMYT breeding program, (4) 40 stem rust differentials lines used to identify races according to their virulence.

Rust severity was also taken in additional field trials independently sown by the Agrovegetal Company, at the same fourth locations in southern Spain, for both yellow rust and stem rust. These trials included the commercial varieties of bread wheat (Arthur Nick, Tejada, Conil, Escacena, Califa), durum wheat (Amilcar, Euroduro, Athoris, Don Ricardo, Calero) and triticale (Bondadoso, Valeroso and Trujillo).

3.3.2 Pathogen isolation

Yellow rust and stem rust differentials in all field trials were infected naturally. Samples of both rusts were sent every year to the Global Rust Reference Center (GRRC) in Denmark (GRRC, 2023), where a phenotypic and/or genetic characterizations on single pustule isolates were carried out on each sample, to identify the local lineages and/or races. As yellow rust and stem rust differentials in all field trials were infected naturally, it is important to know the rainfall in each location and year (Table 3.1).

Table 3.1 Monthly precipitation (mm) during the wheat growing season in the three locations used for rainfed field trials.

Season	Month	Escacena	Écija	Jerez
2015/16	Dec.	147	110	115
2015/16	Jan.	20	15	50
2015/16	Feb.	82	24	62
2015/16	Mar.	112	42	131
2015/16	Apr.	79	35	71
2015/16	May	3	5	1
2015/16	**Total**	**443**	**231**	**430**
2016/17	Dec.	37	120	56
2016/17	Jan.	112	41	67
2016/17	Feb.	48	57	34
2016/17	Mar.	124	24	125
2016/17	Apr.	117	24	82
2016/17	May	2	10	4
2016/17	**Total**	**440**	**276**	**368**
2017/18	Dec.	98	103	90
2017/18	Jan.	110	67	65
2017/18	Feb.	23	56	15
2017/18	Mar.	34	45	18
2017/18	Apr.	14	34	5
2017/18	May	1	2	1
2017/18	**Total**	**280**	**307**	**194**
2018/19	Dec.	78	68	111
2018/19	Jan.	104	99	159
2018/19	Feb.	132	98	77
2018/19	Mar.	63	74	56
2018/19	Apr.	76	65	68
2018/19	May	34	19	23
2018/19	**Total**	**487**	**423**	**494**
2019/20	Dec.	78	87	75
2019/20	Jan.	69	57	112
2019/20	Feb.	35	76	47
2019/20	Mar.	15	14	87
2019/20	Apr.	32	22	54
2019/20	May	4	3	16
2019/20	**Total**	**233**	**259**	**391**
2020/21	Dec.	98	54	109
2020/21	Jan.	54	13	89
2020/21	Feb.	76	45	56
2020/21	Mar.	21	24	79
2020/21	Apr.	12	13	28
2020/21	May	5	2	10
2020/21	**Total**	**266**	**151**	**371**
2021/22	Dec.	86	68	70
2021/22	Jan.	72	89	53
2021/22	Feb.	61	75	97

2021/22	Mar.	43	48	65
2021/22	Apr.	60	46	51
2021/22	May	8	5	8
2021/22	**Total**	**330**	**331**	**344**

[1] Data from RIA (RIA, 2023). Escacena data was from La Palma del Condado station.

3.3.3 Plant disease evaluation

To determine the disease severity in each plot, and the field response (type of reaction to the disease), percentage of foliar area covered by uredinia, according to the modified Cobb scale, was recorded. In addition, the response to infection was scored according to Roelfs et al. (Roelfs, 1992). The disease severity scores were converted into AUDPC (Area Under Disease Progress Curve) (Roelfs, 1992), using the formula:

AUDPC = D [½ (Y1 + Yk) + Y2 + Y3 + …. + Yk-1], being D = Time interval (days between readings), (Y1+YK) = Sum of the first and last score. (Y2 + Y3 +…+ Yk-1) = Sum of all intermediate disease scores. The AUDPC for each entry was converted into relative percentage by using the AUDPC of the check, Atil/Local Red as 100 % (Pandey et al., 1989). To determine the difference between susceptible and resistant lines, a threshold of 30% (stem rust) or 20% (yellow rust) severity relative to the most susceptible line in each trial was set.

3.4 Results

3.4.1 Yellow Rust responses

Based on a combination of DNA analyses conducted at the GRRC from samples collected as part of this study, observations made herein on the set of differentials, and independent reports from different Spanish locations, it appears that the predominant yellow rust lineages present in Spain are PstS4, PstS7, PstS10 PstS13 and PstS14. The virulence spectra of these lineages are shown in Table 3.2, according to the classification from GRRC (GRRC, 2023).

Table 3.2 Virulence on *Yr* genes of the main lineages of yellow rust in Spain, according to GRRC.

	Virulence on *Yr* genes																		**Name**
Lineage	***1***	***2***	***3***	***4***	***5***	***6***	***7***	***8***	***9***	***10***	***15***	***17***	***24***	***25***	***27***	***32***	***Sp***	***Avs***	***Amb***	
PstS4		x				x	X	x		x			x							Triticale 2006
PstS7	x	x	x	x		x	X		x			x		x		x	x	x	x	Warrior
PstS10	x	x	x	x		x	x		x			x		x		x	x	x		Warrior -
PstS13		x				x	x	x	x									x		Triticale 2015
PstS14		x	x			x	x	x	x			x		x		x	x	x		

Virulence on *Yr1* and *Yr4* distinguishes between Warrior and the rest of the lineages, and virulence on cultivar Ambition is between PstS7 and PstS10. If virulence is observed on *Yr8*, the Warrior lineage is not present. If virulence on *Yr8* is observed in addition to virulence on *Yr10* and *Yr24*, lineage PstS4 is most likely present. Virulence on *Yr8*, but not on *Yr10* or *Yr24*, would be an indicator of the presence of PstS13 or PstS14. To distinguish between both latter lineages, we must observe the virulence in the differentials *Yr3*, *Yr17*, *Yr25*, *Yr32*, and *YrSp*. Virulence would indicate the presence of PstS14, avirulence, the presence of PstS13.

During the period of the present study, the lineages detected in the various experiments varied from year to year and between locations within years. In table 3.3 and table 3.4 below, the predominant lineages detected are shown for each combination location/year. In 2016, the first year the differential sets were evaluated as part of the present study, analyses conducted at the GRRC on samples collected from highly infected commercial bread wheat fields indicated that PstS10 (Warrior-) was the major lineage present. In 2017, no samples were sent to the GRRC, but from the set of differentials response, it could be deduced that PstS13 and PstS14 races were the prevailing lineages present. In 2018, only Warrior- was detected in the field trials of the present study, but the presence of PstS7, PstS13 and PstS14 was independently reported in the country. In 2019, both differentials and DNA analysis again indicated the predominance of Psts13 and PstS14, with Warrior- also present. In 2020, only data from Jerez location could be taken and indicated the presence of Warrior-, PstS13 and PstS14. In 2021, the presence of PstS14 was inferred from the evaluation of the set of differentials and DNA analysis by GRRC (GRRC, 2023), confirmed this assumption. In 2022, both results from the set of differentials and DNA analysis revealed the presence of PstS10 (Warrior-), PstS13 and PstS14.

Monitoring the reaction to yellow rust of key commercial cultivars of bread wheat, durum wheat and triticale sown in southern Spain initiated in 2016 by the Agrovegetal company. Results from these evaluations are presented in Table 3.3. While these evaluations relied exclusively on natural field infections, the generally high rust scores observed on susceptible bread wheat cultivar Califa indicate that the environmental conditions, in most location/year combinations reported herein, were conducive to the development of the disease and that virulent races were always present. Similarly high

infections, to a somewhat lesser extent, were observed on susceptible bread wheat cultivar Escacena. The bread wheat cultivar Conil exhibited low to intermediate susceptibility reactions, mostly when Pst10 was present. The other two bread wheat cultivars, Tejada and Arthur Nick consistently exhibited high levels of field resistance, virtually total immunity. So did all the commercial durum wheat and modern triticale cultivars (Bondadoso and Valeroso). They were not at all affected by any of the lineage combinations present during the period of this study, in spite of the conducive environmental conditions. Very minor signs of infection, in some location/year combinations, were observed on commercial durum wheat cultivars starting in 2019 and on triticale cultivar Bondadoso, in 2022. However, infection levels were never high enough to be considered indicative of failing genetic resistance. The only case of emerging non-complete resistance, possibly intermediate susceptibility, is in the case of durum cultivar Athoris. Old (from the 1980s), and now commercially obsolete, triticale cultivar Trujillo was characterized, in most location/year combinations, by intermediate to high infection levels.

Table 3.3 Yellow rust severity data on commercial durum, bread wheat and triticale cultivars grown in southern Spain.

Yellow rust lineage[2]	**ESC 16**[1] PstS10	**ECI 16** PstS10	**JER 16** PstS10	**ESC 17** PstS13 PstS14	**JER 17** PstS13 PstS14	**ECI 18** PstS10	**ESC 19** PstS13 PstS14	**ECI 19** PstS13 PstS14	**JER 19** PstS13	**JER 20** PstS10 PstS13 PstS14	**JER 21** PstS14	**ESC 22** PstS10 PstS13	**ECI 22** PstS10	**JER 22** PstS14 PstS13
Durum wheat cultivars														
Amilcar	0	0	0	0	0	0	0	0	2	1	2	0	0	5
Euroduro	0	0	0	0	0	0	0	0	1	1	1	0	0	3
Athoris	0	0	0	0	0	0	3	0	7	5	9	0	0	22
D. Ricardo	0	0	0	0	0	0	0	0	1	0	1	0	0	1
Calero	0	0	0	0	0	0	0	0	0	0	0	0	0	1
Bread wheat cultivars														
Artur Nick	0	7	2	0	0	0	0	0	0	1	0	0	0	0
Tejada (rc)[3]	0	0	0	0	0	0	0	0	0	0	0	0	0	0
Conil	1	23	30	0	0	30	27	0	13	7	0	3	14	0
Escacena	1	10	63	80	50	40	80	70	35	50	28	35	53	70
Califa (sc)[3]	9	47	87	90	73	80	90	90	70	90	43	90	73	90
Triticale cultivars														
Bondadoso	0	0	0	0	0	0	0	0	0	0	0	1	1	6
Valeroso	0	0	0	0	0	0	0	0	0	0	0	0	0	0
Trujillo	0	5	20	27	20	10	43	57	22	0	12	30	33	33

[1] Locations: ESC = Escacena del Campo, ECI = Ecija, JER = Jerez de la Frontera. The number indicates the year of trial (e.g., 16=2016).
[2] Pst lineages according to GRRC (GRRC, 2023).
[3] Califa and Tejada were the susceptible (sc) and resistant (rc) checks.

To obtain a preliminary indication of what type of genetic option could be useful in breeding against the yellow rust lineages prevailing in southern Spain, two sets of lines with known genes of resistance were evaluated at three locations for their adult plant field reaction from 2016 to 2022. An analysis of variance with genotypes and locations was performed, using years within locations as replications and is presented in Table 3.4. Genotype and location were clearly important factors of variation, but the interaction

between them was not significant, indicating that the genotypes' severity scores were rather correlated between locations.

Table 3.4 Analysis of the variance of yellow rust severity scores of a set of 52 differential lines evaluated under natural field infection at three southern Spain locations from 2016 to 2022, using years of evaluation within location as replicates.

Source	Sum of square III type [1]	df	Mean square	F	Significance
Corrected model	206,729(a)	155	1,334	6.1	0.000
Intersection	184,823	1	184,823	845.2	0.000
Genotype	176,911	51	3,469	15.9	0.000
Location	12,019	2	6,010	27.5	0.000
Genotype Location	23,074	102	226	1.0	0.398
Error	124,857	571	219		
Total	509,127	727			
Total corrected	331,586	726			

[1] R square = 0.623 (R corrected square = 0.521).

The results of the severity scores on the sets of differential lines are presented in Table 3.5. The presence of *Yr2, Yr6,* and *Yr9* in monogenic state was associated with high levels of field susceptibility in all years at all locations, with variability depending on the line's background in some cases, but independently from the lineages present. Of the 52 lines tested, 14 were resistant at all locations and years, even when weather conditions were very favorable to yellow rust as indicated by the high severity scores on the susceptible lines. These lines must have been resistant to PstS10, PstS13 and PstS14 since these lineages were present at these locations during the time of the present study.

Table 3.5 Yellow rust severity scores in two sets of differentials lines evaluated under natural field infection at three southern Spain locations between 2016 and 2022.

Line	ESC 16[1] PstS10[2]	ESC 17 PstS13 PstS14	ECI 17 PstS13 PstS14	JER 17 PstS13 PstS14	ECI 18 PstS10	ESC 19 PstS13 PstS14	ECI 19 PstS13 PstS14	JER 19 PstS13	JER 20 PstS13 PstS14 PstS10	ESC 21 PstS13	ECI 21 PsTs14	JER 21 PsTs14	ESC 22 PstS10 PstS14	ECI 22 PstS10	JER 22 PstS14 PstS13
Yr1/6*Avocet S	30	0	0	0	40	0	0	0	2	0	0	0	30	30	0
Yr5/6*Avocet S	0	0	0	0	0	0	0	0	0	0	0	0	0	0	0
*Yr6/6**Avocet S	60	30	40	20	50	50	40	50	60	40	60	70	70	70	50
*Yr7/6**Avocet S	60	20	40	50	50	60	40	20	70	20	50	60	70	70	70
Yr8/6*Avocet S	5	20	8	10	0	30	20	15	50	15	30	15	30	0	20
Yr9/6*Avocet S	50	40	80	50	60	70	70	10	60	20	70	60	60	90	70
Yr10/6*Avocet S	0	0	0	0	0	0	0	0	0	0	0	0	0	0	0
Yr15/6*Avocet S	0	0	0	0	0	0	0	0	0	0	0	0	0	0	0
Yr17/6*Avocet S	40	2	40	5	40	5	30	0	10	0	25	20	5	50	0
Yr18/6*Avocet S	40	5	80	30	30	30	40	0	20	5	60	70	15	60	30
Yr24/6*Avocet S	5	0	10	10	10	15	20	10	30	0	10	10	0	0	15

Yr26/6*Avocet S	15	2	20	5	5	5	15	5	20	0	10	20	0	0	5
Yr27/6*Avocet S	10	1	7	2	5	15	5	5	5	0	20	20	5	5	10
Yr32/6*Avocet S	50	20	40	10	20	40	20	10	30	2	40	70	10	50	20
YrSp/6*Avocet S	30	2	3	2	20	40	5	5	10	0	50	30	5	10	5
Jupateco R (*Yr18*)	5	5	15	15	5	20	10	0	10	5	20	30	0	5	40
Jupateco S	40	20	15	40	10	70	40	20	40	10	40	80	0	30	80
Avocet R (*YrA*)	30	20	20	40	5	80	50	40	50	5	60	90	60	30	70
Avocet S	70	40	80	50	15	90	70	10	60	10	70	70	40	90	60
Egret	15	40	10	30	20	70	50	5	15	15	50	70	0	40	80
Bowerbird	10	10	15	25	15	20	40	5	30	15	40	20	2	40	80
Brennan	5	5	2	10	5	10	5	0	0	0	40	10	0	10	5
Crusader	5	0	2	2	5	2	15	0	2	0	5	5	0	5	2
H45	30	30	50	60	30	20	80	2	20	20	60	60	2	80	60
Chinese 166 (*Yr1*)	15	1	1	0	5	0	1	0	2	0	0	0	2	50	5
Lee (*Yr7*)	15	2	30	50	10	40	20	0	50	2	50	20	5	30	70
H. Koben(*Yr2,Yr6*)	20	1	40	40	5	50	15	15	60	2	40	30	10	30	40
Vilmorin 23 (*Yr3*)	0	0	20	15	0	10	2	0	0	0	0	5	0	0	0
Moro (*Yr10*)	0	0	0	0	0	0	0	0	0	0	0	0	0	0	0
Strubes Dickkopf	1	0	30	10	1	40	10	0	0	0	40	10	0	10	20
Suwon 92/Omar	15	10	60	60	20	70	30	0	0	20	60	10	80	60	70
Clement (*Yr2, Yr9*)	5	0	30	5	1	15	2	0	0	2	15	2	20	0	5
T. spelta (*Yr5*)	0	0	0	0	0	0	0	0	0	0	0	0	0	0	0
Hybrid 46 (*Yr4*)	0	0	0	0	0	0	0	0	0	0	0	0	0	0	0
Reichersberg42 (*Yr7*)	0	0	0	0	0	0	0	0	0	0	0	0	0	10	5
H. Peko (*Yr2*, *Yr6*)	0	0	0	0	0	5	10	0	0	0	5	2	2	2	0
Nord Desprez	0	0	15	5	0	30	20	2	15	0	5	15	0	0	20
Compare (*Yr8*)	10	2	5	5	5	30	50	10	10	0	40	30	0	5	20
Carstens V (*Yr32*)	0	0	0	0	0	0	0	0	0	0	0	0	0	0	5
S. Prolific (*YrSp*)	2	2	5	5	0	10	50	0	5	0	30	10	0	15	10
Heines VII (*Yr2, Yr25*)	1	0	2	5	-	0	5	0	0	0	0	0	0	5	m
Avocet R (*YrA*)	1	5	0	5	10	50	15	0	0	2	30	10	2	20	m
Kalyansona (*Yr2*)	30	30	5	30	20	90	70	10	50	30	70	80	30	60	70
Trident (*Yr17*)	30	10	10	10	10	50	40	15	25	5	70	60	10	50	70
Yr15/6*AvS	60	0	4	10	40	15	10	2	10	0	5	10	50	10	20
Hugenoot (*Yr25*)	0	0	1	0	0	0	0	0	0	0	0	0	0	2	0
Selkirk (*Yr27*)	20	2	10	5	10	80	20	0	10	0	60	30	0	15	50
EGA Gregory (*Yr33*)	5	0	0	0	0	0	0	0	0	0	0	0	0	0	20
Ellison	-	2	15	5	10	5	20	0	2	0	10	30	0	2	30
Binnu	10	0	1	1	10	10	15	0	2	0	5	5	2	0	0
Breakwell	30	0	2	5	40	20	40	0	15	0	50	5	15	5	5
Tobruk	10	1	0	1	5	40	30	0	30	0	0	0	30	0	40
	0	0	0	0	5	2	0	0	0	0	0	0	5	0	0

[1] Locations: ESC = Escacena del Campo, ECI = Ecija, JER = Jerez de la Frontera. The number indicates the year of trial (e.g., 16=2016).
[2] Pst lineages according to GRRC (GRRC, 2023).

Consistent field resistance in the form of near immunity over years and locations, and over genetic background (some genes were present in lines of different backgrounds) was associated with the presence of *Yr4, Yr5, Yr10* and *Yr15.* Differential lines carrying *Yr24/Yr26* and *Yr27* genes were of particular interest since they should display horizontal resistance. Indeed, the lines known to harbor these genes exhibited low levels of infection

with slow disease progress, never reaching levels of high susceptibility in all trials, as slow-rusting genotypes theoretically should.

In some cases, lines containing the same genes displayed contrasting responses, depending on the genetic background carrying them. This was the case for lines carrying *Yr7, Yr8* and *Yrsp*. The rest of the genes were associated with field reactions typical of race-specificity with high infection in particular seasons and locations, depending on the lineages present, and with no infections in other instances. This was the case of lines carrying genes *Yr1, Yr3, Yr8* (in one background), *Yr17, Yr18, Yr25, Yr33*, and *YrA.*

3.4.2 Stem rust responses

Stem rust reaction in a set of 100 genotypes (2018-2022), as well as a set of commercial cultivars (2021-2022), was recorded in off-season summer trials, under irrigation, at the southern Spain location of Conil de la Frontera.

Results of race and DNA analyses indicated the presence of two races across the five testing seasons involved in the present work: Clade IV-B (TKTTF) and Clade IV-F (TKKTF), which is consistent with the GRRC information for Spain (Table 3.6). The key gene to differentiate the Clade IV-B and Clade IV-F from the Sicilian race is *Sr13*. The Spanish races should be avirulent on this gene, while the Sicilian race is virulent. In the present study, lines carrying *Sr13* genes displayed resistance, albeit partial in its expression in some cases. Similarly, races from Clade IV-B and Clade IV-F could be differentiated from the Ug99 lineage based on virulence on both *Sr31* and *Sr36*. The line harboring *Sr31* was resistant to the Spanish races, while the line with *Sr36* showed susceptibility, confirming that the races present in this study were of Clade IV-B and Clade IV-F.

Table 3.6 Virulence spectrum of the two main races of stem rust reported in southern Spain compared to that of a race from the Ug99 lineage and the Sicilian race.

	Virulence on known *Sr* genes present in wheat differential lines																				
Race name (origin)																					
TKKTF (Spain)	*5*	*21*	*9e*	*7b*	-	*6*	*8a*	*9g*	-	*9b*	*30*	*17*	*9a*	*9d*	*10*	*Tm*	-	*38*	*McN*	-	
TKTTF (Spain)	*5*	*21*	*9e*	*7b*	-	*6*	*8a*	*9g*	*36*	*9b*	*30*	*17*	*9a*	*9d*	*10*	*Tm*	-	*38*	*McN*	-	
TTKSK (Ug99)	*5*	*21*	*9e*	*7b*	*11*	*6*	*8a*	*9g*	-	*9b*	*30*	*17*	*9a*	*9d*	*10*	-	*31*	*38*	*McN*	-	
TTRTF (Sicily)	*5*	*21*	*9e*	*7b*	*11*	*6*	*8a*	*9g*	*36*	*9b*	-	*17*	*9a*	*9d*	*10*	*Tm*	-	*38*	*McN*	*13*	

In Table 3.7, an analysis of variance is shown using genotype as factors and years as replications. The differences between the lines were significant with respect to their severity, showing that the ranking of severity or resistance due to a particular gene remained similar over the years of the study.

Table 3.7 ANOVA Table for stem rust AUDPC for 100 genotypes evaluated for five years (years considered a replications) under natural infection at Conil, in the south of Spain, during the summer counter-season under irrigation.

Source	Sum of Squares	Df	Mean Square	F-Ratio	P-Value
Between groups	3.59	99	3.63	4.0	0.0000
Within groups	3.66	400	914,606		
Total (Corr.)	7.25	499			

With regards to the reaction of commercial cultivars evaluated for two seasons (2021 and 2022), results presented in Table 3.8 indicate that cultivars Athoris and Euroduro were highly susceptible to susceptible, respectively. Cultivar Don Ricardo exhibited an intermediate and possibly useful level of resistance, while cultivars Amilcar and Calero showed high levels of resistance. In bread wheat, cultivar Tocayo was very susceptible, as expected given that it was considered the susceptible check, and cultivar Arthur Nick exhibited a reaction that could be considered as moderately to fully susceptible. Cultivar Tejada was characterized by an intermediate level of resistance, certainly interesting and potentially useful. Finally, cultivars Conil and Escacena were found to have high levels of resistance to the prevailing races. The two modern triticale cultivars, namely Bondadoso and Valeroso, were completely immune to stem rust, while the old and obsolete cultivar Trujillo, exhibited an intermediate level of resistance, but clearly allowing for some development of the pathogen.

Table 3.8 Stem rust AUDPC data calculated for commercial cultivars in off-season field trials (summer under irrigation) under natural infection at the southern Spain location of Conil.

	AUDPC		
Cultivar	2021	2022	**Mean**
Durum Wheat			
Amilcar	14	0	**7**
Euroduro	945	780	**863**
Athoris	1,400	1,135	**1,268**
Don Ricardo	70	78	**74**
Calero (rc)[1]	14	0	**4**
Bread Wheat			
Arthur Nick	574	642	**608**
Tejada	35	215	**125**
Conil	0	78	**39**
Escacena	0	16	**8**
Tocayo (sc)[1]	1,260	1,572	**1,416**
Triticale			
Bondadoso	0	0	**0**
Valeroso	0	0	**0**
Trujillo	14	175	**95**

[1]Tocayo and Calero were susceptible (sc) and resistant (rc) checks.

In order to assess the genetic resistance options available against the Spanish stem rust races, we have assembled a set of 100 genotypes, including the stem rust differentials series, some breeding lines with known reactions to the African races of stem rust (based

on CIMMYT data from the precision phenotyping platforms established in Ethiopia and Kenya), other with known resistance genes introgressed through marker-assisted selection at CIMMYT, and finally some sources of resistance used in the CIMMT program. This set was evaluated under natural infection, during the counter-season under irrigation, at the southern Spain location of Conil for five seasons (2018 to 2022). It was also evaluated at the Jerez location in 2022, when stem rust was observed at high incidence levels during the main season. Results of the AUDPC calculated for each genotype are shown in Table 3.9. In all seasons, the inoculum pressure was strong, the environmental conditions were favorable, and the stem rust severity was ultimately high, allowing for reliable discrimination between genotypes, without possibility of escape.

In the first sub-group of lines, genotypes number 1 to 34, we can observe a general coincidence between the reaction to the Spanish races over the five seasons and the summary information from data collected in Ethiopia and Kenya for the same material. Several exceptions are indeed observed, but the general tendency is present. Lines with good resistance to the African races in Ethiopia and Kenya are, on average, more resistant in Spain than those that are susceptible to the African races. As the resistance to the African races decreases, the susceptibility to the Spanish races increases dramatically.

Within the lines with specific genes of resistance introgressed through marker-assisted selection, the results indicate that *Sr25* (line 35) and *Sr22* (line 38), in monogenic state, provide good to intermediate levels of resistance to the Spanish races, depending on the season. Lines with both *Sr22* and *Sr25* present together (lines 39 and 40) were characterized by the highest levels of resistance among this group. Lines with *Sr38* have shown variable reactions, from complete resistance (line 1) to intermediate resistance (line 36) to outright susceptibility (line 37). Among the sources identified by CIMMYT over the years for their resistance to the Ethiopian races (lines 41 to 60), some maintained high levels of resistance to the Spanish races, including modern cv. Amria (Morocco), CIMMYT breeding line 45, and old landrace type Iumillo (line 42). Another accession of Iumillo (line 54) shows high infection levels indicative of susceptibility, possibly indicating the existence of different biotypes within the landrace or misclassification of the seed source. Among the same group, other sources with good resistance in Ethiopia were characterized by intermediate, possibly interesting, levels of resistance to the Spanish races, including breeding line 46, and modern cvs. Kronos (USA), Westbred 881 (USA), Calero (Spain) and Carpio (Spain), old and tall cvs. Boohai (Ethiopia), Trinakria (Italy), and landrace type Khapli (India). One surprising result was the high level of susceptibility of landrace type Reichenbachii (Turkey) which is one of the sources of resistance most effective against the African races in Ethiopia and Kenya and used significantly in the CIMMYT breeding program. Finally, sources of resistance gene *Sr47* (USA), namely lines 56 to 58, exhibited promising levels of resistance, consistent with their field adult-plant reaction to the African races in Ethiopia. Among the stem rust differentials lines, only line 96, carrying *Sr32*, exhibited high levels of resistance, albeit variable over years. Lines carrying genes *Sr27*, *Sr33* and *Sr35* had intermediate resistance levels on average, again highly variable between years. The rest of the differential lines were characterized by intermediate to very high susceptibility levels.

Table 3.9 Stem rust AUDPC in four sets of differentials in off-season (summer) field trials at Conil (Cadiz) and severity (%) at one normal season (spring 2022, Jerez).

Line	Genotype	Reaction in Ethiopia/Kenya	AUDPC						%Sev.
number	designation	Known genes	2018	2019	2020	2021	2022	Mean	JER22
Lines with known reaction to stem rust in Ethiopia and/or Kenya									
1	CIMMYT LINE 1	Resistant in Ethiopia - *Sr38*	0	0	0	0	0	**0**	**0**
2	CIMMYT LINE 2	Resistant in Ethiopia	89	28	125	738	383	**272**	**10**
3	CIMMYT LINE 3	Resistant in Ethiopia	120	150	125	747	270	**282**	**10**
4	CIMMYT LINE 4	Resistant in Ethiopia & Kenya	134	204	302	737	383	**352**	**0**
5	CIMMYT LINE 5	Resistant in Ethiopia & Kenya	254	275	508	1463	512	**602**	**15**
6	CIMMYT LINE 6	Resistant in Ethiopia & Kenya	178	295	413	1110	693	**538**	**10**
7	CIMMYT LINE 7	Resistant in Ethiopia & Kenya	18	16	38	263	135	**94**	**10**
8	CIMMYT LINE 8	Resistant in Ethiopia & Kenya	147	255	272	940	422	**407**	**20**
9	CIMMYT LINE 9	Resistant in Ethiopia & Kenya	260	304	413	1552	608	**627**	**10**
10	CIMMYT LINE 10	Moderately resistant in Ethiopia & Kenya	291	173	783	1630	869	**749**	**30**
11	CIMMYT LINE 11	Moderately resistant in Ethiopia & Kenya	63	95	310	1033	400	**380**	**20**
12	CIMMYT LINE 12	Moderately resistant in Ethiopia & Kenya	88	155	332	867	555	**399**	**20**
13	CIMMYT LINE 13	Moderately resistant in Ethiopia & Kenya	235	215	550	1334	515	**570**	**20**
14	CIMMYT LINE 14	Susceptible in Ethiopia & resistant in Kenya	228	353	666	1203	473	**584**	**20**
15	CIMMYT LINE 15	Susceptible in Ethiopia & resistant in Kenya	265	428	446	1318	583	**608**	**10**
16	CIMMYT LINE 16	Susceptible in Ethiopia & resistant in Kenya	428	556	783	1883	738	**878**	**10**
17	CIMMYT LINE 17	Susceptible in Ethiopia & resistant in Kenya	158	318	291	737	327	**366**	**15**
18	CIMMYT LINE 18	Susceptible in Ethiopia & resistant in Kenya	291	1128	525	1627	784	**871**	**30**
19	CIMMYT LINE 19	Susceptible in Ethiopia & Kenya	1105	1881	2380	5320	3290	**2795**	**70**
20	CIMMYT LINE 20	Susceptible in Ethiopia & Kenya	1128	1821	2390	5465	3375	**2836**	**40**
21	CIMMYT LINE 21	Susceptible in Ethiopia & Kenya	1040	1528	2390	5325	2922	**2641**	**50**
22	CIMMYT LINE 22	Susceptible in Ethiopia & Kenya	900	1516	1805	5070	2897	**2438**	**50**
23	CIMMYT LINE 23	Susceptible in Ethiopia & Kenya	816	1841	1565	4415	2802	**2288**	**60**
24	CIMMYT LINE 24	Susceptible in Ethiopia & Kenya	731	1971	1655	4928	3745	**2606**	**70**
25	CIMMYT LINE 25	Susceptible in Ethiopia & Kenya	936	2498	2110	5180	4050	**2955**	**70**
26	CIMMYT LINE 26	Susceptible in Ethiopia & Kenya	936	2018	2150	5413	3520	**2807**	**70**
27	CIMMYT LINE 27	Susceptible in Ethiopia & Kenya	458	1350	1350	3828	2915	**1980**	**60**
28	CIMMYT LINE 28	Susceptible in Ethiopia & Kenya	355	743	723	1897	827	**909**	**30**
29	CIMMYT LINE 29	Susceptible in Ethiopia & Kenya	1010	1488	2280	5203	2472	**2491**	**40**
30	CIMMYT LINE 30	Susceptible in Ethiopia & Kenya	961	1635	2355	5040	2290	**2456**	**50**
31	CIMMYT LINE 31	Susceptible in Ethiopia & Kenya	1315	1808	2210	5430	2787	**2710**	**60**
32	CIMMYT LINE 32	Susceptible in Ethiopia & Kenya	1301	1643	2320	5308	2742	**2663**	**40**
33	CIMMYT LINE 33	Susceptible in Ethiopia & Kenya	1026	1449	1980	5010	2517	**2396**	**60**
34	CIMMYT LINE 34	Susceptible in Ethiopia & Kenya	919	1155	1545	4638	2232	**2098**	**50**
Lines with known resistance genes introgressed through marker-assisted selection									
35	CIMMYT LINE 35	Resistant -*Sr25* Monogenic	141	175	185	985	400	**377**	**15**
36	CIMMYT LINE 36	Resistant - *Sr38*	133	285	272	1151	900	**548**	**10**
37	CIMMYT LINE 37	Susceptible - *Sr38* (marker only?)	661	494	1465	2778	1079	**1295**	**40**
38	CIMMYT LINE 38	Resistant - *Sr22*	111	618	163	456	445	**358**	**30**
39	CIMMYT LINE 39	Resistant - *Sr22+Sr25*	5	0	0	0	630	**127**	**0**
40	CIMMYT LINE 40	Resistant - *Sr22+Sr25*	24	8	0	0	225	**51**	**0**
Various sources of resistance and suceptible checks									
41	AMRIA	Resistant in Ethiopia	181	0	60	979	0	**244**	**10**
42	IUMILLO	Resistant in Ethiopia	18	23	0	384	0	**85**	**5**
43	KHAPLI	Resistant in Ethiopia	298	34	0	1395	315	**408**	**0**
44	SNITAN*2/RBC	Resistant in Ethiopia	438	470	555	2067	353	**776**	**40**
45	JUPARE C 2001*2/KHAPLI	Resistant in Ethiopia	5	20	0	155	450	**126**	**10**
46	JUPARE C 2001*2/RBC	Resistant in Ethiopia	191	106	383	798	563	**408**	**30**
47	BOOHAI	Resistant in Ethiopia	215	109	56	1344	113	**367**	**30**
48	KRONOS	Resistant in Ethiopia	446	193	272	1548	315	**555**	**20**
49	TRINAKRIA	Resistant in Ethiopia	234	129	177	867	439	**369**	**20**
50	WESTBRED 881	Resistant in Ethiopia	211	129	56	1290	405	**418**	**0**
51	CALERO	Resistant in Ethiopia	336	135	639	564	1070	**549**	**15**
52	CARPIO	Resistant in Ethiopia	241	251	272	410	468	**328**	**15**
53	ATRED #1	Susceptible in Ethiopia	1495	869	2070	4233	2473	**2228**	**60**
54	IUMILLO	Susceptible in Ethiopia	489	384	1098	2275	685	**986**	**40**
55	REICHENBACHII	Resistant in Ethiopia	486	629	1225	2580	1622	**1308**	**40**
56	RWG35-*Sr47*	Resistant in Ethiopia	85	320	86	630	743	**373**	**10**
57	RWG36-*Sr47*	Resistant in Ethiopia	72	234	12	541	630	**298**	**0**
58	RWG37-*Sr47*	Resistant in Ethiopia	211	523	250	689	332	**401**	**0**
59	ATRED #2	Susceptible in Ethiopia	1248	1623	1565	5180	2410	**2405**	**60**
60	SOOTY_9/RASCON_37	Susceptible in Ethiopia	925	1420	1750	4433	2410	**2188**	**60**

Stem rust differentials									
61	ISR5-RA	CI14159	376	830	978	2102	1070	**1071**	**20**
62	ISR6-RA	-SR6	321	873	1235	2458	1020	**1181**	**40**
63	ISR7B-RA	SR7B-?	370	712	1263	2472	1250	**1213**	**50**
64	ISR8A-RA	CI14176	435	947	1595	2405	1125	**1301**	**30**
65	ISR9A-RA		418	660	1200	2440	817	**1107**	**50**
66	W2691 SR9B	SR9B-?	978	918	930	2440	1825	**1418**	**70**
67	VERNSTEIN-SR9E	CI3686	825	1864	2000	4538	2310	**2307**	**50**
68	CNS TC 2B/LINE E, SR9G		1091	1568	2850	4700	3288	**2699**	**30**
69	ISR9D-RA	SR9D-?	592	1202	3045	2940	1697	**1895**	**30**
70	W2691 SR10	SR10-?	1058	1471	2610	3273	1580	**1998**	**60**
71	ISR11-RA	SR11-?	261	361	570	1545	955	**738**	**50**
72	COMB.VII-SR17,SR13	CRL1.15	459	752	690	1675	1025	**920**	**20**
73	T. MONOCOCCUM-SR21+	CRL5.23	315	811	323	2298	2805	**1310**	**40**
74	LCSR24AG	-SR24	159	503	413	1980	1183	**848**	**30**
75	BTSR30WST	SR30	567	988	723	4588	2565	**1886**	**50**
76	SR31/6*LMPG	-SR31	476	1272	1125	4052	2020	**1789**	**50**
77	W2691SRTT-1	SR36-?	543	1646	1640	4400	1990	**2044**	**50**
78	CNSSRTMP	-SRTMP	501	1297	1153	4012	1621	**1717**	**40**
79	TRIDENT		475	1015	1355	3563	1374	**1556**	**50**
80	MCNAIR-701		618	1320	2300	3300	2062	**1920**	**50**
81	MDS/W2691/-SR7A,SR10	II71.330.11	575	1568	1540	3998	3322	**2201**	**60**
82	BARLETA BENVENUTO,SR8B		593	1528	1200	4320	2675	**2063**	**50**
83	ISR5SB-SR9F	CI14162	357	856	663	2420	1295	**1118**	**60**
84	BTSR 12TC		316	1325	900	2380	1275	**1239**	**50**
85	W2691Sr13		430	1451	1193	1482	439	**999**	**50**
86	W2691*2/NORKA-SR15	CRL1.13	933	1663	2660	4915	3765	**2787**	**70**
87	ISR16RA	SR16-?	252	829	875	2028	1887	**1174**	**60**
88	LC-SR19-MQ		292	913	1350	2560	1677	**1358**	**70**
89	LC-SR20-MQ		508	1206	1500	3683	2930	**1965**	**60**
90	SWSR22T.B.	IL70.565.11-?	530	701	413	1792	1150	**917**	**50**
91	EXCHANGE-SR23,SRMCN	CI12635	530	754	840	2385	1987	**1299**	**50**
92	LC-SR25-ARS		532	703	963	2720	2162	**1416**	**60**
93	EAGLE-SR26,SR9G		616	313	701	2955	2042	**1325**	**60**
94	COORONG TRITICALE-SR27		230	252	538	1295	560	**575**	**20**
95	PUSA/EDCH-SR29		491	533	848	1965	1887	**1145**	**60**
96	C77.19 SR32		225	181	185	497	335	**284**	**20**
97	TETRA CANTHATCH/AE.SQ-S	RL5405	401	310	204	1122	488	**505**	**40**
98	COMPAIR-SR34	PI325842	325	393	808	1795	1445	**953**	**60**
99	W3763-SR35		41	398	375	715	1143	**534**	**15**
100	W2691 SR37TT2	CRL5.171.B	666	1005	1845	2047	700	**1253**	**50**

3.5 Discussion

In southern Spain, wheat is produced primarily under rainfed, often drought-prone, conditions with highly variable, but generally low yields, depending primarily on the amount and distribution of rainfall during the cropping season (Table 3.1). In such an extensive and relatively high-risk production system, the economic viability of any crop requires the maximization of yield potential expression under the prevailing climate conditions in any given year and the minimization of production costs. Genetic control of rust diseases, possibly the biotic factor most likely to prevent maximum yield expression in the region, does both. Not only is it key to the economic viability of wheat, but it also reduces the environmental footprint of the crop and the entire production system. The first step in achieving effective and durable genetic control of rust diseases is the thorough characterization of the lineages/races of the pathogen present in the region and the adjacent areas. The second step involves assessing the previously characterized genetic options available (known resistance genes) as well as non-characterized resistance sources for their suitability against the prevailing lineages/races of the pathogen. The objectives of the present study were to collect such information and provide such an

assessment for the south of Spain, with the ultimate goal of guiding breeding and variety selection programs serving the region in their efforts to develop and deploy cultivars with effective and durable resistance to yellow and stem rust.

The present study relied exclusively on natural infection of both rusts. This ensured that pathogen sampling for race analyses and genotyping did involve lineages/races that were representative of those actually present and relevant in the region. The long duration of the study (seven years) also contributes to the robustness and relevance of our results. The results reported herein were exclusively from location/year combinations where disease incidence was sufficiently high and uniform to enable the reliable differentiation between genotypes. Location/year combinations with too little or no disease incidence were not considered.

Results from samples taken from plots from the present study indicated that yellow rust lineages PstS10 (Warrior-), PstS13, and PstS14 prevailed in southern Spain in recent years. Reports from other areas of Spain also refer to the presence of PstS4 and PstS7 (Warrior). Some of these lineages were known to be present in the Guadalquivir valley (Martínez-Moreno and Solís, 2019), but did not cause serious epidemics until 2015, when an outbreak in northern Spain was attributed to the Warrior race. This race, previously described in Denmark, France, England, Germany, and Sweden, circumvented the resistance of most commercial wheat cultivars in these countries. It is reported to have originated in the Himalayan region of Pakistan, subsequently spreading rapidly throughout the wheat area of Europe (Ma et al., 1995, Hovmoller et al., 2016). The region where our research was conducted, was in fact, one of the last to be reached by this race, probably because it was in the far southwestern corner of Europe with infrequent occurrences of favorable weather conditions. The newer lineages, PstS13 and PstS14, are probably those to pay more attention to, as their presence was generally associated with slightly higher disease incidence on commercial cultivars evaluated in this study. This was particularly visible in the commercial durum wheat cultivars, with the appearance of some incidence, albeit at very low levels, during the last years of the study, as PstS13 and PstS14 became present. PstS14 was detected in 2016 in Morocco and Sicily (Italy) by the GRRC. This lineage (virulent on *Yr2, Yr3, Yr6, Yr7, Yr8, Yr9, Yr17, Yr25, Yr32*, and *YrSp*) was first detected in Spain in 2017 (GRRC, 2023).

The monitoring of the reaction of commercially grown cultivar of bread wheat, durum wheat and triticale has been useful to provide an assessment of the risk facing the southern Spain wheat production sector, and how urgent it is to mitigate it. The fact that highly resistant, locally adapted, commercially successful, cultivars exist for the three crops, is a very positive outcome as they provide immediate genetic solutions to the threat of yellow rust, on the wheat production in southern Spain, solutions that seed companies and growers have successfully deployed and that breeding entities could use as sources of resistance in their improvement programs.

While the number of commercial cultivars of each crop evaluated in this study may be too small to make generalized inferences on the resistance to yellow rust of the different species, our results clearly indicate that the durum wheat and triticale cultivars evaluated were much less affected by the southern Spanish lineages of yellow rust than bread wheat. Durum wheat cultivars were in most instances immune to the disease, and even when some symptoms were present, generally starting the 4th year of the study, they amounted to very low infection scores, too low to consider them susceptible. One possible exception may be the cultivar Athoris, which closely approached a susceptible score, but only at one location in the last year of the study. Recently released commercial triticale cultivars also maintained near-immunity or immunity to yellow rust over the duration of the study. The old cultivar Trujillo, selected from a group of CIMMYT lines released in the early 1980s in several countries worldwide, has lost its resistance to yellow rust (and other diseases) decades ago in Mexico, Spain and Tunisia (M.S. Gharbi, personal communication). While this was reflected during the duration of this study, Trujillo susceptibility levels remained inferior to those observed in the susceptible bread wheats. While resistant bread wheat cultivars Tejada and Arthur Nick exhibited resistance levels similar to that of resistant durum wheat and triticale cultivars, susceptible cultivars Califa and Escacena were characterized by levels of susceptibility unseen in the other two species.

The generally better and, to a certain extent, more frequently seen genetic resistance of durum wheat and triticale compared to bread wheat observed in the small sample of cultivars evaluated in this study, has been observed more widely in the south of Spain and worldwide. Among the germplasm of the three crops annually sent by CIMMYT to southern Spain for the past 20 years, highly susceptible durum or triticale lines were extremely rare, but highly susceptible bread wheat lines were regularly observed, albeit at a low frequency. Unpublished data collected from International Nurseries distributed globally by CIMMYT to numerous cooperators worldwide, indicate that the great majority of the CIMMYT durum wheat germplasm exhibits virtually generalized high level resistance, almost everywhere it is tested. On the other hand, a significant, even though generally low, frequency of susceptibility can be seen in the CIMMYT bread wheat germplasm distributed in the same International Nurseries.

The results of this study and the information discussed in the above paragraph may objectively indicate less of an emergency to work on enhancing the genetic basis for resistance to yellow rust in durum wheat. However, recent developments in the pathogen's populations in Chile should serve as a call for vigilance for breeding programs working with this crop. In 2019, a never-before-seen yellow rust epidemic appeared in commercial durum wheat fields in central Chile and, in the experimental fields of the national program, 70% of the lines evaluated as part of CIMMYT's International Durum Wheat Screening Nursery exhibited, atypically, high levels of susceptibility to the disease (I. Matus, INIA-Chile, personal communication), while the same germplasm maintained its virtually generalized resistance to yellow rust everywhere it was tested outside of Chile (data not published). Thousands of breeding lines from the CIMMYT program were subsequently send to INIA Chile for evaluation of their reaction to the local race of yellow

rust, confirming the very high frequency (close to 70%) of susceptible lines, within this germplasm group. While there is no evidence so far that this race made it out of Chile, durum wheat breeders in the Mediterranean basin, including those providing germplasm to southern Spain, need to assess the risks associated with such a devastating race appearing in their region. The collaboration between INIA-Chile and CIMMYT to address this threat to the local durum production has also resulted in a proactive preventive breeding effort by CIMMYT, to increase the frequency of resistance to the Chilean race in its germplasm pool.

Since the 1970s, a significant part of the spring bread wheat cultivars sown in southern Spain originated from the Mexico-based CIMMYT breeding program. A wide range of *Yr* genes were deployed by this program, such as *Yr6*, *Yr9* and *Yr17*. These were quite common in the past, but their resistance has been overcome by new races. On the other hand, *Yr27*, a gene still used by CIMMYT and most likely present in the bread wheat material planted in Andalusia, is effective against the Warriors lineage (Ali et al., 2017, Hovmoller et al., 2016, Yan et al., 2003). In this study, this gene has provided an intermediate resistance. The other genes that are worth mentioning in terms of their usefulness against the southern Spanish lineages are *Yr5*, *Yr10* and *Yr15*, which presence in the differentials series was associated with an immune reaction for the duration of the study. *Yr5*, located on chromosome 2BL, is effective against most yellow rust races worldwide and originated from *T. spelta* (Yan et al., 2003). *Yr15* is another gene that is performing well all over the world, including against the Warrior races. It originated from wild emmer (*T. turgidum* ssp. *dicoccoides*) and was transferred to chromosome 1BS of bread and durum wheat. It has been recently cloned and found to encode a compound protein kinase-pseudokinase in tandem (Klymiuk et al., 2018). Because of their global effectiveness against most yellow rust races worldwide, and the availability of reliable molecular markers, that could facilitate their introgression in elite germplasm, these genes represent very attractive protective solutions, and are bound to be used extensively by breeding programs worldwide and deployed over large production areas across continents. This could, theoretically, expose them to being circumvented by rapidly evolving pathogen populations, as seen in the past for many such genes. It is therefore useful to keep characterizing new sources of effective resistance to yellow rust, to facilitate their use in breeding and provide wheat breeders and variety developers, with a more ample and diversified set of genetic options to mitigate the threat of yellow rust.

Unlike yellow rust, stem rust is not yet a commercial problem in Spain, but, in recent years, the pathogen occasionally appeared at the end of the regular wheat growing season in the south of the country. Historically, when the very late maturing and generally stem rust susceptible landraces were grown extensively around the Mediterranean basin, the disease was not uncommon. It was a scenario of a susceptible host maintaining green tissue well into the late spring season (May-June) providing the late appearing pathogen with favorable conditions to successfully infect the crop. With the complete displacement of these landraces by the earlier, fast maturing semi-dwarf wheats from the Green Revolution, which also were mostly resistant to the older stem rust races in the region thanks to the effective genes *Sr2* and *Sr31*, the disease virtually disappeared and stopped

being a yield threatening concern. However, recent developments in the pathogen populations and more regular appearances of the disease around the Mediterranean basin, as presented in the introduction, have raised concerns, and prompted us to consider stem rust as a potential emerging threat to wheat production in southern Spain.

All evaluations were again done relying exclusively on natural infections, that occurred during each of the five years of this study and developed into intense epidemics, thanks to the weekly irrigations implemented for the summer sowing (off-season planting), which brings together green leaf tissue from susceptible hosts, a virulent pathogen, and favorable conditions for infection. Based on the off-season field readings from this study and DNA analysis at the GRRC, the predominant groups present during the current study were Clade IV-B (TKKTF) and Clade IV-F (TKTTF) (GRRC, 2023). As reported by Abdedayem et al. (2023), stem rust has recently reappeared in many parts of Europe, and Clade IV-B and Clade IV-F were found to be present in Spain, Italy, France, Morocco, and Tunisia. The presence of the Sicilian TTRTF race in southern Spain and during the present study was considered improbable, as this race is virulent on *Sr13* (Olivera et al., 2021), and the line harboring *Sr13* was always resistant (partial resistance) over the duration of this study. Molecular markers identified 37 strains collected in France in 2021, as part of the sampling campaign from the RustWatch (European project coordinated from the GRRC aimed at characterizing the main rusts races in Europe). All of them clustered into two genetic groups, namely Clade IV-B and Clade IV-F. These two groups were already detected in 2019 and 2020 in nurseries of Île-de-France and in 2018 and 2019 in Italy. All this information strongly indicates that these are indeed the main stem rust races in Mediterranean Europe (Hovmoller et al., 2023), and probably also in North Africa. Besides, according to DNA analyses of samples sent to the GRRC from all parts of Europe, the races of the Ug99 family have not reached Europe. This was confirmed in the case of southern Spain as the local races and the Ug99 lineage differed in their virulence on *Sr24* and *Sr31* (Bhavani et al, 2019, Hale et al., 2013, Shahin et al., 2020).

Another clear difference between yellow and stem rust resides in the level of expression of their resistance. While resistance for yellow rust was often expressed as a fully immune reaction (complete absence of pustules), such reaction was very rare for stem rust (1 genotype out of the 100 evaluated in the present study), including when genes know to have major effects, such as *Sr22*, *Sr25* and the combination of both, were present. None of the differential lines exhibited a near immune reaction indicating that no known *R*-gene would in fact provide such a "clean" reaction. This is consistent with the observations made by Ethiopian and CIMMYT scientists over many years, screening thousands of lines in Ethiopia, at the Debre Zeit experimental site hosted by the Ethiopian Institute of Agricultural Research (EIAR). This different expression of resistance to stem rust is important to point out as breeding programs around the Mediterranean basin have traditionally selected immune types with regards to leaf and yellow rusts. Those contemplating local resistance breeding efforts against stem rust will need to adjust their visual selection thresholds for what would constitute an effective and useful resistance level.

Results from the monitoring of the reaction to stem rust of the main cultivars grown in Spain, clearly indicate suitable commercial genetic solutions are immediately available to farmers in the south of Spain, should this disease become an issue in the main season. While the probability of this happening may be considered low, it did indeed materialize during the present study at the Jerez location in 2022. Durum cultivars Amilcar, Don Ricardo and Calero, bread wheat cultivars Tejada and even Conil, and triticale cultivar Bondadoso and Valeroso, were consistently resistant to both yellow and stem rusts. While the commercial availability of locally adapted cultivars with such resistance is a very positive result, it is important to keep in mind the virulence spectrum of the races these commercial cultivars were resistant to, particularly with regards to the avirulence of the Spanish races on *Sr13*. Virulence on *Sr13*, a gene that has substantially contributed to the protection of durum wheat from several germplasm pool, while still absent in Spain, is present in the south of Italy, and it is unavoidable to assume that this virulence will soon reach the south of Spain. Results from screening a large collection of durum wheat lines from different germplasm pools against the race JRCQC (with combined virulence on *Sr9e* and *Sr13*) (Olivera et al., 2012), revealed a very low frequency of resistance, reportedly 5.2% (Olivera et al., 2010). The very low frequency of resistance against the Ethiopian races, with combined virulence on *Sr9e* and *Sr13*, was consistently confirmed upon screening thousands of CIMMYT lines over years in Ethiopia (data not published). In this context, it becomes clear that the races currently present in Spain do not represent an unmanageable threat to the local wheat production, but that the most important and consequential threat would come from an eventual appearance of races with *Sr13* virulence. Any preventive breeding effort or variety selection program to provide stem rust resistant cultivars for the south of Spain should be aiming at resistance to races with combined virulence on *Sr13/Sr9e*, and not resistance merely to the races currently present in Spain. This can be effectively addressed using recent CIMMYT germplasm that was pre-screened for resistance to the African races, either to the Ug99 lineages via the selection in Kenya for bread wheat or to the *Sr13/Sr9e* virulence, via evaluation of lines in Ethiopia for durum wheat. Results from the present study confirm the suitability of this approach, as many of the durum lines known to have acceptable levels of resistance in Ethiopia and Kenya were also resistant to the currently present races in the south of Spain.

In terms of the usefulness for the south of Spain of single genes or gene combinations known to provide good resistance to stem rust globally, *Sr22* and *Sr25* in a monogenic state, were found to provide adequate protection against the Spanish races in the present study, while also known to be effective against the African stem rust races (data not published). *Sr22* originated from *T. monococcum ssp. boeoticum* and *T. monococcum* and the translocated segment has been mapped on chromosome 7AL of wheat (Khan et al., 2005). It has not been extensively used due to an associated yield penalty and a delay in heading date (Khan et al., 2005). In fact, the *Sr22* introgression line used in this study, is agronomically inferior and, based on unpublished CIMMYT data, has limited yield potential and drought tolerance, and was therefore never distributed globally, but used as new donor of the gene for subsequent crossing/selection to pyramid

with other resistance genes, while selecting for better agronomic types with the least possible yield penalty. *Sr25*, linked to *Lr19*, was transferred to bread wheat in a translocated segment from *Lophopyrum ponticum*, also mapping on chromosome 7AL. It has been extensively deployed in many spring bread wheat cultivars of the middle and lower Volga regions of Russia (Sibikeev et al., 2021); with some presence in the CIMMYT bread wheat germplasm. When introgressed into durum wheat, this gene provides good levels of resistance to the Spanish races (as indicated in the present study), as well as to the Ethiopian durum races. The first generation of CMMYT lines with *Sr25* introgressed expressed variable levels of yield penalties, especially under drought. After two cycles of crossing/selection, new CIMMYT germplasm carrying *Sr25* with no yield penalty has been developed (data not published). The combination *Sr22+Sr25* is attractive to use in breeding as loci for the two genes, are very closely linked on chromosome 7AL. Once assembled in the correct genetic configuration, they should effectively be inherited together with very little probability of being separated in further cycles of crossing/selection. The combination was found to be the most effective against the current Spanish races of stem rust, with reactions generally close to an immune response in the present study. Its use in spring bread wheat breeding programs in Russia was found to be associated with a higher ratio of dough tenacity to extensibility and lower flour strength, porosity, and bread volume (Sibikeev et al., 2021). In CIMMYT durum wheat backgrounds, the first generation of lines carrying both genes were characterized by severe yield and drought tolerance penalties, but after two cycles of crossing/selection, the last generation of such lines have compensated for much yield or drought tolerance penalties, making them useful improved parents to use in any breeding programs.

Other genes, such as *Sr38*, with limited usefulness in bread wheat breeding against stem rust may still be useful for durum wheat. Included in a translocated 2NS fragment from *T. ventricosum* onto bread wheat chromosome 2AS (Bariana et al., 1993), it was extensively used for its triple resistance to rusts, as it carries genes *Lr37* and *Yr18*, in addition to *Sr38*. This gene is now considered to have limited utility against stem rust in bread wheat. In the present study, it was carried by the cultivar Trident that was found to be susceptible to the Spanish races. However, when introgressed into a durum background, it had a variable effect against the Spanish races, ranging from complete immunity to complete susceptibility. The original introgression line (line 36) had and intermediate level of resistance to the Spanish races, with highly resistant field reactions to the African durum races in Ethiopia and Kenya. The other *Sr38* introgression line (line 37), had a rather susceptible reaction to the Spanish races, and was characterized by an intermediate to susceptible reaction against the Ethiopian races, suggesting a possible recombination between the molecular marker used in the introgression and the actual gene. Line 1 of the set evaluated herein, was a result of introgression of *Sr38* via marker-assisted selection in a CIMMYT elite background, that had already a good level of resistance to the African races of stem rust, hence its immune reaction, likely due to additive effects of several genes, including *Sr38*. Rust resistance genes with limited to no usefulness in bread wheat but with significant value for durum wheat breeding are not unheard off. A clear example is that of *Lr14a* gene for leaf rust resistance. It is useless in

bread wheat breeding, as most bread wheat leaf rust races are virulent on this gene. However, most races that are virulent on durum wheat are avirulent on *Lr14a* gene, making it one of the most useful sources of genetic resistance in durum wheat for many years (Maccaferri et al., 2010), until it was recently circumvented around the Mediterranean basin (Soleiman et al., 2016), but continues to be highly effective everywhere else, to this day.

The only other known and well characterized genes, to consider in developing/selecting stem rust resistant cultivars for the south of Spain, are *Sr27*, *Sr32* and *Sr35*. These were characterized by very low levels of infection in the presence of the Spanish races (this study) and are also provide good protection against the Ug99 lineage and derivatives (Jin et al., 2007, Upadhyaya et al., 2021, Mago et al., 2013). *Sr27* is located on a segment from chromosome 3R of rye translocated onto chromosome 3A of bread wheat (Upadhyaya et al., 2021). *Sr32* originated from *A. speltoides* and was transferred to chromosome 2DS in bread wheat (Mago et al., 2013). Finally, *Sr35* is located on chromosome 3AL of bread wheat, and was transferred from *T. monococcum* (Jin et al., 2007). As for several of the previously mentioned, the origin of these genes is a translocated segment from wild relatives of wheat, which will require an assessment of the likely yield or quality penalties that could come with the resistance genes, especially if they are to be transferred to durum wheat.

3.6 Conclusions

Results of the present study clearly indicated that the main lineages of yellow rust detected in recent years in southern Spain were PstS13, PstS14 and PstS10 (Warrior-), and those for stem rust were Clade IV-B and Clade IV-F, both avirulent on the important gene *Sr13*, as seen in most of Europe and North Africa, with the exception of southern Italy, with its Sicilian races harboring virulence on *Sr13*. For both diseases, the high and/or useful levels of resistance to the Spanish lineages/races exhibited by some of the most widely grown commercial cultivars of bread wheat, durum wheat and triticale indicate that, on the short term, the threat to these crop production may be effectively mitigated. Various known resistance genes were shown to be potentially useful in breeding for resistance to either disease and could provide effective protection in the near future. However, future breeding efforts will need to consider not only the lineages/races currently present in Spain, but also the rapidly evolving pathogen populations in and outside the Mediterranean basin, implementing strategies that include resistance to linages/races currently absent locally but that could potentially come in and threaten the wheat production in southern Spain in the near future.

Capítulo 4. Tackling unbalanced datasets for yellow and leaf rust detection in wheat. A novel methodological approach

4.1 Abstract

This study assesses the efficacy of hyperspectral data in detecting yellow and leaf rust in wheat. Machine learning models—ANN, SVM, RF, and GNB—were evaluated, with SVM and RF models demonstrating the highest accuracies, particularly when SMOTE-enhanced datasets were used. For yellow rust, the RF model achieved 70% accuracy using unaltered data, while for leaf rust, the SVM model performed best, with an accuracy of 78.35% when SMOTE was applied to the training set. The study underscores the potential of spectral data and machine learning in plant disease detection and calls for advanced research in data processing techniques, particularly in the application of SMOTE and its impact on model performance.

4.2 Introduction

Wheat is most cultivated crop in the world, with an annual area of about 220 Mha in 2022/23 (Faostat, 2023). The severity of foliar diseases, such as the rusts is directly related to decreased yield and grain quality (Sauceda-Acosta et al., 2015). Yield loss caused by diseases like the wheat rusts vary depending on the resistance/susceptibility of the cultivars deployed in particular regions, the climate and soil of the region, and the rust species affecting the crop (Savary et al., 2019). Potential loss may reach up to 1% in resistant varieties but, in susceptible cultivars, this value can be almost 100% under favorable conditions for the disease (Beard et al., 2005). Consequently, early disease-detection is essential to optimize their management and maximize crop production (Salvagiottu et al., 2005; Orchi et al., 2021).

As it was mentioned before, crop disease identification has primarily relied on human visual inspection (Yadav et al., 2019). However, this method is subjective, time-consuming, and prone to human error (Bock et al., 2010). As an alternative to visual methods, many technologies based on remote sensing have been developed to achieve more accurate, rapid, and cost-effective detection of crop diseases (Zhang et al., 2019). These technologies offer great potential for early and non-destructive detection of plant diseases, enabling timely intervention (Terentev et al., 2021).

From a remote-sensing perspective, disease detection is carried out using various tools (Yang, 2020). However, in the past year, the use of spectral information has gained significance, as highlighted by Wan et al. (2022). The reliance on spectral information is based on the understanding that each disease induces unique spectral reflectivity patterns in crops, resulting from the harm inflicted on plant tissues (Clevers, 1999). The changes

can be detected by hyperspectral sensors (spectroradiometers and cameras), considered the state of the art for disease detection in crops (Guzmán-Álvarez et al., 2022). These sensors offer an exceptional level of spectral resolution, capturing data related to biotic and abiotic stresses that might not be easily detected by other sensors with lower spectral resolution (Di Bella et al., 2008).

Among the hyperspectral sensors, hyperspectral cameras have emerged as a promising alternative to spectroradiometers. They provide the unique capability to capture a high-resolution spectrum for each pixel in an image. Despite their advantages, hyperspectral images do have several limitations, including the equipment's cost that should be considered. According to the work conducted by Roberts et al. (2018), the issues are related to the availability of robust commercial instrumentation and the large amount of data generated during the analysis. Due to the large amount of data generated, hyperspectral images require extensive processing work, which involves a significant amount of time and complex algorithms to reduce spectral dimensionality (Paoletti et al., 2019). In this regard, spectroradiometers, while less precise because they don't provide an image as an outcome, are a more affordable solution both from an economic standpoint and in terms of data processing.

Many approaches have been derived for data processing of spectroradiometers and hyperspectral cameras. One of the most widely used approaches is the application of vegetation spectral indices, obtained from the combination of specific spectral bands (Gilabert et al., 1997). These indices may detect crop diseases by observing changes in the leaf external (i.e., necrosis and chlorosis,) and internal architecture (i.e., chloroplast dysfunction) as is explained by Ling et al. (2017). Extensive research has been conducted to detect diseases using spectral indices. As an example, Devadas et al. (2009) showed the suitability of specific indices like the Anthocyanin Reflectance Index (ARI) to discriminate between healthy and rust-infected wheat leaves at a medium-late growth stage, and the Transformed Chlorophyll Absorption in Reflectance Index (TCARI) to detect wheat leaf rust. Other studies, such as the one conducted by Ashourloo et al. (2014), demonstrated remarkable accuracies exceeding 85% in estimating disease severity using a Leaf Rust Disease Severity Index (LRDSI). While the LRDSI has been successful, it has limitations in the early detection of symptoms due to the spectral similarity between affected and healthy leaf areas. Spectral indices offer valuable insights; however, in certain scenarios, they may fall short, as they don't encompass the comprehensive data required for in-depth research analysis.

An alternative to employing spectral indices for disease identification is leveraging the full spectrum of radiation reflected and captured by hyperspectral sensors. However, given the vastness of hyperspectral datasets and their intricate processing requirements, the integration of machine learning (ML) models with hyperspectral data for disease identification has garnered increased interest in recent years. In this sense, models such as Artificial Neural Network (ANN), Support Vector Machine (SVM), Random Forest (RF) or Gaussian Naïve Bayes (GNB), among others, have been proposed (Su et al., 2020, Singh et al., 2016).

While there has been success in utilizing hyperspectral information for disease detection, the research thus far often relies on datasets with limited data volume. This is particularly concerning in the context of machine learning. For the construction of a resilient ML model, a comprehensive and balanced dataset is essential for achieving broad generalization. However, field data collection requires considerable effort and resources, which limits the availability of data for analysis. Because of this, it is common to employ data augmentation techniques to improve the overall learning procedure and performance of ML models. Data augmentation is primarily performed on imbalanced datasets, which exhibit a significant disparity in the number of data instances in each class (Hadad et al., 2009). This imbalance has consequences for the learning process by resulting in low predictive accuracy for the minority class (Daskalaki et al., 2006), as many performance measures used to guide training penalize minority classes. Rules that predict minority classes are highly specialized and have low coverage, which often causes them to be discarded in favor of more general rules. In addition, the treatment of noise may affect the classification of minority classes, as they may be erroneously discarded as noise (Pulgar et al., 2018).

According to the literature review by Kamilaris and Prenafeta-Boldú (2018), 37% of the reviewed articles apply data augmentation and highlight the importance of such techniques in scientific works with small hyperspectral datasets (i.e., images). Regarding the augmentation of hyperspectral data obtained through spectroscopy, little information is available. Chawla et al. (2002) introduced the Synthetic Minority Over-sampling Technique (SMOTE), which interpolates between minority class instances to address data imbalance. This tool augments the minority class by generating new synthetic data based on existing examples. From an agriculture perspective, researchers like Ma et al. (2019) employed SMOTE to balance the imbalanced training dataset, aiming to develop a model that distinguishes between powdery mildew and aphid infestations in winter wheat using bi-temporal Landsat-8 imagery. A more recent study by Divakar et al. (2021) utilized SMOTE to classify areas affected by wilt disease in bananas.

Based on the aforementioned literature review and to the best of our knowledge, this technique has rarely been applied to agricultural tasks, particularly for the detection of wheat leaf rust. Hence, this study aims to evaluate the feasibility of differentiating cultivars affected by yellow rust and leaf rust in bread and durum wheat, respectively, using full spectral signatures acquired through spectroscopy. Moreover, it will assess the impact of the SMOTE algorithm on the development of machine learning models for the accurate detection of both types of rust.

4.3 Materials and Methods

4.3.1 Greenhouse experiment and data collection

The greenhouse experiment was conducted in the facilities at the School of Agricultural Engineering, University of Seville (37°21′9″ N, 5 ° 56 ′ 10.5 ′ W; Datum: WGS84), Spain, during the growing season 2020/2021. The experiment involved two separate trials: one with durum wheat (*Triticum turgidum* L. ssp. *durum* (Desf.) Husn.) and another with bread wheat (*Triticum aestivum* L. ssp. *aestivum*). The first trial comprised three cultivars of durum wheat with different types of resistance to leaf rust: Don Ricardo (resistant), Amilcar (intermediate resistant), and Kiko Nick (susceptible); while the second trials involved three cultivars of bread wheat with different degrees of resistance to yellow rust: Arthur Nick (resistant), Conil (intermediate resistant), and Califa (susceptible). In both trials, four seeds of each cultivar were sown in 3 liters pots (filled with a peatmoss and sand mix, 2:1 vol./vol.) to finally get two healthy plants. Pots were arranged in a randomized design with twelve pots per cultivar, resulting in an experiment of 36×2=72 pots. All plants were properly irrigated and fertilized throughout the experiment. Wheat plants were inoculated at DC 53 (flag leaf extended and a quarter of the ear emerged) (Zadoks et al., 1974), on days 87 and 94 after sowing for bread and durum wheat, respectively. The plants of six pots of each cultivar were rust inoculated, while the other six remained rust free. Durum wheat plants were inoculated with leaf rust isolate CONDJA13 (BBBSJ) (Aoun et al., 2020), while the other half were used as uninfected checks. The plants of the 18 pots of each trial were inoculated by dusting a mix of uredospores and talcum powder (20 mg of spores: 1.200 mg of talcum powder). The leaves of the plants were manually bent to a semi-horizontal position that facilitated the inoculation and deposition of the spores. Inoculated plants were placed in an incubation compartment within the greenhouse at 18–20 ºC, with darkness and humidity at saturation for 15 hours. Then, pots were placed back to their grown compartment. In the same way, six pots of each bread wheat cultivar were inoculated with yellow rust isolate ECIJER18 (PstS10 or Warrior-) (Ali et al., 2017), but plants were incubated for 24 hours. Infection type was assessed visually about 16 days after inoculation according to the McNeal scale. This scale is 0–9, where infection type lower than 7 indicated a resistant response, and infection type of 7 or more indicated a susceptible response (McNeal et al., 1971). Besides, rust severity was taken weekly during three times, beginning the day of infection type scoring. Severity was assessed following the modified Cobb scale (Peterson et al., 1948), expressed as a proportion of foliar surface covered by pustules with respect to the total plant (from 0 to 100%). In the resistant cultivars, necrosis (yellowish) tissue surrounding the pustules were also measured as a proportion of total foliar area.

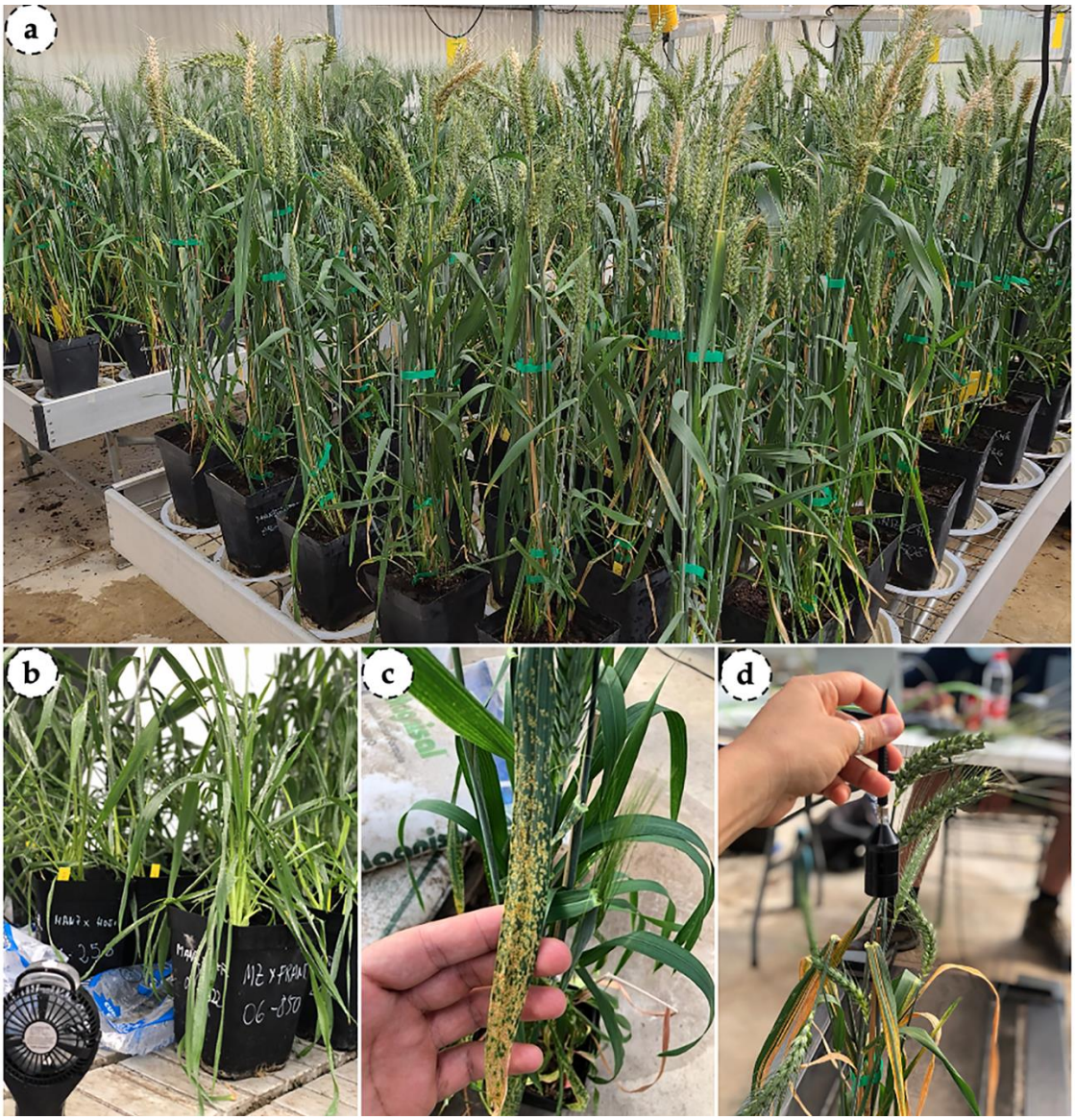

Figure 4.1 Illustration showing the experimental design (a), the inoculation process (b) a detailed view of leaves with leaf rust (c) and, the position of the spectroradiometer during the measurements (d).

Simultaneously, three spectral measurements were acquired for each pot from a distance of 0.15 m around the plant. These measurements were taken by directly targeting the affected areas using a portable spectroradiometer (UNISPEC-DC, PP-systems, Inc., Amesbury, MA, USA). This sensor allows the measurement of reflectance from two optical fibers, channels A and B. One channel records the incident radiation while the other records the reflected radiation. Each channel includes a photodiode detector that covers a spectral region ranging from 310 to 1100 nm. The sensor offers a spectral resolution between 3.1 and 3.4 nm. To calibrate the spectroradiometer, a white reference (99% reflectance Spectralon panel) was utilized. Hyperspectral data were collected around noon under completely sunny conditions, with data collection performed for each pot at intervals of 3-4 days. Seven measurements were made on pots inoculated with yellow rust on DAS (days after sowing): 87, 94, 98, 101, 105, 108, and 112 DAS, and six

measurements were made on pots inoculated with leaf rust on days 94, 98, 101, 105, 108, and 112 DAS.

4.3.2 Data preprocessing

For each wavelength (λ), the spectral reflectance (R_λ) was calculated following equation 1:

$$R_\lambda\ (\%) = \frac{L_\lambda^r}{L_\lambda^i} \times 100 \qquad \text{(Eqn. 1)}$$

where L_λ^r denotes the spectral radiance reflected by the crop surface in wavelength λ and L_λ^i is the spectral radiance received by the crop surface in wavelength λ.

The spectral signature of each pot was obtained by calculating the mean of the three measurements taken. This resulted in a total of 36 spectral signatures for bread wheat and 36 for durum wheat. These spectra were classified into three groups: 'Healthy' (H) for non-inoculated plants, 'Asymptomatic Leaf' (AL) for inoculated plants without visible symptoms, and 'Symptomatic Leaf' (SL) for inoculated plants displaying visual symptoms. The selection of these categories was deliberate, as they served as target variables for prediction. Each category was carefully designed to encompass a variety of instances, ensuring the creation of accurate and robust prediction models. Subsequently, the spectra underwent standardization using the Scikit-learn package version 1.2.2, scaling the values within the range of 0 to 1. Machine learning estimators often need standardization procedures as they perform optimally when features exhibit approximately normal distribution. Following standardization, was applied with the following parameters: a window frame length of 11, polynomial order of 4, and the first derivative.

To mitigate the substantial variance in the quantity of data entries across categories, SMOTE (Synthetic Minority Over-sampling Technique) was utilized to augment the available data. The SMOTE technique generated synthetic samples for the underrepresented categories, thereby equalizing the dataset's distribution. A random state of 888 was employed to ensure reproducibility. Table 4.1 illustrates the data points for each category both prior to and following the application of the SMOTE technique. Furthermore, it provides the proportion of actual data within each category subsequent to the SMOTE procedure.

Table 4.1 Comparative data on bread wheat and durum wheat cultivars. The table presents the number and percentage of actual data for each category: Healthy (H), Asymptomatic Leaf (AL), and Symptomatic Leaf (SL).

Categories	Bread wheat		Durum wheat	
	Number of actual data	Actual data (%)	Number of actual data	Actual data (%)
H	125	100	107	100
AL	44	35.2	54	50.46
SL	64	51.2	36	33.64

Various dataset processing techniques were utilized to assess the influence of synthetic data generated by SMOTE on the development of prediction models. Throughout all scenarios, the H category was solely composed of actual data. The distinct processing methods are as follows:

- No SMOTE applied: no synthetic data were introduced.
- SMOTE applied to the entire data set: synthetic data were introduced into the training, testing and second validation sets.
- SMOTE applied to the training set only: The testing and second validation sets consisted exclusively of actual data.

4.3.3 Training of machine learning models

After the preprocessing step, the dataset was split into two parts: 30% for testing and 70% for training the models. The flowchart (Figure 4.2) provides the workflow associate of the different stages involved in disease detection.

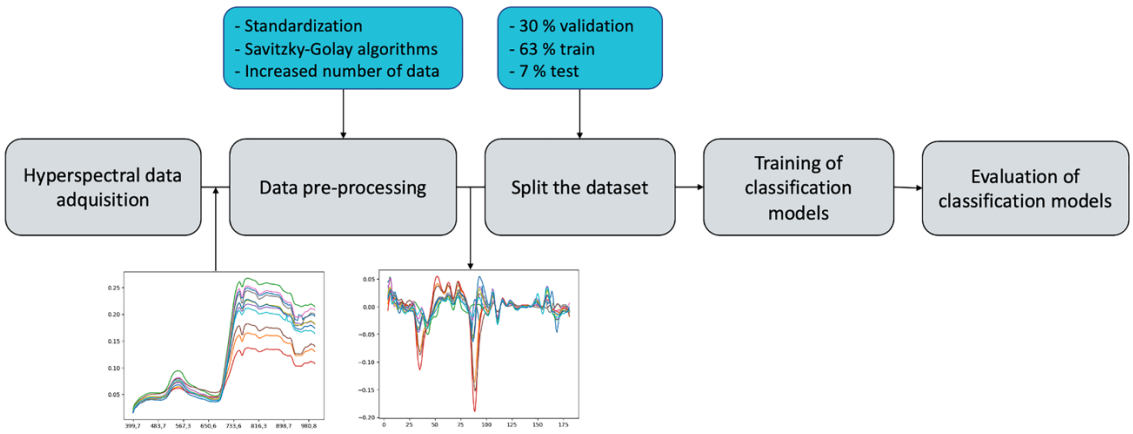

Figure 4.1 Workflow of hyperspectral data processing for disease classification in wheat. The process begins with hyperspectral data acquisition, followed by data pre-processing that includes standardization and Savitzky-Golay filtering, with an increase in the number of data points. The dataset is then split into 63% for training, 30% for validation, and 7% for testing. Subsequently, the training of classification models is conducted, culminating in the evaluation of the models' performance.

This study implemented four models with the scikit-learn library: Artificial Neural Network (ANN), Support Vector Machine (SVM), Random Forest (RF), and Gaussian Naive Bayes (GNB). The Random Forest and Gaussian Naive Bayes models were configured with default parameters. For the SVM model, a second-degree polynomial kernel was employed, with an independent term value of 2 in the kernel function.

The development of the Artificial Neural Network (ANN) entailed utilizing RandomizedSearchCV to optimize the parameter settings. A total of 50 interactions were performed, with a random state set to 42. The parameters considered during the optimization process were alpha, hidden layer sizes, and learning rate init. For yellow rust, alpha was set to 0.0001, hidden layer sizes were 20 and 20, and the learning rate was set to 0.001. Conversely, for leaf rust, alpha was set to 0.1, hidden layer size was 30, and the learning rate was set to 0.01. The solver employed for the yellow rust dataset was Adam, while for leaf rust, LBFGS was selected due to its better suitability for the data structure. All other parameters retained the default configuration of Scikit Learn. The ANN models developed using the dataset without SMOTE application served as a reference due to achieving the highest accuracy results (Table 4.2).

4.3.4 Metrics for model evaluation

The entire data processing was conducted using Google Collaboratory, which provides the necessary Python environment and libraries for data analysis and visualization. In terms of statistical assessment, the classification models were compared based on their network classification accuracy. Accuracy (Equation 2) quantifies the percentage of instances in which the model has made correct predictions, and it is defined as follows:

$$\text{Accuracy} = \frac{\text{Number of correct predictions}}{\text{Total number of predictions}} \quad (2)$$

For each category with balanced data, evaluation was performed using the F1_score (Equation 3) derived from the confusion matrix, and it is defined as:

$$\text{F1\_score} = \frac{2 \text{ x precision x recall}}{\text{precision + recall}} \quad (3)$$

where precision (Equation 4) and recall (Equation 5) are defined as follows:

$$\text{Precision} = \frac{\text{TP}}{\text{TP + FP}} \quad (4)$$

$$\text{Recall} = \frac{\text{TP}}{\text{TP + FN}} \quad (5)$$

where TP represents True Positive, FP stands for False Positive, and FN represents False Negative. For models trained with imbalanced categories, precision was employed for their evaluation.

4.4 Results

4.4.1 Spectral reflectance analysis

Figure 4.3 illustrates the reflectance obtained for each category of yellow (4.3a) and leaf (4.3b) rust. The lines on the plot represent the average values, while the shaded areas indicate the standard deviations of the data.

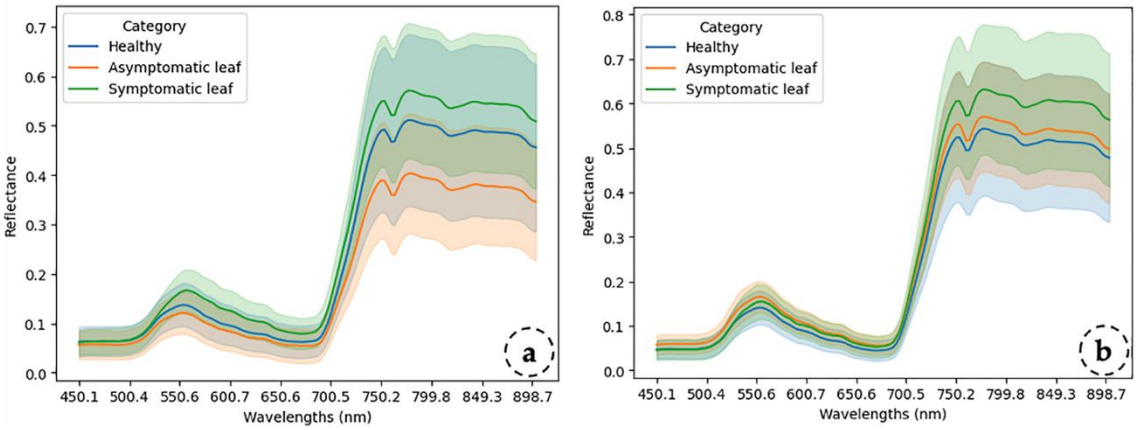

Figure 4.3. Reflectance spectra for healthy, asymptomatic, and symptomatic leaf categories are presented, illustrating the spectra of wheat leaves affected by yellow rust (a) and leaf rust (b). Mean reflectance values and standard deviations have been computed for these predefined categories.

As can be observed in Figure 3, the mean values can vary between categories, especially for yellow rust (Fig. 4.3a). However, in leaf rust (Fig. 4.3b), the mean values exhibit a higher degree of overlap between categories. Overall, the mean reflectance values obtained for leaf rust are higher than in the case of yellow rust. In both cases, the greatest degree of overlap occurs in the visible spectrum region, although it also occurs between the "H" and "AL" categories for leaf rust. Both types of rust show considerable standard deviations, leading to considerable overlap across all categories. To address with this issue, specific classification models have been developed for each rust type to enhance accuracy in categorization. Notably, for yellow rust, the mean value of the healthy category exceeds that of the asymptomatic leaf category, while the reverse is true for leaf rust.

A careful look at each plot at yellow rust level revealed (Figure 4.3a) that the category with the lowest mean reflectance value is the asymptomatic leaf, followed by the healthy category, while the symptomatic leaf category exhibits the highest mean reflectance value. This trend remains consistent in both the visible-spectrum (400-700 nm) region and the NIR region (700-800 nm). All categories exhibit a standard deviation wide enough to cause overlap, although the healthy category displays the highest variability. In the visible spectrum region, the similarity in mean reflectance values between the healthy and asymptomatic leaf categories is noteworthy, with the symptomatic category achieving a higher mean value than both. In the NIR region, the mean reflectance difference increases between the healthy and asymptomatic leaf categories, while it decreases between the healthy and symptomatic leaf categories.

In Figure 4.3b, the mean reflectance and standard deviation values obtained for the different categories of wheat leaves infested with leaf rust. In the visible spectrum region, the mean reflectance values and standard deviations are quite similar across categories. However, in the NIR region, the mean reflectance value within the symptomatic leaf category shows and increased difference compared to the others. This implies that the category corresponding to healthy and asymptomatic plants is very similar along the spectral signature, which cause difficulties in early detection. Similarly, to yellow rust, the data obtained from leaf rust also exhibit significant standard deviations, resulting in overlap among categories.

4.4.2 Models performance

The classification model was constructed using the training dataset, encompassing labeled data from all wheat varieties. The model was fine-tuned using the validation dataset. Subsequently, the developed model was tested for performance using the test set, comprising spectral data from all varieties within each wheat type. The corresponding accuracy (%) of each model used in this study, based on their respective datasets, is presented in Table 4.2

Table 4.2 Performance comparison of ML models for yellow and leaf rust classification. The table presents the accuracy percentages of Artificial Neural Networks (ANN), Support Vector Machines (SVM), Random Forests (RF), and Gaussian Naive Bayes (GNB) with and without the application of Synthetic Minority Over-sampling Technique (SMOTE) during training.

Models	**Yellow rust**			**Leaf rust**		
	Without SMOTE	SMOTE	SMOTE on training	Without SMOTE	SMOTE	SMOTE on training
ANN	65.71	76	60	57	76.3	55
SVM	68.6	85	62.86	58	78.35	63
RF	70	81.5	68.5	53	73.2	55
GNB	64	61	57	37	60	38

The results obtained show that the models' accuracies are consistently higher for classifying yellow rust than leaf rust. Among the models, the GNB model displayed the least accuracy in both yellow and leaf rust contexts. Consequently, our analysis will primarily concentrate on the outcomes achieved by the ANN, SVM, and RF models.

For the dataset where SMOTE was not applied, the highest accuracy was obtained by the SVM model, immediately followed by ANN model, for leaf rust and RF model for yellow rust. Similarly, in cases where the dataset was augmented using SMOTE, the highest accuracy values were obtained by SVM models. The accuracy achieved in this dataset is the highest among all models compared to the results obtained in the remaining datasets. Furthermore, these models also excel in the dataset where the SMOTE algorithm was exclusively applied during training. Nevertheless, it is noteworthy that the accuracies

obtained in the SMOTE dataset during training decreased in comparison to the datasets where SMOTE was and was not applied, for all models. However, the exception to this trend is observed for the SVM and RF models in the case of leaf rust. In the SVM model, the accuracy of the model trained with the original data increased by 5 points compared to the model where SMOTE was applied in training. For the RF model, this increase was 2 points.

Table 4.3 presents the F1-score values of ANN models across different categories and datasets utilized.

Table 4.3 F1-scores achieved by the ANN (Artificial Neural Network) model for wheat disease classification are presented for the categories: Healthy (H), asymptomatic leaf (AL), and Symptomatic Leaf (SL) across datasets for both yellow rust and leaf rust. The table compares model performance without the use of SMOTE, with SMOTE, and with SMOTE applied during the training phase.

	Yellow rust			**Leaf rust**		
Categories	Without SMOTE	SMOTE	SMOTE on training	Without SMOTE	SMOTE	SMOTE on training
H	0.73	0.63	0.65	0.66	0.66	0.67
AL	0.45	0.77	0.50	0.47	0.81	0.61
SL	0.62	0.87	0.59	0.37	0.82	0.63

Regarding the yellow rust trial, it was observed that in the dataset without SMOTE, the “H” category, characterized by a more substantial number of data points, achieved higher values. In contrast, the “AL” category displayed the lowest value. It is worth noting that this category was composed of a smaller number of data compared to the others. In the dataset where the algorithm was fully implemented, notable enhancements were observed in the “AL” and “SL” categories, both of which incorporated synthetic data. However, the “H” category, comprised solely of actual data, obtained a lower score than the dataset where SMOTE was not applied. Conversely, in the dataset where SMOTE was only applied to the training dataset, it was observed that the “H” category maintained a similar outcome to that of the dataset with full SMOTE application and a decrease relative to the original dataset. However, the “SL” and “AL” categories obtained similar and slightly higher results, respectively, than the dataset where the SMOTE algorithm was not applied.

For leaf rust, a similar trend to yellow rust is observed. The category “H” results were consistent across all three datasets. In n the categories “AL” and “SL,” higher values were obtained in the dataset where SMOTE was fully applied. In contrast to the trend observed in yellow rust, in the dataset where SMOTE was only used in the training, categories SL and AL increased their accuracy by 26 and 14 points, respectively, compared to the dataset where SMOTE was not applied.

The F1-score results obtained from the SVM models, as shown in Table 4.4, exhibit similar behavior to the ANN model. The “H” category demonstrates consistent performance across all three datasets with slight variations. For the “AL” and “SL” categories, a notable enhancement is observed when SMOTE is applied to the entire dataset, contrasting the non-SMOTE dataset performance. However, in the dataset where

SMOTE was solely used during training The obtained accuracy decreases by 3-4 points for yellow rust and increases for leaf rust. In the latter case, it is worth noting the 15-point increase in the SL category compared to the original dataset.

Table 4.4 F1-scores achieved by the SVM (Support Vector Machine) model for wheat disease classification are presented for the categories: Healthy (H), asymptomatic leaf (AL), and Symptomatic Leaf (SL) across datasets for both yellow rust and leaf rust. The table compares model performance without the use of SMOTE, with SMOTE, and with SMOTE applied during the training phase.

Categories	**Yellow rust**			**Leaf rust**		
	Without SMOTE	SMOTE	SMOTE on trainning	Without SMOTE	SMOTE	SMOTE on trainning
H	0.75	0.77	0.68	0.70	0.64	0.74
AL	0.54	0.87	0.50	0.46	0.75	0.54
SL	0.67	0.89	0.63	0.29	0.94	0.44

Table 4.5 displays the F1-score results of the RF model. In the case of yellow rust, the "H" category maintains consistency across all datasets, with a slight advantage in the non-SMOTE dataset. The "AL" category shows improvement with SMOTE applied during training, while "SL" remains unchanged. A similar pattern is observed for the "H" category in the context of leaf rust. Interestingly, the dataset containing actual data yielded the lowest values for "AL" and "SL", but the application of SMOTE during training increased their values in 12 and 20 points respectively.

Table 4.5 F1-scores achieved by the RF (Random Forest) model for wheat disease classification are presented for the categories: Healthy (H), asymptomatic leaf (AL), and Symptomatic Leaf (SL) across datasets for both yellow rust and leaf rust. The table compares model performance without the use of SMOTE, with SMOTE, and with SMOTE applied during the training phase.

Categories	**Yellow rust**			**Leaf rust**		
	Without SMOTE	SMOTE	SMOTE on training	Without SMOTE	SMOTE	SMOTE on training
H	0.78	0.70	0.73	0.66	0.59	0.64
AL	0.32	0.84	0.50	0.34	0.71	0.46
SL	0.71	0.88	0.74	0.17	0.89	0.37

When comparing the results obtained for each model, it can be observed that the best accuracies are achieved by the models that used datasets augmented which the SMOTE algorithm. However, the presence of synthetic data in the test dataset may raise concerns about the reliability of the results. Regarding the dataset for the category consisting solely of actual data, RF was the best model for yellow rust classification. For leaf rust, it was the SVM model the one that performed better when the same dataset was used.

The SVM model achieved the highest F1-score for the "AL" category in both rusts Conversely, for yellow rust, it occurred in the original dataset and for leaf rust, it occurred in dataset where SMOTE was applied during training. Finally, the best F1-score for the "SL" category in yellow rust was achieved by the RF model, and for leaf rust, it was the SVM model, both using the dataset with SMOTE applied during training.

4.4.3 Confusion matrix

The confusion matrices generated for each dataset in the RF and SVM models are displayed in Figure 4.4

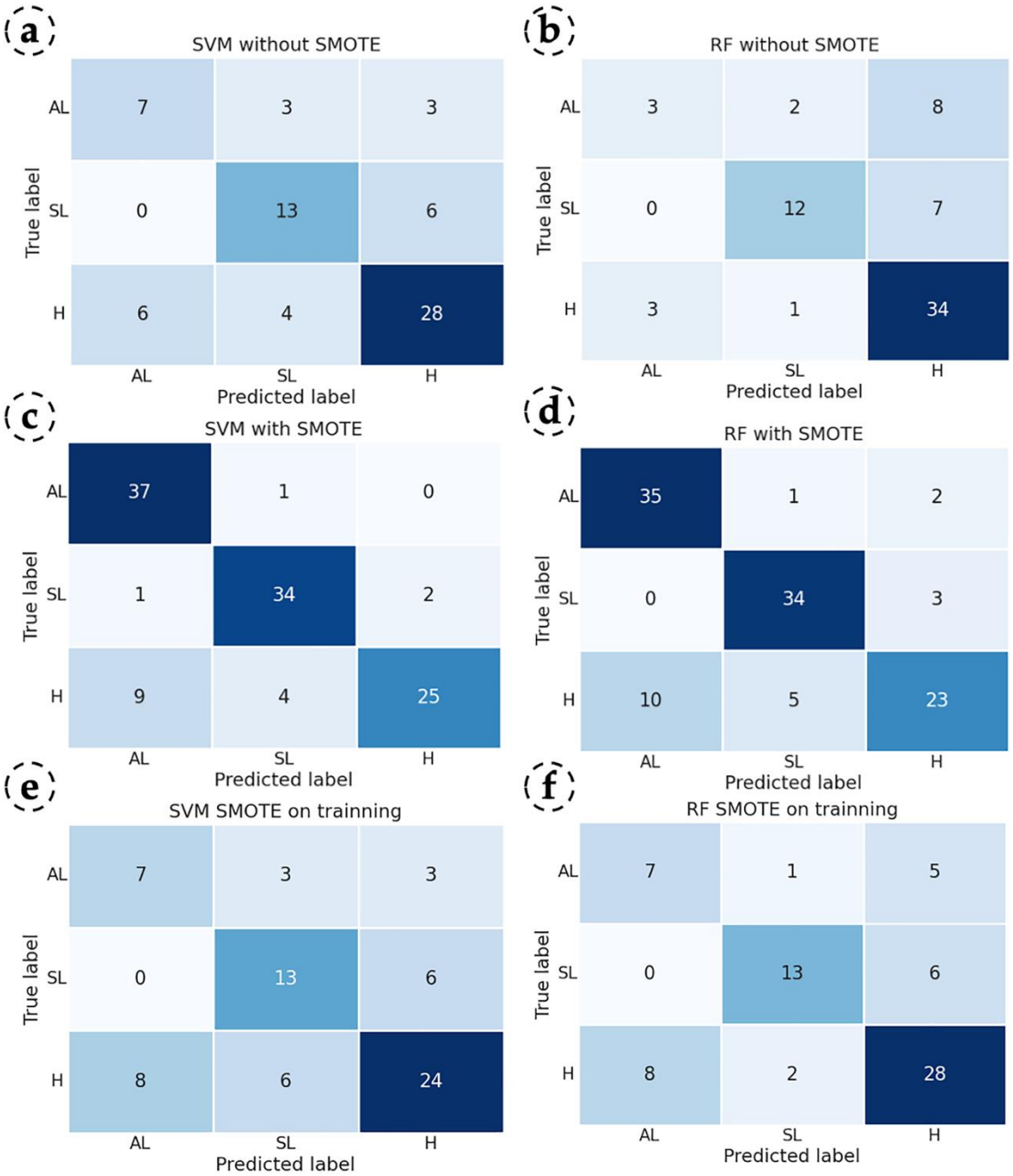

Figure 4.4 Confusion matrix with three datasets for two machine learning models with categories H, SL, and AL, in yellow rust. SVM for the dataset without SMOTE (a), RF for the dataset without SMOTE (b), SVM for the dataset with SMOTE (c), RF for the dataset with SMOTE (d), SVM for the dataset with SMOTE on training (e), RF for the dataset with SMOTE on training (f).

For the set of confusion matrices shown in Figure 4.4, it was observed that in the dataset where SMOTE was not applied, both models had a similar total number of errors. However, the number of classification errors by categories differs significantly. In the SVM model, the category with the highest number of errors was "H," particularly in

distinguishing it from the "AL" category. It is also noteworthy the high number of errors in classifying the "SL" and "H" categories. On the other hand, in the RF model, there is a drastic decrease in the error rate for classifying the "H" category, which represents an improvement compared to the SVM model. However, we observe an increase in misclassifications in the "AL" and "SL" categories, especially when distinguishing them from the "H" category.

In the dataset where SMOTE was applied entirely, both models exhibited the highest number of correct predictions in the categories “AL” and “SL,” which contained synthetic data. However, most errors occurred in the category “H”, composed entirely of actual data, particularly in distinguishing between “H” and “AL”. It's worth noting that the number of errors in this distinction is higher in this dataset than in the dataset composed entirely of original data.

Finally, in the dataset where SMOTE was exclusively applied to the training set, a similar pattern was observed as in the dataset where SMOTE was not applied. The category with the most correct predictions was “H,” showing better RF results than SVM. For this category, the SVM model made a greater number of incorrect predictions with the 'SL' category. On the other hand, for the 'AL' category in the SVM model, the number of errors was balanced with the 'SL' and 'H' categories. However, in the RF model, it is observed that the majority of incorrect predictions were made mainly with respect to the 'H' category.

Based on the data obtained in Figures 4.4a, 4.4b, 4.4e, and 4.4f, we observe that the RF model is better at classifying the majority category 'H,' which is exclusively composed of real data. Regarding the 'SL' category, whose spectral characteristics differed the most from the other categories, all options behave similarly. Finally, for the 'AL' category, it is noteworthy that the SVM and RF models with SMOTE applied during training both perform well. However, both models misclassify differently, with the RF model standing out. This is because, within the error, it is capable of more accurately approximating two categories with similar spectral characteristics, namely 'AL' and 'H'. The confusion matrix generated by each dataset for the SVM model with the highest accuracy are displayed in Figure 4.5

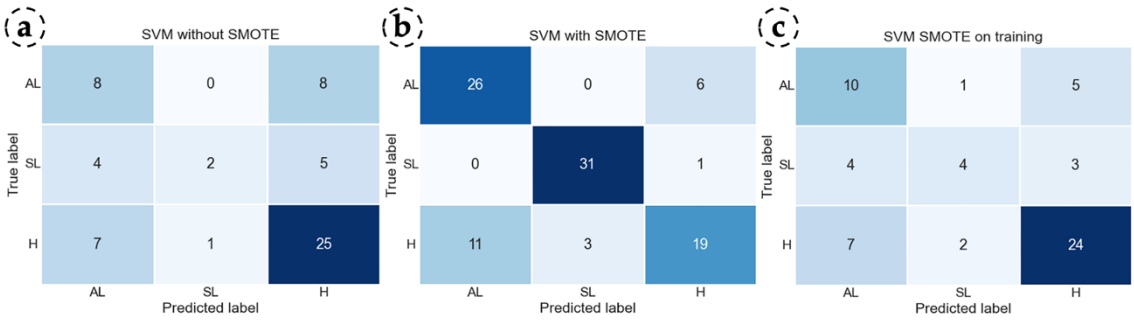

Figure 4.5 Confusion matrix with three datasets for two machine learning models with categories H, SL, and AL, in leaf rust. SVM for the dataset without SMOTE (a), SVM for the dataset with SMOTE (b), SVM fir the dataset with SMOTE on training (c)

For the set of confusion matrices shown in Figure 4.5, it was observed that in the dataset in which SMOTE was not applied, it can be observed that the category with the highest number of correct predictions is 'H.' Within this category, it is noteworthy that the highest number of errors was made with the 'AL' category. This same trend is repeated for the 'AL' category, as all incorrect predictions were made with the 'H' category. In the case of the 'SL' category, the highest number of errors occurred, with these being distributed among the remaining categories.

In the dataset where SMOTE was applied entirely, the same trend is observed as that which occurred for yellow rust. Finally, in the dataset where SMOTE was exclusively applied to the training set, the trend noted for the 'H' category in the dataset where no data augmentation was performed repeats itself. However, for the 'SL' and 'AL' categories, there is a slight increase in the number of correct predictions, and the error ratio remains consistent with respect to the original dataset. For this reason, this latter model exhibits the highest efficiency in category distinction, although the 'SL' category exhibits serious deficiencies.

4.5 Discussion

In the present study, the accuracy and F1-score results have been analyzed across different models and datasets. The datasets used can be considered comparatively small to other studies that utilize public datasets such as Plant Village (Thakur et al., 2022), which has 54,305 images of 14 plant species, for machine learning training The study conducted by Lu et al. (2021) is one of the few works that highlights a significant challenge. This challenge pertains to the current inadequacy of dataset size and diversity in the application of disease classification models in plants. Furthermore, it is essential to consider all possible capture conditions, symptom variations, and sensor characteristics used (Barbedo, 2018). Due to these reasons, it is inevitable to have complete datasets, and therefore, the models in their application have limited scope.

There are several alternatives to address the effects of using incomplete datasets, with one of the most common being data augmentation through various techniques that can be combined with each other. However, according to the literature reviewed by Kobayashi et al., (2018), each data augmentation technique affects the model's accuracy in a different way. Finding a design pattern for selecting the most optimal method presents a challenge.

In this study, the SMOTE algorithm is applied at varying degrees to a small dataset for a single disease with three categories. This demonstrates how overall accuracy increases with the application of data augmentation techniques. This result aligns with those obtained in the study conducted by Uguz & Ulysal (2021), where a dataset of 3400 hyperspectral images was used to differentiate between two diseases and healthy plants across three categories. However, their results demonstrate an increase in accuracy across

all categories, whereas in the present study, accuracy does not increase in the category consisting of original data.

Regarding the dataset where the SMOTE algorithm was applied only to the training set, the results are consistent with those obtained by Singh & Arora (2020), as the category with the highest accuracy is the one composed of the original data. However, the overall accuracy of the models differs from the results obtained by Kannan et al. (2020) in which a dataset of 12.206 hyperspectral images is used and 75% of the dataset comprised synthetic data. In that study, the overall accuracy increases by 2.5%, whereas in the current study, it decreases for yellow rust and increases to a lesser extent for leaf rust.

The classification models that achieved the highest accuracy values in this study were SVM and RF. Both models fall within the realm of classical machine learning (Li et al., 2020). They differ from studies like the one conducted by Patil et al. (2017), where three machine learning models were compared for late blight detection. In that study, the best classifier was ANN, followed by SVM and RF, which represents a contrary trend to what was found in this article. The variation in the obtained results may be attributed to differences in the characteristics of the datasets used in this study. Specifically, in this study, there are two categories, namely 'H' and 'AL,' which exhibit similar characteristics. Additionally, the dataset's size and the percentage of synthetic data within each category could also contribute to these differences.

In terms of the achieved overall accuracy result, there is a limited body of research utilizing the complete spectrum of a spectroradiometer for disease detection. The study conducted by Naidu et al., (2021) is one of the few that show cases the potential of such data combined with machine learning. In this study, the LDA model was employed, and the results obtained align with those in the present study, yielding high accuracy rates for healthy plants and higher classification errors for categories with similar spectral characteristics. The study conducted by Khosrokhani & Nasr (2022), demonstrates higher accuracies by combining machine learning with vegetation spectral indices, achieving 85% for the RF model and 89.5% for the SVM model. In conclusion, the findings in this study contributes to the nuanced understanding of how data augmentation, particularly SMOTE, influences ML performance in the context of plant disease detection, underscoring the need for extensive datasets and the judicious application of augmentation techniques.

4.6 Conclusions

This study evaluated the capability of different ML models using datasets, composed of complete spectral signatures, with varying degrees of SMOTE to detect yellow and leaf rust in wheat crops based on hyperspectral data obtained through spectroscopy. The study demonstrates how the application of SMOTE in training and testing sets the accuracy obtained in all models compared to the dataset where SMOTE

was not applied. This increase in accuracy is particularly pronounced within the minority categories, which contain a larger quantity of synthetic data. This phenomenon may introduce a distortion in the accuracy of the model in real-world scenarios. On the other hand, the best models for disease detection in a small dataset were for yellow rust, the RF (70%) model with the dataset composed entirely of actual data, and for leaf rust, the SVM (63%) model in the dataset where SMOTE was applied to the training set. Furthermore, it is noteworthy that these models were capable of distinguishing between the features more effectively. An exception to this trend was observed between the 'H' and 'AL' categories, which exhibit similar spectral characteristics. Regarding the results obtained by classes, it was observed that class composed exclusively of actual data “H” is negatively affected by the application of SMOTE in RF and SVM models. However, the presence of synthetic data in the training of the minority categories ("AL" and "SL") increased the accuracy in both models, achieving an accuracy of 61% for the "AL" category in the case of leaf rust. Therefore, the application of data augmentation techniques during training is beneficial for achieving higher category-level accuracy, resulting in a more comprehensive and balanced model.

Finally, these results suggest the potential of using complete spectral signatures obtained through spectroradiometry combined with machine learning methods. Likewise, it underscores the need for further research into new data processing methods and how data augmentation techniques affect different model architectures.

Capítulo 5. Diagnosis leaf rust and yellow rust detection using point clouds from LiDAR sensor in wheat

5.1 Abstract

Leaf and yellow rust, a significant threat to wheat production, necessitates early and accurate detection to mitigate yield losses. In this context, the current study leverages 3D LiDAR technology to discern the impact of rust diseases on wheat cultivars. Despite rust inoculation, variations in plant height and biomass were negligible; however, notable declines in grain yield were recorded, especially in varieties susceptible to rust. LiDAR-derived data demonstrated substantial correlation with disease severity, underscoring its promise for reliable biomass assessment and early rust detection. The study affirms the vital role of LiDAR in precision agriculture, offering a proactive approach to disease management and safeguarding the stability of wheat yields.

Keywords: Lidar, phenotyping, leaf rust, yellow rust

5.2 Introduction

Wheat is the third most produced cereal grain worldwide behind corn and rice (Igrejas and Branlard, 2020). In terms of area planted and production, wheat is grown in almost all the planet's surface with the exception of the polar and tropics-equatorial zones (Le Gouis *et al*., 2020). Its production reached around 780 million tons in 2023 annually, according to the FAO database (FAOSTAT, 2023). However, according to Choudhary *et al.* (2020) wheat production needs to be increased by 2% annually in the coming years (Jasrotia *et al*., 2020). As if not all this were enough, the future global climate change scenarios and an estimated population of 9.6 billion by 2050 must be added together (Bahar *et al*., 2020). Furthermore, based on the literature review, wheat yields are, on average, around 20% lower than potential yields due to the effects of biotic (disease) and abiotic (drought) factors. In this context, a profit rate of around 2% per year is required to meet global food demands, but currently only a 1% annual increase in yield has been reached (De La Fuente *et al*., 2013; Ray *et al*., 2013). With the large amounts of factors that can affect wheat production fungal diseases (i.e., foliar and stem-base) have become the major concern expressed by farmers (Vergara-Diaz *et al*., 2015).

Among the various fungal diseases that can affect wheat, rust is exceptionally destructive. Wheat cultivars susceptible to leaf rust often experience yield losses ranging from 5% to 15%, depending on the crop's developmental stage. In cases where the variety is highly susceptible and weather conditions favor disease development, losses can reach as high as 60%. (Kolmer, 1996). One of the primary factors contributing to reduced wheat yields, with rust being particularly detrimental, is the indirect impact of rust on plant architecture (Yuan et al., 2018). Infection typically coincides with the grain filling stage,

diminishing both the interception and absorption of radiation. This, in turn, leads to reduce assimilate supply per grain, resulting in a decrease in both grain count and ear weight, as well as alterations in crop biomass (Roelfs et al., 1992). The current method for assessing disease occurrence relies on visual inspection by the human eye, which is effective when pustules are visible (Kumar and Kukreja, 2022). However, this inspection is constrained to specific areas, such as individual leaves, and does not provide comprehensive information about the entire crop architecture.

In the pursuit of more efficient crop monitoring methods, the integration of remote-sensing technology into phenotyping techniques has emerged as a highly promising approach for the non-destructive measurement of crop parameters (Winterhalter et al., 2013; Araus and Cairns, 2014). These innovative tools are particularly crucial as they facilitate a rapid acceleration of the breeding cycle, an advancement unprecedented in modern agriculture (Yao et al., 2018). While molecular data is readily available, there is a notable gap in phenotypic data, which these remote phenotyping technologies aim to fill (Montes et al., 2011). Breeders traditionally select leaf rust-resistant wheat cultivars by considering yield data and relying on their expertise an approach that is constrained by its dependence on end-of-season outcomes, making it inherently slow. Recognizing this limitation, research has highlighted that leaf rust not only affects yield but also causes architectural changes in wheat plants, such as reduced biomass, shorter plant stature, and altered leaf orientation (Holman et al., 2016; Jay et al., 2015; Li et al., 2017). Given these insights, there is a clear necessity for advanced techniques capable of early discrimination between wheat varieties based on their response to rust infection. Such techniques should enable the analysis of three-dimensional structural changes in plants from the earliest stages of infection, providing breeders with timely information to make informed decisions without the need to wait for the crop to reach maturity.

The characterization of plant architecture through 3D modeling has advanced significantly, with LiDAR technology becoming a key instrument for extracting crop parameters (Boogaard et al., 2021; Rebetzke et al., 2022). Although the application of LiDAR has been widespread, its use for monitoring leaf rust in wheat remains in the early stages. Li et al. (2021) were pioneers in utilizing 3D data to enhance leaf rust detection, underscoring the method's promise for crop health management.

The first early detections of wheat diseases was heavily dependent on hyperspectral imaging techniques. Research by Whetton et al. (2018) and Devadas et al. (2015) has confirmed the effectiveness of these cameras in identifying diseases. Nonetheless, the practical application of hyperspectral imaging is limited by the substantial costs involved, which pose a financial challenge for low-margin crops like wheat. Another method for early disease detection involves predictive models that use meteorological data (Rodriguez-Moreno et al., 2020). Despite being a creative solution, these models have not consistently achieved the necessary accuracy for dependable disease prediction. The ongoing challenge is to strike an optimal balance between the cost-effectiveness and accuracy of disease monitoring techniques for wheat.

Therefore, the development of an effective early detection system for rust in wheat has been initiated. This system employs LIDAR sensors, which offer a combination of affordability and precision, to identify leaf rust in durum wheat and yellow rust in bread wheat. While the use of LIDAR sensors has primarily been for analyzing plant morphology—as demonstrated in the study of wheat leaf morphology by Li et al. (2022) and in the segmentation of cucumber plant parts by Boogaard et al. (2021)—the current focus is on refining 3D point cloud applications. The main goal of this initiative is to perfect an early detection system for leaf rust, which is being tested on commercial varieties of durum wheat, and for yellow rust, which is under evaluation in commercial varieties of bread wheat. This system aspires to deliver precise, cost-effective rust detection by leveraging the capabilities of LIDAR sensors and 3D point cloud technology.

5.3 Materials and methods

5.3.1 Greenhouse experiment description

The greenhouse experiment was conducted in the facilities at the School of Agricultural Engineering, University of Seville (37°21′9″ N, 5 ° 56 ′ 10.5 ′ W; Datum: WGS84), Spain, during the growing season 2020/2021. The experiment involved two separate trials: one with durum wheat (*Triticum turgidum* L. ssp. *durum* (Desf.) Husn.) and another with bread wheat (*Triticum aestivum* L. ssp. *aestivum*). The first trial comprised three cultivars of durum wheat with different types of resistance to leaf rust: Don Ricardo (resistant), Amilcar (intermediate resistant), and Kiko Nick (susceptible); while the second trials involved three cultivars of bread wheat with different degrees of resistance to yellow rust: Arthur Nick (resistant), Conil (intermediate resistant), and Califa (susceptible). In both trials, four seeds of each cultivar were sown in 3 liters pots (filled with a peatmoss and sand mix, 2:1 vol./vol.) to finally get two healthy plants. Pots were arranged in a randomized design with twelve pots per cultivar, resulting in an experiment of 36×2=72 pots. All plants were properly irrigated and fertilized throughout the experiment. Wheat plants were inoculated at DC 53 (flag leaf extended and a quarter of the ear emerged) (Zadoks et al., 1974), on days 87 and 94 after sowing for bread and durum wheat, respectively. The plants of six pots of each cultivar were rust inoculated, while the other six remained rust free. Durum wheat plants were inoculated with leaf rust isolate CONDJA13 (BBBSJ) (Aoun et al., 2020), while the other half were used as uninfected checks. The plants of the 18 pots of each trial were inoculated by dusting a mix of uredospores and talcum powder (20 mg of spores: 1.200 mg of talcum powder). The leaves of the plants were manually bent to a semi-horizontal position that facilitated the inoculation and deposition of the spores. Inoculated plants were placed in an incubation compartment within the greenhouse at 18–20 ºC, with darkness and humidity at saturation for 15 hours. Then, pots were placed back to their grown compartment. In the same way, six pots of each bread wheat cultivar were inoculated with yellow rust isolate ECIJER18 (PstS10 or Warrior-) (Ali et al., 2017), but plants were incubated for

24 hours. Infection type was assessed visually about 16 days after inoculation according to the McNeal scale. This scale is 0–9, where infection type lower than 7 indicated a resistant response, and infection type of 7 or more indicated a susceptible response (McNeal et al., 1971). Besides, rust severity was taken weekly during three times, beginning the day of infection type scoring. Severity was assessed following the modified Cobb scale (Peterson et al., 1948), expressed as a proportion of foliar surface covered by pustules with respect to the total plant (from 0 to 100%). In the resistant cultivars, necrosis (yellowish) tissue surrounding the pustules were also measured as a proportion of total foliar area.

Additionally, regular height measurements were taken for all plants. Upon harvest at about 120 days after sowing, various parameters such as biomass, number of ears, number of grains per plant, and wheat production were measured to assess the impact of rust disease on different wheat cultivars, both in terms of inter-cultivar differences and the effects within the same cultivar.

5.3.2 Collection of crop parameters information

At the end of the growing season, all pots, both inoculated and non-inoculated, were harvested to measure various crop parameters that would serve as ground truth data, alongside the severity measurements taken on the specified days after inoculation (DAIs). The plants were cut at soil level in the pots, and their weight was measured using a balance; this weight was recorded as the biomass. Subsequently, the ears were collected individually to determine the number of ears (NoE), the number of grains (NoG), and the grain weight (Gw).

5.3.3 Lidar data measurements

To conduct 3D plant reconstruction, a 2D LiDAR laser scanner (Model LMS-111, Sick AG, located in Waldkirch, Germany) was employed. The scanner was mounted at the front of the platform, positioned approximately 0.5 meters above the crop canopy. This specific sensor placement aligns with the LiDAR sensor principle, where a pulsed laser beam is emitted, and its reflection is detected by a photodiode. The distance to an object is determined based on the time taken for the emitted signal to return after reflection. Notably, this sensor boasts a 0.5-degree angular resolution, a 270-degree field of view, a working range spanning from 0.5 to 20 meters, and operates at a frequency of 50 Hz.

To ascertain the platform's position, an odometer system was integrated, as depicted in Figure 5.1. This system was directly affixed to the wheel axle and featured an incremental optical encoder (Model E6B2-CWZ6C, OMRON Corporation, Kyoto, Japan). The rotary encoder generated 1000 pulses per revolution, offering a 1.8 mm

resolution in the direction of platform movement. The cumulative pulse count from the odometer was collected using a low-cost open-hardware Arduino Nano V3.0 microcontroller (Arduino Project, Italy) programmed through the open-source Arduino Software (IDE). After being collected by the microcontroller, the pulse data was transmitted to a computer via a USB interface, where it was synchronized with the LiDAR data to construct a 3D point cloud. These communication and computational processes were executed on an Ubuntu 18.04.5 LTS desktop workstation, and the Robot Operating System (ROS) Melodic (version 1.14.10) was employed for sensor control and data recording. The LiDAR point cloud data was stored in a bag file, which serves as a raw file format for storing ROS message data.

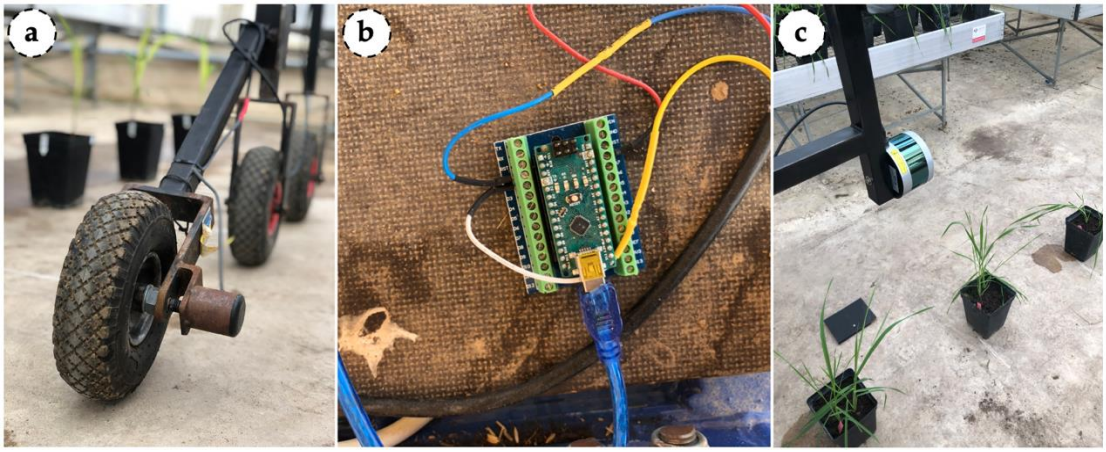

Figure 5.1 The setup includes a ground wheel odometry system affixed to the HTFPP chassis (a), with the encoder's wires linked to the Arduino board (b), and the LiDAR device actively scanning a selection of the pots utilized in the experiment (c).

5.3.4. Lidar data analysis

After data collection, all the ROS bag files generated by the LiDAR sensor were converted into PCD (Point Cloud Data) using specific ROS commands. Each LiDAR point cloud obtained was then processed to estimate the biomass, measured by the volume occupied by the canopy, and severity, using several methods (Figure 5.2, which are described as follows:

Evol: this method involves estimating plant volume using LiDAR data by modeling the plants as prisms. It excludes the outer 2% of lateral points to avoid edge anomalies and removes the bottom 20% of points deemed to represent soil, ensuring the volume calculation pertains solely to the plant.

Parea: this method involves estimating plant volume using LiDAR data by modeling the plants through a projection of all the data points onto the ground surface.

Prop10, Prop20, Prop30, Prop40, Prop50: this method consists of estimating plant volume by modeling the plants with a specific proportion of the data points from the top, using LiDAR data.

To estimate severity, the LiDAR-provided reflectance or intensity, which functions analogously to spectral sensors, was utilized. Intensity has been identified by Gregorio and Llorens (2021) as a potential feature for segmenting fruit within the canopy of apple orchards. In this study, the mean reflectance was calculated using the aforementioned proportions of data points. Therefore, the options explored were **Int10, Int20, Int30, Int40, and Int50**. Finally, the actual plant height (**Aph**) was estimated by calculating the average height of the top 3% of points.

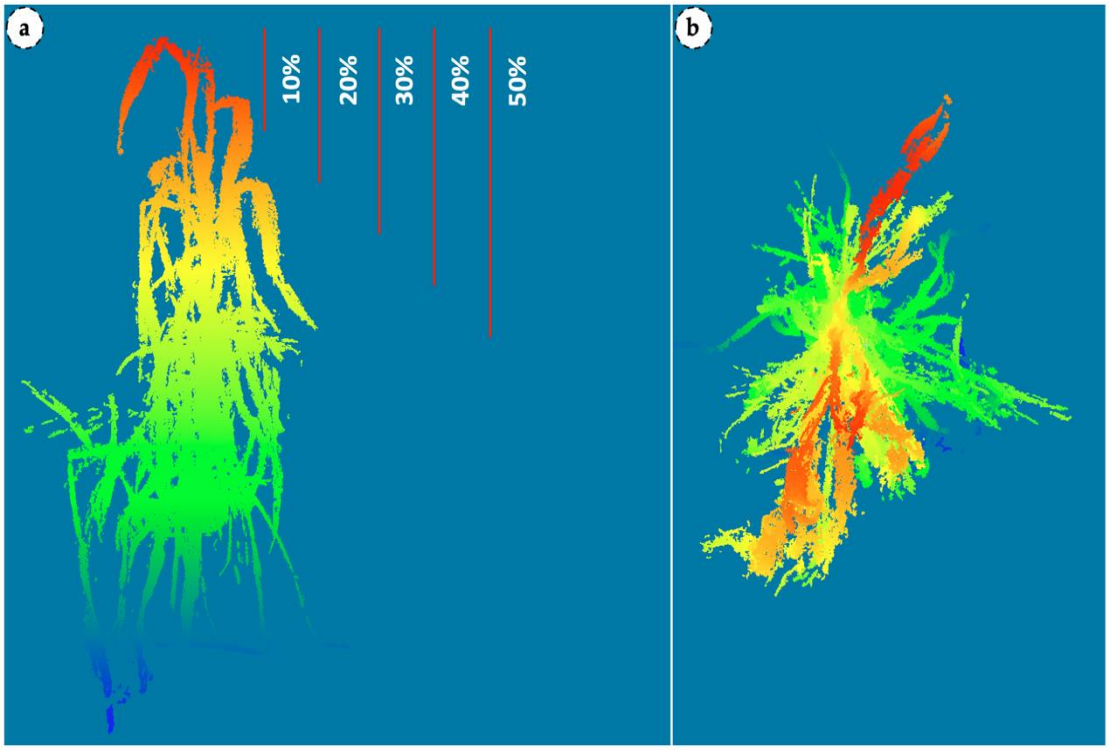

Figure 5.2. Frontal view of a LiDAR point cloud displaying the percentage of points used to estimate the volume and severity (a), alongside a top view of the 3D point cloud utilized for estimating volume as a projection (Parea).

5.3.5 Statistical analysis

The statistical analyses in this study were carried out using Python, version 3.11. The graphical plots vital for illustrating the findings were also generated using this programming language. Linear correlation plots and matrix correlations employing the Pearson r-value were utilized to evaluate the quality of the predictions.

5.4 Results and discussion

5.4.1 Ground truth values obtained evolution

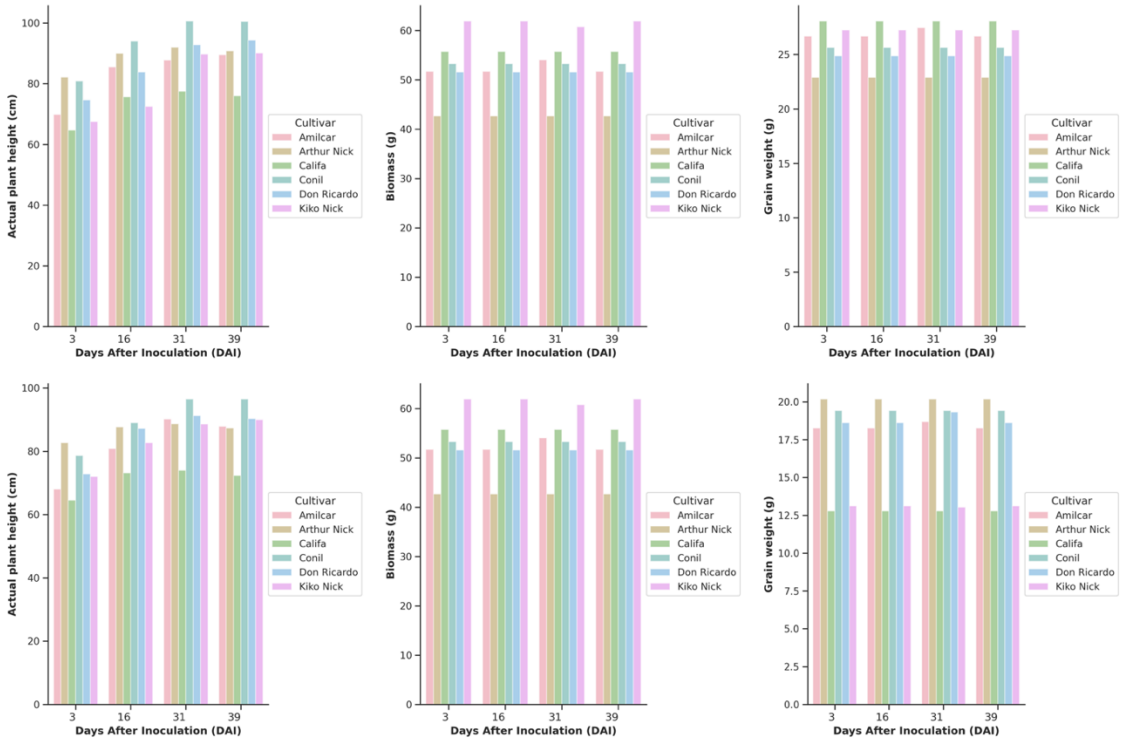

Figure 5.3 Bar plots illustrate the progression of the measured crop parameters across all cultivars, with the first row representing non-inoculated cultivars and the second row depicting those that were inoculated.

In Figure 5.3, no differences were observed in the parameters of plant height and biomass between plants inoculated with rust and their non-inoculated counterparts, across both resistant and susceptible varieties. This indicates that neither leaf rust nor yellow rust has a significant impact on these growth parameters. Contrastingly, the grain production parameter (grain weight) demonstrates a significant reduction, exceeding 50% in certain instances. This was particularly notable in durum wheat cultivar Kiko Nick, which presented high susceptibility to leaf rust, and the bread wheat cultivar Califa, highly susceptible to yellow rust. Among other durum wheat varieties inoculated with leaf rust, Don Ricardo showed an approximate 20% decrease in production, while the intermediate-resistant Amilcar suffers a grain weight loss of about 30%. Similarly, among the bread wheat cultivar inoculated with yellow rust, Arthur Nick underwent a production decrease of about 10%, and Conil experienced a reduction of around 20%. This confirms that in terms of grain weight, there was a noticeable difference of more than 50% in production, especially in the durum wheat cultivar Kiko Nick, which was susceptible to leaf rust, and the bread wheat cultivar Califa, which was susceptible to yellow rust. In other hand wheat cultivars inoculated with leaf rust, Don Ricardo showed an approximate 20% loss in production, and Amilcar around 30%. In the other bread wheat varieties inoculated with

yellow rust, Arthur Nick experienced a loss of about 10%, whereas the inoculated Conil lost around 20% of grain weight.

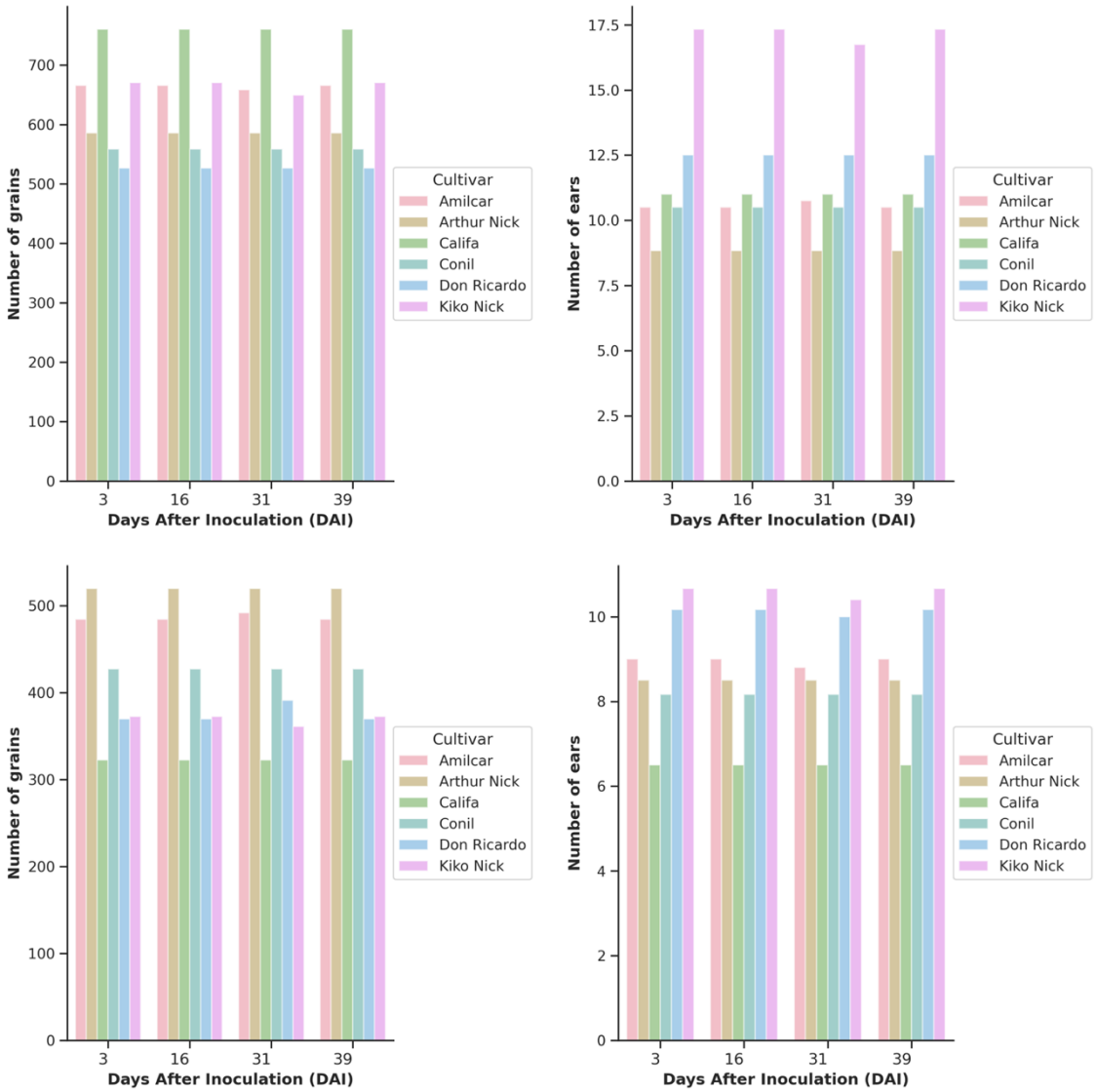

Figure 5.4 Bar plots illustrate the progression of the measured crop parameters across all cultivars, with the first row representing non-inoculated cultivars and the second row depicting those that were inoculated.

Figure 5.4 illustrates the impact of both leaf and yellow rust on the number of grains per plant. In the durum wheat cultivars resistant to leaf rust, such as Amilcar and Don Ricardo, there was a decline in grain number exceeding 20%, while the susceptible cultivar Kiko Nick experienced a nearly 50% reduction. Among the bread wheat cultivars inoculated with yellow rust, the resistant cultivar Arthur Nick only showed a 10% decrease in grain number. The yellow rust-resistant Conil suffered a grain reduction over 20%, and the susceptible Califa underwent a 60% grain number reduction. It is important to note that the number of spikelets per ear is not as directly correlated with yield as the number of grains or the grain weight. A plant susceptible to rust infection may produce smaller ears with fewer grains. Nonetheless, it has been noted that all cultivars, with the

sole exception of Arthur Nick, showed a reduction in the number of spikelets per ear in the inoculated plants.

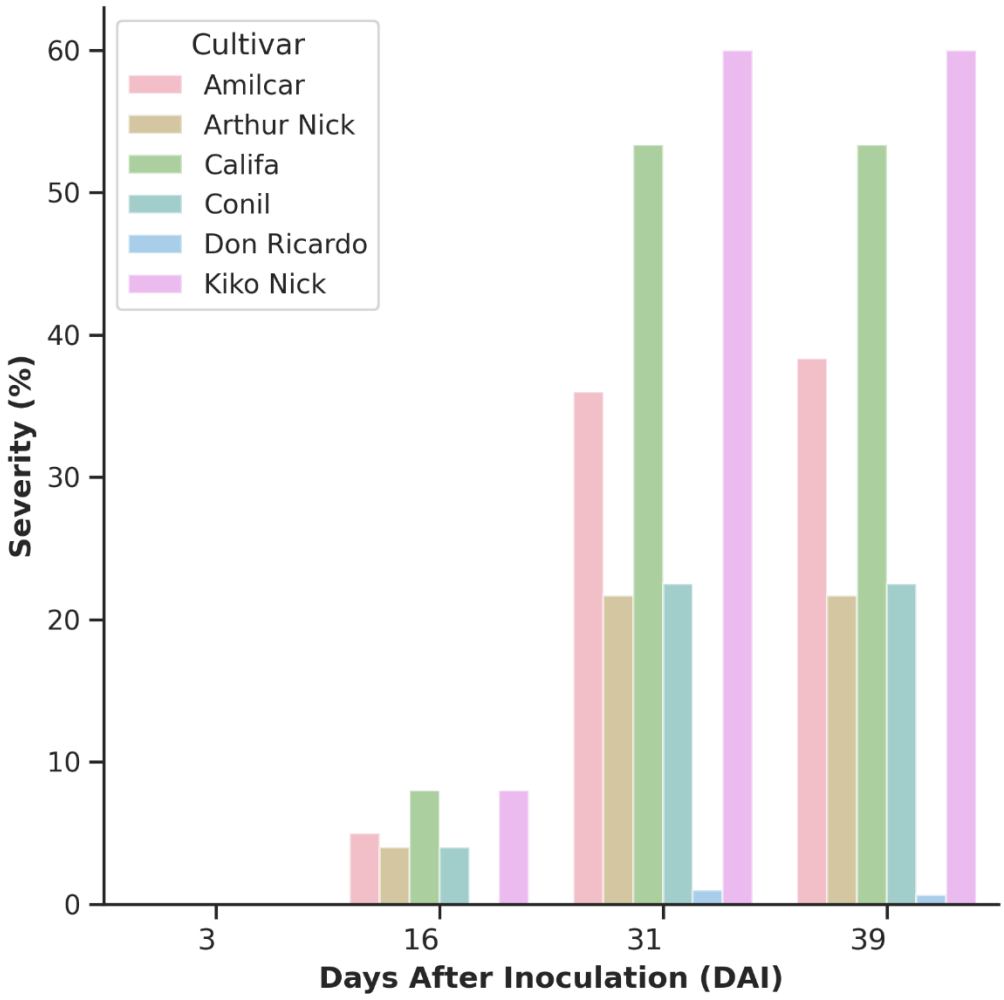

Figure 5.5 Bar plots demonstrate the evolution of severity on days after inoculation (DAI) 3, 16, 31, and 39 across all inoculated cultivars.

Figure 5.5 presents a bar chart that tracks the progression of disease severity as a percentage over time, measured at intervals of 3, 16, 31, and 39 DAI (days after inoculation) across the six wheat cultivars. Initially, at 3 DAI, no cultivars displayed any symptoms of disease. As time progresses to 16 DAI, there was a noticeable increase in severity for all cultivars, with Arthur Nick and Kiko Nick experiencing a more pronounced rise. By 31 DAI, the severity escalated further, with Kiko Nick exhibiting the highest leaf rust severity, closely followed by Arthur Nick-yellow rust. Califa and Don Ricardo present moderate severity scores, while Amilcar maintains the lowest severity among the cultivars. At the final measured interval of 39 DAI, the pattern of increasing severity continues, with Kiko Nick still showing the most substantial severity (leaf rust). Notably, Arthur Nick and Califa demonstrated a significant increase in (yellow rust) severity, suggesting that these cultivars possess intermediate levels of resistance. This pattern of progression is typical for rust infections, as reported by Roelfs et al. (1992).

5.4.2 Correlations between all the crop parameter measured manually and the severity

This section delves into the analysis of correlations between various crop parameters to determine their significance. Identifying those parameters that have a considerable impact on disease severity is especially critical, as this investigation forms a core part of the study's objectives. Subsequently, Figure 5.6 presents the correlation matrices for all measured crop parameters in non-inoculated cultivars. Within the Don Ricardo matrix, strong positive correlations are evident between Biomass and both Gw and Nog (r^2 = 1.0), suggesting either potential redundancy or a pronounced relationship among these growth-related traits for this variety. Aph demonstrates moderate to strong correlations with the remaining traits, aside from a weaker link with Noe (r^2 = 0.3). In contrast, Arthur Nick exhibits generally lower correlation coefficients compared to Don Ricardo, with the most notable correlation occurring between Gw and Nog (r^2 = 1.0). The correlations involving Aph are only modest, indicating a less marked interdependency among traits for this variety. The Kiko Nick matrix reveals a diverse correlation landscape, with the most significant correlation observed between Biomass and Gw (r^2 = 1.0). Aph is also strongly correlated with Biomass (r^2 = 0.8) and Gw (r^2 = 0.7). In contrast, Noe has a broad correlation spectrum, ranging from a strong positive association with Gw (r^2 = 0.8) to a moderate negative correlation with Aph (r^2 = -0.3).

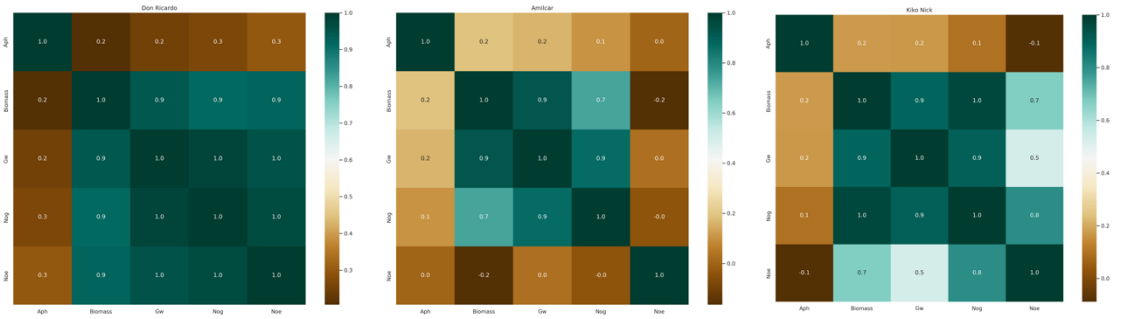

Figure 5.6 Heat map showing correlation between the crop parameters measured in cultivars non-inoculated for durum wheat. Number of ears (Noe), number of grains (Nog), grain weight (Gw) and actual plant height (Aph).

Figure 5.7 depicts heat maps that illustrate the correlations between crop parameters mentioned before measured in non-inoculated bread wheat cultivars. The Arthur Nick cultivar matrix indicates robust positive correlations across all the growth-related traits, with Biomass, Gw, and Nog exhibiting a perfect correlation (r^2 = 1.0). This suggests these traits may be highly interrelated or may exhibit redundancy within this particular cultivar. Aph shows a strong correlation with these traits, ranging from r^2 = 0.6 with Noe to r^2 = 0.8 with Biomass. In the Califa cultivar matrix, the correlations are generally moderate. The strongest correlation is again observed between Gw and Nog (r^2 = 1.0), indicating a tight linkage between these two traits. Other traits show moderate correlations with one another, with Aph displaying the least degree of association with Noe (r^2 = 0.6). The Conil cultivar matrix presents a different pattern, with the highest

correlations involving Aph, notably with Biomass (r^2 = 0.8) and Gw (r^2 = 0.7). However, Noe is less correlated with the other traits, shown by its varied correlation coefficients, the strongest being with Gw (r^2 = 0.8) and the weakest with Aph (r^2 = 0.4).

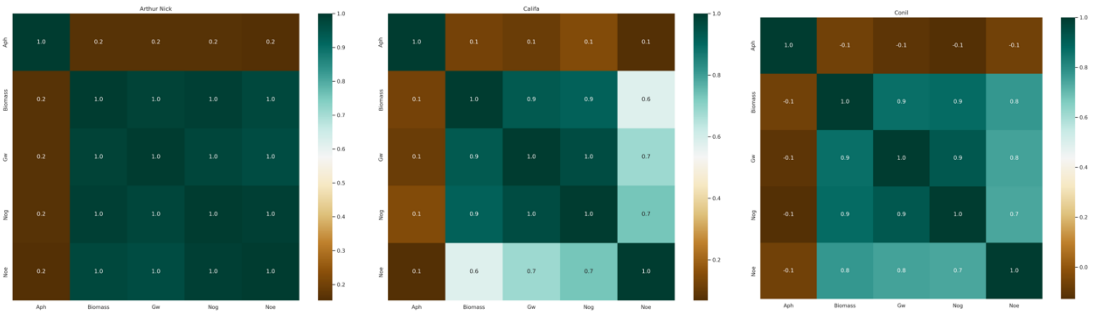

Figure 5.7 Heat map showing correlation between the crop parameters measured in cultivars non-inoculated in bread wheat. Number of ears (Noe), number of grains (Nog), grain weight (Gw) and actual plant height (Aph).

Figure 5.8 presents a series of heatmaps for three durum wheat cultivars: Kiko Nick, Don Ricardo, and Amilcar, following inoculation. The Kiko Nick heatmap reveals a significant positive correlation between Severity and Aph (r^2 = 0.8), indicating a potential relationship between plant height and disease severity. A strong interdependence is observed between Biomass and both Gw and Nog (r^2 = 1.0), suggesting these growth traits are closely linked in this cultivar's response to inoculation. The heatmap for Don Ricardo displays generally weaker correlations. The growth-related traits of Biomass, Gw, and Nog are perfectly correlated (r^2 = 1.0), denoting a tight association. Conversely, Severity exhibits a negative correlation with these traits, most notably with Gw (r^2 = -0.5), which could imply a detrimental effect of disease on growth parameters. In the heatmap for Amilcar, moderate to strong correlations are evident among the growth traits, with Biomass exhibiting substantial positive correlations with Gw (r^2 = 0.9) and Nog (r^2 = 1.0). The lack of significant correlation between Severity and the growth traits suggests that in Amilcar, disease severity may not be closely linked to these growth metrics.

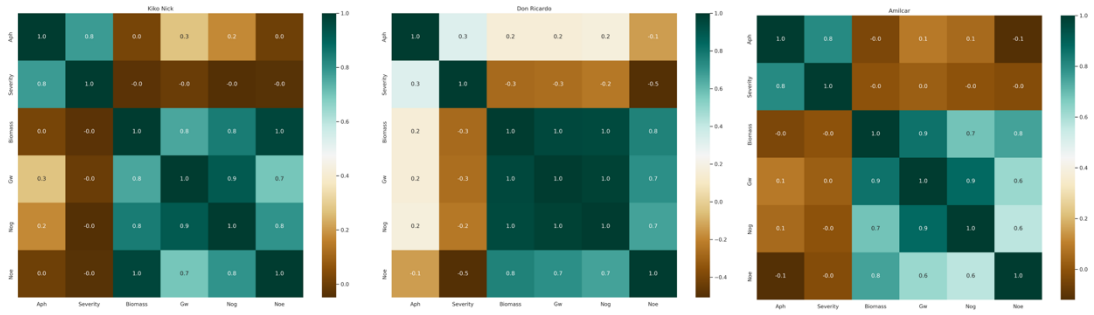

Figure 5.8 Heat map showing correlation between the crop parameters measured in cultivars inoculated of durum wheat. Number of ears (Noe), number of grains (Nog), grain weight (Gw) and actual plant height (Aph).

Figure 5.9 represents correlation matrices for the three bread wheat cultivars: Conil, Califa and Arthur Nick. In the Conil heatmap, there is a notable positive correlation between Aph and Severity (r^2 = 0.6), while most other variables such as Biomass, Gw, Nog, and Noe exhibit strong positive inter-correlations (r^2 = 1), suggesting potential redundancy or a high degree of association between these measurements within this group. The Califa heatmap shows generally weaker correlations across all variables, with the strongest positive correlation observed between Nog and Gw (r^2 = 1.0), and between Nog and Noe (r^2 = 0.9). The Aph and Severity variables display no significant correlation (r^2 = 0.0). In the Arthur Nick heatmap, moderate positive correlations are observed between Aph and Severity (r^2 = 0.6), and Aph and Gw (r^2 = 0.5). Conversely, a slight negative correlation is seen between Aph and Noe (r^2 = -0.3). The variables Nog and Noe again show a perfect positive correlation (r^2 = 1.0), consistent with observations in the Conil heatmap.

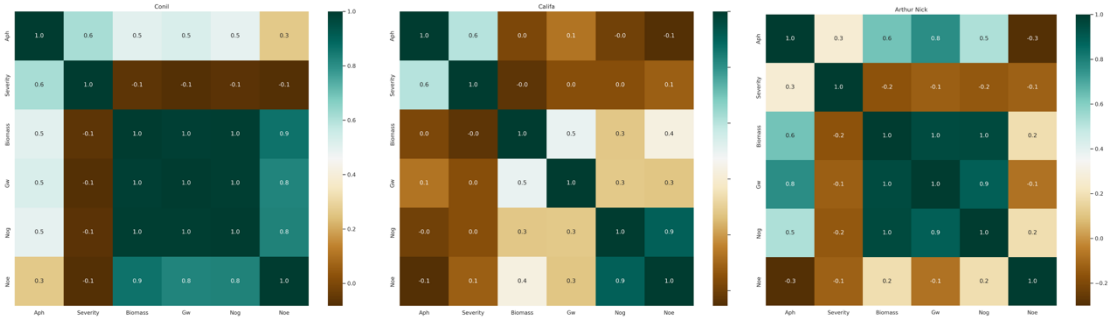

Figure 5.9 Heat map showing correlation between the crop parameters measured in cultivars inoculated of bread wheat. Number of ears (Noe), number of grains (Nog), grain weight (Gw) and actual plant height (Aph).

5.4.3 Estimation of crop parameters of interest in leaf rust detection

In Section 5.4.2, the most relevant crop parameters associated with disease severity were examined, as well as those that can be readily derived from 3D point cloud data. This section presents the findings on the estimation of plant height and biomass. Figure 5.10 depicts the correlation between Aph and Eph across three varieties of bread wheat under non-inoculated and inoculated conditions. The non-inoculated panel reveals varying degrees of positive linear associations: Arthur Nick exhibits a moderate correlation (r^2 = 0.64), Califa a relatively stronger one (r^2 = 0.57), and Conil demonstrates a weaker correlation (r^2 = 0.35). These disparities suggest that Eph's predictive accuracy for Aph varies among the varieties in the absence of inoculation. In the inoculated panel, each variety shows an enhanced correlation strength. 'Conil' presents a notably high coefficient of determination (r^2 = 0.81), indicating a strengthened predictive relationship following inoculation. Arthur Nick and Califa also display significant correlations (r^2 = 0.72 and r^2 = 0.53, respectively), suggesting inoculation potentially increases the reliability of Eph in predicting Aph.

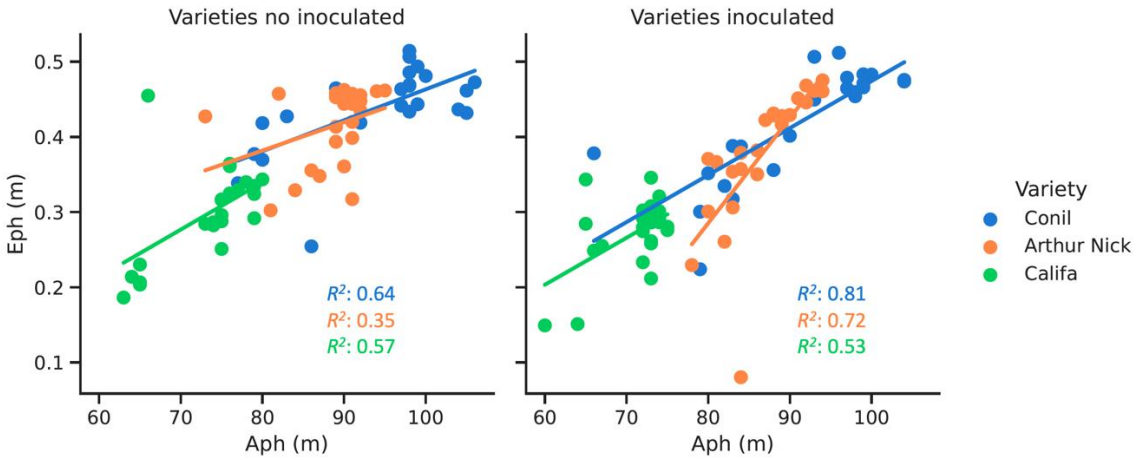

Figure 5.10 Comparative analysis of actual plant height (Aph) and estimated plant eeight (Eph) in non-inoculated and inoculated bread wheat cultivars.

On the other hand, Figure 5.11 presents a comparative linear regression analysis between Aph and Eph for three durum wheat varieties under two distinct conditions: non-inoculated (left panel) and inoculated (right panel). In the non-inoculated panel, the scatter plot reveals a range of positive linear relationships between Aph and Eph. Kiko Nick displays the strongest correlation (r^2 = 0.63), followed by Amilcar (r^2 = 0.56), and Don Ricardo (r^2 = 0.41). This variation indicates a differential accuracy in Eph's estimation of Aph when inoculation is not applied. Conversely, the inoculated panel indicates a generally stronger correlation across all varieties. Notably, Don Ricardo exhibits a substantial rise in the coefficient of determination (r^2 = 0.76) relative to its non-inoculated counterpart. Kiko Nick and Amilcar also demonstrate increased r^2 values of 0.64 and 0.48, respectively, suggesting that inoculation may improve Eph's predictive capability regarding Aph.

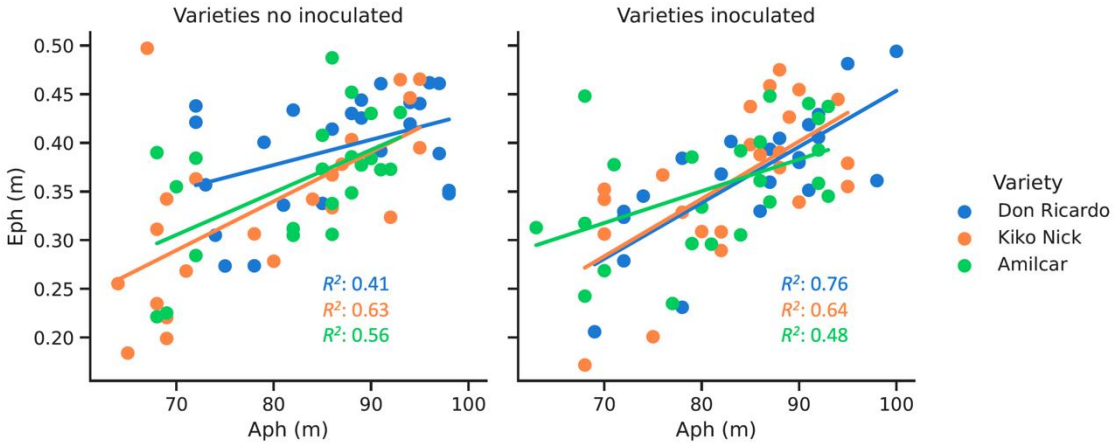

Figure 5.11 Comparative analysis of actual plant height (Aph) and estimated plant eeight (Eph) in non-inoculated and inoculated durum wheat cultivars.

Although biomass is not strongly correlated with disease severity, as mentioned previously, this parameter is typically measured only at the end of the growing season.

LiDAR data enable non-destructive estimation of biomass throughout the season. Furthermore, biomass exhibits a high correlation with other parameters integral to determining final yield. Figure 5.12 illustrates heatmaps of the Pearson correlation coefficients between actual biomass and estimated biomass derived from varying percentages (Prop10 to Prop50) of 3D point cloud data for three durum wheat cultivars: Don Ricardo, Amilcar, and Kiko Nick. These proportions represent incremental captures of the 3D plant structure used to estimate biomass at different growth stages. For the majority of cultivars and methods, the heatmaps reveal generally low correlation values, underscoring the challenge of accurately estimating biomass from 3D point cloud data. This challenge is particularly pronounced when plants are in their green matter phase, as opposed to the actual biomass measurements recorded post-senescence at season's end. An exception to this trend is observed with the inoculated Kiko Nick cultivar, where an acceptable level of positive correlation is evident. This suggests that the methods employed for Kiko Nick may have been more effective in capturing the nuances of biomass changes during the inoculated state.

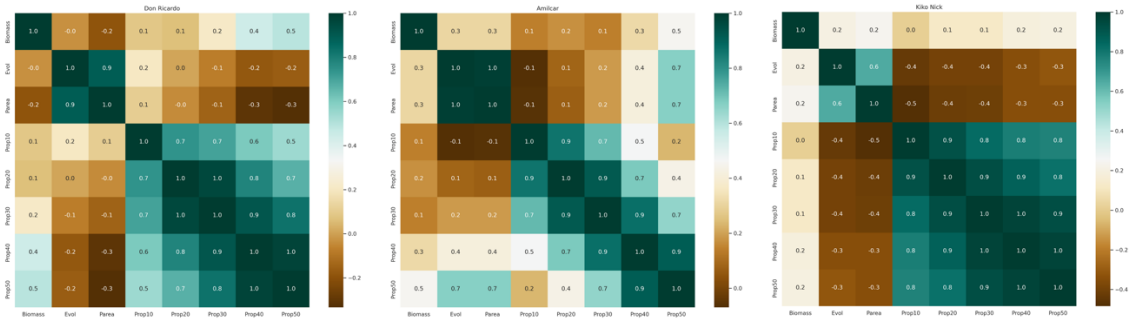

Figure 5.12 Heatmap analysis of biomass estimation with three methods: Evol, Parea and based on percentages (Prop10 to Prop50) of 3D point cloud data for durum wheat non-inoculated.

On the other hand, in Figure 5.13, the heat maps for bread wheat cultivars are depicted. In Arthur Nick, the correlations are generally moderate, peaking at Prop50, which indicates that utilizing a higher percentage of 3D point data aligns more closely with actual biomass measurements. Califa shows a progressive increase in correlation values, culminating in strong correlations at higher data proportions. This trend suggests that as more comprehensive point cloud data is employed, the accuracy of biomass estimation improves. Conil follows a similar pattern, with the most substantial correlations occurring at the later proportions (Prop30 to Prop50), signifying that estimates based on denser point cloud data are more reflective of the actual biomass.

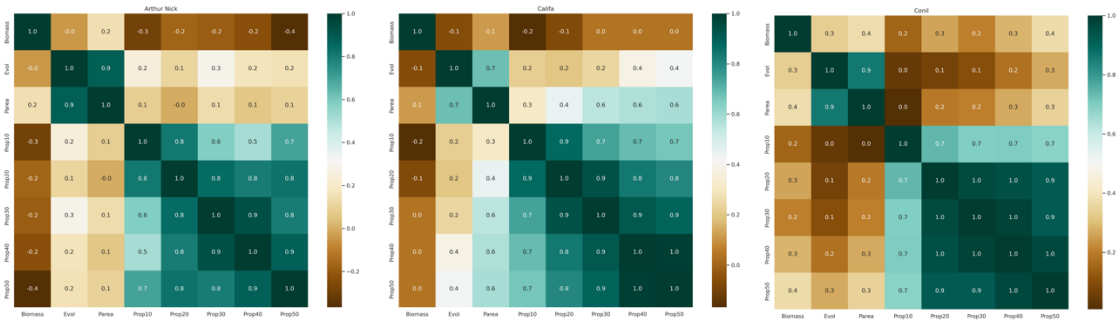

Figure 5.13 Heatmap analysis of Biomass estimation three methods: Evol, Parea and based on percentages (Prop10 to Prop50) of 3D point cloud data for bread wheat non-inoculated.

Alighted with the previous description, In Figure 5.14, the results are depicted for inoculated durum wheat cultivars, showcasing the correlation between biomass estimates and plant characteristics derived from 3D point cloud data. In Kiko Nick, there is a moderate correlation between actual biomass and plant characteristics estimated from the 3D point cloud data, with the strongest correlation at the higher proportions (Prop40 and Prop50). This suggests that the accuracy of biomass estimation improves with a greater percentage of point cloud data. The Don Ricardo heatmap shows a similar trend, with stronger correlations emerging at the higher data proportions, indicating that the completeness of the point cloud data can lead to more accurate biomass estimations. Conversely, Amilcar presents strong positive correlations across all data proportions, reflecting a consistent and reliable relationship between the point cloud data and actual biomass across all sampled percentages.

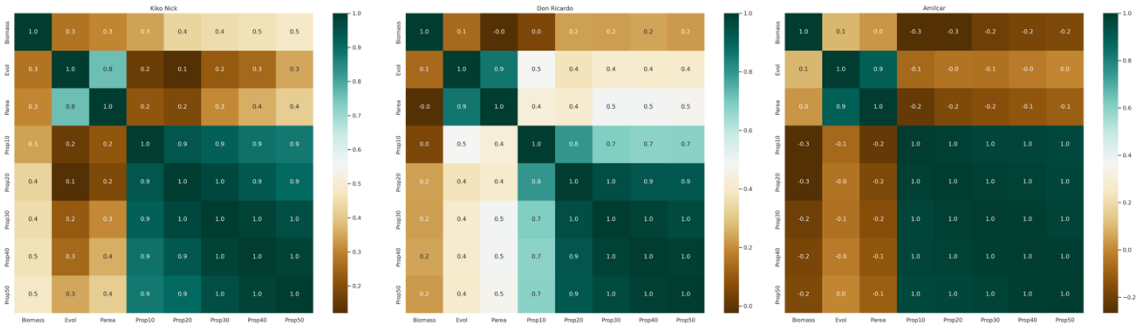

Figure 5.14 Heatmap analysis of biomass estimation with three methods: Evol, Parea and based on percentages (Prop10 to Prop50) of 3D point cloud data for durum wheat inoculated.

In Figure 5.15, for Conil the heatmap indicates weak to moderate correlations between the actual biomass and the estimated proportions from the point cloud data, with some improvement noted as the proportion of data used for estimation increases. However, the overall low correlation values suggest challenges in biomass estimation for this cultivar when utilizing point cloud data. The Califa heatmap reveals a trend of increasing correlation coefficients with higher proportions of point cloud data, signifying that more comprehensive data capture may enhance the accuracy of biomass estimation for this cultivar. A similar observation is noted for Arthur Nick, although the correlations

are generally stronger across all data proportions, indicating a more consistent relationship between the estimated and actual biomass.

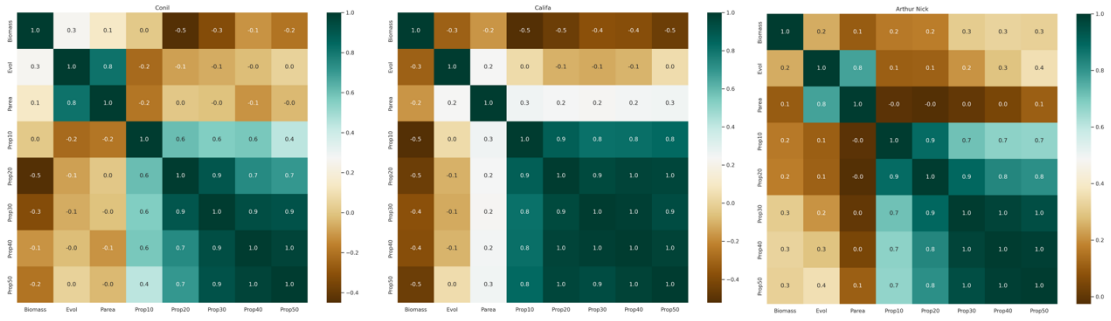

Figure 5.15 Heatmap analysis of biomass estimation with three methods: Evol, Parea and based on percentages (Prop10 to Prop50) of 3D point cloud data for bread wheat inoculated.

5.4.4 Severity estimation

Figure 5.16 presents a series of heatmaps that analyze the correlation between disease severity and varying intensities of LiDAR reflectance across three inoculated durum wheat cultivars: Kiko Nick, Don Ricardo, and Amilcar. Each heatmap corresponds to a cultivar and illustrates the correlation coefficients at different intensity thresholds, ranging from 10% (Int10) to 50% (Int50) of the reflectance data. In the Kiko Nick heatmap, a strong positive correlation is consistently observed between severity and all intensity thresholds, with the correlation generally increasing with higher intensity data, reaching up to 0.9 at Int50. This indicates that for Kiko Nick, higher reflectance intensities are closely associated with greater disease severity. For Don Ricardo, the heatmap depicts a different pattern, with a lack of significant correlation at lower intensity thresholds (Int10 and Int20). However, a modest positive correlation emerges at higher thresholds (Int30 to Int50), suggesting that the relationship between disease severity and reflectance intensity becomes more pronounced when considering a broader range of data. The Amilcar heatmap shows moderate to strong correlations across all intensity thresholds. This cultivar exhibits a consistent relationship between disease severity and LiDAR reflectance, indicating that even at lower intensity thresholds, there is a significant correlation that can be utilized for disease assessment.

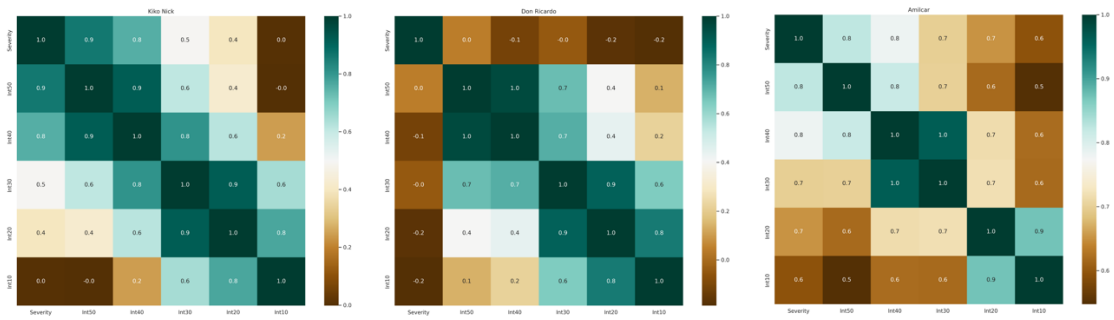

Figure 5.16 The heatmap displays the correlation analysis of disease severity and LiDAR reflectance intensities in durum wheat cultivars.

Figure 5.17 depicts heatmaps that demonstrate the correlation between disease severity and reflectance intensities measured by a LiDAR sensor for three bread wheat cultivars: Conil, Califa, and Arthur Nick. In the Conil heatmap, there is a noticeable trend of increasing correlation with higher percentages of data points. The correlation is particularly strong at Int50, suggesting a more accurate estimation of disease severity when a larger dataset is analyzed. The Califa heatmap exhibits a similar pattern, with correlations strengthening at higher data point percentages. The strongest correlation is at Int50, which indicates a robust relationship between the intensity of LiDAR reflectance and the severity of disease symptoms in this cultivar. Conversely, Arthur Nick shows a consistent level of high correlation across all percentages, with only a slight increase observed, as more data points are included. This implies a stable and significant relationship between LiDAR reflectance and disease severity, regardless of the data sample size.

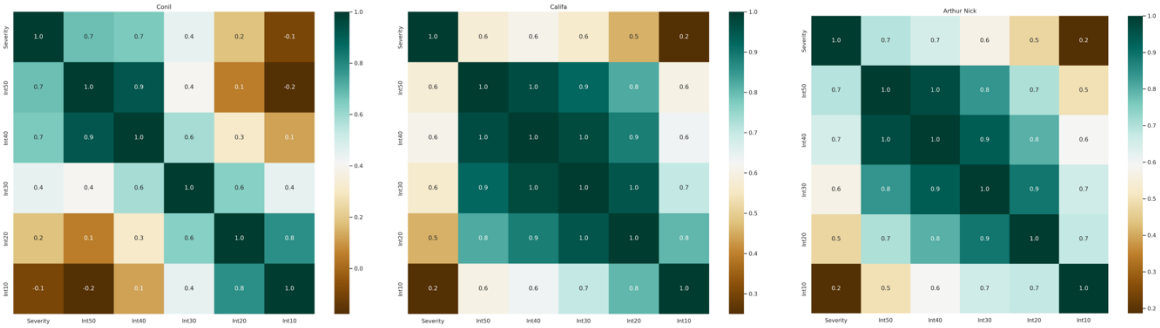

Figure 5.17 The heatmap displays the correlation analysis of disease severity and LiDAR reflectance intensities in bread wheat cultivars.

5.5 Discussion

The estimation of disease severity using LiDAR reflectance intensities presents a novel method that aligns with the growing interest in precision agriculture and the need for timely disease management. The findings of this study reveal that disease severity can be quantitatively assessed through LiDAR, supporting previous research that suggests remote sensing technologies are viable tools for monitoring plant health (Shakoor et al., 2017; Zhang et al., 2019). In inoculated durum wheat cultivars, the strong positive correlations between LiDAR reflectance intensities and disease severity, especially in Kiko Nick, align with findings by Fahey et al. (2020), who reported the utility of LiDAR in detecting foliar diseases due to the distinct light absorption and reflection properties of diseased tissue. The consistency of this relationship across intensity thresholds in Amilcar cultivar further demonstrates that even subtle variations in reflectance can be indicative of disease presence.

For Don Ricardo, the emergence of significant correlations at higher intensity thresholds may suggest that the manifestation of disease symptoms is more discernible at advanced stages, where the spectral signature of the plant's surface changes more

noticeably. This delayed correlation is consistent with the findings by Khaled et al. (2018), which indicated that the spectral detection of certain plant diseases becomes more reliable as symptoms become more pronounced. However, the relatively weaker correlations in Conil and Califa suggest that the detection of disease through LiDAR reflectance may be more complex, potentially influenced by factors such as the cultivar's canopy structure or the disease's spatial distribution within the field (Azadbakht et al., 2019). These discrepancies underscore the need for calibrating LiDAR-based severity estimation models to accommodate cultivar-specific and disease-specific factors, as also suggested by Oblinger et al. (2020). Moreover, the results corroborate the potential of LiDAR as a non-invasive method that can offer real-time data to farmers, enabling more precise applications of fungicides, which can lead to reduced chemical usage and associated costs (Mahlein et al., 2012). Implementing LiDAR in integrated disease management programs could thus contribute to more sustainable agricultural practices (Khan et al., 2021).

In conclusion, while the application of LiDAR technology for severity estimation is promising, it is imperative to consider the variability among different wheat cultivars and the stages of disease progression. Future studies should focus on refining the estimation models and exploring the integration of LiDAR data with other remote sensing modalities to enhance the accuracy and reliability of disease severity assessments.

5.6 Conclusions

It is evident that rust infection both leaf and yellow significantly impacts grain weight across various wheat cultivars, with notable reductions exceeding 50% in susceptible varieties. This effect is less pronounced on growth parameters such as plant height and biomass, which remain relatively unaffected by rust infection. The strong correlations observed between actual biomass and larger proportions of 3D point cloud data underscore the potential of LiDAR technology for non-destructive biomass estimation. However, the accuracy of these predictions varies among cultivars and is contingent upon the developmental stage, highlighting the need for cultivar-specific calibration. Moreover, disease severity can be reliably assessed using LiDAR reflectance intensities, particularly when larger datasets are analyzed, demonstrating the technology's utility in precision agriculture for disease monitoring and management. Overall, the integration of 3D point cloud data presents a promising avenue for enhancing crop parameter estimation and disease severity assessment, thereby supporting informed decision-making in crop management.

Capítulo 6. Discusión general

6.1 Roya de la hoja en trigo duro en Andalucía

En el sur de España, el trigo se produce principalmente en condiciones de secano, a menudo propensas a la sequía, con rendimientos muy variables, pero generalmente bajos, que dependen principalmente de la cantidad y distribución de las precipitaciones durante la temporada de cultivo (Martínez-Moreno y Solís, 2017). En un sistema de producción tan extensivo y de riesgo relativamente alto, la viabilidad económica de cualquier cultivo requiere la maximización de la expresión del potencial de rendimiento bajo las condiciones climáticas predominantes en un año determinado y la minimización de los costes de producción (Borlaug, 2007). El control genético de las royas, el factor biótico más importante en la región, logra ambas cosas (Patpour et al., 2020). No sólo es clave para la viabilidad económica del trigo, sino que también reduce la huella ambiental del cultivo y de todo el sistema de producción (Martínez-Moreno et al., 2020). El primer paso para lograr un control genético eficaz y duradero de las royas del trigo es la caracterización exhaustiva de los linajes (o grupos de razas) / razas del patógeno presente en la región y las áreas adyacentes (Hovmoller et al., 2023). El segundo paso implica evaluar las opciones genéticas disponibles previamente caracterizadas (genes de resistencia conocidos), así como las fuentes de resistencia no caracterizadas, para determinar su idoneidad frente a los linajes / razas predominantes del patógeno (Hovmoller et al., 2023).

La roya de la hoja ha sido la especie de roya más frecuente en Andalucía, tanto en trigo harinero como en trigo duro. Sin embargo, el trabajo de empresas e instituciones de mejora vegetal como el CIMMYT, ha producido cultivares resistentes, y el control eficiente de esta enfermedad (Borlaug, 2007). *P. tritici-duri* es otra especie de roya del trigo presente en Marruecos, sur de Portugal y sur de España, descrita desde hace décadas, y que afecta principalmente a trigo duro (Roelfs, 1992). En el presente trabajo hemos descrito el daño causado por esta especie de roya sobre cultivares de trigo duro. Es un daño variable entre años, pero la respuesta es bastante uniforme en todos los cultivares tanto, en campo como en invernadero. Cuando infecta a los cultivares de trigo duro, casi todos muestran una resistencia intermedia que, en ausencia de otras enfermedades, causan un daño apreciable. Existen muy pocos cultivares con un buen nivel de resistencia, como Calero.

P. tritici-duri ha estado presente en la zona Mediterránea occidental durante mucho tiempo (Anikster et al., 1997). Curiosamente, *Anchusa azurea* (el huésped alternativo de *P. tritici-duri*) infectada por roya, fue citada en España antes de 1902 (Navarro, 1902), y más específicamente en el sur de España, poco antes de 1918 (González-Fragoso, 1918). La investigación sobre la roya de la hoja del trigo duro se reactivó a nivel mundial cuando, en 2001, apareció en México y más tarde en otras partes del mundo una nueva raza de roya de la hoja (BBG/BN), virulenta en *Lr72* (un gen

frecuentemente utilizado en cultivares de trigo duro a nivel mundial) (Herrera-Foessel et al., 2014). Hasta ese momento, la resistencia a la roya en trigo duro a nivel mundial dependía principalmente de dos genes, *Lr72* y *Lr14a* (Singh et al., 2004). Pero el desarrollo de razas virulentas frente a estos dos genes convirtió a *P. triticina* en una enfermedad importante en el trigo duro a nivel mundial, incluida España (Martínez-Moreno y Solís, 2019).

Aunque en principio *P. tritici-duri* fue detectada en el área de distribución geográfica de *Anchusa azurea*, es posible que haya podido desplazarse de esta región a otras sin ningún huésped alternativo. Esta capacidad de la roya para sobrevivir y coexistir sin el huésped alternativo ha sido descrita previamente como lo indica la expansión de *P. triticina*, fuera del área de su huésped alternativo, *Thalictrum spp.*, en el sur de Europa (Anikster et al., 1997).

Las royas siempre han sido un problema en el trigo, su naturaleza evolutiva y el rápido desarrollo de virulencia hacia cultivares con resistencia efectiva es una característica de estos patógenos (Figueroa et al., 2020). La roya de la hoja no es una excepción, y la aparición de razas virulentas a cultivares de trigo duro que contienen el gen *Lr14a* en España en 2013, es un buen ejemplo (Soleiman et al., 2016). Sin embargo, en este estudio ha surgido otra especie de roya de la hoja, *P. tritici-duri*, en los campos de trigo duro de Andalucía occidental. Esta especie de roya no es nueva, ya que ha estado presente en Marruecos, Portugal e incluso en el sur de España durante mucho tiempo, pero el impacto en el desarrollo del trigo fue limitado (D´Oliveira y Samborski, 1966; Anikster et al. 1997). Estos países han tenido una gran tradición en la plantación de trigo duro, especialmente Marruecos, pero también en el sur de la Península Ibérica (Martínez-Moreno et al., 2020). La distancia entre Marruecos y el sur de España es muy corta, y las condiciones climáticas son similares, por lo que las diferentes razas de roya vuelan fácilmente y se desplazan de un país a otro (Martínez-Moreno y Solís, 2019). Aunque *P. tritici-duri* puede estar presente en la zona desde hace mucho tiempo, el reciente aumento de la incidencia en el trigo duro en Andalucía desde 2020 ha sido muy significativo y alarmante para una región en la que se siembra el 60% de la superficie triguera, de trigo duro (Martínez-Moreno y Solís, 2019).

P. triticina y *P. tritici-duri* mostraron diferencias importantes, principalmente en el tamaño de sus pústulas, siendo las de *P. tritici-duri* más grandes que las de *P. triticina*. La otra diferencia, fue la velocidad con la que se desarrollan los telios, los primeros lo hacen a los 26 días después de la inoculación, mucho más rápido que los segundos, que desarrollan telios a los 45 días en las mismas condiciones. Estos resultados fueron consistentes con lo publicado por Anikster et al. (1997). Los espectros de virulencia en el conjunto diferencial de Thatcher también fueron bastante diferentes, siendo las razas de *Puccinia triticina* recolectadas de trigo duro, avirulentas en *Lr1, Lr3ka, Lr9, Lr17* y virulentas en *Lr18* y *Lr20*. *P. tritici-duri* presentó una reacción mesotética (mezcla de pústulas con diferentes tipos de infección en la misma hoja) hacia casi todas las líneas isogénicas Thatcher, donde las lesiones de infección tipo 1 se mezclaron con pústulas bien formadas, pero pocas, de infección tipo 2-3. Sólo los genes *Lr24, Lr26* y *Lr28* fueron

claramente eficaces contra *P. tritici-duri*. *Lr24* está ubicado en el cromosoma 3D y no puede transferirse al trigo duro mediante cruzamiento y selección regular, y su transferencia requeriría transferencias citogenéticas antes de poder usarse en programas de mejora regulares. *Lr26,* ubicado en el cromosoma translocado 1B/1R y originario del centeno, se ha utilizado ampliamente durante décadas en el trigo harinero (McIntosh et al., 1995), pero, hasta donde sabemos, no se ha implementado comercialmente en el trigo duro. Es necesario evaluar críticamente su uso potencial como opción de resistencia contra *P. tritici-duri*, ya que se sabe que la translocación 1B/1R causa tenacidad en las masas inadecuadas en el trigo harinero y también podría afectar la fuerza del gluten y las características del trigo duro. Finalmente, *Lr28,* ubicado en el cromosoma 4A y originario de *T. speltoides* (McIntosh, 1995), se ha utilizado de manera más limitada en el trigo harinero, pero se ha descrito que la virulencia de este gen es muy frecuente en poblaciones de *P. triticina* en todo el mundo (McIntosh, 1995). Según los resultados de este estudio, los pocos genes de resistencia de plántulas bien caracterizados, utilizados en el trigo harinero, que podrían usarse en el trigo duro como opciones de resistencia contra *P. tritici-duri,* presentan importantes inconvenientes, que pueden desaconsejar su uso en programas de mejora de trigo duro.

P. tritici-duri está presente en Andalucía occidental y, aunque esporádicamente, puede suponer un problema grave en el trigo duro, porque se han identificado muy pocos genotipos completamente resistentes (Huerta-Espino et al., 2014). La mayoría de los cultivares y genotipos evaluados en este estudio, y en conjuntos más grandes se caracterizan por la misma reacción intermedia severa (Huerta-Espino et al., 2014). La mayoría de los cultivares considerados resistentes a la roya de la hoja, como Don Ricardo (*Lr27+Lr31*), que es, desde hace muchos años el cultivar más sembrado en Andalucía (Martínez-Moreno y Solís, 2017), son susceptibles a *P. tritici-duri.* Otros genotipos con genes *Lr* diferentes, como *LrCamayo,* presente en el cultivar mexicano Cirno C2008, también se han visto afectados significativamente por esta especie de roya. *Lr19* y *Lr47* son genes globalmente eficaces que se originan a partir de parientes silvestres del trigo (Kthiri et al., 2017). Se introdujeron en el trigo harinero dando una respuesta casi inmune, y recientemente en el trigo duro (Ammar, c.p.). *P. tritici-duri* parece superar fácilmente la resistencia de estos dos genes. Hasta la fecha, entre los cultivares liberados cultivados en Andalucía, sólo Calero mostró una resistencia interesante frente a las dos razas de *P. tritici-duri* empleadas en este estudio. Es probable que la resistencia de Calero hacia las razas de *P. triticina* esté ubicada en los cromosomas 6B, muy cerca de *Lr61*, ya que las pruebas de alelismo entre Calero y Guayacán, la fuente de *Lr61* (Herrera et al., 2008b) no han arrojado ninguna planta susceptible recombinante, basada en estudios realizados en el CIMMYT (Ammar, c.p.). Si esta es, o no, la base subyacente a la resistencia de Calero a *P. tritici-duri* no se podrá saber hasta que se realicen los estudios adecuados.

Dados los niveles casi generalizados y variables de susceptibilidad, observados en los conjuntos relativamente pequeños de germoplasma evaluados en el sur de España contra *P. tritici-duri*, y las limitadas opciones disponibles con genes de resistencia conocidos para proporcionar resistencia completa a *P. triticina*, para los mejoradores, será necesario explorar y encontrar nuevas fuentes de resistencia adecuada en conjuntos de

germoplasma más amplios y diversos. Estas actividades de búsqueda de resistencia deberán realizarse en condiciones que aseguren la presencia exclusiva de *P. tritici-duri* sin el efecto de confusión de *P. triticina*. Sin embargo, antes de que se tomen iniciativas tan costosas, es importante evaluar con precisión la probabilidad de que *P. tritici-duri* se convierta en un patógeno importante que limite el rendimiento en el sur de España, y estimar el coste económico real, a través de la pérdida de rendimiento, cuando el patógeno está presente en los cultivares que sean resistentes a *P. triticina.*

6.2 Roya amarilla y del tallo en Andalucía

En cuanto al estudio de roya amarilla y del tallo, se basó exclusivamente en la infección natural de ambas royas. Esto aseguró que el muestreo de patógenos para análisis raciales y genotipado involucrara linajes/razas que fueran representativos de aquellos realmente presentes en la región. Los resultados indicaron que los linajes de roya amarilla PstS10 (Warrior-), PstS13 y PstS14 fueron los más habituales en el sur de España desde el 2016 hasta la actualidad. Informes previos del GRRC de otras zonas de España también hacen referencia a la presencia de PstS4 y PstS7 (Warrior) (GRRC, 2023). Se sabía que algunos de estos linajes estaban presentes en el valle del Guadalquivir (Martínez-Moreno et al., 2019), pero no causaron epidemias graves hasta 2015, cuando se atribuyó una fuerte infección en el norte de España a la raza Warrior. Esta raza, descrita anteriormente en Dinamarca, Francia, Inglaterra, Alemania y Suecia, superó la resistencia de la mayoría de los cultivares de trigo comerciales en estos países (Hovmoller et al, 2016). Parece que se originó en la región del Himalaya de Pakistán y posteriormente se extendió rápidamente por toda la zona triguera de Europa (Hovmoller et al., 2016). La zona del sur de España fue, de hecho, una de las últimas en ser alcanzada por esta dispersión, probablemente porque estaba en el extremo suroeste de Europa con condiciones climáticas menos favorables. Los linajes más nuevos, PstS13 y PstS14, son probablemente aquellos a los que se debe prestar más atención, ya que su presencia generalmente se asoció con una mayor severidad en los cultivares comerciales evaluados en este estudio. Esto fue particularmente visible en los cultivares de trigo duro, con la aparición de cierta incidencia, aunque en niveles muy bajos, durante los últimos años del estudio, a medida que PstS13 y PstS14 se hicieron más presentes. En 2016 se detectó PstS14 en Marruecos y Sicilia (Italia) por el GRRC. Este linaje (virulento en *Yr2, Yr3, Yr6, Yr7, Yr8, Yr9, Yr17, Yr25, Yr32* y *YrSp*) se detectó por primera vez en España en 2017 (GRRC, 2023).

El seguimiento de la reacción de cultivares de trigo harinero, trigo duro y triticale, ha sido útil para proporcionar una evaluación de una posible mayor infección de roya amarilla. El hecho de que existan cultivares resistentes y con buenos rendimientos para los tres cultivos es un resultado muy positivo, ya que proporcionan soluciones genéticas inmediatas frente a la roya amarilla sobre la producción de trigo en el sur de España, soluciones que las entidades de mejora vegetal podrían utilizar como fuentes de resistencia en sus programas de mejora.

Si bien, el número de cultivares estudiado ha sido pequeño, nuestros resultados indican que los cultivares de trigo duro y triticale fueron menos afectados por los linajes de roya amarilla del sur de España, que de trigo harinero. Los cultivares de trigo duro, fueron en la mayoría de los casos, inmunes a la enfermedad, e incluso cuando algunos síntomas estaban presentes, generalmente a partir del cuarto año del estudio, mostraron una severidad muy baja. El cultivar Athoris tuvo una severidad mayor, pero sólo en una ubicación durante el último año del estudio. Los cultivares de triticales evaluados, también mantuvieron inmunidad o casi inmunidad a la roya amarilla durante la duración del estudio. El antiguo cultivar Trujillo perdió su resistencia a la roya amarilla (y a otras enfermedades) hace décadas en México, España y Túnez (M.S. Gharbi, c.p.). Mientras que los cultivares resistentes de trigo harinero Tejada y Arthur Nick exhibieron niveles de resistencia similares a los de los cultivares resistentes de trigo duro y triticale, los cultivares Califa y Escacena fueron claramente susceptibles, se caracterizaron por niveles de susceptibilidad, no observados en las otras especies.

La mayor resistencia del trigo duro y triticale respecto al trigo harinero se ha observado más ampliamente en todo el mundo. Entre el germoplasma de los tres cultivos enviados anualmente por el CIMMYT al sur de España durante los últimos 20 años, las líneas de trigo duro o triticale altamente susceptibles eran poco frecuentes, pero se observaban regularmente algunas líneas de trigo harinero altamente susceptibles. Por otra parte, se puede observar una frecuencia baja de susceptibilidad en el germoplasma de trigo harinero del CIMMYT, distribuido en los mismos viveros internacionales.

Los resultados de este estudio indican que es menos urgente trabajar para mejorar la base genética de la resistencia a la roya amarilla en trigo duro. En 2019, una epifitia de roya amarilla nunca vista, apareció en campos comerciales de trigo duro en el centro de Chile y, en los campos experimentales del programa nacional, un 70% de las líneas evaluadas como parte del Vivero Internacional de Detección de Trigo Duro del CIMMYT fueron susceptibles (I. Matus, INIA-Chile, c.p.), mientras que el mismo germoplasma mantuvo su resistencia prácticamente generalizada a la roya amarilla en ensayos fuera de Chile (datos no publicados). Posteriormente, miles de líneas de mejora del programa del CIMMYT fueron enviadas al INIA Chile para evaluar su reacción a la raza local de roya amarilla, confirmando la alta frecuencia (cerca del 70%) de líneas susceptibles dentro de este grupo de germoplasma. Si bien, hasta el momento, no hay evidencia de que esta raza haya salido de Chile, los mejoradores de trigo duro de la cuenca mediterránea, incluidos los que suministran germoplasma al sur de España, deben evaluar los riesgos asociados con la aparición de una raza peligrosa para su región.

Desde la década de 1970, una parte importante de los cultivares de trigo harinero de primavera, sembrados en el sur de España, se originaron en el programa de mejora del CIMMYT, con sede en México. Este programa implementó una amplia gama de genes *Yr*, como *Yr6, Yr9* e *Yr17*, los cuales eran bastante comunes en el pasado, pero su resistencia ha sido superada por nuevas razas. Por otro lado, *Yr27*, un gen todavía utilizado por el CIMMYT, y probablemente presente en el material de trigo harinero plantado en Andalucía, ya que es eficaz contra el linaje Warrior (Hovmoller et al., 2016).

En este estudio, este gen ha proporcionado una resistencia intermedia. Los otros genes que cabe destacar por su utilidad frente a los linajes del sur de España son *Yr5*, *Yr10* e *Yr15*, cuya presencia en las series diferenciales se asoció a una reacción inmune durante todos los años. El gen *Yr5*, ubicado en el cromosoma 2BL, es eficaz contra la mayoría de las razas de roya amarilla en todo el mundo y se originó a partir de *T. spelta* (Yan et al., 2003). *Yr15* es otro gen que está funcionando bien en todo el mundo, incluso contra las razas Warriors. Debido a su eficacia global, contra la mayoría de las razas de roya amarilla en todo el mundo, y a la disponibilidad de marcadores moleculares confiables, que podrían facilitar su introgresión en el germoplasma de élite, estos genes representan soluciones protectoras muy atractivas, y seguramente, serán utilizados ampliamente en programas de mejora en todo el mundo. En teoría, esto podría exponerlos a las poblaciones de patógenos en rápida evolución, como se ha visto en el pasado con muchos otros genes.

A diferencia de la roya amarilla, la roya del tallo aún no es un problema comercial en España, pero, en los últimos años, el patógeno apareció ocasionalmente al final de la temporada regular de cultivo del trigo en el sur del país. Históricamente, cuando las variedades locales de maduración muy tardía, y generalmente susceptibles a la roya del tallo, se cultivaban extensamente en la cuenca mediterránea, la enfermedad era muy habitual. Era un escenario en el que un huésped susceptible, mantenía el tejido verde hasta finales de la temporada de primavera (mayo-junio), proporcionando al patógeno de aparición tardía condiciones favorables para infectar con éxito el cultivo (Pretorius et al., 2000). Con el desplazamiento completo de estas variedades locales por cultivares semienanos y de rápida maduración de la Revolución Verde, (que también eran en su mayoría resistentes a las razas antiguas de roya del tallo en Andalucía y España, gracias a los genes efectivos *Sr2* y *Sr31),* la enfermedad prácticamente desapareció y dejó de ser una preocupación que amenazaba el rendimiento. No solo desapareció de España, sino de casi todo el mundo en el periodo 1955-1998 (Pretorius et al., 2012). Sin embargo, la evolución reciente de las razas de patógenos, y la aparición más regular de la enfermedad en la cuenca mediterránea, han generado preocupación y nos han llevado a considerar la roya del tallo, como una posible amenaza emergente para la producción de trigo en el sur de España.

Todas las evaluaciones se realizaron nuevamente basándose exclusivamente en infecciones naturales, que ocurrieron durante cada uno de los cinco años de este estudio, y se convirtieron en intensas epidemias gracias a los riegos semanales implementados para la siembra de verano (plantación fuera de temporada o contraestación), que reúne tejido foliar verde de huéspedes susceptibles, un patógeno virulento y condiciones favorables para la infección.

Según las lecturas de campo de este estudio y el análisis de ADN en el GRRC, los grupos predominantes presentes durante el estudio actual fueron el Clade IV-B (TKKTF) y el Clade IV-F (TKTTF) (GRRC, 2023). Según lo informado por Abdedayem et al. (2023), la roya del tallo ha reaparecido recientemente en muchas partes de Europa y norte de África. La presencia de la raza TTRTF, también llamada raza siciliana, en el sur de

España, se consideró improbable, ya que esta raza es virulenta frente al gen *Sr13* (Olivera et al., 2021), y la línea que alberga *Sr13* siempre fue resistente (resistencia parcial), durante la duración de este estudio. Los marcadores moleculares identificaron 37 aislados recolectados en Francia en 2021 en el marco de la campaña de muestreo del RustWatch (proyecto europeo coordinado por el GRRC destinado a caracterizar las principales razas de royas en Europa). Todos ellos se agruparon en dos grupos genéticos, Clade IV-B y Clade IV-F. Estos dos grupos ya fueron detectados en 2019 y 2020 en Francia y en 2018 y 2019 en Italia. Toda esta información indica claramente que estas son las principales razas de roya del tallo en la Europa mediterránea (Hovmoller et al., 2023), y probablemente en el norte de África. Además, según los análisis de ADN de muestras enviadas al GRRC desde todas partes de Europa, las razas del linaje Ug99 no han llegado a Europa. Esto se confirmó en el caso del sur de España, ya que las razas locales y el linaje Ug99, diferían en su virulencia sobre *Sr24* y *Sr31*.

Otra clara diferencia entre la roya amarilla y la roya del tallo reside en el nivel de expresión de su resistencia. Mientras que la resistencia a la roya amarilla a menudo se expresaba como una reacción totalmente inmune (ausencia total de pústulas), la resistencia a la roya del tallo es casi siempre incompleta, como la debida a los genes *Sr22* o *Sr25*.

Los resultados del seguimiento de la reacción a la roya del tallo, de las principales variedades sembradas en el sur de España, indican que los agricultores de esta región disponen de soluciones genéticas comerciales adecuadas, en caso de que esta enfermedad se convierta en un problema. Si bien, la probabilidad de que esto suceda puede considerarse baja, de hecho, se materializó durante el presente estudio en la localidad de Jerez en 2022. Los cultivares de trigo duro Amílcar, Don Ricardo y Calero, los cultivares de trigo harinero Tejada e incluso Conil, y los cultivares de triticale Bondadoso y Valeroso, fueron consistentemente resistentes tanto a la roya amarilla como a la roya del tallo. En España las razas de roya del tallo no son virulentas frente al gen *Sr13*, aunque la virulencia sí está presente en el sur de Italia, por lo que, seguramente, pronto llegará a España. Los resultados de la selección de una gran colección de líneas de trigo duro de diferentes conjuntos de germoplasma contra la raza JRCQC (con virulencia combinada en *Sr9e* y *Sr13*) (Olivera et al., 2012), revelaron una frecuencia muy baja de resistencia, supuestamente del 5,2%. La baja frecuencia de resistencia contra las razas etíopes con virulencia combinada en *Sr9e* y *Sr13* se confirmó al examinar miles de líneas del CIMMYT a lo largo de años en Etiopía (Ammar c.p.). En este contexto, queda claro que las razas actualmente presentes en España no representan una amenaza inmanejable para la producción local de trigo, sino que la amenaza más importante vendría de una eventual aparición de razas con virulencia al gen *Sr13*. Cualquier esfuerzo de mejora preventiva o programa de selección de variedades para proporcionar cultivares resistentes a la roya del tallo para el sur de España, debería apuntar a la resistencia a razas con virulencia combinada en *Sr13/Sr9e*, y no simplemente de la resistencia a las razas actualmente presentes en España. Esto se puede abordar eficazmente usando germoplasma reciente del CIMMYT, que fue, previamente seleccionado, para detectar resistencia a las razas africanas, ya sea a los linajes Ug99, mediante la selección en Kenia para trigo harinero, o

a la virulencia *Sr13/Sr9e,* mediante la evaluación de líneas en Kenia y Etiopía para el trigo duro. Los resultados del presente estudio confirman la idoneidad de este enfoque, ya que muchas de las líneas de trigo duro, que se sabe que tienen niveles aceptables de resistencia en Etiopía y Kenia, también eran resistentes a las razas actualmente presentes en el sur de España.

En términos de utilidad para el sur de España, se encontró que los genes *Sr22* y *Sr25* proporcionaron una protección adecuada contra las razas españolas en el presente estudio, al igual que se sabe también que es eficaz contra las razas africanas de roya del tallo (Ammar c.p.). El gen *Sr22* se originó a partir de *T. monococcum,* y se ha mapeado en el cromosoma 7AL del trigo. Sin embargo, no se ha utilizado muchodebido a una penalización de rendimiento (Khan et al., 2019). El gen *Sr25*, ligado a *Lr19*, se transfirió al trigo harinero en un segmento que también se mapeó en el cromosoma 7AL. Se ha utilizado ampliamente en muchos cultivares de trigo harinero de primavera, de las regiones media y baja del Volga en Rusia (Sibikeev et al., 2021), con cierta presencia en el germoplasma de trigo harinero del CIMMYT. Cuando se introduce en trigo duro, este gen proporciona buenos niveles de resistencia a las razas españolas (como se indica en el presente estudio), así como a las razas de trigo duro etíopes. La primera generación de líneas CMMYT con *Sr25,* experimentó mermas en el rendimiento, especialmente en condiciones de sequía. Después de dos ciclos de cruzamiento/selección, se desarrolló nuevo germoplasma del CIMMYT, que porta *Sr25* sin penalización en el rendimiento (Ammar c.p.). La combinación *Sr22+Sr25* es atractiva para su uso en la mejora, ya que ambos genes están estrechamente vinculados en el cromosoma 7AL. Una vez ensamblados en la configuración genética correcta, deberían efectivamente heredarse juntos con muy poca probabilidad de ser separados en ciclos posteriores de cruce/selección. Se descubrió que era la combinación más eficaz contra las razas españolas actuales de roya del tallo, con reacciones generalmente cercanas a una respuesta inmune en el presente estudio. En material de trigo duro del CIMMYT, la primera generación de líneas portadoras de ambos genes se caracterizó por severas penalizaciones en rendimiento y tolerancia a la sequía, pero después de dos ciclos de cruce/selección, la última generación de dichas líneas tuvo menor pérdida de rendimiento y tolerancia a la sequía, lo que hace que sean parentales mejorados útiles para usar en cualquier programa de mejora.

Otros genes, como el *Sr38,* con utilidad limitada en la mejora del trigo harinero contra la roya del tallo, aún pueden ser útiles para el trigo duro. Incluido en un fragmento 2NS translocado al cromosoma 2AS del trigo harinero, se utilizó ampliamente por su triple resistencia a las royas, ya que además porta los genes *Lr37* e *Yr18*. Actualmente se considera que el gen *Sr38* tiene una utilidad limitada contra la roya del tallo del trigo harinero. En el presente estudio fue transmitido por el cultivar Trident, que resultó ser susceptible a las razas españolas. Sin embargo, cuando se introdujo en un fondo genético de trigo duro, tuvo un efecto variable contra las razas españolas, que iba desde la completa inmunidad hasta la completa susceptibilidad. La línea de introgresión original (línea 36) tenía un nivel intermedio de resistencia a las razas españolas, con reacciones de campo altamente resistentes a las razas africanas de trigo duro en Etiopía y Kenia. La otra línea

de introgresión *Sr38* (línea 37) tuvo una reacción bastante susceptible a las razas españolas, y se caracterizó por una reacción intermedia-susceptible contra las razas etíopes, lo que sugiere una posible recombinación entre el marcador molecular utilizado en la introgresión y el gen real. La línea 1 del conjunto evaluado en nuestro trabajo fue el resultado de la introgresión de *Sr38* mediante selección asistida por marcadores en un fondo genético de élite del CIMMYT que ya tenía un buen nivel de resistencia a las razas africanas de roya del tallo, de ahí su reacción inmune, probablemente debido a efectos aditivos de varios genes, incluido el *Sr38*. Los genes de resistencia a la roya con utilidad limitada o nula en el trigo harinero, pero con un valor significativo para la mejora del trigo duro, no son desconocidos. Un claro ejemplo es el del gen *Lr14a* de resistencia a la roya de la hoja. Es completamente ineficaz en la mejora del trigo harinero, ya que la mayoría de las razas de roya de la hoja del trigo harinero son virulentas en este gen. Sin embargo, la mayoría de las razas que son virulentas en trigo duro, son avirulentas frente al gen *Lr14a*, lo que lo convierte en una de las fuentes más útiles de resistencia genética en el trigo duro durante muchos años (Macaferri et al., 2010). De todas formas, su efecto fue vencido en España en 2013 y otras zonas de la cuenca mediterránea (Soleiman et al., 2016), pero sigue siendo muy eficaz en otras partes del mundo hasta el día de hoy.

6.3 Eficacia de los datos hiperespectrales para detectar la roya amarilla y de la hoja en el trigo

Respecto al estudio de sensores, la precisión y los resultados de la puntuación F1 se analizaron en diferentes modelos y conjuntos de datos. Los conjuntos de datos utilizados pueden considerarse comparativamente pequeños con respecto a otros estudios que utilizan conjuntos de datos públicos como PlantVillage (Thakur et al., 2022), que tiene 54.305 imágenes de 14 especies de plantas, para el entrenamiento de aprendizaje automático. El estudio realizado por Lu et al. (2021) es uno de los pocos trabajos que destaca un desafío importante. Este desafío se relaciona con la insuficiencia actual del tamaño y la diversidad de los conjuntos de datos en la aplicación de modelos de clasificación de enfermedades en plantas. Además, es fundamental considerar todas las posibles condiciones de captura, variaciones de síntomas y características de los sensores utilizados (Barbedo, 2018). Por estas razones, es inevitable tener conjuntos de datos completos y, por lo tanto, los modelos en su aplicación tienen un alcance limitado.

Existen varias alternativas para abordar los efectos del uso de conjuntos de datos incompletos, siendo una de las más comunes el aumento de datos a través de varias técnicas que se pueden combinar entre sí. Sin embargo, según la literatura revisada por Kobayashi et al., (2018), cada técnica de aumento de datos afecta la precisión del modelo de manera diferente.

En este estudio, el algoritmo SMOTE se aplica en diversos grados a un pequeño conjunto de datos para una sola enfermedad con tres categorías. Esto demuestra cómo la precisión general aumenta con la aplicación de técnicas de aumento de datos. Este

resultado se alinea con los obtenidos en el estudio realizado por Uguz y Ulysal (2021), donde se utilizó un conjunto de datos de 3.400 imágenes hiperespectrales para diferenciar entre dos enfermedades y plantas sanas en tres categorías. Sin embargo, sus resultados demuestran un aumento en la precisión en todas las categorías, mientras que, en el presente estudio, la precisión no aumenta en la categoría que consta de datos originales.

6.4 Detección de roya de la hoja y amarilla en cultivares de trigo, usando sensor LiDAR

Respecto al conjunto de datos donde se aplicó el algoritmo SMOTE únicamente al conjunto de entrenamiento, los resultados son consistentes con los obtenidos por Singh & Arora (2020), pues la categoría con mayor precisión es la compuesta por los datos originales. Sin embargo, la precisión general de los modelos difiere de los resultados obtenidos por Kannan et al. (2020), en el que se utiliza un conjunto de datos de 12.206 imágenes hiperespectrales, y el 75% del conjunto de datos estaba compuesto por datos sintéticos. En ese estudio, la precisión general aumenta en un 2,5%, mientras que, en el estudio actual, disminuye para la roya amarilla y aumenta en menor medida para la roya de la hoja.

Los modelos de clasificación que alcanzaron los valores de precisión más altos en este estudio fueron SVM y RF. Ambos modelos entran dentro del ámbito del aprendizaje automático clásico (Li et al., 2020). Se diferencian de estudios como el realizado por Patil et al. (2017), donde se compararon tres modelos de aprendizaje automático para la detección del tizón tardío. En ese estudio, el mejor clasificador fue ANN, seguido de SVM y RF, lo que representa una tendencia contraria a lo encontrado en este artículo. La variación en los resultados obtenidos puede atribuirse a diferencias en las características de los conjuntos de datos utilizados en este estudio. Específicamente en este estudio, hay dos categorías, a saber, 'H' y 'AL', que exhiben características similares. Además, el tamaño del conjunto de datos y el porcentaje de datos sintéticos dentro de cada categoría, también podrían contribuir a estas diferencias.

En términos del resultado de precisión general logrado, existe un conjunto limitado de investigaciones que utilizan el espectro completo de un espectroradiómetro para la detección de enfermedades. El estudio realizado por Naidu et al. (2021) es uno de los pocos que muestra el potencial de dichos datos combinados con el aprendizaje automático. En este estudio, se empleó el modelo LDA y los resultados obtenidos se alinean con los del presente estudio, lo que arroja altas tasas de precisión para plantas sanas, y mayores errores de clasificación, para categorías con características espectrales similares. El estudio realizado por Khosrokhani y NasR (2022) demuestra mayor precisión, al combinar el aprendizaje automático, con índices espectrales de vegetación, logrando un 85% para el modelo RF y un 89,5% para el modelo SVM.

Conclusiones

1. *P. tritici-duri* infecta a casi todos los cultivares de trigo duro sembrados en el sur de España, y en el invernadero mostró un tipo de infección mesotético frente a la mayoría de las líneas isogénicas Thatcher, y frente a una colección de cultivares y líneas de trigo duro resistentes a *P. triticina*. Esta resistencia intermedia no es suficiente para detener al patógeno, que produce daños importantes en todos los cultivares y líneas estudiadas, excepto en Calero, Thatcher-*Lr24*, Thatcher-*Lr26* y Thatcher-*Lr28*. Los programas de mejora deberán identificar nuevas fuentes de resistencia en conjuntos de germoplasma más amplios. Los aislados de *P. tritici-duri* obtenidos en este estudio serán útiles para estudios futuros.

2. Las principales razas de roya amarilla detectadas en los últimos años en el sur de España fueron PstS13, PstS14 y PstS10 (Warrior-). Esta especie de roya infecta más a los trigos harineros que a los trigos duros o triticales. Aun así, algunos cultivares de trigo harinero como Arthur Nick o Tejada fueron resistentes frente a estas razas. El gen *Yr27* utilizado frecuentemente por el CIMMYT está presente en numerosas variedades cultivadas en Andalucía y ofrece una protección intermedia frente a la raza PstS10 (Warrior -). Los genes *Yr5*, *Yr10* e *Yr15* son potencialmente interesantes por su resistencia a todas las razas de roya amarilla de Andalucía, y podrían emplearse en programas de mejora.

3. Las razas de roya del tallo encontradas en Andalucía en contraestación (en Conil de la Frontera) y estación (Jerez de la Frontera) fueron Clade IV-B y Clade IV-F, (que son las más frecuentes en la mayor parte del territorio europeo). Ambas son avirulentas frente al gen *Sr13*, muy importante en la protección de numerosas variedades de trigo duro. La peligrosa raza siciliana y la familia Ug99, no fueron detectadas en el sur de España, pero podrían llegar en un futuro próximo. Afectan de forma parecida a trigos harineros y duros, mientras que los triticales son más resistentes. Los cultivares de trigo harinero Escacena y Conil, los cultivares de trigos duros Calero, Amílcar y Don Ricardo, y el cultivar de triticale Bondadoso fueron resistentes a la roya del tallo. Los genes *Sr27* y *Sr35* son potencialmente interesantes ya que las líneas que portaban esos genes presentaron una menor severidad de roya del tallo.

4. El estudio demuestra cómo la aplicación de SMOTE, en entrenamiento y pruebas, establece la precisión obtenida en todos los modelos, en comparación con el conjunto de datos donde no se aplicó SMOTE. Por otro lado, los mejores modelos para la detección de enfermedades fueron, para la roya amarilla, el modelo RF, (70%), con el conjunto de datos compuesto enteramente de datos reales, y para la roya parda, el modelo SVM, (63%). Además, cabe destacar que estos modelos eran capaces de distinguir entre las diferentes características de forma más eficaz.

Se observó una excepción a esta tendencia entre las categorías 'H' y 'AL', que exhiben características espectrales similares.

5. Los resultados obtenidos sugieren el potencial de utilizar firmas espectrales completas, obtenidas mediante información hiperespectral, y combinadas con métodos de aprendizaje automático. Asimismo, subraya la necesidad de seguir investigando sobre nuevos métodos de procesamiento de datos, y cómo las técnicas de aumento de datos afectan las diferentes arquitecturas de modelos.

6. La infección por roya, tanto de la hoja como amarilla, impacta significativamente en el peso del grano en varios cultivares de trigo, con reducciones notables, que superan el 50% en los cultivares más susceptibles. Las fuertes correlaciones observadas entre la biomasa real y los datos proporcionados por las nubes de puntos 3D, subrayan el potencial de la tecnología LiDAR para la estimación de biomasa no destructiva. Sin embargo, la precisión de estas predicciones varía entre cultivares, y depende de la etapa de desarrollo, lo que destaca la necesidad de una calibración específica de cada cultivar. En general, la integración de datos de nubes de puntos 3D, presenta una vía prometedora para mejorar la estimación de los parámetros en los cultivares, y la evaluación de la gravedad de las enfermedades, apoyando así la toma de decisiones en el manejo del cultivo del trigo.

Glosario

Se incluyen varias definiciones relacionadas con la presente tesis doctoral, muchas de ellas de acuerdo a Niks et al. (2019) y otras tantas del sector de la digitalización.

Adam (Adaptive Moment Estimation): en aprendizaje automático es un algoritmo de optimización utilizado para actualizar los pesos de la red neuronal durante el entrenamiento. Combina las ventajas de otros dos métodos de optimización: Momentum y RMSprop, ajustando los pesos de manera más eficiente. Adam mantiene tasas de aprendizaje adaptativas para diferentes parámetros, lo que lo hace efectivo en práctica para una amplia gama de problemas.

Aislado: Muestra de un patógeno que es almacenado vivo o mantenido en aislamiento sobre plantas o en medio nutritivo (isolate).

Algoritmo: Secuencia de pasos finitos bien definidos que resuelven un problema (algorithm).

Artificial Neural Network (ANN): una red neuronal artificial es un modelo computacional inspirado en la estructura y funcionamiento de las redes neuronales biológicas. Consiste en capas de nodos, o "neuronas", conectadas por "sinapsis" que transmiten señales. Estas redes aprenden a realizar tareas ajustando los pesos de las conexiones, basándose en los datos de entrada y su retroalimentación durante el entrenamiento, lo que las hace muy efectivas para tareas complejas como reconocimiento de patrones, clasificación y predicción.

Avirulencia: Es la propiedad de un patógeno de no poder infectar a una planta huésped debido a la efectividad de uno o más genes mayores para resistencia (hipersensible). El término implica que opera una relación gen a gen (avirulence).

Diferenciales (conjunto): Un grupo de líneas o cultivares mediante el cual se pueden distinguir o caracterizar los patotipos de un enemigo natural (cultivar differential set).

Efector: proteína del patógeno que manipula las funciones celulares de la planta huésped. Cuando un efector del patógeno es detectado por la planta, puede actuar también como factor de avirulencia para inducir una respuesta hipersensible (effector).

Enfermedad: Cualquier alteración fisiológica de una planta o, de una parte considerable de la misma, causada por un factor de estrés biótico o una combinación de factores de estreses resultando en la manifestación de síntomas (disease).

Epifitia: Fenómeno consistente en que una enfermedad afecte simultáneamente a un gran número de plantas de la misma especie en la misma región. Puede deberse a agentes químicos, físicos o bióticos (epiphytia).

Gaussian naive bayes: Algoritmo de clasificación en aprendizaje automático que se basa en el teorema de Bayes con la suposición de independencia entre las características. Específicamente, utiliza la distribución gaussiana (o normal) para modelar las

características continuas. Este algoritmo es eficiente y efectivo, particularmente en tareas de clasificación donde las características son continuas y se asume que siguen una distribución normal.

Haustorio: Estructura que forman algunos hongos patogénicos en la célula viva de la planta y que les sirve para extraer nutrientes de esa célula (haustorium).

Huésped (planta): Especie de planta que es susceptible a un patógeno y le sirve como fuente de alimento y como sustrato para vivir (host plant).

Hipersensibilidad: Capacidad de una planta para defenderse de un patógeno o parásito mediante una reacción de muerte celular programada (apoptosis) de células vegetales en el sitio de infección (hypersensitivity).

Infección: El uso de una planta como fuente de nutrientes por un patógeno resultando generalmente en reproducción de ese enemigo (infection).

Inmunidad: Resistencia del organismo frente a un agente infeccioso externo.

Machine Learning (ML): el aprendizaje automático es una rama de la inteligencia artificial que se centra en desarrollar algoritmos y técnicas que permitan a las computadoras aprender y hacer predicciones o tomar decisiones basadas en datos, sin ser explícitamente programadas para cada tarea. Utiliza patrones y estructuras de datos históricos para crear modelos que mejoran automáticamente a través de la experiencia y la incorporación de nueva información.

Marcador molecular: es un elemento (normalmente un fragmento de ADN) que nos permite diferenciar los alelos de un locus (molecular marker).

Mesotética (reacción): Respuesta de infección indefinida en un cultivar, donde se observan pústulas pequeñas rodeadas de necrosis, y pústulas grandes rodeadas de clorosis. Es decir, en la misma planta, se pueden observar pústulas tipo 1-2 y pustulas tipo 3-4, guiándonos por la escala de Stackman, llegando al punto, de no saber diferenciar si el cultivar es resistente o susceptible a la raza de roya por la que ha sido infectado (mesothetic).

Patógeno: Microorganismo que explotan la planta como fuente de nutrientes (pathogen).

Patosistema vegetal: Combinación de una especie hospedante y de una de sus especies de enemigo natural (plant pathosystem).

Periodo de latencia: Periodo desde el momento de la inoculación hasta el inicio de la esporulación del patógeno. En el caso de la roya se mide mejor calculando el tiempo en el cual han aparecido el 50% de las pústulas (latency period).

Patotipo: Grupo de genotipos dentro de una especie de patógeno que sedistinguen por su espectro de virulencia. Es sinónimo del término raza (pathotype/race).

Piramidar: Proceso por el cual se combinan, en un único genotipo, varios genes de resistencia de diversas fuentes genéticas (gene pyramiding).

Postulación de genes: Método para averiguar el gen de resistencia de un genotipo asumiendo una relación gen a gen entre planta y patógeno. La forma más frecuente es usar genotipos con genes conocidos (diferenciales) e inocularlas con una serie de patotipos diferentes. El tipo de infección de estos genotipos se compara con el tipo de infección del genotipo cuyo gen(es) de resistencia queremos averiguar (gene postulation).

Pústula: ver uredinio (pustule).

Random forest: es un algoritmo de aprendizaje supervisado que combina múltiples árboles de decisión para formar un "bosque". Cada árbol en el Random Forest produce una predicción y la clase con la mayoría de los votos se convierte en la predicción del modelo. Este método mejora la precisión y controla el sobreajuste, aprovechando la diversidad de los árboles.

Randomizedsearch CV: es una técnica en aprendizaje automático que se utiliza para seleccionar de manera aleatoria y eficiente los mejores hiperparámetros para un modelo. A diferencia de la búsqueda en cuadrícula (GridSearchCV) que prueba todas las combinaciones posibles, RandomizedSearchCV explora un número fijo de configuraciones de hiperparámetros seleccionadas al azar dentro de los rangos predefinidos. Esto lo hace más rápido y a menudo más efectivo para encontrar una buena combinación de hiperparámetros, especialmente cuando se trabaja con grandes espacios de búsqueda.

Relación gen a gen: Relación hospedante-patógeno en la cual cada gen de resistencia en la planta puede ser fenotípicamente expresado sólo cuando el patógeno posee un correspondiente gen de avirulencia (gene for gene relationship).

Resistencia: Capacidad de una planta para reducir o detener el crecimiento, desarrollo y reproducción del patógeno después del establecimiento de un contacto íntimo (resistance).

Resistencia horizontal: Es una resisntecia, de una cultivar frente a un organismo infeccioso, que está determinada por la presencia y acción de muchos genes. No suele ser una resistencia total, pero en cambio, suele ser muy duradera en el tiempo (horizontal resistant).

Resistencia parcial: Resistencia que produce una menor tasa epidémica por parte del patógeno, a pesar de que manifiesta un tipo de infección susceptible, o sea, que no se observa hipersensitividad (partial resistance).

Resistencia vertical: Es una resistencia, de un cultivar frente a un organismo infeccioso, que está determinada por la presencia de un solo gen de resistencia R, suele tener una respuesta de resistencia total, pero puede ser poco duradera en el tiempo, ya que venciendo al gen R, por ejemplo, con un pequeño cambio de raza del patógeno, el cultivar se vuelve susceptible.

Resistencia raza específica: Resistencia que es efectiva contra genotipos específicos (avirulentos) de un patógeno (race specific resistance).

Rotura de la resistencia: Es el fenómeno donde la efectividad de la resistencia contra un enemigo natural decrece como resultado de los cambios en la población de ese enemigo. También se le llama erosión (breaking down of resistance).

Scikit learn: Es una biblioteca de software libre y de código abierto para Python que proporciona herramientas sencillas y eficientes para análisis de datos y aprendizaje automático. Incluye algoritmos para clasificación, regresión, agrupación, reducción de dimensionalidad, selección de modelos y preprocesamiento de datos, siendo ampliamente utilizada tanto en la academia como en la industria por su versatilidad y facilidad de uso.

SMOTE (Synthetic Minority Over-sampling Technique): es una técnica de preprocesamiento de datos utilizada en aprendizaje automático para abordar el desbalance en los conjuntos de datos de clasificación. Funciona generando muestras sintéticas de la clase minoritaria para igualar la cantidad de muestras en la clase mayoritaria. Esto se logra seleccionando muestras existentes de la clase minoritaria y creando nuevas muestras sintéticas que son variaciones ligeras, utilizando interpolación entre muestras y sus vecinos más cercanos. SMOTE ayuda a mejorar el rendimiento de los modelos de clasificación en conjuntos de datos desequilibrados.

Support Vector Machine (SVM): es un algoritmo de aprendizaje supervisado utilizado principalmente para tareas de clasificación y regresión. Funciona encontrando el hiperplano óptimo que separa las clases de datos con el mayor margen posible. En casos no lineales, utiliza un truco conocido como el "kernel" para transformar los datos a un espacio donde puedan ser linealmente separables. Las SVM son conocidas por su eficacia en espacios de alta dimensión y su capacidad para manejar datos no lineales.

Susceptibilidad: Incapacidad de una planta para reducir el crecimiento, desarrollo y reproducción de un enemigo natural (susceptibility).

Tipo de infección: Reacción o respuesta de la planta a una infección (o intento de infección) por un patógeno, la cual se expresa por un número de acuerdo a una escala normalizada. El término es sinónimo de ‘tipo de reacción’ (infection type).

Uredinio (o uredio): Síntoma típico de infecciones de roya en la planta huésped principal. Consiste en manchas de color generalmente rojizo o anaranjado que aparecen, sobre todo, en las hojas de las plantas infectadas. En realidad, son erupciones de esporas (urediniosporas) producidas en el interior de la hoja por una unidad de infección de roya que ha progresado y ha creado una colonia. En esta colonia se producen tal cantidad de nuevas esporas que éstas presionan y rompen finalmente la epidermis foliar para dispersarse en el exterior. Es sinónimo de pústula (uredinium; plural, uredinia).

Urediniospora: Es el nombre que se da a las esporas de las royas que infectan a la planta huésped principal. Son transportadas por los vientos a grandes distancias, a veces miles de kilómetro. Es sinónimo de uredospora (uredospore).

Virulencia: Capacidad de un patógeno para infectar una planta con uno o más genes mayores de resistencia (hipersensibilidad), debido a que no posee ninguno de los genes complementarios de avirulencia (virulence).

Bibliografía

Abdedayem, W., Patpour, M., Laribi, M., Justesen, A. F., Kouki, H., Fakhfakh, M., ... & Ben M'Barek, S. (2023). Wheat Stem Rust Detection and Race Characterization in Tunisia. *Plants*, *12*(3), 552.

Abdullaeva, Y., Manirajan, B. A., Honermeier, B., Schnell, S., & Cardinale, M. (2021). Domestication affects the composition, diversity, and co-occurrence of the cereal seed microbiota. *Journal of Advanced Research*, *31*, 75-86.

Aboelghar, M., Ali, A. R., & Arafat, S. (2014). Spectral wheat yield prediction modeling using SPOT satellite imagery and leaf area index. *Arabian Journal of Geosciences*, *7*, 465-474.

Ahmad, S., Afzal, M., Noorka, I. R., Iqbal, Z., Akhtar, N., Iftkhar, Y., & Kamran, M. (2010). Prediction of yield losses in wheat (*Triticum aestivum* L.) caused by yellow rust in relation to epidemiological factors in Faisalabad. *Pak. J. Bot.*, *42*(1), 401-407.

Ahmed, H. G. M. D., Zeng, Y., Shah, A. N., Yar, M. M., Ullah, A., & Ali, M. (2022). Conferring of drought tolerance in wheat (*Triticum aestivum* L.) genotypes using seedling indices. *Frontiers in Plant Science*, *13*, 961049.

Ali, S., Gladieux, P., Leconte, M., Gautier, A., Justesen, A. F., Hovmøller, M. S., ... & de Vallavieille-Pope, C. (2014). Origin, migration routes and worldwide population genetic structure of the wheat yellow rust pathogen *Puccinia striiformis* f. sp. *tritici*. *PLoS Pathogens*, *10*(1), e1003903.

Ali, S., Rodriguez-Algaba, J., Thach, T., Sørensen, C. K., Hansen, J. G., Lassen, P., ... & Hovmøller, M. S. (2017). Yellow rust epidemics worldwide were caused by pathogen races from divergent genetic lineages. *Frontiers in Plant Science*, *8*, 1057.

Ali, S., Khan, M. I., Shahbaz, M., Nabi, G., Zeeshan, M., Aleem, S., & Hussain, M. (2022). Environmental Factors and Yellow Rust Epidemic on Wheat Varieties in Punjab, Pakistan. *Journal of Agriculture and Food*, *3*(1), 86-96.

Amiridis, V., Balis, D. S., Giannakaki, E., Stohl, A., Kazadzis, S., Koukouli, M. E., & Zanis, P. (2009). Optical characteristics of biomass burning aerosols over Southeastern Europe determined from UV-Raman lidar measurements. *Atmospheric Chemistry and Physics*, *9*(7), 2431-2440.

Anikster, Y., Bushnell, W.R., Eilam, T., Manisterski, J., & Roelfs, A.P., 1997. *Puccinia recondita* causing leaf rust on cultivated wheat, wild wheat, and rye. *Canadian Journal of Botany*, *75*, 2082–2096.

Aoun, M., Kolmer, J. A., Breiland, M., Richards, J., Brueggeman, R. S., Szabo, L. J., & Acevedo, M. 2020. Genotyping-by-Sequencing for the Study of Genetic Diversity in *Puccinia triticina*. *Plant Dis.*, *104*(3), 752-760. doi: 10.1094/PDIS-09-19-1890-RE.

Apolo-Apolo, O. E., Egea Cegarra, G., Martínez Guanter, J., & Pérez Ruiz, M. (2019). *Estimación de parámetros biofísicos de interés para la mejora de trigo usando inteligencia artificial* (No. COMPON-2019-agri-3398).

Apolo-Apolo, O. E., Martínez-Guanter, J., Egea, G., Raja, P., & Pérez-Ruiz, M. (2020). Deep learning techniques for estimation of the yield and size of citrus fruits using a UAV. *European Journal of Agronomy*, *115*, 126030.

Appeltans, S., Apolo-Apolo, O. E., Rodríguez-Vázquez, J. N., Pérez-Ruiz, M., Pieters, J., & Mouazen, A. M. (2021). The automation of hyperspectral training library construction: a case study for wheat and potato crops. *Remote Sensing*, *13*(23), 4735.

Araus, J. L., & Cairns, J. E. (2014). Field high-throughput phenotyping: the new crop breeding frontier. *Trends in Plant Science, 19*(1), 52-61.

Aryal, J. P., Jat, M. L., Sapkota, T. B., Rahut, D. B., Rai, M., Jat, H. S., ... & Stirling, C. (2020). Learning adaptation to climate change from past climate extremes: Evidence from recent climate extremes in Haryana, India. *International Journal of Climate Change Strategies and Management*, *12*(1), 128-146.

Ashourloo, D., Mobasheri, MR., Huete, A. (2014). Evaluating the Effect of Different Wheat Rust Disease Symptoms on Vegetation Indices Using Hyperspectral Measurements. *Remote Sensing, (6)*, 5107-5123. https://doi.org/10.3390/rs6065107

Azadbakht, Mohsen, et al. 2019. Wheat leaf rust detection at canopy scale under different LAI levels using machine learning techniques. *Computers and Electronics in Agriculture, 156*, 119-128.

Babu, P., Baranwal, D. K., Harikrishna, Pal, D., Bharti, H., Joshi, P., ... & Singh, A. (2020). Application of genomics tools in wheat breeding to attain durable rust resistance. *Frontiers in Plant Science, 11*, 567147.

Bade, C. I. A., & Carmona, M. A. (2011). Comparison of methods to assess severity of common rust caused by *Puccinia sorghi* in maize. *Tropical Plant Pathology*, *36*, 264-266.

Bagnato, C., Conde, C., Noe, Y., Caride, C., Baeza, S., Paoli, H., ... & Paruelo, J. M. (2012). Utilización de firmas espectrales de alta resolución temporal para la elaboración de mapas de uso agrícola y estimaciones de superficie cultivada a escala de lote en Argentina y Uruguay. In *Congreso Argentino de Teledetección* (pp. 18-21). Cordoba, Argentina: Universidad Nacional de Córdoba.

Bahar, N. H., Lo, M., Sanjaya, M., Van Vianen, J., Alexander, P., Ickowitz, A., & Sunderland, T. (2020). Meeting the food security challenge for nine billion people in 2050: What impact on forests. *Glob. Environ. Chang., 62*, 102056. https://doi.org/10.1016/j.gloenvcha.2020.102056

Bahri, H., Annabi, M., M'Hamed, H. C., & Frija, A. (2019). Assessing the long-term impact of conservation agriculture on wheat-based systems in Tunisia using APSIM simulations under a climate change context. *Science of the Total Environment*, *692*, 1223-1233.

Balasundram, S K., Golhani, K., & Shamshiri, R. R. (2019). Non-Invasive Approaches for oil palm disease assessment and monitoring. Palmas, 40 (Especial Tomo I), 204-219.

Barbedo, J.G.A. (2018). Impact of dataset size and variety on the effectiveness of deep learning and transfer learning for plant disease classification. *Computers and Electronics in Agriculture*, *153*, 46-53. https://doi.org/10.1016/j.compag.2018.08.013

Bariana, H. S., & McIntosh, R. A. (1993). Cytogenetic studies in wheat. XV. Location of rust resistance genes in VPM1 and their genetic linkage with other disease resistance genes in chromosome 2A. *Genome*, *36*(3), 476-482.

Bartoš, P., Stuchlíková, E., & Hanušová, R. (1997). Adaptation of wheat rusts to the wheat cultivars in former Czechoslovakia. In *Adaptation in Plant Breeding: Selected*

Papers from the XIV EUCARPIA Congress on Adaptation in Plant Breeding held at Jyväskylä, Sweden from July 31 to August 4, 1995 (pp. 109-117). Springer Netherlands.

Bates, J. S., Montzka, C., Schmidt, M., & Jonard, F. (2021). Estimating canopy density parameters time-series for winter wheat using UAS Mounted LiDAR. *Remote Sensing*, *13*(4), 710.

Beard, C. Loughman, R. & Thomas, G. (2005). Managing stripe rust and leaf rust. Farmnote núm. 43/2005. Department of Agriculture. Government of Western Australia.

Beard, C., Jayasena, K., Thomas, G., & Loughman, R. (2006). Managing stem rust of wheat. *Managing stem rust of wheat, 73*.

Beddow, J. M., Pardey, P. G., Chai, Y., Hurley, T. M., Kriticos, D. J., Braun, H. J., ... & Yonow, T. (2015). Research investment implications of shifts in the global geography of wheat stripe rust. *Nature Plants*, *1*(10), 1-5.

Bellido, L. L. (1991). *Cultivos herbáceos: cereales* (Vol. 1). Mundi-Prensa.

Bhattacharya, S. (2017). Deadly new wheat disease threatens Europe's crops. *Nature*, *542*(7640).

Bhavani, P., Hussain, M., & Park, Y. K. (2022). Recent advancements on the sustainable biochar based semiconducting materials for photocatalytic applications: A state of the art review. *Journal of Cleaner Production*, *330*, 129899.

Bhavani, S., Hodson, D. P., Huerta-Espino, J., Randhawa, M. S., & Singh, R. P. (2019). Progress in breeding for resistance to Ug99 and other races of the stem rust fungus in CIMMYT wheat germplasm. *Front. Agr. Sci. Eng.*, *6*(3), 210-224.

Bian, Z., Fan, R., & Xie, L. (2022). A novel cuproptosis-related prognostic gene signature and validation of differential expression in clear cell renal cell carcinoma. *Genes*, *13*(5), 851.

Bock, C. H., Poole, G. H., Parker, P. E., & Gottwald, T. R. (2010). Plant disease severity estimated visually, by digital photography and image analysis, and by hyperspectral imaging. *Crit. Rev. Plant Sci.*, *29*(2), 59-107. https://doi.org/10.1080/07352681003617285

Boogaard, F. P., van Henten, E. J., & Kootstra, G. (2021). Boosting plant-part segmentation of cucumber plants by enriching incomplete 3D point clouds with spectral data. *Biosystems Engineering*, *211*, 167-182. https://doi.org/10.1016/j.biosystemseng.2021.09.004

Borlaug, N. (2007). Feeding a hungry world. *Science*, *318*(5849), 359-359.

Braun, H. J., Atlin, G., & Payne, T. (2010). Multi-location testing as a tool to identify plant response to global climate change. In *Climate change and crop production* (pp. 115-138). Wallingford UK: CABI.

Camacho, A., Vargas, C. A., & Arguello, H. (2016). A comparative study of target detection algorithms in hyperspectral imagery applied to agricultural crops in Colombia. *Tecnura*, *20*(49), 86-99.

Castro-Valdecantos, P., Apolo-Apolo, O. E., Pérez-Ruiz, M., & Egea, G. (2022). Leaf area index estimations by deep learning models using RGB images and data fusion in maize. *Precision Agriculture*, *23*(6), 1949-1966.

Chacón-Iznaga, A., Rodríguez-Orozco, M., Aguila-Alcantara, E., Colás-Sánchez, A., González-Aguiar, D., Alvarez-Vázquez, D. L., ... & Saeys, W. (2019). Comparación de firmas espectrales vis-NIR de suelos cultivados con caña de azúcar (*Sacharum* sp.) en la provincia de Villa Clara. *Centro Agrícola*, *46*(4), 13-20.

Chairi, F., Aparicio, N., Serret, M. D., & Araus, J. L. (2020). Breeding effects on the genotype× environment interaction for yield of durum wheat grown after the Green Revolution: The case of Spain. *The Crop Journal*, *8*(4), 623-634.

Chen, C., Clark, B., Martin, M., Matny, O., Steffenson, B. J., Franckowiak, J. D., ... & Dracatos, P. M. (2020). Ancient BED-domain-containing immune receptor from wild barley confers widely effective resistance to leaf rust. *bioRxiv*, 2020-01.

Chen, W., Wellings, C., Chen, X., Kang, Z., & Liu, T. (2014). Wheat stripe (yellow) rust caused by *Puccinia striiformis* f. sp. *tritici*. *Molecular Plant Pathology*, *15*(5), 433-446.

Chester, K.S., (1946). *The nature and prevention of the cereal rusts as exemplified in the leaf rust of wheat*. Chronica Botanica Co. Waltham, Mass.; Win. Dawson and Sons, Ltd., London, 270 p

Choudhary, R. L., & Behera, U. K. (2013). Effect of sequential tillage practices and N levels on energy relations and use-efficiencies of irrigation water and N in maize (Zea mays)–wheat (*Triticum aestivum*) cropping system. *Indian J. Agron.*, *58*(1), 27-34. https://doi.org/10.20546/ijcmas.2020.904.075

Choudhary, K. M., Jat, H. S., Nandal, D. P., Bishnoi, D. K., Sutaliya, J. M., Choudhary, M., ... & Jat, M. L. (2018). Evaluating alternatives to rice-wheat system in western Indo-Gangetic Plains: crop yields, water productivity and economic profitability. *Field Crops Research*, *218*, 1-10.

Clevers, J. G. P. W. (1999). The use of imaging spectrometry for agricultural applications. *ISPRS Journal of Photogrammetry and Remote sensing*, *54*(5-6), 299-304. https://doi.org/10.1016/S0924-2716(99)00033-7

Curtis, B. C., Rajaram, S., & Gómez Macpherson, H. (2002). *Bread wheat: improvement and production*. Food and Agriculture Organization of the United Nations (FAO). https://www.fao.org/3/Y4011E/y4011e00.htm

Dabove, P., & Manzino, A. M. (2014). GPS & GLONASS mass-market receivers: positioning performances and peculiarities. *Sensors*, *14*(12), 22159-22179.

Dammer, K. H., Garz, A., Hobart, M., & Schirrmann, M. (2022). Combined UAV-and tractor-based stripe rust monitoring in winter wheat under field conditions. *Agronomy Journal*, *114*(1), 651-661.

Daskalaki. S., Kopanas, I., Avouris, N. (2006). Evaluation of classifiers for an uneven class distribution problem. *Appl Artif Intel.*, *20*(5), 381-417. https://doi.org/10.1080/08839510500313653

De La Fuente, G. N., Frei, U. K., & Lübberstedt, T. (2013). Accelerating plant breeding. *Trends in Plant Science*, *18*(12), 667–672. https://doi.org/10.1016/j.tplants.2013.09.001

Demidova, L., & Klyueva, I. (2017). SVM Classification: Optimization with the SMOTE Algorithm for the Class Imbalance Problem. In 2017 6th Mediterranean Conference on Embedded Computing (MECO) (pp. 1-4). Bar, Montenegro. DOI: 10.1109/MECO.2017.797713

Devadas, R., Lamb, D.W., & Simpfendorfer, S. (2009). Evaluating ten spectral vegetation indices for identifying rust infection in individual wheat leaves. *Precision Agric., 10*, 459–470. https://doi.org/10.1007/s11119-008-9100-2

Devadas, R., Lamb, D.W., Backhouse, D. et al., (2015). Sequential application of hyperspectral indices for delineation of stripe rust infection and nitrogen deficiency in wheat. *Precision Agric., 16*, 477–491. https://doi.org/10.1007/s11119-015-9390-0

Di Bella, C.M., Posse, G., Beget, M.E., Fischer, M.A., Mari, N., Veron, S. (2008). La teledetección como herramienta para la prevención, seguimiento y evaluación de incendios e inundaciones. *Ecosistemas, 17*(3), 39-52.

Ding, Y., Cuddy, W. S., Wellings, C. R., Zhang, P., Thach, T., Hovmøller, M. S., ... & Park, R. F. (2021). Incursions of divergent genotypes, evolution of virulence and host jumps shape a continental clonal population of the stripe rust pathogen *Puccinia* striiformis. *Molecular Ecology*, *30*(24), 6566-6584.

Divakar, S., Bhattacharjee, A., & Priyadarshini, R. (2021). Smote-DL: A Deep Learning-Based Plant Disease Detection Method. In 6th International Conference for Technological Convergence (I2CT), Maharashtra, India, 2021 (pp. 1-6). doi: 10.1109/I2CT51068.2021.9417920

D'Oliveira, B., and Samborski, D.J., 1966. Aecial stage of *Puccinia recondita* on *Ranunculaceae* and *Boraginaceae* in Portugal. Pp. 133-150. *Proceedings of Cereal Rusts Conferences*, Cambridge, United Kingdom.

Dubcovsky, J., Ordon, F., Perovic, D. *et al.* (2011). Conflicting mapping results for stem rust resistance gene *Sr13*. *Theor. Appl. Genet., 122*, 659. https://doi.org/10.1007/s00122-010-1495-2

Duplessis, S., Lorrain, C., Petre, B., Figueroa, M., Dodds, P. N., & Aime, M. C. (2021). Host adaptation and virulence in heteroecious rust fungi. *Annual Review of Phytopathology*, *59*, 403-422.

Egea, G., Padilla-Díaz, C. M., Martinez-Guanter, J., Fernández, J. E., & Pérez-Ruiz, M. (2017). Assessing a crop water stress index derived from aerial thermal imaging and infrared thermometry in super-high density olive orchards. *Agricultural Water Management*, *187*, 210-221.

El Amil, R., De Vallavieille-Pope, C., Leconte, M., & Nazari, K. (2019). Diversity of genes for resistance to stripe rust in wheat elite lines, commercial varieties and landraces from Lebanon and Syria. *Phytopathologia Mediterranea*, *58*(3), 607-628.

El-Ghamry, A., Darwish, A., & Hassanien, A. E. (2023). An optimized CNN-based intrusion detection system to reduce risks in smart agriculture. *Computers & Electrical Engineering, 22*, 100709. doi: 10.1016/j.compeleceng.2023.100709

Ellis, J. G., Lagudah, E. S., Spielmeyer, W., & Dodds, P. N. (2014). The past, present and future of breeding rust resistant wheat. *Frontiers in Plant Science*, *5*, 641.

Espinosa, K. C. S., Vázquez, L. D., Fernández-González, M., Almaguer, M., & Rodríguez-Rajo, F. J. (2023). Aeromycological studies in the crops of the main cereals: A systematic review. *Journal of Agriculture and Food Research*, 100732.

Ezzahiri, B., and Roelfs, A.P., 1992. *Anchusa italica* as an Alternate Host for Wheat Leaf Rust in Morocco. B. Ezzahiri. *Plant Disease*, 76, 1185. Doi: 10.1094/PD-76-1185A.

FAOSTAT. (Food and Agriculture Organization of the United Nations, 2023). http://www.fao.org/faostat/es/#home

Faris, J. D. (2014). Wheat domestication: Key to agricultural revolutions past and future. *Genomics of Plant Genetic Resources: Volume 1. Managing, sequencing and mining genetic resources*. In R. Tuberosa, A. Graner & E. Frison (Eds.), *Genomics of Plant Genetic Resources* (pp. 439-464). Springer. https://doi.org/10.1007/978-94-007-7572-5_18

Fernández, A., García, S., Herrera, F. y Chawla, NV (2018). SMOTE para aprender de datos desequilibrados: avances y desafíos, conmemorando el 15 aniversario. Diario de investigación de inteligencia artificial , 61 , 863-905. https://doi.org/10.1613/jair.1.11192

Ferreira, M., Ogren, M., Dias, J. N., Silva, M., Gil, S., Tavares, L., ... & Aguiar, S. I. (2021). Liposomes as antibiotic delivery systems: A promising nanotechnological strategy against antimicrobial resistance. *Molecules*, *26*(7), 2047.

Ferreira, R. A., Correia, S. F., Monguzzi, A., Liu, X., & Meinardi, F. (2020). Spectral converters for photovoltaics–What's ahead. *Materials Today*, *33*, 105-121.

Figueroa, M., Hammond-Kosack, K. E., & Solomon, P. S. (2018). A review of wheat diseases—a field perspective. *Molecular Plant Pathology*, *19*(6), 1523-1536.

Figueroa, M., Dodds, P.N., & Henningsen, E.C., 2020. Evolution of virulence in rust fungi multiple solutions to one problem. *Current Opinion in Plant Biology* 56: 20–27. https://doi.org/10.1016/j.pbi.2020.02.007

Fisher, L. V., & Barron, A. R. (2022). Effect of functionalized and unfunctionalized basic oxygen steelmaking slag on the growth of cereal wheat (*Triticum aestivum*). *Resources, Conservation & Recycling Advances*, *15*, 200092.

Flor, H. H. (1956). The complementary genic systems in flax and flax rust. *Advances in Genetics*, *8*, 29-54.

Flor, H. H. (1971). Current status of the gene-for-gene concept. *Annual review of phytopathology*, *9*(1), 275-296.

Furbank, R. T., & Tester, M. (2011). Phenomics–technologies to relieve the phenotyping bottleneck. *Trends in Plant Science*, *16*(12), 635-644.

Gilabert, M. A., González-Piqueras, J., & García-Haro, J. (1997). Acerca de los índices de vegetación. *Revista de teledetección*, *8*(1), 1-10

Global Rust Reference Center (GRRC), Aarhus University (Denmark). Available online: https://agro.au.dk/en/research/research-areas/global-rust-reference-center (accessed on 24 October 2023).

González-Fragoso, R., 1918. *La roya de los vegetales*. Publisher: Junta para Ampliación de Estudios e Investigaciones Científicas (Imp. de Fortanet, Libertad 29), Madrid, Spain, 267 p.

Guerrero García, A. (1999). *Cultivos herbáceos extensivos*. Ediciones Mundi-Prensa.

Gultyaeva, E., Shaydayuk, E., & Gannibal, P. (2021). Leaf rust resistance genes in wheat cultivars registered in Russia and their influence on adaptation processes in pathogen populations. *Agriculture*, *11*(4), 319.

Gultyaeva, E., & Shaydayuk, E. (2023). Resistance of Modern Russian Winter Wheat Cultivars to Yellow Rust. *Plants*, *12*(19), 3471.

Guo, J., Borges, P. V., Park, C., & Gawel, A. (2019). Local descriptor for robust place recognition using lidar intensity. *IEEE Robotics and Automation Letters*, *4*(2), 1470-1477.

Gupta, S. K., Charpe, A., Prabhu, K. V., & Haque, Q. M. R. (2006). Identification and validation of molecular markers linked to the leaf rust resistance gene *Lr19* in wheat. *Theoretical and Applied Genetics*, *113*, 1027-1036.

Guzmán-Álvarez, J. A., González-Zuñiga, M., Fernandez, J. A. S., & Calvo-Alvarado, J. C. (2022). Uso de sensores remotos en la agricultura: aplicaciones en el cultivo del banano. *Agronomy Mesoamerican*, 48279-48279.

Hadad, A., Evin, D., & Drozdowicz, B. (2009). Modelo para el tratamiento de datos desbalanceados basado en redes neuronales autoorganizadas. In XVII Congreso Argentino de Bioingeniería, Rosario, Santa Fe.

Hafeez, A. N., Arora, S., Ghosh, S., Gilbert, D., Bowden, R. L., & Wulff, B. B. (2021). Creation and judicious application of a wheat resistance gene atlas. *Molecular Plant*, *14*(7), 1053-1070.

Haider, M. W., Kaur, J., Bala, R., Singh, S., Srivastava, P., Sharma, A., ... & Kumari, J. (2023). Stripe rust resistance gene (s) postulation in wheat germplasm with the help of differentials and tagged molecular markers. *Scientific Reports*, *13*(1), 9007.

Hale, I. L., Mamuya, I., & Singh, D. (2013). *Sr31*-virulent races (TTKSK, TTKST, and TTTSK) of the wheat stem rust pathogen *Puccinia graminis* f. sp. *tritici* are present in Tanzania. *Plant Disease*, *97*(4), 557-557.

Hawku, M. D., He, F., Bai, X., Islam, M. A., Huang, X., Kang, Z., & Guo, J. (2022). A R2R3 MYB transcription factor, TaMYB391, is positively involved in wheat resistance to *Puccinia striiformis* f. sp. *tritici*. *International Journal of Molecular Sciences*, *23*(22), 14070.

He, J., Wang, S., Liu, Y., Ma, H., & Liu, Q. (2017). Examining the relationship between urbanization and the eco-environment using a coupling analysis: Case study of Shanghai, China. *Ecological Indicators*, *77*, 185-193.

Heinzler, R., Schindler, P., Seekircher, J., Ritter, W., & Stork, W. (2019, June). Weather influence and classification with automotive lidar sensors. In *2019 IEEE intelligent vehicles symposium (IV)* (pp. 1527-1534). IEEE.

Herrera-Foessel, S.A., Singh, R.P., Huerta-Espino, J., Crossa, J., Djurle, A. & Yuen, J., 2007. Evaluation of slow rusting resistance components to leaf rust in CIMMYT durum wheats. *Euphytica*, *155*, 361–369.

Herrera-Foessel, S.A., Singh, R.P., Huerta-Espino, J., William, H. M., Garcia, V., Djurle, A., Yuen, J., 2008a. Identification and Molecular Characterization of Leaf Rust Resistance Gene *Lr14a* in Durum Wheat. *Plant Disease*, *92*, 469–473. https://doi.org/10.1094/PDIS-92-3-0469

Herrera-Foessel, S. A., Singh, R. P., Huerta-Espino, J., William, H. M., Djurle, A., Yuen, J., 2008b. Molecular mapping of a leaf rust resistance gene on the short arm of chromosome 6B of durum wheat. *Plant Disease*, *92*, 1650–1654.

Herrera-Foessel, S. A., Lagudah, E. S., Huerta-Espino, J., Hayden, M. J., Bariana, H. S., Singh, D., & Singh, R. P. (2011). New slow-rusting leaf rust and stripe rust resistance genes *Lr67* and *Yr46* in wheat are pleiotropic or closely linked. *Theoretical and Applied Genetics*, *122*, 239-249.

Holman, F. H., Riche, A. B., Michalski, A., Castle, M., Wooster, M. J., & Hawkesford, M. J. (2016). High throughput field phenotyping of wheat plant height and growth rate in field plot trials using UAV based remote sensing. *Remote Sensing*, *8*(12), 1031. https://doi.org/10.3390/rs8121031

Hovmøller, M. S., Sørensen, C. K., Walter, S., & Justesen, A. F. (2011). Diversity of *Puccinia striiformis* on cereals and grasses. *Annual Review of Phytopathology*, *49*, 197-217.

Hovmøller, M. S., Walter, S., Bayles, R. A., Hubbard, A., Flath, K., Sommerfeldt, N., ... & de Vallavieille-Pope, C. (2016). Replacement of the European wheat yellow rust population by new races from the centre of diversity in the near-Himalayan region. *Plant Pathology*, *65*(3), 402-411.

Hovmøller, M. S., Thach, T., & Justesen, A. F. (2023). Global dispersal and diversity of rust fungi in the context of plant health. *Current Opinion in Microbiology*, *71*, 102243.

Huerta-Espino, J., Singh, R. P., German, S., McCallum, B.D., Park, R.F., Chen, W.Q., Bhardwaj, S.C., Goyeau, H., 2011. Global status of wheat leaf rust caused by *Puccinia triticina*. *Euphytica*, *179*, 143–160.

Huerta-Espino, J., Singh, R. P., Villaseñor-Mir, H. E., & Ammar, K. (2023). Mining sources of resistance to durum leaf rust among tetraploid wheat accessions from CIMMYT's germplasm bank. *Plants*, *12*(1), 49.

Huerta-Mora, E. A., González-Huitrón, V., Rodríguez-Rangel, H., & Amabilis-Sosa, L. E. (2020). Detección de enfermedades foliares con arquitecturas de redes neuronales convolucionales. *RINDERESU, 5*(1), 18-40

Hyles, J., Bloomfield, M. T., Hunt, J. R., Trethowan, R. M., & Trevaskis, B. (2020). Phenology and related traits for wheat adaptation. *Heredity*, *125*(6), 417-430.

Igrejas, G., & Branlard, G. (2020). The importance of wheat. In Wheat quality for improving processing and human health (pp. 1-7). Springer, Cham.

Jasrotia, S., & Sharma, M. (2020). Climate Change Impact on Tourism-Based Livelihood and Related Youth Migration—A Case. Advances in Water Pollution Monitoring and Control: Select Proceedings from HSFEA 2018, 67.

Jay, S., Rabatel, G., Hadoux, X., Moura, D., & Gorretta, N. (2015). In-field crop row phenotyping from 3D modeling performed using Structure from Motion. *Computers and Electronics in Agriculture, 110*, 70-77. https://doi.org/10.1016/j.compag.2014.09.021

Jimenez-Berni, J. A., Deery, D. M., Rozas-Larraondo, P., Condon, A. T. G., Rebetzke, G. J., James, R. A., ... & Sirault, X. R. (2018). High throughput determination of plant height, ground cover, and above-ground biomass in wheat with LiDAR. *Frontiers in Plant Science*, *9*, 237.

Jin, J., & Jiang, C. (2002). Spatial variability of soil nutrients and site-specific nutrient management in the PR China. *Computers and Electronics in Agriculture, 36*(2-3), 165-172. https://doi.org/10.1016/S0168-1699(02)00099-

Jin, Y., Singh, R. P., Ward, R. W., Wanyera, R., Kinyua, M., Njau, P., ... & Yahyaoui, A. (2007). Characterization of seedling infection types and adult plant infection responses of monogenic *Sr* gene lines to race TTKS of *Puccinia graminis* f. sp. *tritici*. *Plant Disease*, *91*(9), 1096-1099.

Johnson, R. (1984). A critical analysis of durable resistance. *Annual review of phytopathology*, *22*(1), 309-330.

Kamilaris, A., & Prenafeta-Bold, F.X. (2018). Deep learning in agriculture: A survey. *Computers and Electronics in Agriculture, 147*, 70-90. doi: 10.1016/j.compag.2018.02.016

Kannan, N., Kaushik, M., Prakash, P., Ajay, R., & Veni, S. (2020). Detection of tomato leaf diseases using a convolutional neural network with data augmentation. Fifth International Conference on Communication and Electronics Systems (ICCES) (pp. 1125-1132). Coimbatore, India. doi: 10.1109/ICCES48766.2020.9138030

Karkman, A., Pärnänen, K., & Larsson, D. J. (2019). Fecal pollution can explain antibiotic resistance gene abundances in anthropogenically impacted environments. *Nature communications*, *10*(1), 80.

Kashyap, P. L., Kumar, S., Jasrotia, P., Singh, D. P., & Singh, G. P. (2020). Nanotechnology in wheat production and protection. *Environmental Nanotechnology Volume 4*, 165-194.

Khan, R. R., Bariana, H. S., Dholakia, B. B., Naik, S. V., Lagu, M. D., Rathjen, A. J., ... & Gupta, V. S. (2005). Molecular mapping of stem and leaf rust resistance in wheat. *Theoretical and Applied Genetics*, *111*, 846-850.

Khan, Z. S., Rizwan, M., Hafeez, M., Ali, S., Javed, M. R., & Adrees, M. (2019). The accumulation of cadmium in wheat (*Triticum aestivum*) as influenced by zinc oxide nanoparticles and soil moisture conditions. *Environmental Science and Pollution Research*, *26*, 19859-19870.

Khanal, S., Kc, K., Fulton, J. P., Shearer, S., & Ozkan, E. (2020). Remote sensing in agriculture—accomplishments, limitations, and opportunities. *Remote Sensing*, *12*(22), 3783.

Khosrokhani, M., & Nasr, A. H. (2022). Applications of the remote sensing technology to detect and monitor the rust disease in the wheat – a literature review. *Geocarto International, 37*(26), 13268-13290. doi:10.1080/10106049.2022.2076922

Kiani, S., Rezaei, P., & Fakhr, M. (2021). Dual-frequency microwave resonant sensor to detect noninvasive glucose-level changes through the fingertip. *IEEE Transactions on Instrumentation and Measurement*, *70*, 1-8.

Klindworth, D. L., Miller, J. D., Jin, Y., & Xu, S. S. (2007). Chromosomal locations of genes for stem rust resistance in monogenic lines derived from tetraploid wheat accession ST464. *Crop Science*, *47*(4), 1441-1450.

Klymiuk, V., Yaniv, E., Huang, L., Raats, D., Fatiukha, A., Chen, S., ... & Fahima, T. (2018). Cloning of the wheat *Yr15* resistance gene sheds light on the plant tandem kinase-pseudokinase family. *Nature Communications*, *9*(1), 3735.

Kobayashi, K., Tsuji, J., & Noto, M. (2018). Evaluation of Data Augmentation for Image-Based Plant-Disease Detection. In 2018 IEEE International Conference on Systems, Man, and Cybernetics (SMC) (pp. 2206-2211). Miyazaki, Japan. doi: 10.1109/SMC.2018.00379.

Kolmer, J. A. (1996). Genetics of resistance to wheat leaf rust. *Annual Review of Phytopathology*, *34*(1), 435-455.

Kolmer, J. (2013). Leaf rust of wheat: pathogen biology, variation and host resistance. *Forests*, *4*(1), 70-84.

Kolmer, J.A., Hughes, M.E., (2018). Physiologic Specialization of *Puccinia triticina* on Wheat in the United States in 2016. *Plant Disease, 102*, 10661071. https://doi.org/10.1094/PDIS-11-17-1701-*SR*

Kolmer, J. A., & Fajolu, O. (2022). Virulence phenotypes of the wheat leaf rust pathogen, *Puccinia triticina*, in the United States from 2018 to 2020. *Plant Disease*, *106*(6), 1723-1729.

Kthiri, D., 2017. Genetic and Molecular Characterization of Leaf Rust Resistance from Uncharacterized Sources of Durum Wheat (*Triticum turgidum* L. ssp. *durum*). PhD. University of Saskatchewan, Canada. Available at: https://harvest.usask.ca/handle/10388/7928

Kthiri, D., Loladze, A., MacLachlan, P.R., N'Diaye, A., Walkowiak, S., Nilsen, K., 2018. Characterization and mapping of leaf rust resistance in four durum wheat cultivars. *PLOS ONE, 13*(5). https://doi.org/10.1371/journal.pone.0197317

Kumar, R., Kumar, P., Tripathi, R., Gupta, G. P., Islam, A. N., & Shorfuzzaman, M. (2022). Permissioned blockchain and deep learning for secure and efficient data sharing in industrial healthcare systems. *IEEE Transactions on Industrial Informatics*, *18*(11), 8065-8073.

Lamberti, G. (2015). Microwave technology applied in post-harvest treatments of cereals and legumes. *Chem. Eng. Trans.*, *44*, 13-8.

Lee, S., Franklin, S., Hassani, F. A., Yokota, T., Nayeem, M. O. G., Wang, Y., ... & Someya, T. (2020). Nanomesh pressure sensor for monitoring finger manipulation without sensory interference. *Science*, *370*(6519), 966-970.

Le Gouis, J., Oury, F. X., & Charmet, G. (2020). How changes in climate and agricultural practices influenced wheat production in Western Europe. *Journal of Cereal Science*, *93*, 102960. https://doi.org/10.1016/j.jcs.2020.102960

Leonova, I. N., Skolotneva, E. S., & Salina, E. A. (2020). Genome-wide association study of leaf rust resistance in Russian spring wheat varieties. *BMC Plant Biology*, *20*(1), 1-13.

Levy, A. A., & Feldman, M. (2022). Evolution and origin of bread wheat. *The Plant Cell*, *34*(7), 2549-2567.

Lewis, C. M., Persoons, A., Bebber, D. P., Kigathi, R. N., Maintz, J., Findlay, K., ... & Saunders, D. G. (2018). Potential for re-emergence of wheat stem rust in the United Kingdom. *Communications biology*, *1*(1), 13.

Li, L., Ma, Z., Niinemets, Ü., & Guo, D. (2017). Three key sub-leaf modules and the diversity of leaf designs. *Frontiers in Plant Science, 8*, 1542. https://doi.org/10.3389/fpls.2017.01542

Li, Minhui (2021) Impact of camera viewing angle for estimating leaf parameters of wheat plants from 3D point clouds. *Agriculture*, *563*. https://doi.org/10.3390/agriculture11060563

Li, M., Shamshiri, R. R., Schirrmann, M., Weltzien, C., Shafian, S., & Laursen, M. S. (2022). UAV Oblique Imagery with an Adaptive Micro-Terrain Model for Estimation

of Leaf Area Index and Height of Maize Canopy from 3D Point Clouds. *Remote Sensing*, *14*(3), 585. https://doi.org/10.3390/rs14030585

Li, W., Chern, M., Yin, J., Wang, J., & Chen, X. (2019). Recent advances in broad-spectrum resistance to the rice blast disease. *Current Opinion in Plant Biology*, *50*, 114-120.

Li, Y., Nie, J., & Chao, X. (2020). Do we really need deep CNN for plant diseases identification? *Computers and Electronics in Agriculture, 178*, 105803. https://doi.org/10.1016/j.compag.2020.105803

Lin, Y., Zhinyan, B., Haibo, Z., Yuntao, Z., Xi, L. (2017). Habitat monitoring to evaluate crop disease and pest distributions based on multi-source satellite remote sensing imagery. *Optik Optics, 145*, 66-73. https://doi.org/10.1016/j.ijleo.2017.06.071

Liu, C., Zhong, Y., Qi, X., Chen, M., Liu, Z., Chen & Chen, S. (2020). Extension of the in vivo haploid induction system from diploid maize to hexaploid wheat. *Plant Biotechnology Journal*, *18*(2), 316.

Lozada-Portilla, William Alexander, Suarez-Barón, Marco Javier, & Avendaño-Fernández, Eduardo. (2021). Aplicación de redes neuronales convolucionales para la detección del tizón tardío *Phytophthora infestans* en papa *Solanum tuberosum*. Revista UDCA Actualidad & Divulgación Científica , 24 (2), e1917. Epub 06 de diciembre de 2021. https://doi.org/10.31910/rudca.v24.n2.2021.1917

Lu, J., Tan, L., & Jiang, H. (2021). Review of Convolutional Neural Network (CNN) Applied to Plant Leaf Disease Classification. *Agriculture, 11*(8), 707. MDPI AG. http://dx.doi.org/10.3390/agriculture11080707.

Luig, N. H. (1971). *Advances in plant breeding* (No. 11). P. Parey.

Luo, M., Xie, L., Chakraborty, S., Wang, A., Matny, O., Jugovich, M., ... & Ayliffe, M. (2021). A five-transgene cassette confers broad-spectrum resistance to a fungal rust pathogen in wheat. *Nature Biotechnology*, *39*(5), 561-566.

Ma, H., Singh, R. P., & Mujeeb-Kazi, A. (1995). Resistance to stripe rust in *Triticum turgidum, T. tauschii* and their synthetic hexaploids. *Euphytica*, *82*, 117-124.

Mabrouk, O. I., El-Orabey, W. M., & Esmail, S. M. (2019). Evaluation of wheat cultivars for slow rusting resistance to leaf and stem rust diseases in Egypt. *Egyptian Journal of Phytopathology*, *47*(2), 1-19.

Maccaferri, M., Sanguineti, M.C., Mantovani, P., Demontis, A., Massi, A., Ammar, K., Kolmer, J.A., Czembor, J.H., Ezrati, S., Tuberosa, R., 2010. Association mapping of leaf rust response in durum wheat. *Molecular Breeding*, *26*, 189–228.

Mago, R., Verlin, D., Zhang, P., Bansal, U., Bariana, H., Jin, Y., ... & Dundas, I. (2013). Development of wheat–Aegilops speltoides recombinants and simple PCR-based markers for *Sr32* and a new stem rust resistance gene on the 2S# 1 chromosome. *Theoretical and Applied Genetics*, *126*, 2943-2955.

Mahlein, A. K., Oerke, E. C., Steiner, U., & Dehne, H. W. (2012). Recent advances in sensing plant diseases for precision crop protection. *European Journal of Plant Pathology, 133*, 197-209.

MAPA (Ministerio de Agricultura, Pesca y Alimentación), 2022. Available at: https://www.mapa.gob.es/es/

Mapuranga, J., Zhang, N., Zhang, L., Chang, J., & Yang, W. (2022). Infection strategies and pathogenicity of biotrophic plant fungal pathogens. *Frontiers in Microbiology*, *13*, 799396.

Marikkar, N., Nagaraja, R., Somawathie, K. M. S., Hewapathirana, H. P. T. D., Yalegama, C., Littardi, P., & Chiavaro, E. (2020). Effect of coconut testa flour on cookie characteristics. *Italian Journal of Food Science*, *32*(1).

Martínez, F., Sillero, J.C., Rubiales, D., (2005). Pathogenic specialization of *Puccinia triticina* in Andalusia from 1998 to 2000. *Journal of Phytopathology, 153*, 344–349.

Martínez-Guanter, J., Garrido-Izard, M., Valero, C., Slaughter, D. C., & Pérez-Ruiz, M. (2017). Optical sensing to determine tomato plant spacing for precise agrochemical application: Two scenarios. *Sensors*, *17*(5), 1096.

Martínez-Guanter, J., Egea, G., Pérez-Ruiz, M., & Apolo-Apolo, O. E. (2019). Estimation of the leaf area index in maize based on UAV imagery using deep learning techniques. In *Precision agriculture,* (p. 1304). Wageningen Academic Publishers.

Martínez-Moreno F., & Solís, I., (2017). Evolución histórica de variedades de trigo duro en España. *Vida Rural*, Sep, 60–66.

Martínez-Moreno, F., & Solís, I., (2019). Wheat rust evolution in Spain: an historical review. *Phytopathologia Mediterranea*, *58*(1), 3–16. Doi: 10.13128/Phytopathol_Mediterr-22561

Martínez-Moreno, F., Solís, I., Noguero D., et al. (2020). Durum wheat in the Mediterranean Rim: historical evolution and genetic resources. *Genetic Resources and Crop Evolution* 67, 1415–1436. https://doi.org/10.1007/s10722-020-00913-8

Martínez-Moreno, F., Ammar, K., & Solís I. (2022). Global Changes in Cultivated Area and Breeding Activities of Durum Wheat from 1800 to Date: A Historical Review. *Agronomy, 12*(5), 1135. https://doi.org/10.3390/agronomy12051135

Mashaheet, A. M., Burkey, K. O., Saitanis, C. J., Abdelrhim, A. S., Rafiullah, & Marshall, D. S. (2020). Differential ozone responses identified among key rust-susceptible wheat genotypes. *Agronomy*, *10*(12), 1853.

Mboup, M., Bahri, B., Leconte, M., De Vallavieille-Pope, C., Kaltz, O., & Enjalbert, J. (2012). Genetic structure and local adaptation of European wheat yellow rust populations: the role of temperature-specific adaptation. *Evolutionary Applications*, *5*(4), 341-352.

McCallum, B., Hiebert, C., Huerta-Espino, J., & Cloutier, S. (2012). Wheat leaf rust. Disease resistance in wheat. *CABI plant protection series, 1*, 33–62

McCarthy, C. L., Hancock, N. H., & Raine, S. R. (2010). Applied machine vision of plants: a review with implications for field deployment in automated farming operations. *Intelligent Service Robotics*, *3*(4), 209-217.

McIntosh, R.A., Wellings, C.R., & Park, R.F. (1995). *Wheat Rusts. An atlas of resistance genes*. CSIRO, University of Sidney, Australia, 205 p.

McIntosh, R. A., Yamazaki, Y., Dubcovsky, J., Rogers, J., Morris, C., & Appels, R. (2013, September). Catalogue of gene symbols for wheat. In *Proceedings of the 12th international wheat genetics symposium* (pp. 8-13). Yokohama Japan.

McNeal, F. H., C. F. Konzak, E. P. Smith, W. S. Tate, & T.S. Russell. (1971). A uniform system for recording and processing cereal research data. USDA, Agricultural Research Service, Washington, D.C. ARS, 34-121.

Meivel, S., & Maheswari, S. (2022). Monitoring of potato crops based on multispectral image feature extraction with vegetation indices. *Multidimensional Systems and Signal Processing*, *33*(2), 683-709.

Miah, G., Rafii, M. Y., Ismail, M. R., Puteh, A. B., Rahim, H. A., Asfaliza, R., & Latif, M. A. (2013). Blast resistance in rice: a review of conventional breeding to molecular approaches. *Molecular Biology Reports*, *40*, 2369-2388.

Miedaner, T., & Korzun, V. (2012). Marker-assisted selection for disease resistance in wheat and barley breeding. *Phytopathology*, *102*(6), 560-566.

Moerschbacher, B. M., Noll, U., Gorrichon, L., & Reisener, H. J. (1990). Specific inhibition of lignification breaks hypersensitive resistance of wheat to stem rust. *Plant Physiology*, *93*(2), 465-470.

Montes, J. M., Technow, F., Dhillon, B. S., Mauch, F., & Melchinger, A. E. (2011). High-throughput non-destructive biomass determination during early plant development in maize under field conditions. *Field Crops Research*, *121*(2), 268-273. https://doi.org/10.1016/j.fcr.2010.12.017

Morgounov, A., Pozherukova, V., Kolmer, J., Gultyaeva, E., Abugalieva, A., Chudinov, V., ... & Shamanin, V. (2020). Genetic basis of spring wheat resistance to leaf rust (*Puccinia* triticina) in Kazakhstan and Russia. *Euphytica*, *216*, 1-15.

Murugan, D., Garg, A., Ahmed, T., & Singh, D. (2016, December). Fusion of drone and satellite data for precision agriculture monitoring. In *2016 11th International Conference on Industrial and Information Systems (ICIIS)* (pp. 910-914). IEEE.

Naidu, R. A., Perry E. M., Pierce F. J., & Mekuria T. (2009). The Potential of Spectral Reflectance Technique for the Detection of Grapevine Leafroll-Associated Virus-3 in Two Red-Berried Wine Grape Cultivars. *Computers and Electronics in Agriculture* *66*(1), 38–45. doi:10.1016/j.compag.2008.11.007.

Navarro, L., 1902. *Enfermedades de los trigos*. Imprenta de los hijos de M.G. Hernández, Madrid, Spain, 299 p.

Navarro, J. R., & Arauz, L. F. (1999). Exactitud y repetibilidad de dos métodos para la evaluación de la severidad de enfermedades fúngicas en el fruto de la papaya *(Carica papaya)*, *23*(3), 45-57).

Newcomb, M., Olivera, P. D., Rouse, M. N., Szabo, L. J., Johnson, J., Gale, S., ... & Jin, Y. (2016). Kenyan isolates of *Puccinia graminis* f. sp. *tritici* from 2008 to 2014: Virulence to *SrTmp* in the Ug99 race group and implications for breeding programs. *Phytopathology*, *106*(7), 729-736.

Nicolaides, N. C., & Charmandari, E. (2021). Primary generalized glucocorticoid resistance and hypersensitivity syndromes: a 2021 update. *International Journal of Molecular Sciences*, *22*(19), 10839.

Niks, R. E., Qi, X., & Marcel, T. C. (2015). Quantitative resistance to biotrophic filamentous plant pathogens: concepts, misconceptions, and mechanisms. *Annual Review of Phytopathology*, *53*, 445-470.

Niks, D., & Hille, R. (2019). Molybdenum-and tungsten-containing formate dehydrogenases and formylmethanofuran dehydrogenases: Structure, mechanism, and cofactor insertion. *Protein Science*, *28*(1), 111-122.

Nirmala, J., Saini, J., Newcomb, M., Olivera, P., Gale, S., Klindworth, D., ... & Rouse, M. N. (2017). Discovery of a novel stem rust resistance allele in durum wheat that

exhibits differential reactions to Ug99 isolates. *G3: Genes, Genomes, Genetics*, *7*(10), 3481-3490.

Ochsendorf, B. B., Ellerbroek, L. E., Chini, R., Hartoog, O. E., Hoffmeister, V., Waters, L. B. F. M., & Kaper, L. (2011). First firm spectral classification of an early-B pre-main-sequence star: B275 in M 17. *Astronomy & Astrophysics*, *536*, L1.

Oehler, M., Ling, V., Melhorn, K., & Schilling, M. (2008). A multichannel portable ECG system with capacitive sensors. *Physiological Measurement*, *29*(7), 783.

Olivera, P. D., Jin, Y., Badebo, A., & Singh, D. (2010). Races of *Puccinia graminis* f. sp. *tritici* with virulence on *Sr13* and *Sr9e* in durum screening nursery in Ethiopia. Borlaug Global Rust Initiative (BGRI), Technical Workshop; Abstracts of oral and poster presentations, St. Petersburg (Russia); 30-31 May 2010. In *TBorlaug Global Rust Initiative (BGRI), Technical Workshop; Abstracts of oral and poster presentations, St. Petersburg (Russia); 30-31 May 2010 St. Petersburg (Russia) C2010* (No. CIS-6294. CIMMYT.).

Olivera, P. D., Jin, Y., Rouse, M., Badebo, A., Fetch Jr, T., Singh, R. P., & Yahyaoui, A. (2012). Races of *Puccinia graminis* f. sp. *tritici* with combined virulence to Sr13 and *Sr9e* in a field stem rust screening nursery in Ethiopia. *Plant Disease*, *96*(5), 623-628.

Olivera, P., Newcomb, M., Szabo, L. J., Rouse, M., Johnson, J., Gale, S., ... & Jin, Y. (2015). Phenotypic and genotypic characterization of race TKTTF of *Puccinia graminis* f. sp. *tritici* that caused a wheat stem rust epidemic in southern Ethiopia in 2013–14. *Phytopathology*, *105*(7), 917-928.

Olivera Firpo, P. D., Newcomb, M., Flath, K., Sommerfeldt-Impe, N., Szabo, L. J., Carter, M. & Jin, Y. (2017). Characterization of *Puccinia graminis* f. sp. *tritici* isolates derived from an unusual wheat stem rust outbreak in Germany in 2013. *Plant Pathology*, *66*(8), 1258-1266.

Olivera Firpo, P. D., Bulbula, W. D., Badebo, A., Bockelman, H., Edae, E., & Jin, Y. (2021). Field resistance to wheat stem rust in durum wheat accessions deposited at the USDA National Small Grains Collection.

Olivera, P. D., Villegas, D., Cantero-Martínez, C., Szabo, L. J., Rouse, M. N., Luster, D. G., ... & Jin, Y. (2022). A unique race of the wheat stem rust pathogen with virulence on *Sr31* identified in Spain and reaction of wheat and durum cultivars to this race. *Plant Pathology*, *71*(4), 873-889.

Omara, R. I., Nehela, Y., Mabrouk, O. I., & Elsharkawy, M. M. (2021). The emergence of new aggressive leaf rust races with the potential to supplant the resistance of wheat cultivars. *Biology*, *10*(9), 925.

Orchi, H., Sadik, M., & Khaldoun, M. (2021). On Using Artificial Intelligence and the Internet of Things for Crop Disease Detection: A Contemporary Survey. *Agriculture*, *12*(1), 9. MDPI AG. http://dx.doi.org/10.3390/agriculture12010009

Orellana-Torrejon, C., Vidal, T., Boixel, A. L., Gélisse, S., Saint-Jean, S., & Suffert, F. (2022). Annual dynamics of *Zymoseptoria tritici* populations in wheat cultivar mixtures: A compromise between the efficacy and durability of a recently broken-down resistance gene? *Plant Pathology*, *71*(2), 289-303.

Otto, R., Silva, A. D., Franco, H. C. J., Oliveira, E. D., & Trivelin, P. C. O. (2011). High soil penetration resistance reduces sugarcane root system development. *Soil and Tillage Research*, *117*, 201-210.

Ozdogan, B., Gacar, A., & Aktas, H. (2017). Digital agriculture practices in the context of agriculture 4.0. *Journal of Economics Finance and Accounting*, *4*(2), 186-193.

Pandey, H. N., & Rao, M. V. (1989). Effect of heterogeneous populations on yield and spread of stem rust in *Triticum durum*. *Indian Journal of Genetics and Plant Breeding*, *49*(03), 297-308.

Paoletti, M. E., Haut, J. M., Plaza, J., & Plaza, A. (2019). Deep learning classifiers for hyperspectral imagery: A review. *ISPRS Journal of Photogrammetry and Remote Sensing*, *158*, 279-317. https://doi.org/10.1016/j.isprsjprs.2019.09.006

Park, R., Bansal, U., Bariana, H., Singh D., (2020). Rust resistance genotypes and expected rust responses of Australian common wheat, durum wheat and triticale varieties. *Cereal Rust Report*, 2020, 17(3).

Pascual, L.; Ruiz, M.; López-Fernández, M.; Pérez-Penã, H.; Benavente, E.; Vázquez, J.F.; Sansaloni, C.; Giraldo, P. (2020). Genomic analysis of Spanish wheat landraces reveals their variability and potential for breeding. BMC Genom. 21, 122.

Patil, P., Yaligar, N., & Meena, S. M. (2017). Performance comparison of classifiers: SVM, RF, and ANN in potato late blight disease detection using leaf images. In 2017 IEEE International Conference on Computational Intelligence and Computing Research (ICCIC) (pp. 1-5). Coimbatore, India. doi: 10.1109/ICCIC.2017.8524301-Pulgar, F. J.,

Patoliya, J., Mewada, H., Hassaballah, M., Khan, M. A., & Kadry, S. (2022). A robust autonomous navigation and mapping system based on GPS and LiDAR data for unconstraint environment. *Earth Science Informatics*, *15*(4), 2703-2715.

Patpour, M., Justesen, A. F., Tecle, A. W., Yazdani, M., Yasaie, M., & Hovmøller, M. S. (2020). First report of race TTRTF of wheat stem rust (*Puccinia graminis* f. sp. *tritici*) in Eritrea. *Plant Disease*, *104*(3), 973.

Patpour, M., Hovmøller, M. S., Rodriguez-Algaba, J., Randazzo, B., Villegas, D., Shamanin, V. P., ... & Justesen, A. F. (2022). Wheat stem rust back in Europe: Diversity, prevalence and impact on host resistance. *Frontiers in Plant Science*, *13*, 882440.

Paz Pellat, F., Romero Sanchez, M. E., Palacios Vélez, E., Bolaños González, M., Valdez Lazalde, J. R., & Aldrete, A. (2015). Alcances y limitaciones de los índices espectrales de la vegetación: análisis de índices de banda ancha. *Terra Latinoamericana*, *33*(1), 27-49.

Pazda, M., Kumirska, J., Stepnowski, P., & Mulkiewicz, E. (2019). Antibiotic resistance genes identified in wastewater treatment plant systems–a review. *Science of the Total Environment*, *697*, 134023.

Pérez-Ruiz, M., Agüera, J., Gil, J. A., & Slaughter, D. C. (2011). Optimization of agrochemical application in olive groves based on positioning sensor. *Precision Agriculture*, *12*, 564-575.

Pérez-Ruiz, M., Rallo, P., Jiménez, M. R., Garrido-Izard, M., Suárez, M. P., Casanova, L., ... & Morales-Sillero, A. (2018). Evaluation of over-the-row harvester damage in a super-high-density olive orchard using on-board sensing techniques. *Sensors*, *18*(4), 1242.

Pérez-Ruiz, M., Prior, A., Martínez-Guanter, J., Apolo-Apolo, O. E., Andrade-Sanchez, P., & Egea, G. (2020). Development and evaluation of a self-propelled electric

platform for high-throughput field phenotyping in wheat breeding trials. *Computers and Electronics in Agriculture*, *169*, 105237.

Peterson, R.F., Campbell, A.B., Hannan, A.E., 1948. A diagrammatic scale for estimating rust intensity of leaves and stem of cereals. *Canadian Journal of Research*, *26*, 496–500.

Porras, R., Miguel-Rojas, C., Pérez-de-Luque, A., & Sillero, J. C. (2022). Macro-and Microscopic Characterization of Components of Resistance against *Puccinia striiformis* f. sp. *tritici* in a Collection of Spanish Bread Wheat Cultivars. *Agronomy*, *12*(5), 1239.

Prasad, P., Savadi, S., Bhardwaj, S. C., & Gupta, P. K. (2020). The progress of leaf rust research in wheat. *Fungal biology*, *124*(6), 537-550.

Pretorius, Z. A., Singh, R. P., Wagoire, W. W., & Payne, T. S. (2000). Detection of virulence to wheat stem rust resistance gene *Sr31* in *Puccinia graminis* f. sp. *tritici* in Uganda. *Plant disease*, *84*(2), 203-203.

Pretorius, Z. A., Jin, Y., Bender, C. M., Herselman, L., & Prins, R. (2012). Seedling resistance to stem rust race Ug99 and marker analysis for *Sr2*, *Sr24* and *Sr31* in South African wheat cultivars and lines. *Euphytica*, *186*, 15-23.

Radici, A., Martinetti, D., & Bevacqua, D. (2022). Early-detection surveillance for stem rust of wheat: insights from a global epidemic network based on airborne connectivity and host phenology. *Environmental Research Letters*, *17*(6), 064045.

Ramezani, H., & Dietz, H. (2020). Building machines with DNA molecules. *Nature Reviews Genetics*, *21*(1), 5-26.

Rasti, B., Chang, Y., Dalsasso, E., Denis, L., & Ghamisi, P. (2021). Image restoration for remote sensing: Overview and toolbox. *IEEE Geoscience and Remote Sensing Magazine*, *10*(2), 201-230.

Ray, D. K., Mueller, N. D., West, P. C., & Foley, J. A. (2013). Yield Trends Are Insufficient to Double Global Crop Production by 2050. *PLoS ONE*, *8*(6). https://doi.org/10.1371/journal.pone.0066428

Rebetzke, G. J., Jimenez-Berni, J., Fischer, R. A., Deery, D. M., & Smith, D. J. (2019). High-throughput phenotyping to enhance the use of crop genetic resources. *Plant Science*, *282*, 40-48. https://doi.org/10.1016/j.plantsci.2018.06.017.

Red de Información Agroclimática de Andalucía (RIA). https://www.juntadeandalucia.es/agriculturaypesca/ifapa/riaweb/web/

Ren, X., Wang, C., Ren, Z., Wang, J., Zhang, P., Zhao, S., ... & Wang, X. (2023). Genetics of resistance to leaf rust in wheat: an overview in a genome-wide level. *Sustainability*, *15*(4), 3247.

Reynolds, M. P., & Braun, H. J. (2022). Wheat improvement. In *Wheat Improvement: Food Security in a Changing Climate* (pp. 3-15). Cham: Springer International Publishing.

Riaz, M., & Wong, Y. (2017). Estimation of Yield Losses due to Leaf Rust and Late Seeding on Wheat (*Triticum aestivum* L.) Variety Seher-06 in District Faisalabad, Punjab, Pakistan. *Adv. Biotech. Micro*, *4*(10.19080).

Rivera, A. J., Charte, F., & del Jesus, M. J. (2018). Análisis del impacto de datos desbalanceados en el rendimiento predictivo de redes neuronales convolucionales. In

XVIII Conferencia de la Asociación Española para la Inteligencia Artificial (pp. 1213-1218.

Roberts, J., Power, A., Chapman, J., Chandra, S., & Cozzolino, D. (2018). A brief update on the advantages, applications, and limitations of hyperspectral and chemical imaging in food authentication. *Applied Sciences, 8*(4), 505. https://doi.org/10.3390/app8040505

Rodríguez-Moreno, V. M., Jiménez-Lagunes, A., Estrada-Avalos, J., Mauricio-Ruvalcaba, J. E., & Padilla-Ramírez, J. S. (2020). Weather-data-based model: an approach for forecasting leaf and stripe rust on winter wheat. *Meteorological Applications, 27*(2), e1896. https://doi.org/10.1002/met.1896

Rodríguez-Vázquez, J. N., Ammar, K., Solís, I., & Martínez-Moreno, F. (2023). Virulence of *Puccinia triticina* and *Puccinia tritici-duri* on durum wheat in southern Spain, from 2020 to 2022. *Phytopathologia Mediterranea, 62*(1), 29-34. doi: 10.36253/phyto-14227

Rodríguez-Vázquez JN, Ammar K, Solís I, Martínez-Moreno F. (2023). Characterization of Wheat Yellow Rust and Stem Rust Virulence in Southern Spain. *Agriculture, 13*(12), 2202. https://doi.org/10.3390/agriculture13122202

Roelfs, A. P. (1985). Wheat and rye stem rust. In *Diseases, distribution, epidemiology, and control* (pp. 3-37). Academic Press.

Roelfs, A. P. (1992). Las royas del trigo: Conceptos y métodos para el manejo de esas enfermedades. CIMMYT.

Ruan, G., Li, X., Yuan, F., Cammarano, D., Ata-UI-Karim, S. T., Liu, X., ... & Cao, Q. (2022). Improving wheat yield prediction integrating proximal sensing and weather data with machine learning. *Computers and Electronics in Agriculture*, *195*, 106852.

Sabouri, H., Kazerani, B., Fallahi, H. A., Dehghan, M. A., Alegh, S. M., Dadras, A. R., ... & Mastinu, A. (2022). Association analysis of yellow rust, fusarium head blight, tan spot, powdery mildew, and brown rust horizontal resistance genes in wheat. *Physiological and Molecular Plant Pathology*, *118*, 101808.

Sadeghipoor, Z., Lu, Y. M., & Süsstrunk, S. (2015, February). Gradient-based correction of chromatic aberration in the joint acquisition of color and near-infrared images. In *Digital photography XI* (Vol. 9404, pp. 94-104). SPIE.

Sagan, V., Peterson, K. T., Maimaitijiang, M., Sidike, P., Sloan, J., Greeling, B. A., ... & Adams, C. (2020). Monitoring inland water quality using remote sensing: Potential and limitations of spectral indices, bio-optical simulations, machine learning, and cloud computing. *Earth-Science Reviews*, *205*, 103187.

Saini, D. K., Chahal, A., Pal, N., Srivastava, P., & Gupta, P. K. (2022). Meta-analysis reveals consensus genomic regions associated with multiple disease resistance in wheat (*Triticum aestivum* L.). *Molecular Breeding*, *42*(3), 11.

Salazar, J., Branas, M., & Martinez, M., (1976). Physiological specialization of wheat leaf rust in Spain, 1972-1975. *Cereal Rusts Conferences*, Interlaken, Switzerland.

Salcedo, A., Rutter, W., Wang, S., Akhunova, A., Bolus, S., Chao, S., & Akhunov, E. (2017). Variation in the Avr*Sr35* gene determines *Sr35* resistance against wheat stem rust race Ug99. *Science*, *358*(6370), 1604-1606.

Sansaloni, C., Franco, J., Santos, B., Percival-Alwyn, L., Singh, S., Petroli, C., ... & Pixley, K. (2020). Diversity analysis of 80,000 wheat accessions reveals consequences and opportunities of selection footprints. *Nature Communications*, *11*(1), 4572.

Sauce-Acosta, C., Lugo-García, G., Villaseñor-Mir, H., Partida-Ruvalcaba, L., Reyes-Olivares, A. (2015). Un método preciso para medir severidad de roya de la hoja (*Puccina triticina Eriks)* en trigo. *Revista Fitotecnia Mexicana, 38*(4), 427-434.

Savary, S., Willocquet, L., Pethybridge, S. J., Esker, P., McRoberts, N. & Nelson, A., (2019). The global burden of pathogens and pests on major food crops. *Nature Ecology & Evolution, 3*(3), 430–439.

Semagn, K., Iqbal, M., Jarquin, D., Crossa, J., Howard, R., Ciechanowska, I., ... & Spaner, D. (2022). Genomic predictions for common bunt, FHB, stripe rust, leaf rust, and leaf spotting resistance in spring wheat. *Genes*, *13*(4), 565.

Shahin, A., Youssif, W., & EL-Naggar, D. (2020). Detection of Ug99 (TTKSK) of wheat stem rust fungus and new virulence races of *Puccinia graminis* f. sp. *tritici* in Egypt. *Egyptian Journal of Phytopathology*, *48*(1), 14-28.

Shakoor, A., Grant, J., Grande, M., & Cumming, D. R. (2019). Towards portable nanophotonic sensors. *Sensors*, *19*(7), 1715.

Shakoor, N., Lee, S., & Mockler, T. C. (2017). High throughput phenotyping to accelerate crop breeding and monitoring of diseases in the field. *Current Opinion in Plant Biology, 38*, 184-192

Sharma, S., & Bhattarai, K. (2019). Progress in developing bacterial spot resistance in tomato. *Agronomy*, *9*(1), 26.

Shewry, P. R. (2009). Wheat. *Journal of Experimental Botany*, *60*(6), 1537-1553.

Shrawat, A. K., & Armstrong, C. L. (2018). Development and application of genetic engineering for wheat improvement. *Critical Reviews in Plant Sciences*, *37*(5), 335-421.

Sibikeev, S.N., Baranova, O.A., Druzhin, A.E. (2021). A prebreeding study of introgression spring bread wheat lines carrying combinations of stem rust resistance genes, *Sr22+Sr25* and *Sr35+Sr25*. *Vavilovskii Zhurnal Genet. Selektsii.*, *25*(7), 713-722. doi: 10.18699/VJ21.081.

Singh, A., Ganapathysubramanian, B., & Sarkar, S. (2016). Machine learning for High-Throughput Stress Phenotyping in Plants. *Trends in Plant Science, 21*(2), 110 – 124. https://doi.org/10.1016/j.tplants.2015.10.015

Singh, A., & Arora, M. (2020). CNN-Based Detection of Healthy and Unhealthy Wheat Crops. In 2020 International Conference on Smart Electronics and Communication (ICOSEC) (pp. 121-125). Trichy, India. doi: 10.1109/ICOSEC49089.2020.9215340

Singh, R.P., Huerta–Espino, J., Pfeiffer, W., & Figueroa–Lopez, P., 2004. Occurrence and impact of a new leaf rust race on durum wheat in northwestern Mexico from 2001 to 2003. *Plant Disease*, 88, 703–708.

Singh, R. P., Hodson, D. P., Huerta-Espino, J., Jin, Y., Njau, P., Wanyera, R., ... & Ward, R. W. (2008). Will stem rust destroy the world's wheat crop? *Advances in Agronomy*, *98*, 271-309.

Singh, R. P., Huerta-Espino, J., Bhavani, S., Herrera-Foessel, S. A., Singh, D., Singh, P. K., ... & Crossa, J. (2011). Race non-specific resistance to rust diseases in CIMMYT spring wheats. *Euphytica*, *179*, 175-186.

Singh, R. P., Hodson, D. P., Jin, Y., Lagudah, E. S., Ayliffe, M. A., Bhavani, S., ... & Hovmøller, M. S. (2015). Emergence and spread of new races of wheat stem rust fungus: continued threat to food security and prospects of genetic control. *Phytopathology*, *105*(7), 872-884.

Singh, S., & Bowden, R. L. (2011). Molecular mapping of adult-plant race-specific leaf rust resistance gene *Lr12* in bread wheat. *Molecular Breeding*, *28*, 137-142.

Soko, T., Bender, C. M., Prins, R., & Pretorius, Z. A. (2018). Yield loss associated with different levels of stem rust resistance in bread wheat. *Plant Disease*, *102*(12), 2531-2538.

Soleiman, N. H., Solis, I., Sillero, J. C., Herrera-Foessel, S. A., Ammar, K., & Martinez, F. (2014). Evaluation of macroscopic and microscopic components of partial resistance to leaf rust in durum wheat. *Journal of Phytopathology*, *162*(6), 359-366.

Soleiman, N.H., Solís, I., Soleiman, M.H., Sillero, J.C., Villegas, D., Álvaro, F., Martínez-Moreno, F., (2016). Emergence of a new race of leaf rust with combined virulence to *Lr14a* and *Lr72* genes on durum wheat. *Spanish Journal of Agricultural Research, 14*(3), e10SC02.

Song, S., Demirel, Y. K., Atlar, M., Dai, S., Day, S., & Turan, O. (2020). Validation of the CFD approach for modelling roughness effect on ship resistance. *Ocean Engineering*, *200*, 107029.

Song, L., Liu, J., Cao, B., Liu, B., Zhang, X., Chen, Z. & Ni, Z. (2023). Reducing brassinosteroid signalling enhances grain yield in semi-dwarf wheat. *Nature*, 1-7.

Soylak, M., Agirbas, M., & Yilmaz, E. (2021). A new strategy for the combination of supramolecular liquid phase microextraction and UV–Vis spectrophotometric determination for traces of maneb in food and water samples. *Food Chemistry*, *338*, 128068.

Stakman, E.C., Stewart, D.M., Loegering, W.Q. (1962). *Identification of physiologic races of Puccinia* graminis *var.* tritici. United States Department of Agriculture, Agricultural Research Service, E617, Minnesota, USA, 54p. Available at: https://naldc.nal.usda.gov/download/CAT10243018/PDF

Taddia, Y., Russo, P., Lovo, S., & Pellegrinelli, A. (2020). Multispectral UAV monitoring of submerged seaweed in shallow water. *Applied Geomatics*, *12*, 19-34.

Terentev, A., Dolzhenko, V., Fedotov, A. y Eremenko, D. (2022). Current State of Hyperspectral Remote Sensing for Early Plant Disease Detection: A Review. *Sensors*, *22*(3), 757. http://dx.doi.org/10.3390/s22030757

Thakur, P. S., Khanna, P., Sheorey, T., & Ojha, A. (2022). Trends in vision-based machine learning techniques for plant disease identification: A systematic review. *Expert Systems with Applications*, *208*, 118117. https://doi.org/10.1016/j.eswa.2022.118117

Thirugnana Sambandham, V., Shankar, P., & Mukhopadhaya, S. (2022). Early Onset Yellow Rust Detection Guided by Remote Sensing Indices. *Agriculture*, *12*(8), 1206.

Tomar, S. M. S., Singh, S. K., & Sivasamy, M. (2014). Wheat rusts in India: Resistance breeding and gene deployment-A review. *Indian Journal of Genetics and Plant Breeding*, *74*(02), 129-156.

Trendov, N. M., Varas, S., & Zeng, M. (2019). Tecnologías digitales en la agricultura y las zonas rurales. Organización de las Naciones Unidas para la Alimentación y la Agricultura. Roma, FAO.

Uğuz, S., & Uysal, N. (2021). Classification of olive leaf diseases using deep convolutional neural networks. *Neural Computing and Applications*, *33*, 4133-4149. https://doi.org/10.1007/s00521-020-05235-5

Upadhyaya, N. M., Mago, R., Panwar, V., Hewitt, T., Luo, M., Chen, J. & Dodds, P. N. (2021). Genomics accelerated isolation of a new stem rust avirulence gene–wheat resistance gene pair. *Nature Plants*, *7*(9), 1220-1228.

Vanderplank, J. E. (2012). *Disease resistance in plants*. Elsevier.

Vásquez-Dolande, Eduardo, Morales, Ethel y Achkar, Marcel. (2021). Evaluación del uso de sensores remotos para identificar manchas de crudo en áreas costa afuera del Uruguay. *Boletín de Geología*, *43*(2), 185-202. https://doi.org/10.18273/revbol.v43n2-2021010

Vergara-Diaz, O., Kefauver, S. C., Elazab, A., Nieto-Taladriz, M. T., & Araus, J. L. (2015). Grain yield losses in yellow-rusted durum wheat estimated using digital and conventional parameters under field conditions. *Crop Journal*, *3*(3), 200–210. https://doi.org/10.1016/j.cj.2015.03.003

Viennot-Bourgin G., (1941). Diagnose Latine de *Puccinia tritici-duri*. Ann. Ecole Nationale Agric. Grignon Paris. C Amat Ser. 2: 146.

Weiss, M., Jacob, F., & Duveiller, G. (2020). Remote sensing for agricultural applications: A meta-review. *Remote Sensing of Environment*, *236*, 111402.

Wellings, C. R. (2011). Global status of stripe rust: a review of historical and current threats. *Euphytica*, *179*(1), 129-141.

Whetton, R. L., Waine, T. W., & Mouazen, A. M. (2018). Hyperspectral measurements of yellow rust and fusarium head blight in cereal crops: Part 2: On-line field measurement. *Biosystems engineering*, *167*, 144-158. https://doi.org/10.1016/j.biosystemseng.2018.01.004

Winterhalter, L., Mistele, B., & Schmidhalter, U. (2013). Evaluation of active and passive sensor systems in the field to phenotype maize hybrids with high-throughput. *Field Crops Research*, *154*, 236-245. https://doi.org/10.1016/j.fcr.2013.09.006

Wulff, B. B., & Krattinger, S. G. (2022). The long road to engineering durable disease resistance in wheat. *Current Opinion in Biotechnology*, *73*, 270-275.

Xu, W., Wang, D., & Tang, B. Z. (2021). NIR-II AIEgens: a win–win integration towards bioapplications. *Angewandte Chemie International Edition*, *60*(14), 7476-7487.

Yadav, R., Kumar Rana, Y., Nagpal, S. (2019). Plant Leaf Disease Detection and Classification Using Particle Swarm Optimization. En: Renault, É. Mühlethaler, P., Boumerdassi, S. (eds) Machine Learning for Networking. MLN 2018. Lecture Notes in Computer Science (), vol 11407. Springer, Cham. https://doi.org/10.1007/978-3-030-19945-6_21

Yan, G., Chen, X., Line, R., & Wellings, C. (2003). Resistance gene-analog polymorphism markers co-segregating with the *Yr5* gene for resistance to wheat stripe rust. *Theoretical and Applied Genetics*, *106*, 636-643.

Yang, Z., Zheng, J., Liu, C., Wang, Y., Condon, A. G., Chen, Y. & Y.G., Hu. (2015). Effects of the GA-responsive dwarfing gene Rht18 from tetraploid wheat on agronomic traits of common wheat *Field Crops Research* 183 (92–101).

Yao, Y., Luo, Z., Li, S., Shen, T., Fang, T., & Quan, L. (2019). Recurrent mvsnet for high-resolution multi-view stereo depth inference. In *Proceedings of the IEEE/CVF conference on computer vision and pattern recognition* (pp. 5525-5534).

Yao, Z., He, D., & Lei, Y. (2018). Thermal imaging for early nondestructive detection of wheat stripe rust. In 2018 ASABE Annual International Meeting (p. 1). American Society of Agricultural and Biological Engineers.

Yuan, Z., Wen, Y., & Li, G. (2018). Production of bioethanol and value added compounds from wheat straw through combined alkaline/alkaline-peroxide pretreatment. *Bioresource Technology, 259*, 228-236. https://doi.org/10.1016/j.biortech.2018.03.044

Zadoks, J.C., Chang, T.T., & Konzak, C.F., (1974). A decimal code for the growth stages of cereals. *Weed Research, 14*, 415–421.

Zadoks, J. C., & Bouwman, J. J. (1985). Epidemiology in Europe. In *Diseases, Distribution, Epidemiology, and Control* (pp. 329-369). Academic Press.

Zhang, J., Huang, Y., Pu, R., González-Moreno, P., Yuan, L., Wu, K., & Huang, W. (2019). Monitoring plant diseases and pests through remote sensing sensor technology: A review. *Computers and Electronics in Agriculture, 165*. https://doi.org/10.1016/j.compag.2019.104943

Zhao, X., Guo, Y., Kang, L., Yin, C., Bi, A., Xu, D., & Lu, F. (2023). Population genomics unravels the Holocene history of bread wheat and its relatives. *Nature Plants*, *9*(3), 403-419.

Zheng, Q., Wenjiang H., Ximin C., Yue S., and Linyi L. (2018). New Spectral Index for Detecting Wheat Yellow Rust Using Sentinel-2 Multispectral Imagery. *Sensors*, *18*(3), 868. https://doi.org/10.3390/s18030868

Zheng, Q., Weng, Q., & Wang, K. (2019). Developing a new cross-sensor calibration model for DMSP-OLS and Suomi-NPP VIIRS night-light imageries. *ISPRS Journal of Photogrammetry and Remote Sensing*, *153*, 36-47.

Zhu, C., Leung, V. C., Rodrigues, J. J., Shu, L., Wang, L., & Zhou, H. (2018). Social sensor cloud: framework, greenness, issues, and outlook. *IEEE Network*, *32*(5), 100-105.

Zohary, D., & Hopf, M. (2000). *Domestication of plants in the Old World: The origin and spread of cultivated plants in West Asia, Europe and the Nile Valley* (No. Ed. 3). Oxford University Press.